

**SRC/SEMATECH Engineering Research Center
for Environmentally Benign Semiconductor Manufacturing**

2010 ANNUAL REPORT

**SRC Core Projects
and
Customized, Intel Initiative and Seed Projects**

February 2010

Environmental Safety and Health (ESH) Impacts of Emerging Nanoparticles and Byproducts from Semiconductor Manufacturing

Tasks 425.023 and 425.024

Research Team

PIs:

- **Jim A Field, Dept. Chemical and Environmental Engineering, UA**
- **Scott Boitano, Dept. of Physiology & Arizona Respiratory Center, UA**
- **Buddy Ratner, University of Washington Engineered Biomaterials Center, UWEB**
- **Reyes Sierra, Dept. Chemical and Environmental Engineering, UA**
- **Farhang Shadman, Dept. Chemical and Environmental Engineering, UA**

Graduate Students:

- **Isabel Barbero: PhD candidate, Chemical and Environmental Engineering, UA**
- **Christopher Barnes, PhD completed, Chemical Engineering, UW**
- **Rosa Daneshvar: PhD candidate, Chemical Engineering, UW**
- **Cara L Sherwood: PhD candidate, Cell Biology and Anatomy, UA**
- **Hao Wang: PhD candidate, Chemical and Environmental Engineering, UA**

Other Researchers:

- **Antonia Luna, Postdoctoral Fellow, Chemical and Environmental Engineering, UA**
- **Citlali Garcia, Postdoctoral Fellow, Chemical and Environmental Engineering, UA**
- **Angel Cobo, Exchange MS Student, Chemical and Environmental Engineering, UA**
- **Jacky Yao, Research Scientist, Chemical and Environmental Engineering, UA**

Cost Share (other than core ERC funding):

- **\$80k from UA Water Sustainability Program**

Overall Objectives

- **Characterize toxicity of current and emerging nanoparticles (NP) & NP byproducts**
- **Develop new rapid methodologies for assessing and predicting toxicity**

ESH Metrics and Impact

1. *Reduction in the use or replacement of ESH-problematic materials*

This project will evaluate the toxicity of various types of nanoparticles utilized or considered for application in semiconductor manufacturing, and the impact of manufacturing steps on their toxicity. This information can assist in selecting materials which are candidates for replacement or use reduction.

2. *Reduction in emission of ESH-problematic material to environment*

The knowledge gained can be utilized to modify the manufacture of nanoparticles so that they have a lowered toxicity and thus a lowered environmental impact.

Surface Physical Characterization

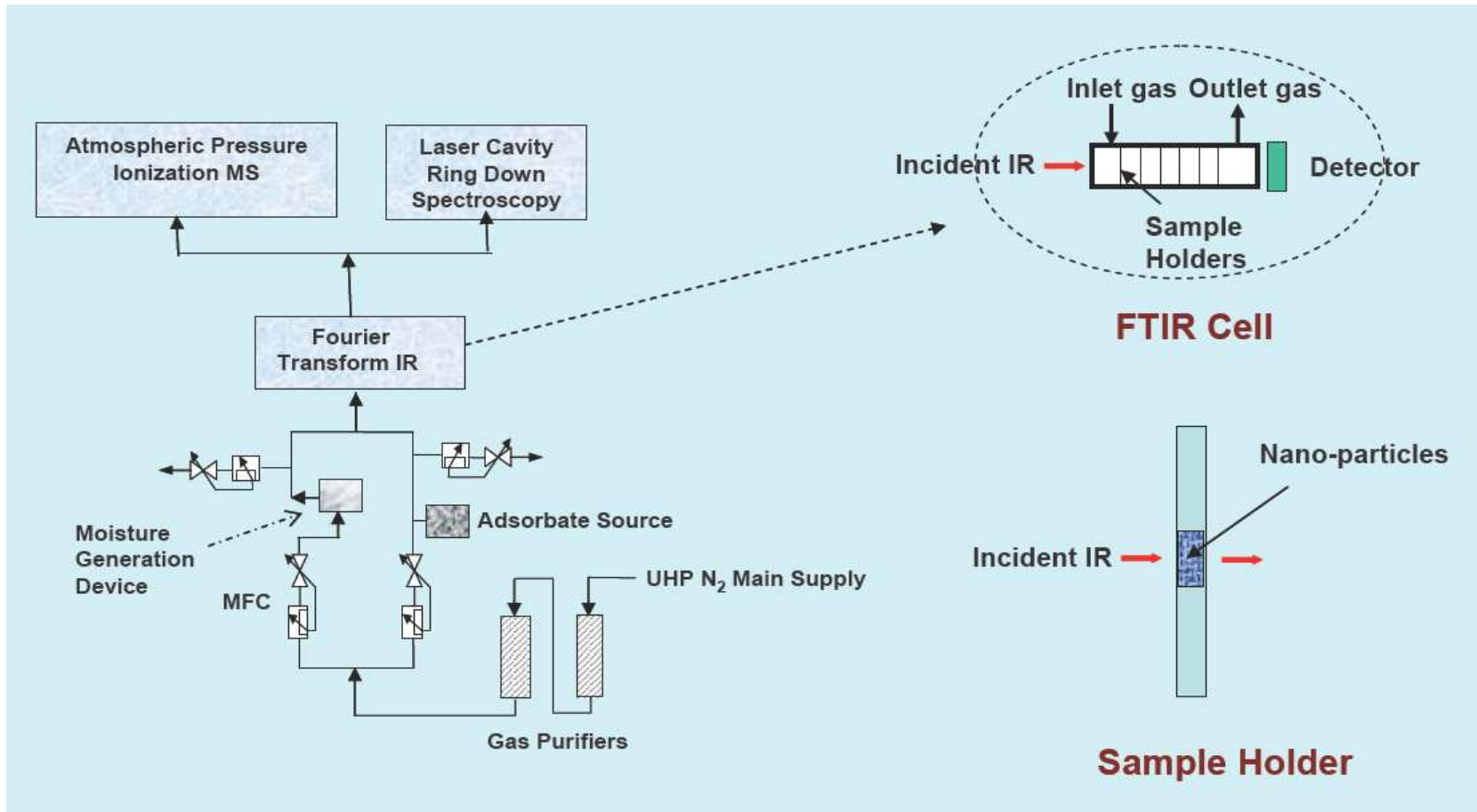
Hypothesis: The size and size distribution of nanoparticles intrinsically makes them more adsorptive to external chemicals, and these surface molecules lead to the observed toxic effects of nanoparticles on cells.

Surface Physical Characterization

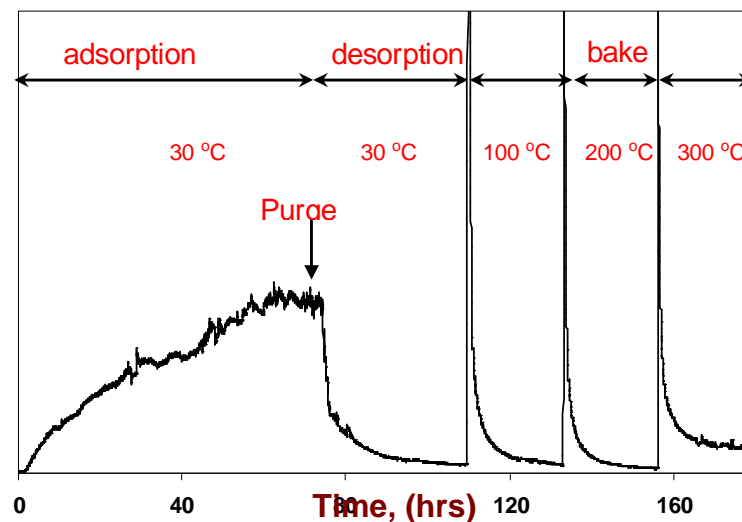
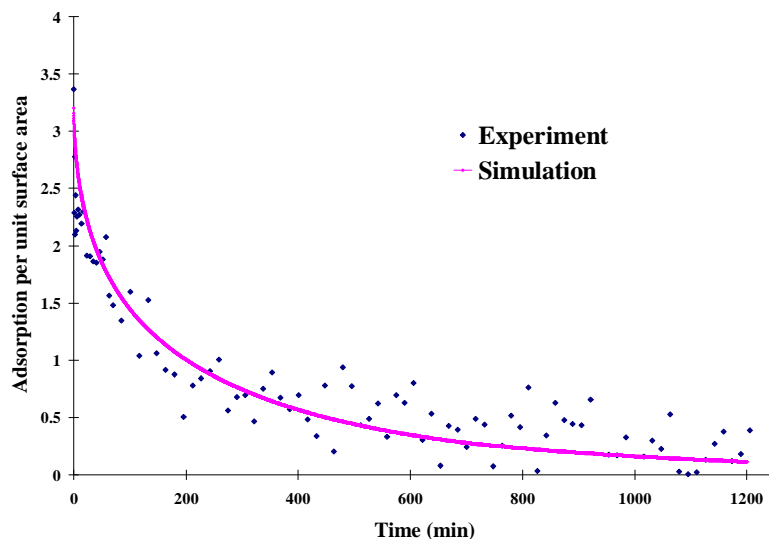
- **Particle size distribution (dynamic light scattering)**
- **Specific area (area/volume or area/mass of NP)**
- **Active site density; site energetics**
- **Physical adsorption vs chemical adsorption**
- **Ability of the surface to concentrate bulk contaminants (selective adsorption)**
- **Retention of contaminants**

Surface Physical Characterization

Objective: determine surface ability to concentrate and retain bulk contaminants. Key parameters are specific area, active site density, and surface energetics for selective adsorption



Experimental Method & Typical Results

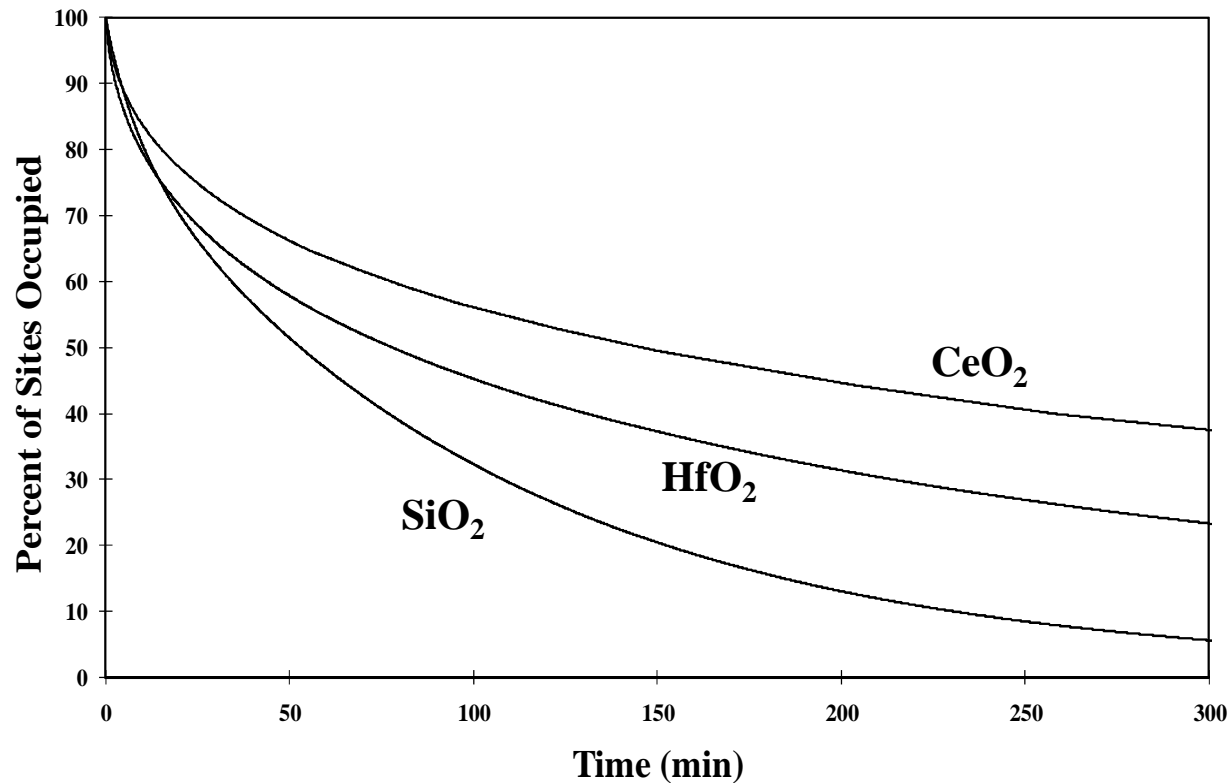


- Physical adsorption of inert adsorbent (similar to BET isotherm) for area measurement
- Chemical adsorption of reactive adsorbent for measuring site density

- Temperature-Programmed Interaction (TPI) for measuring site energetics

Comparison of Surface Activity of Different NP Materials

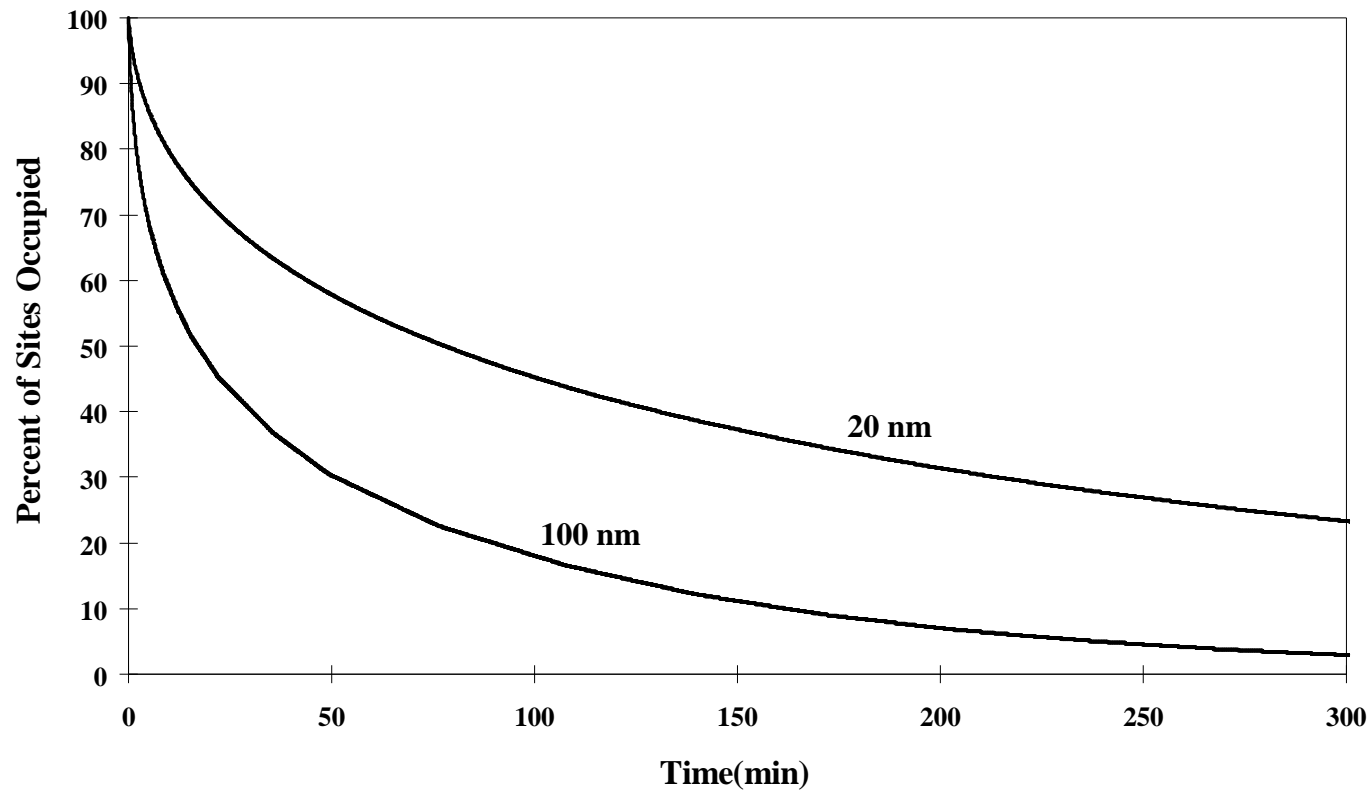
Experimental data using moisture adsorption on 20 nm NPs



Contamination retention is compound dependent: highest for CeO₂ and lowest for SiO₂; adsorption on CeO₂ seems to be strong chemisorption

NPs Retention of Contaminants

Dynamics of Moisture Desorption



Contamination retention of NPs is size dependent (smaller NPs show higher retention)

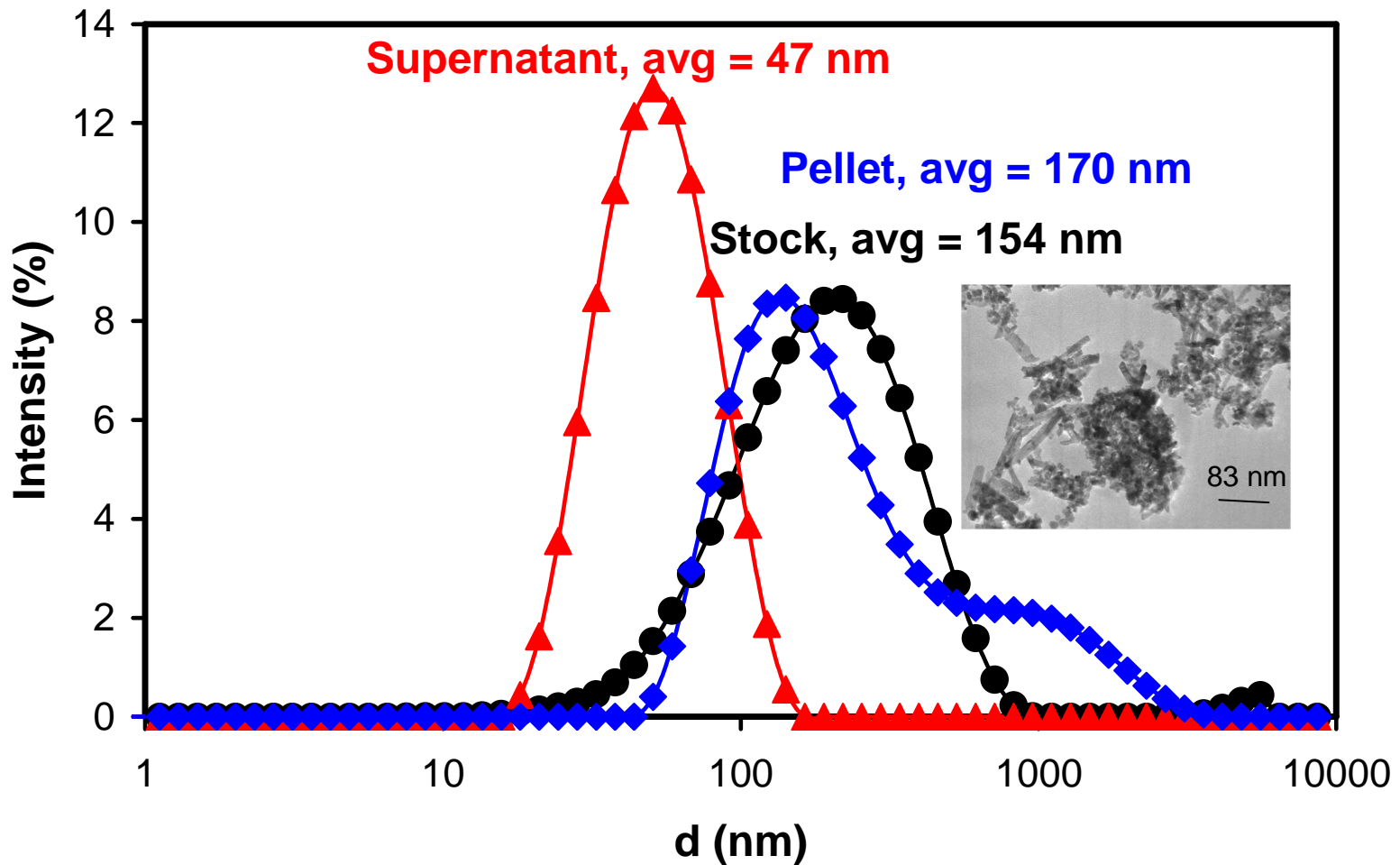
Surface Characterization

	Particle Size	Adsorption Rate Coeff.	Desorption Rate Coeff.	Active Site Density	Adsorption Capacity
	d_p (nm)	k_a ($\text{cm}^3 \text{mol}^{-1} \text{s}^{-1}$)	k_d (s^{-1})	S_0 (mol/cm^2)	C_{s0} (mol/cm^2)
HfO_2	20	3.30E+08	2.4	7.00E-10	6.56E-10
HfO_2	100	8.00E+08	0.8	2.50E-10	2.48E-10
SiO_2	20	5.30E+08	360	2.00E-08	2.74E-09
CeO_2	20	3.00E+08	1	8.75E-10	8.49E-10

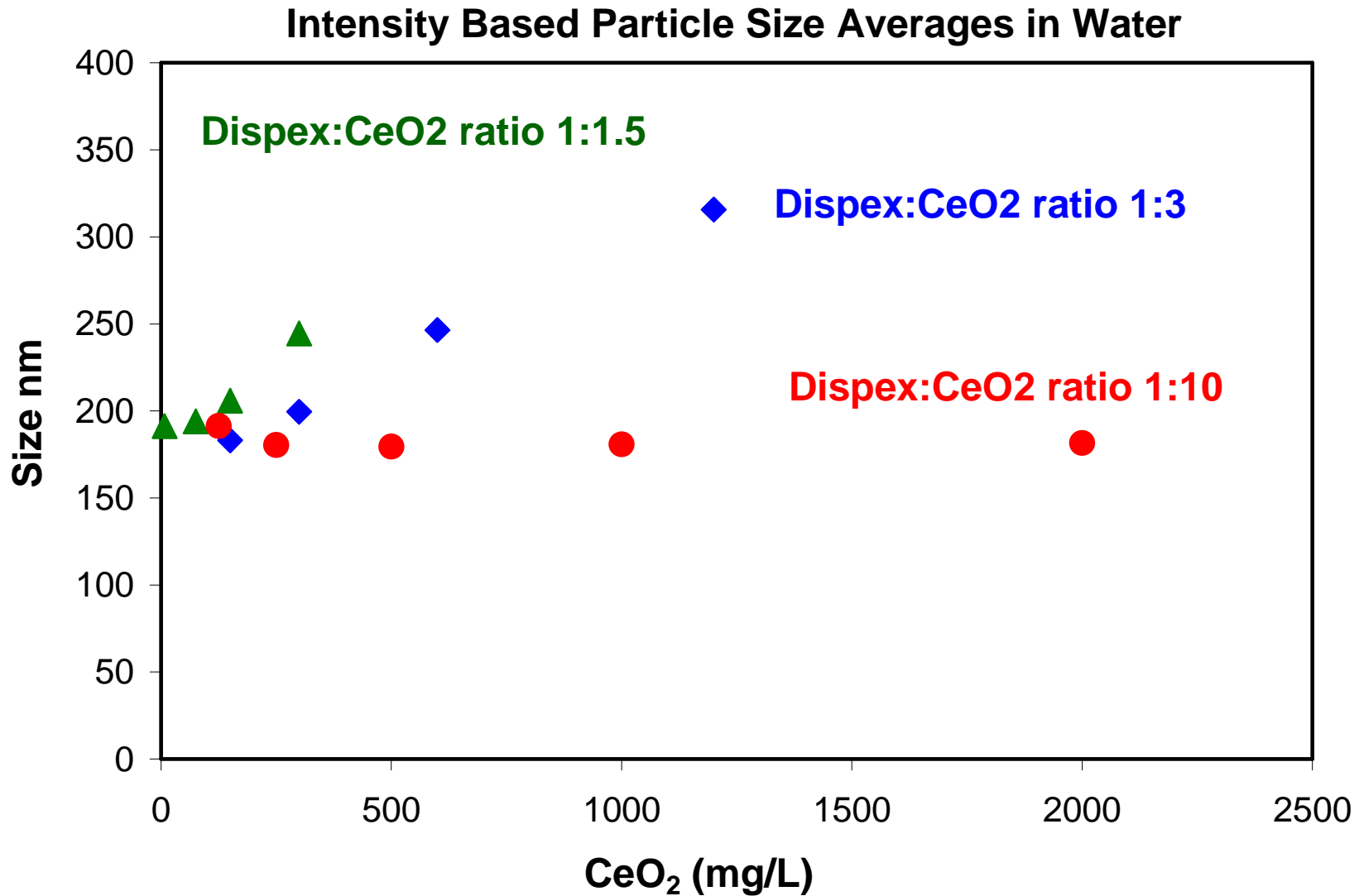
- Small HfO_2 particles adsorbed contaminants more energetically than larger particles (*higher activation energy*)
- Small particles have higher *capacity* for adsorption and retention of secondary contaminants

Fractionation of CeO₂ by Centrifugation

Fractioning CeO₂ 2g/L Eppendorf Centrifuge 4500 rpm



Role Surfactant Conc. on CeO₂ NP Size



Impact Biological Media on NP Dispersions

Intensity Based Particle Size Averages in Water (DLS)
(units = nm)

<u>MEDIUM</u>	<u>MATERIAL</u>		<u>Comment</u>
	<u>HfO₂</u>	<u>CeO₂</u>	
MQ Water	359 ± 12	1741 ± 275	
MQ Water + dispex	138 ± 2	209 ± 25	
MTT	284 ± 2		MTT = mitochondrion toxicity test medium
HBSS	3242 ± 270		HBSS = Hanks' Balanced Salt Solutions
DMEM	593 ± 252		DMEM = Dulbecco's Modified Eagle Medium (+25KBS, no HCO ₃)
Microtox	901 ± 406	236 ± 21	

Surface Chemical Characterization

The University of Washington has a strong campus resource facility permitting us to perform state-of-the-art nanoparticle surface analysis. Instrumentation that is available for this purpose includes:

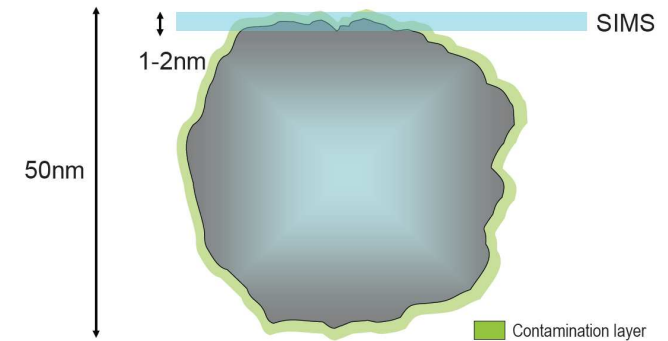
- Electron spectroscopy for chemical analysis (ESCA)**
- Secondary ion mass spectrometry (SIMS)**
- Surface plasmon resonance (SPR)**
- Atomic force microscopy (AFM)**
- Sum Frequency Generation (SFG)**
- Attenuated Total Reflectance IR (ATR-IR)**

Secondary Ion Mass Spectrometry (SIMS)

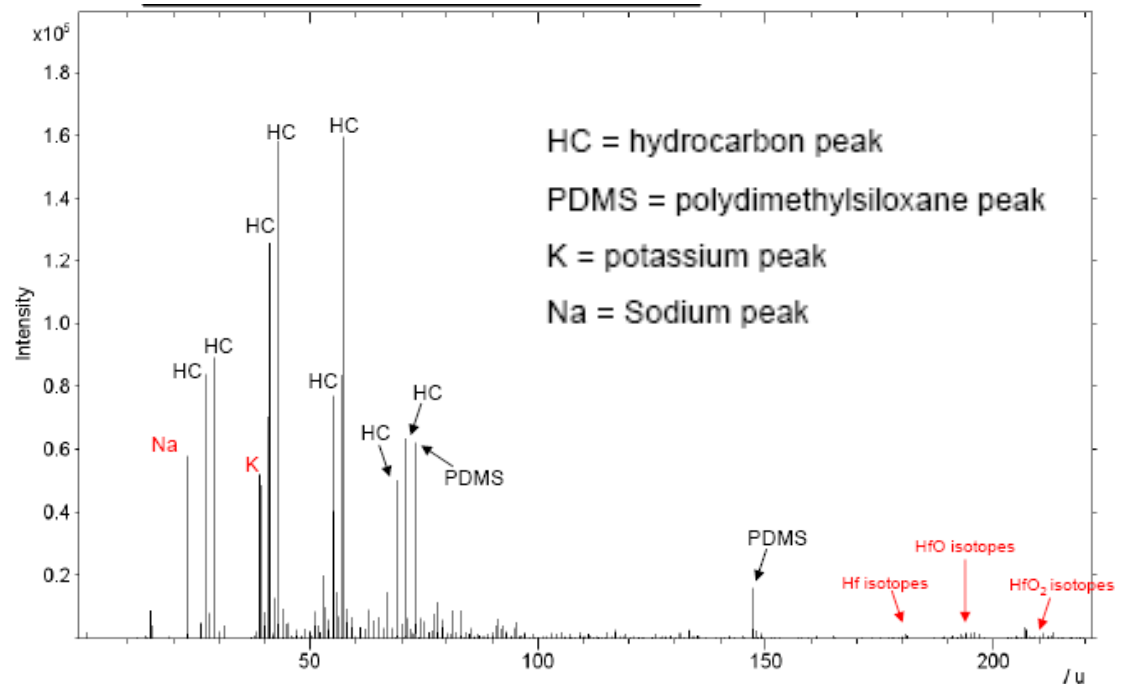
Time-of-flight (ToF) SIMS; Static SIMS



- Probably the most information-rich of the modern surface analysis methods
- Various organic/inorganic contaminants detected on the surface of HfO_2 NPs



- Positive and negative spectra can be used to identify impurities including metals from fabrication or organics from unidentified sources



Nanoparticle Impurities – ToF SIMS

Positive Spectra Impurities

mass	ID	Ref Micron	NP1 20 nm	NP2 1-2 nm	NP3 100 nm
27	Al	+	+		+
28	CH ₂ N	+	++		++
30	CH ₄ N	+	+		+
40	Ca	++			+
45	C ₂ H ₅ O	++		++	+
46	C ₂ H ₆ O	+		+	+
52	C ₃ H ₂ N		+		+
55	Fe	+			+
58	Ni		+		
78	C ₂ H ₆ O ₃		+		
90	Zr	++	+		+
118	C ₅ H ₁₂ NO ₂	+		+	+
135	C ₉ H ₁₁ O	++		++	+
161	C ₁₁ H ₁₃ O	++		+++	+

“+” represents presence of listed fragment. “++” and “+++” are used to indicate relative amounts of listed fragments within row and cannot be used to compare rows one to another.

Nanoparticle Impurities – ToF SIMS

Negative Spectra Impurities

mass	ID	Ref Micron	NP1 20 nm	NP2 1-2 nm	NP3 100 nm
19	F	+++	+	++	++
26	CN	+	++		+
31	P		+		
35	Cl	+++	+	+	++
47	PO	+	++		
51	CIO	+			
59	C ₂ H ₃ O ₂	+		++	
78	C ₃ H ₇ OF		+		
78.96	PO ₃		+		
78.92	⁷⁹ Br	+	++		
81	⁸¹ Br	+	++		
104	C ₃ H ₈ N ₂ O ₂		+		
127	I	+			
205	C ₁₃ H ₁₉ NO			+	

“+” represents presence of listed fragment. “++” and “+++” are used to indicate relative amounts of listed fragments within row and cannot be used to compare rows one to another.

SRC/Sematech Engineering Research Center for Environmentally Benign Semiconductor Manufacturing

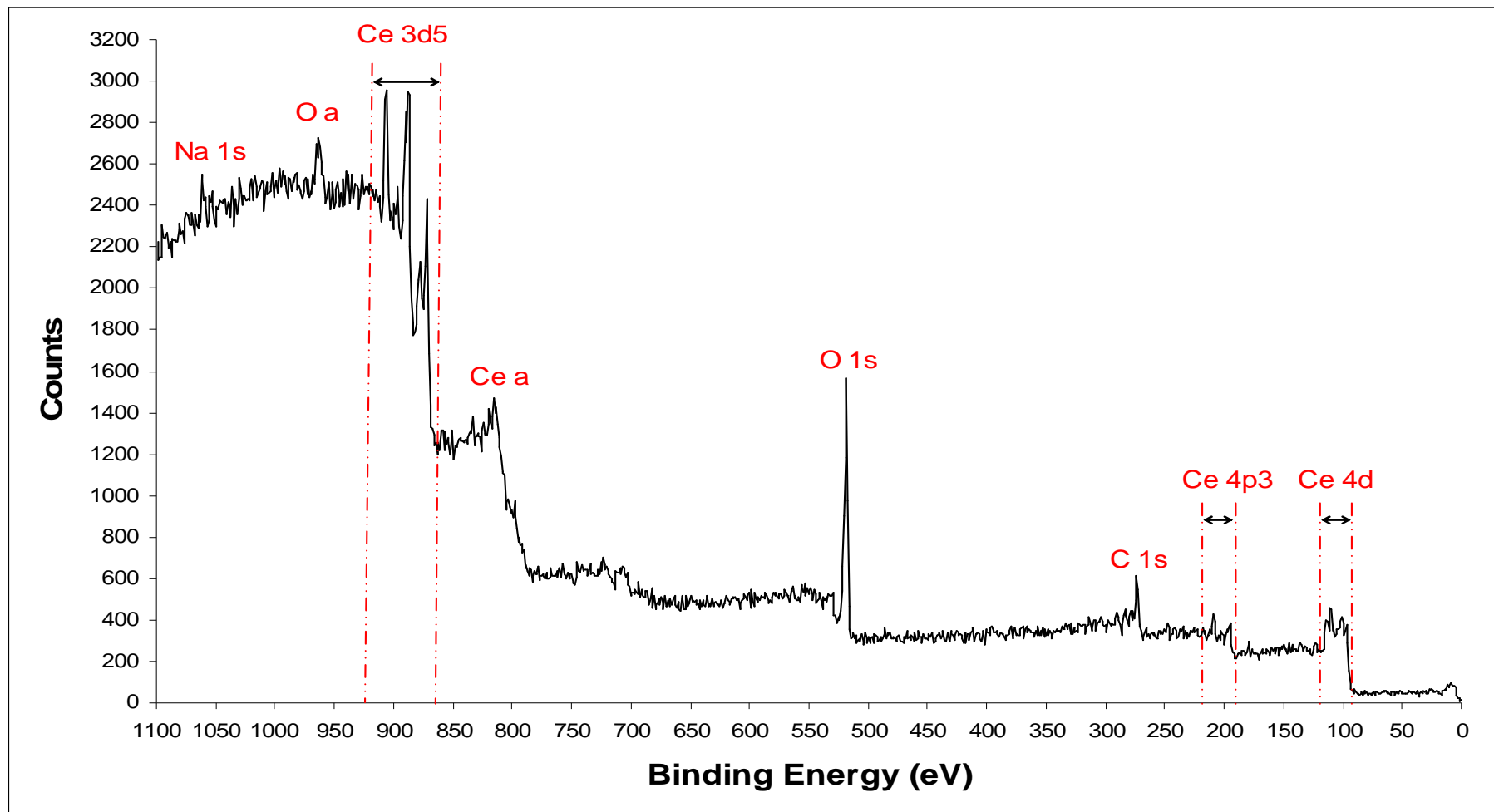
Surface Characterization

Summary/Preliminary Conclusions

SIMS Analysis

Impurity	Ref Micro	NP1 20 nm	NP2 1-2 nm
Light Organics (<100 MW)	+	+	+
Heavy Organics (>100 MW)			+
Silicon	+		+
Chlorine	+	+	
Bromine		+	
Rare Earth Metals	+	+	+

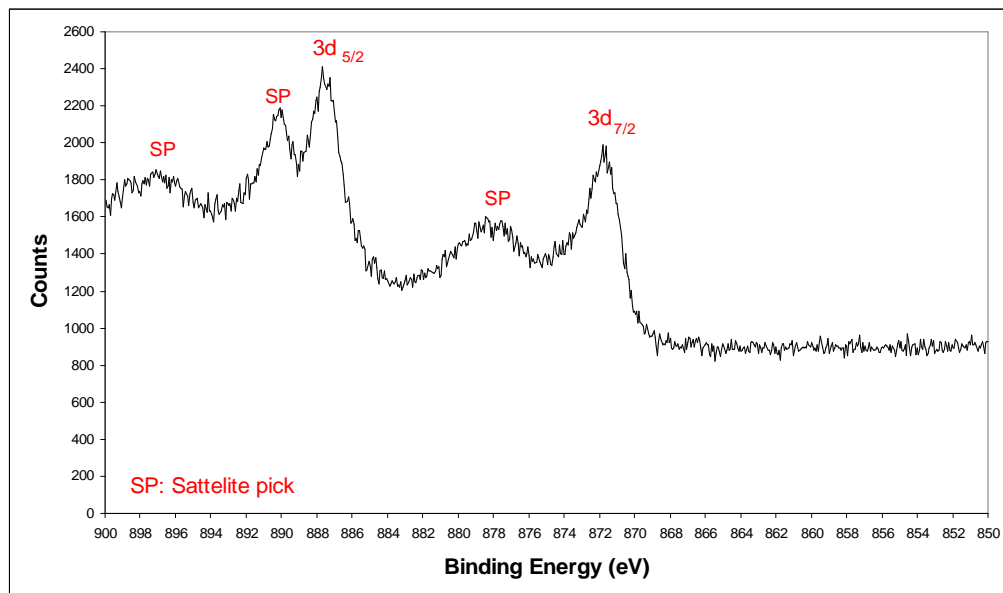
Catechol Treated CeO₂ XPS Spectra



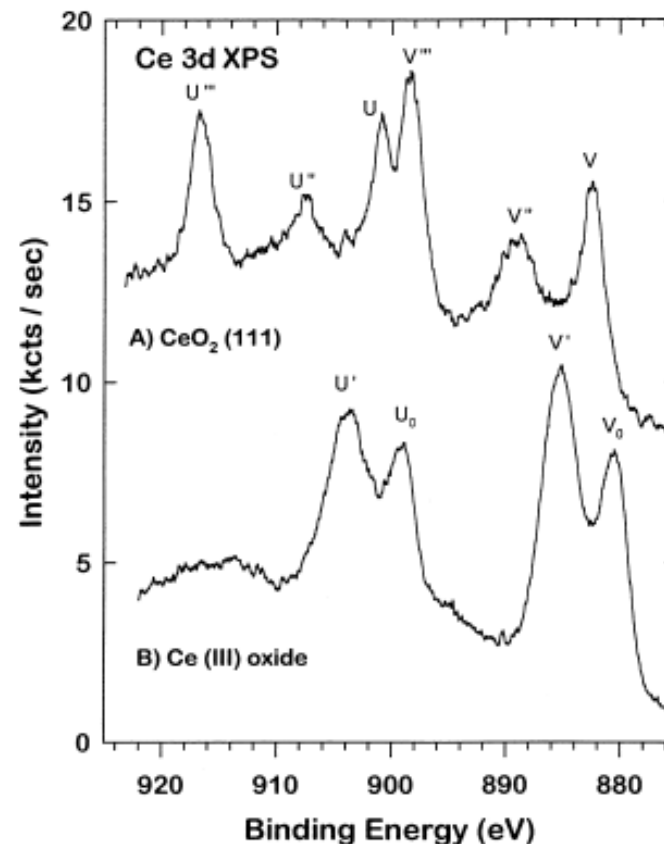
Sodium, carbon, cerium and oxygen were observed in the spectrum

SRC/Sematech Engineering Research Center for Environmentally Benign Semiconductor Manufacturing

CeO₂ Core Level XPS Spectra Comparison



High resolution XPS spectra of catechol treated CeO₂



Ce 3d core level photoemission spectra from (A) CeO₂ (111), (B) Ce (III) oxide*

* D.R. Mullins, S.H. Overbury, D. R. Huntley. Surface Science 409 (1998) 307-319.

Surface Chemistry Results and Future Plans

- **Our central hypothesis about the presence of surface contaminant species and high surface adsorptiveness of these nanoparticles is supported by our data.**
- **Comparison between Ce3d photoemission spectra of catechol treated CeO₂ and literature suggests that sample is in Ce⁴⁺ state.**
- **It has been shown in the literature that X-ray emission might have an effect on the oxidative state of the sample.**
- **In order to find the oxidative state of a pristine sample, the effect of x-ray on CeO₂ nanoparticles should be investigated.**

Toxicity Assessment and Prediction

Objectives

- **Establish role for reactive oxygen species (ROS) and oxidative stress as a potential marker for NP toxicity assessment**
- **Develop predictable models of toxicity based on physico-chemical properties elucidated by advanced surface analysis techniques**
- **Validate toxicity assessments and predictions with organ skin cultures (and advanced lung cultures)**

Materials

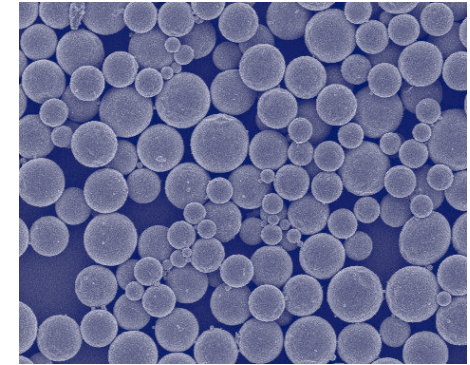
- Nanoparticles

Hafnium Oxide (HfO_2), immersion lithography

Silica Oxide (SiO_2), CMP

Ceria Oxide (CeO_2), CMP

Others (Al_2O_3 , carbon and germanium- nanotubes, quantum dots *etc*)



- Biological targets

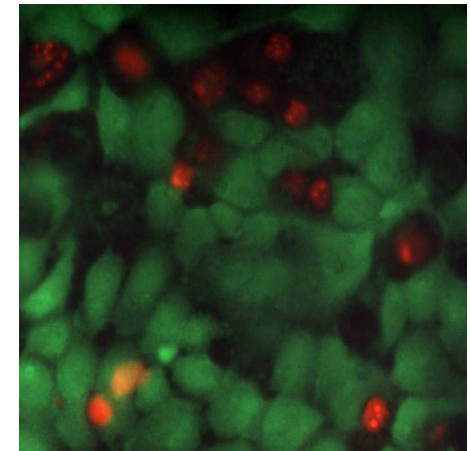
Human skin cell line (HaCat)

Human lung epithelial cell line (16HBE14o-)

Human foreskin rafted organ culture (ROC)

Bacterium (*Vibrio fischeri*) Microtox test

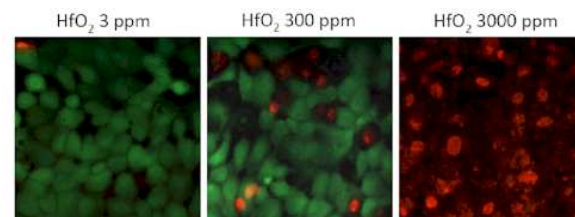
Others (methanogens, bacterial cultures, yeast *etc*)



Methods

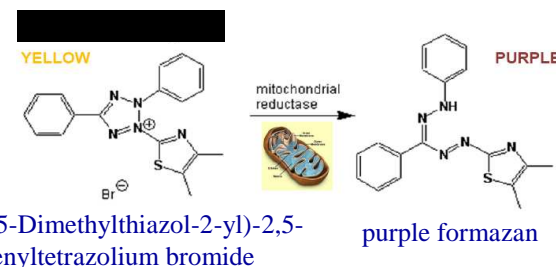
- Main Toxicity Tests Utilized

Live/Dead Assay with HaCat Skin Cell Line (HaCat)



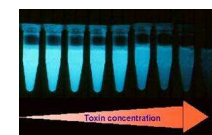
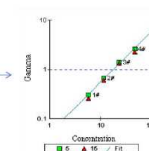
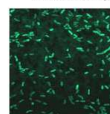
Live: calcein AM) Dead: ethidium homodimer-1

Mitochondrial Toxicity test (MTT) (ureter cells)



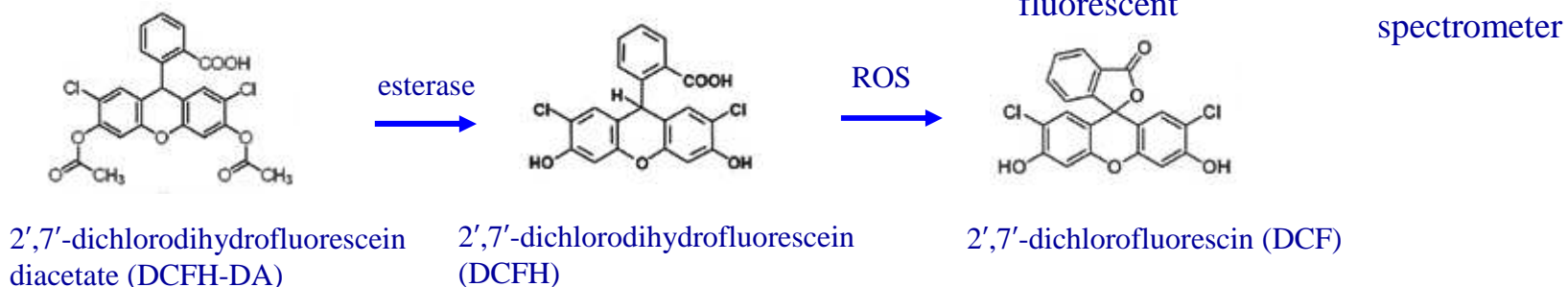
Microtox (*Vibrio fischeri*)

Methanogenic Activity



- Chemical: Reactive Oxygen Species (ROS) Production

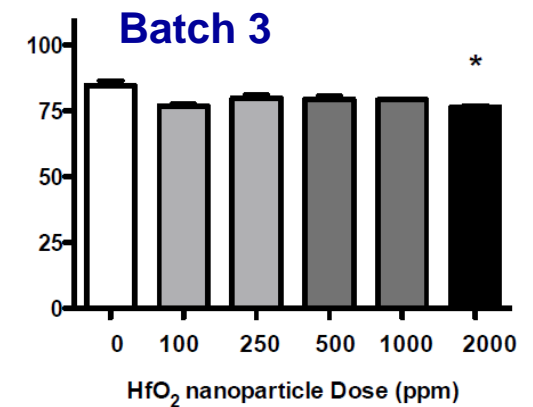
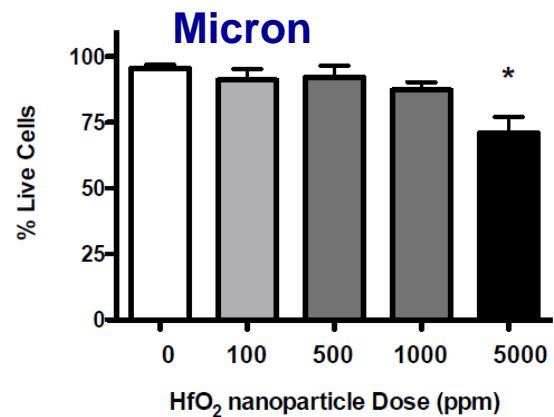
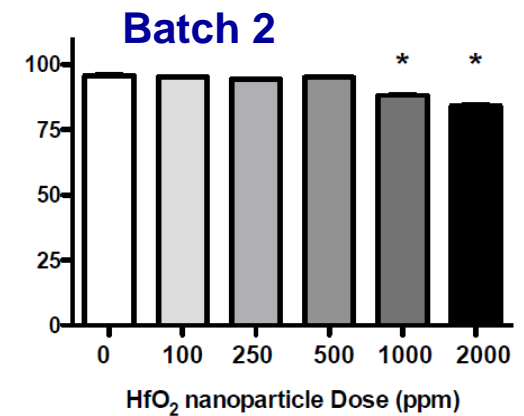
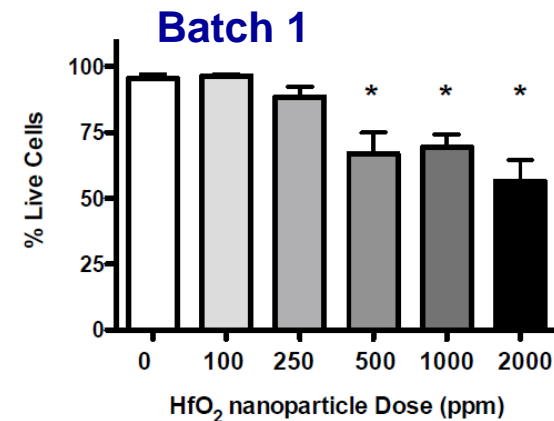
Detection of fluorescent ROS-sensitive dye



Results on HfO₂

Four distinct batches of hafnium oxide tested. Example Live/Dead test (HaCat skin cells)

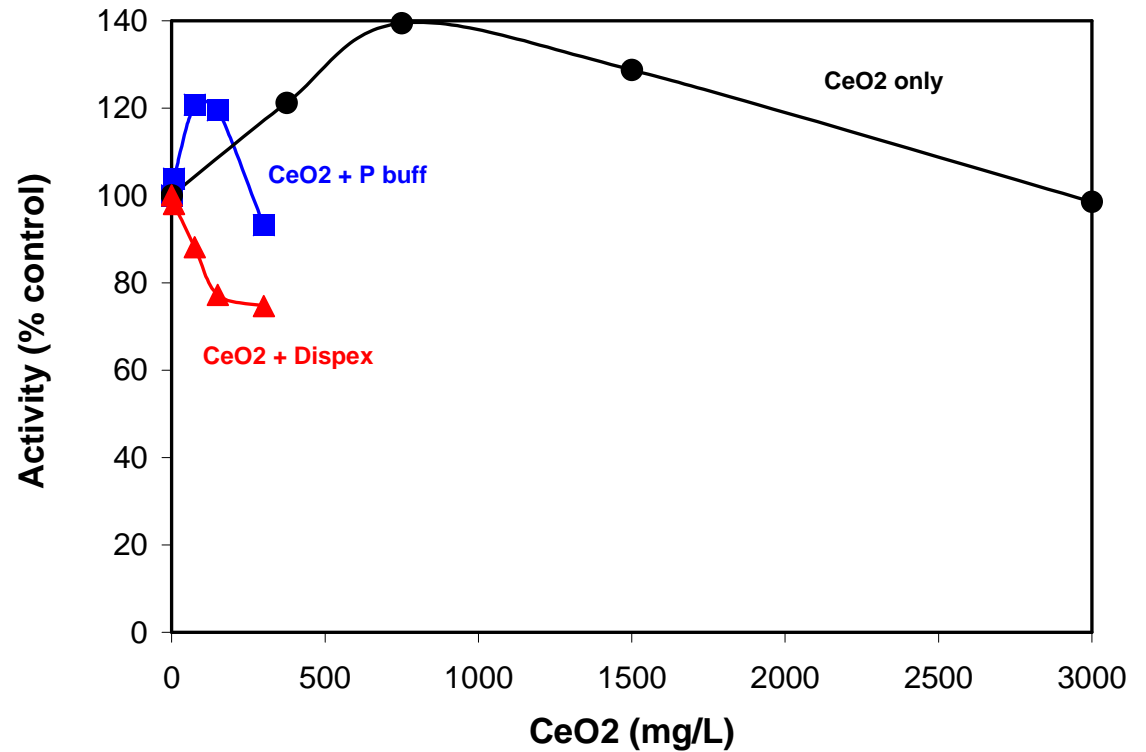
Batch	Measured ----- avg size (nm) -----	Manufact. Reported
Batch 1	360	20
Batch 2	224	2
Batch 3	169	100
Micron	6000	< 44,000



Results on CeO₂

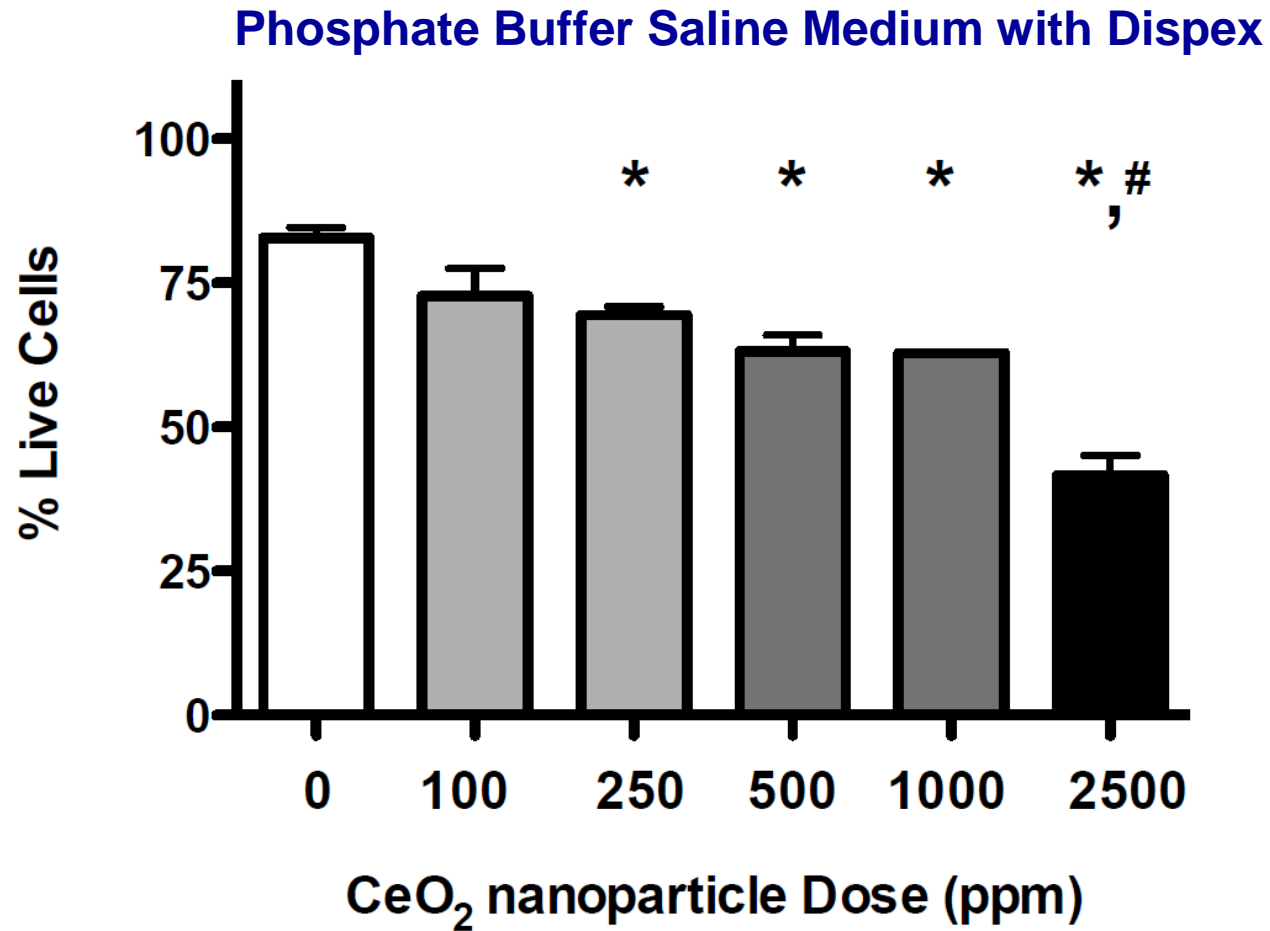
Cerium oxide (MTI, "20 nm"). Example Microtox Test

Prep.	Measured avg size (nm)
Water	1741
+ Dispex	183



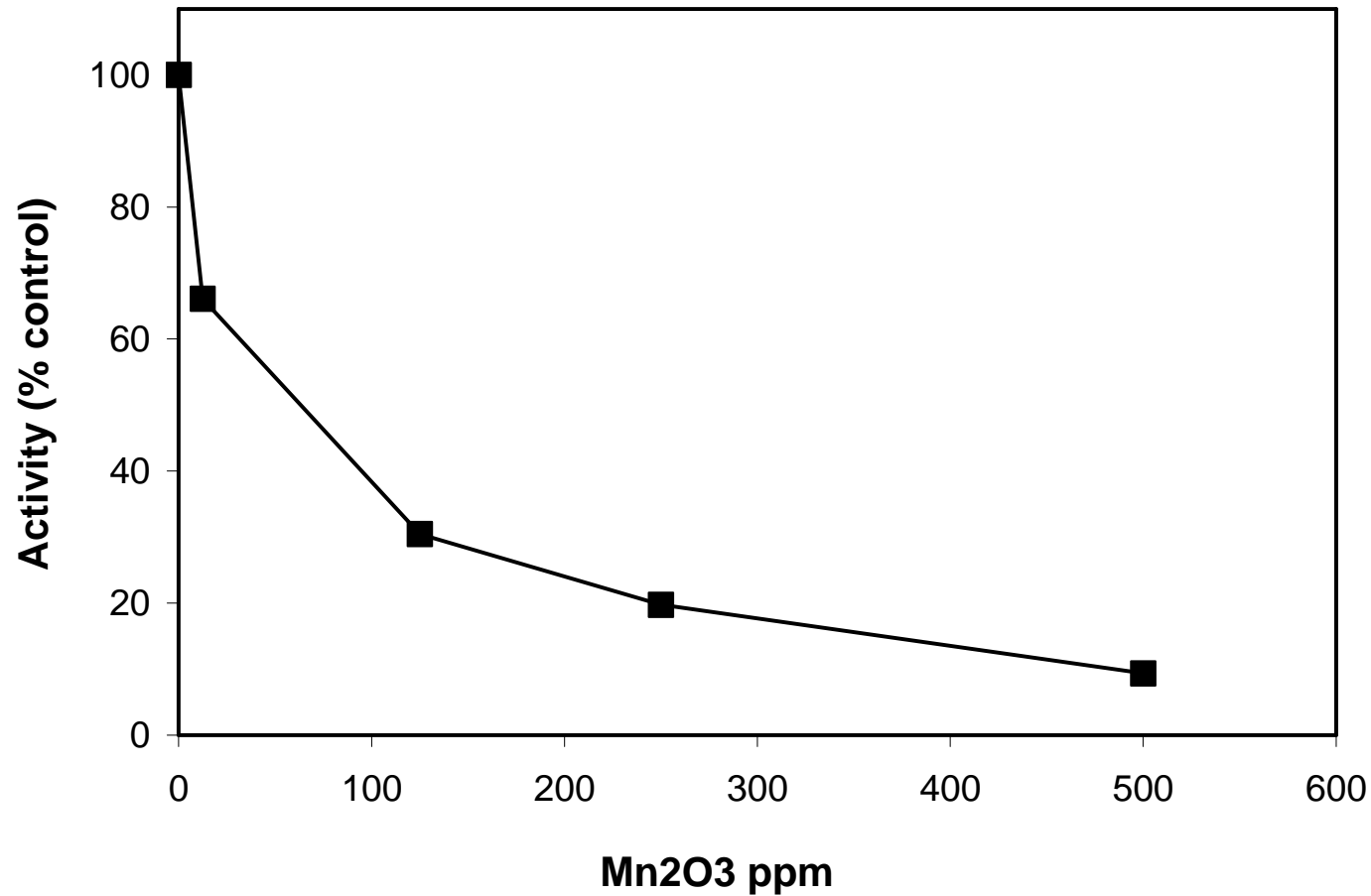
Results on CeO₂

Cerium oxide (MTI, “20 nm”). Example Live/Dead with Dispex

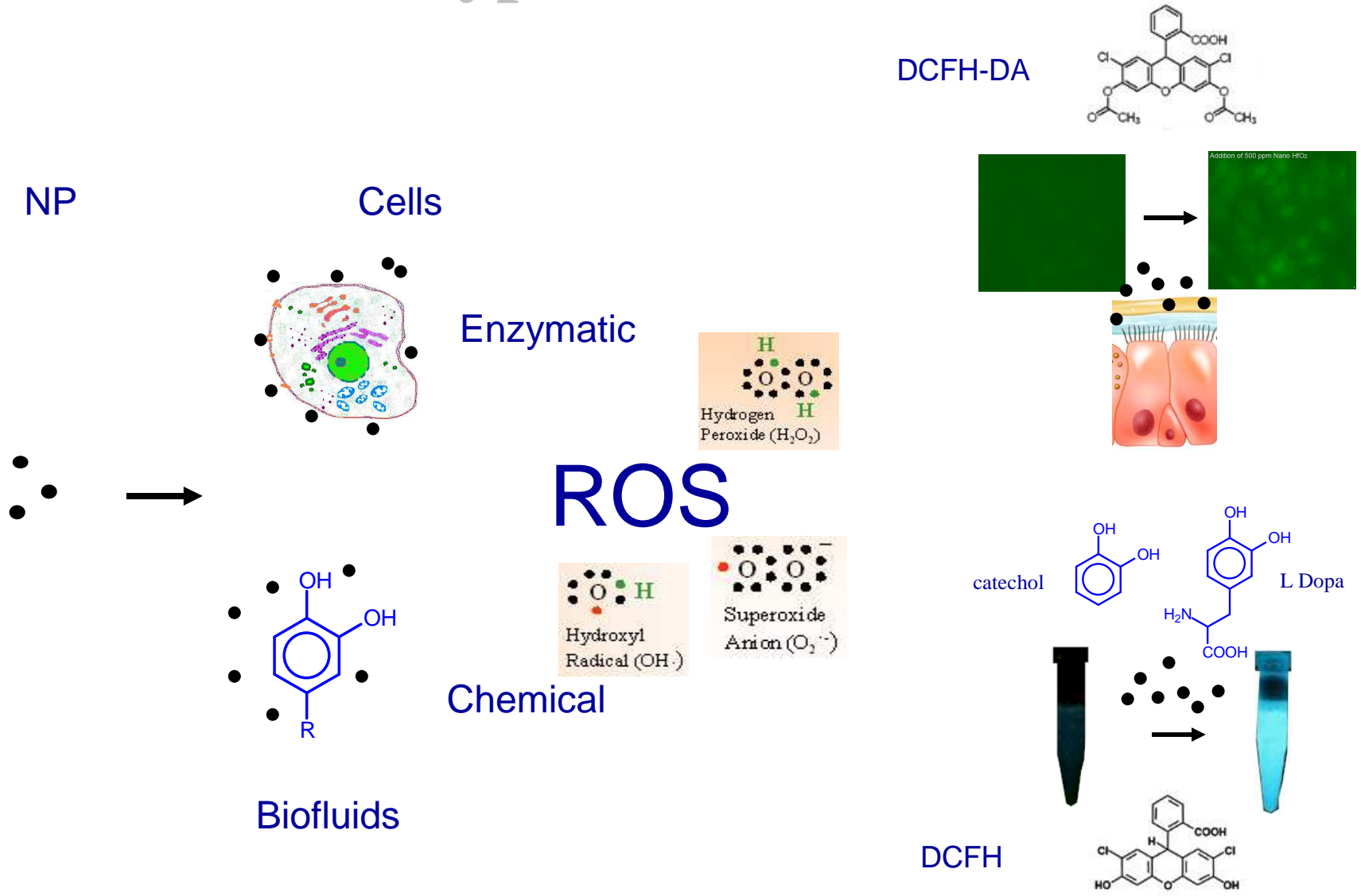


Results on Mn₂O₃

Manganese Oxide (SSNano, “40-60 nm”). Example Microtox with Dispex

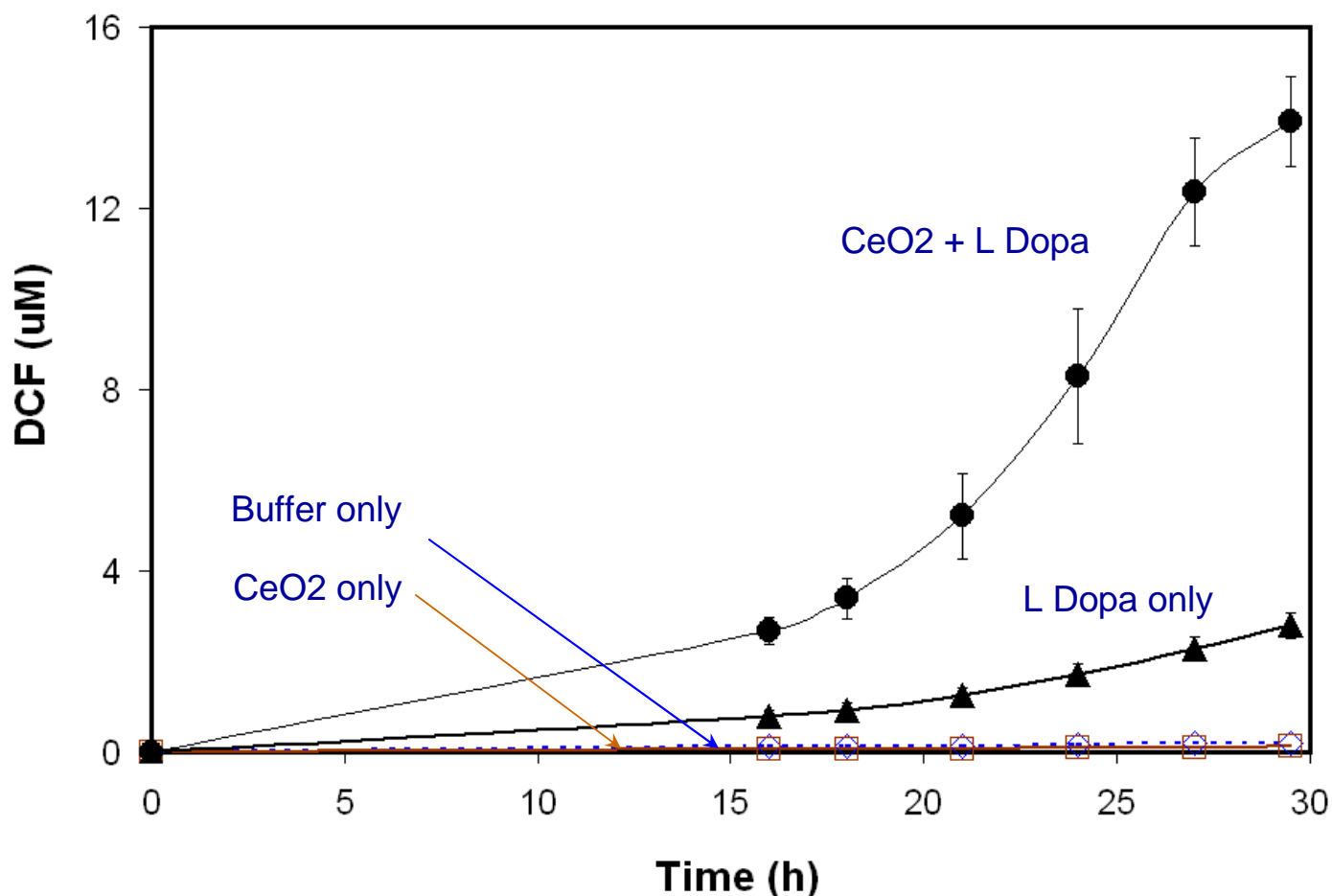


Hypothesis ROS



Chemical Production ROS

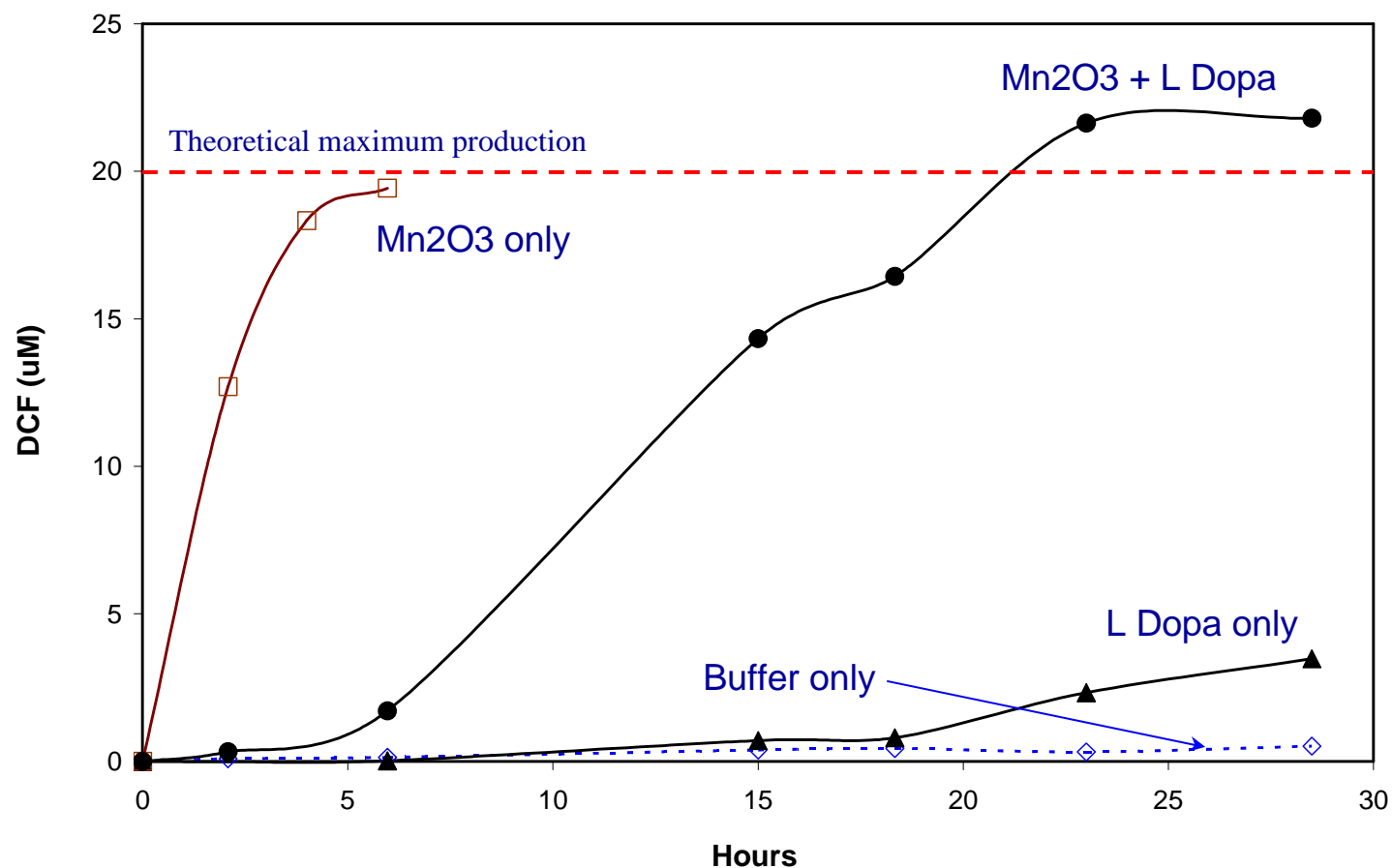
CeO₂ (MTI, “20 nm”)



Results indicate that the oxidation of L Dopa by CeO₂ NP produces ROS. Direct reaction of CeO₂ with dissolved oxygen and water does not produce ROS

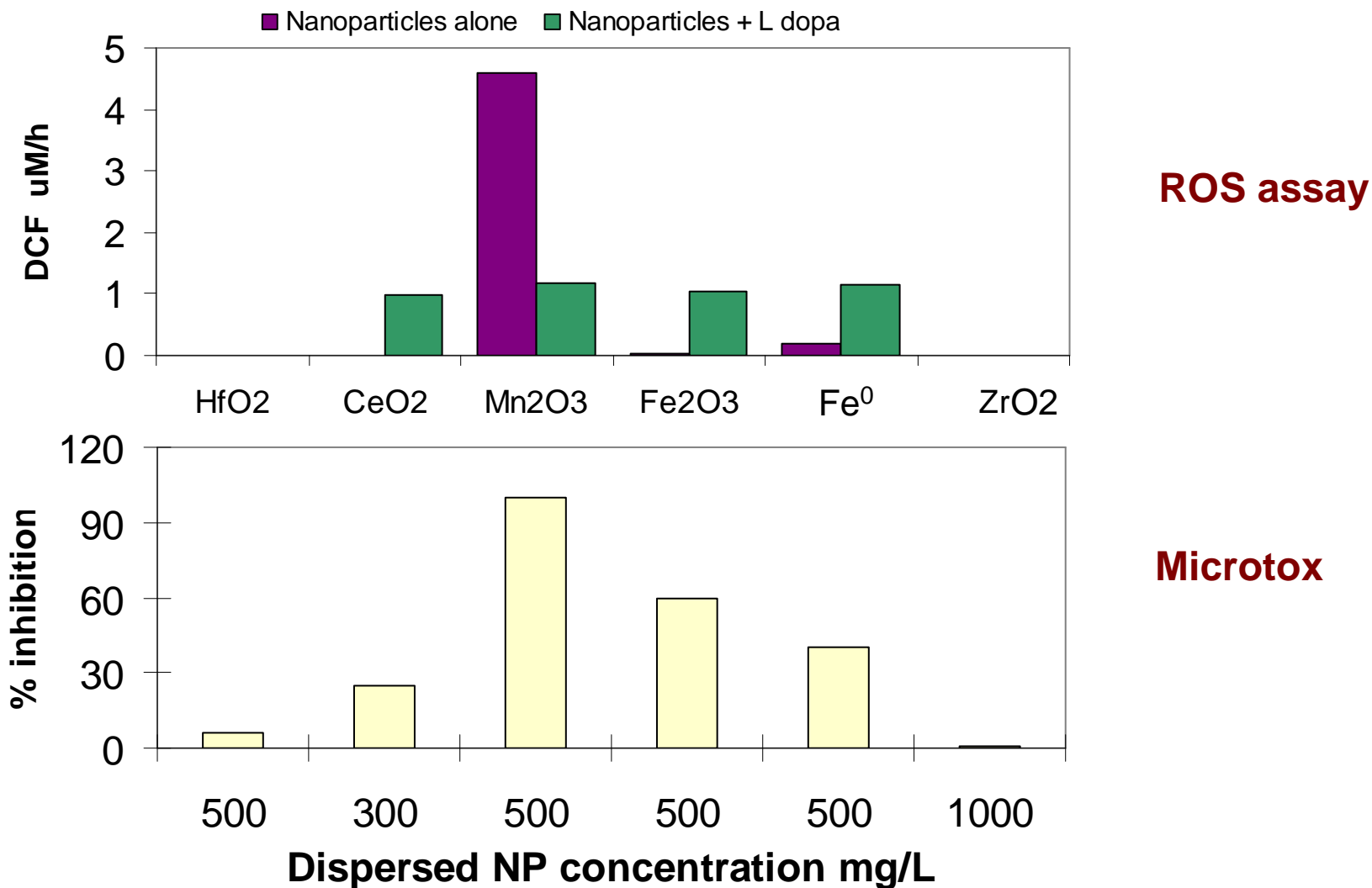
Chemical Production ROS

Mn₂O₃ SSNano “40-60 nm”).



Results indicate that the interaction of Mn₂O₃ NP with water and dissolved oxygen causes the formation of ROS. L Dopa inhibits the formation of ROS by Mn₂O₃

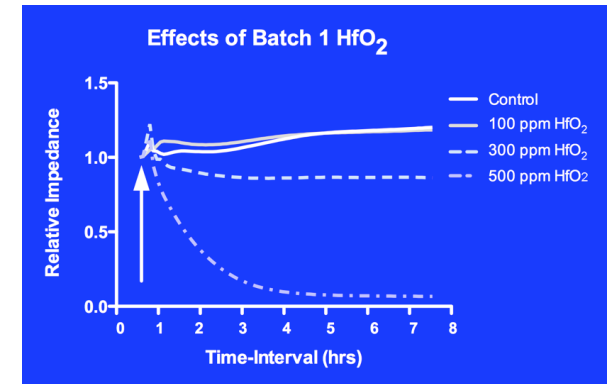
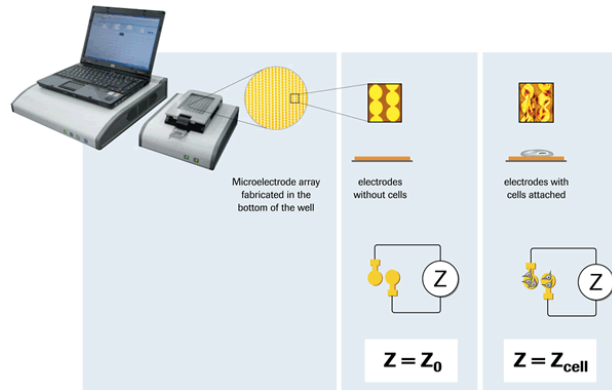
Correspondence ROS Versus Inhibition



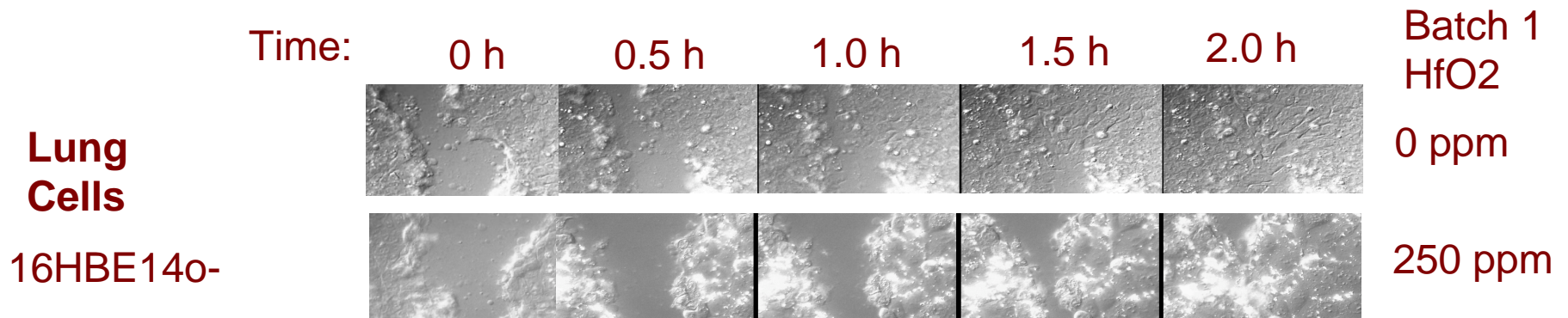
Development New Techniques

New dye-free techniques that are less prone to interferences

- xCELLigence based on measuring impedance



- Wound healing assay, based on time to close scrape wound

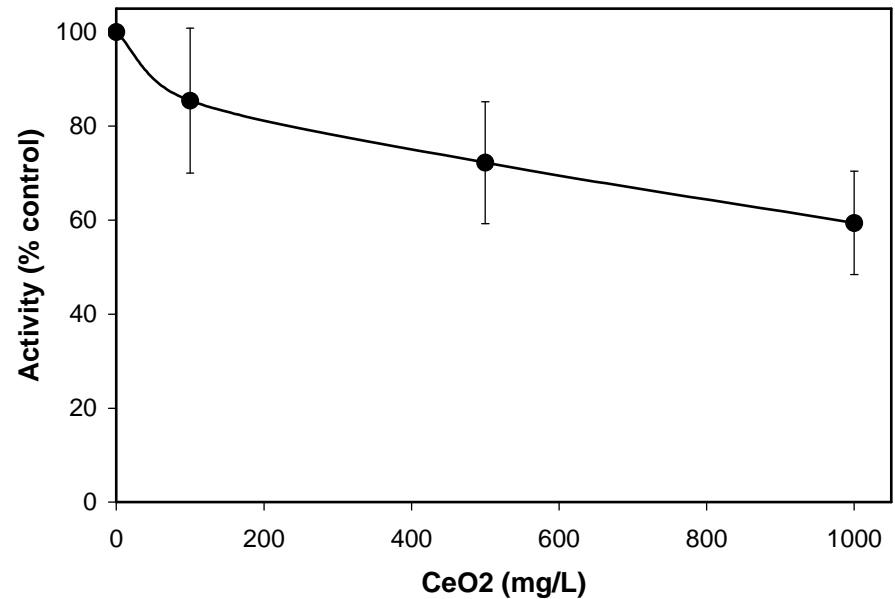
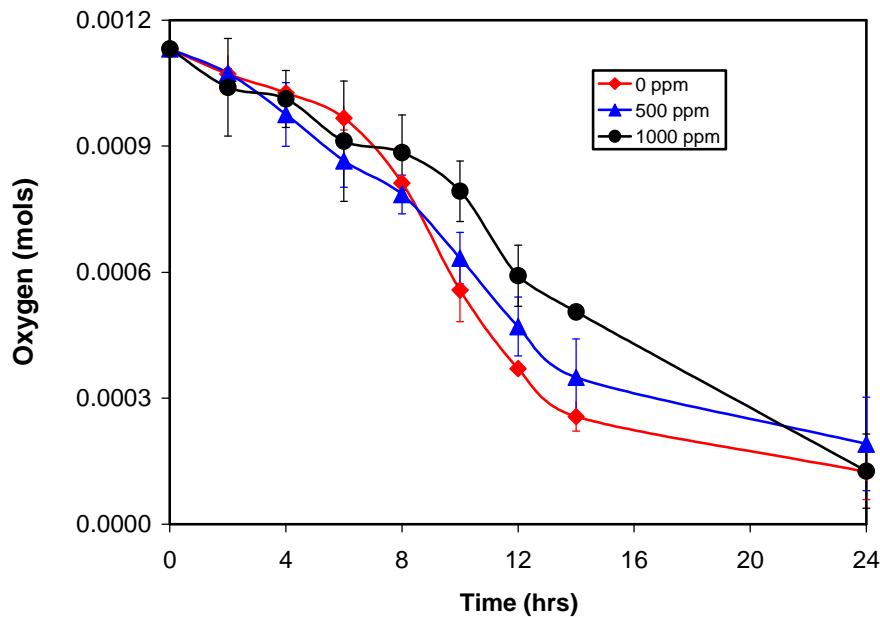


Development New Techniques

New dye-free techniques that are less prone to interferences (continued)

- O₂ uptake assay for yeast and bacterial cells

Inhibition of Yeast, *Saccharomyces cerevisiae*, by CeO₂



Preliminary Conclusions

- HfO₂, ZrO₂ and CeO₂ NPs mild to no toxicity.

Higher Toxicity of Batch 1 HfO₂ may be due to chemical contamination (from synthesis)

	L/D	Microtox	Methanog
	50% death	50% inhib	50% inhib
	----- mg/L -----		
HfO₂ *	>2000	3000	>2500
CeO₂	2500**	>300**	>1000
ZrO₂		>1000**	

*batch3 **with dispersant

- NPs producing ROS directly in water most toxic. Chemical ROS production indicative of NP toxicity

Mn₂O₃ 50% IC microtox = 70 mg/L

Fe₂O₃ 50% IC microtox ≅ 500 mg/L

Fe⁰ 50% IC microtox ≅ 500 mg/L

Industrial Interactions and Technology Transfer

- **ISMI-Sematech (Steve Trammell, Laurie Beu)**
- **AMD (Reed Content)**
- **IBM (Arthur T. Fong)**
- **Intel (Steve W. Brown, Paul Zimmerman, Mansour Moinpour)**

Future Plans

Next Year Plans

- Fractionation of CeO₂ for toxicity study size fractions
- Biochemical indicators of oxidative stress
- Complete development of new non-dye based techniques

Long-Term Plans

- Rapid screening protocols of for assessing NP toxicity
- Toxicity to organ models

Publications, Presentations

- **Brownbag presentation: Nanoparticle Interaction with Biological Wastewater Treatment Processes, Water Sustainability Program, Phoenix, Arizona Jan 20th, 2010 at Arizona Cooperative Extension**
- **Sierra-Alvarez, R. 2009. Toxicity characterization of HfO₂ nanoparticles. SRC/Sematech Engineering Research Center for Environmentally Benign Semiconductor Manufacturing Teleseminar Series. August 6.**
- **Boitano, S. 2009. Measuring cytotoxicity of nanoparticles in human cells. SRC/Sematech Engineering Research Center for Environmentally Benign Semiconductor Manufacturing Teleseminar Series. Sept. 17.**
- **Ratner, B. 2009. Static SIMS: A Powerful Tool to Investigate Nanoparticles and Biology. SRC/Sematech Engineering Research Center for Environmentally Benign Semiconductor Manufacturing Teleseminar Series. May 14.**

Development of Quantitative Structure-Activity Relationship for Prediction of Biological Effects of Nanoparticles Associated with Semiconductor Industries *(Task Number: 425.025)*

PIs:

- **Yongsheng Chen, Environmental Engineering, Georgia Institute of Technology (GIT)**

Graduate Students:

- **Wen Zhang: PhD student, Environmental Engineering, GIT**
- **Steven Klein: PhD student, Mechanical engineering, ASU**

Other Researchers:

- **Trevor J. Thornton, Electric Engineering, ASU**
- **Jonathan Posner, Mechanical Engineering, ASU**

Cost Share (other than core ERC funding):

- **\$25 k start-up fund from ASU**
- **\$152k funds from GIT for AFM and other lab instrument purchase**

Objectives

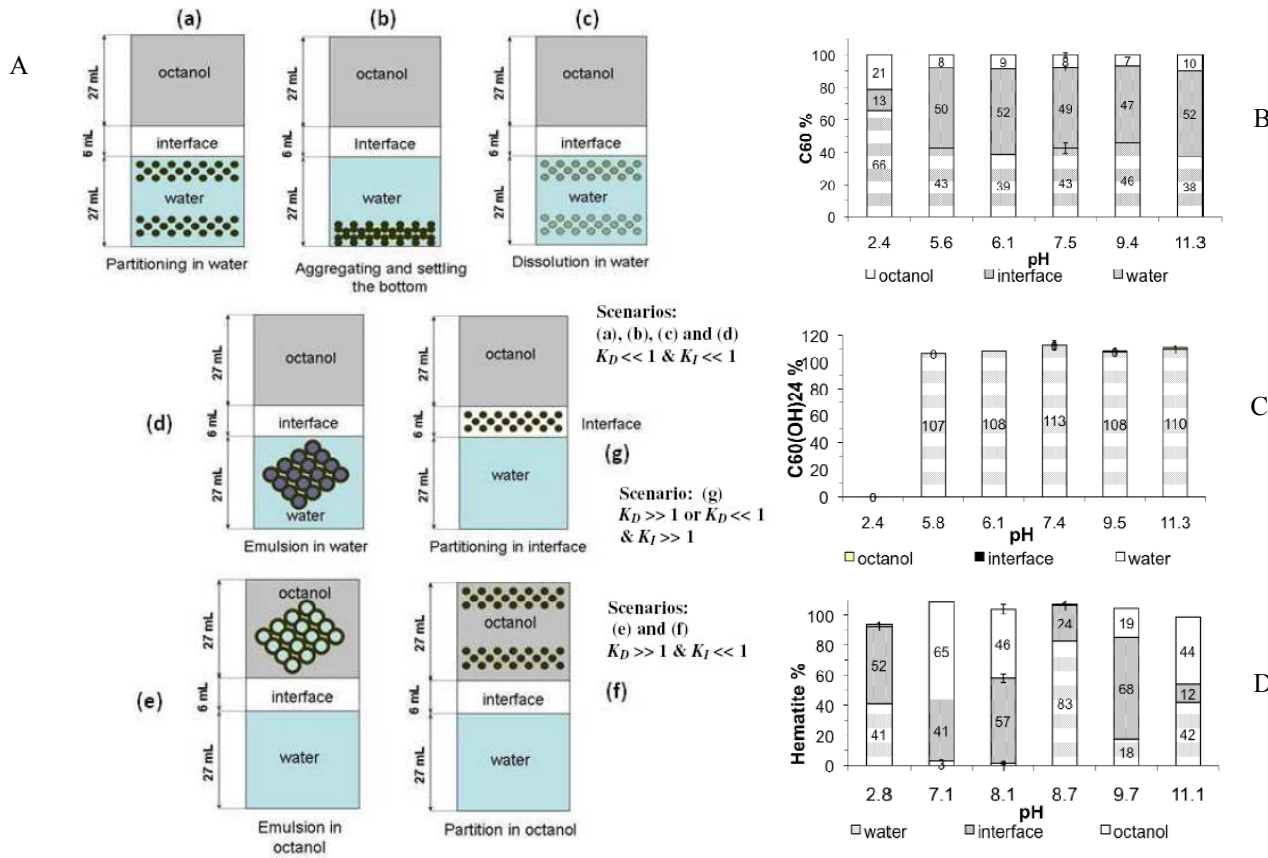
Develop a quantitative structure-activity relationships (QSARs) model for prediction of the biological effects of engineered nanoparticles (NPs) associated with semiconductor industries. To pursue this goal, our approach mainly includes:

- Development of new surrogate descriptors (relative to those for conventional contaminants) for NPs and Methodology development of experimental measurement.**
- Correlation of the descriptors with their environmental behaviors and impact.**

ESH Metrics and Impact

1. *Our work aims at new descriptor development for cytotoxicity of NPs to human health and provides a comprehensive understanding and clear definition of ESH-problematic manufactured nanomaterials.*
2. *Based on the quantitative structure-activity relationship (QSAR) model we plan to establish, problematic nanomaterials from industrial manufacturers could be identified and effectively reduced, and more environmental benign nanomaterials can be designed.*

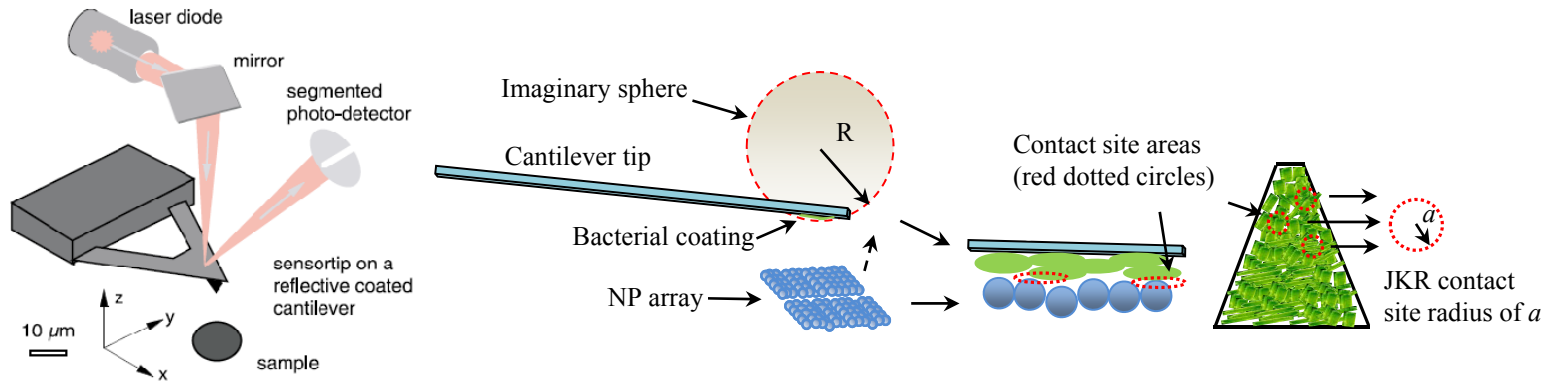
Bias of traditional descriptors for NPs: study of octanol-water partitioning coefficients (K_{ow})



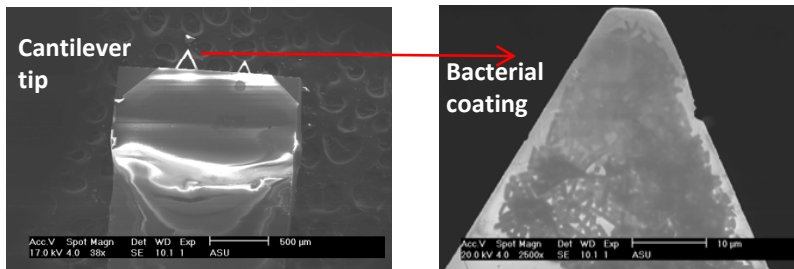
A: Boundary partitioning scenarios (a~g) of nanoparticles in the octanol and aqueous phases and the interface. B: Partitioning of n-C₆₀, C: n-C₆₀(OH)₂₄ D: hematite nanoparticles in the interface, octanol, and aqueous phases at different pH values in the presence of 1 mM NaHCO₃ buffer.

Method and materials: New descriptor development

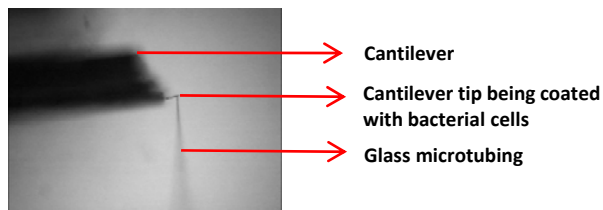
1. Adhesion force measurement with AFM



Demonstrations of adhesion force measurement with AFM and determination of contact area with JKR model. Cantilever probe coated with bacterial cells is approaching to NP array and the contact surface of the probe is assumed to be a part of the surface on the imaginary sphere (R). Multiple contact sites (indicated by the red circles) between bacteria and NPs add up to a total contact site area of πa^2 .

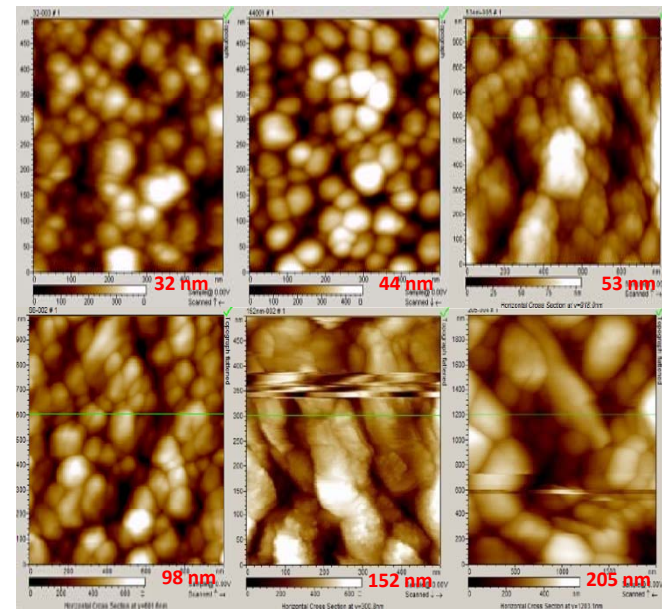


Coating process with micromanipulator



Images of NP array achieved by tapping mode AFM:

NP array composed of NPs (different sizes were determined by Malvern Zetasizer)

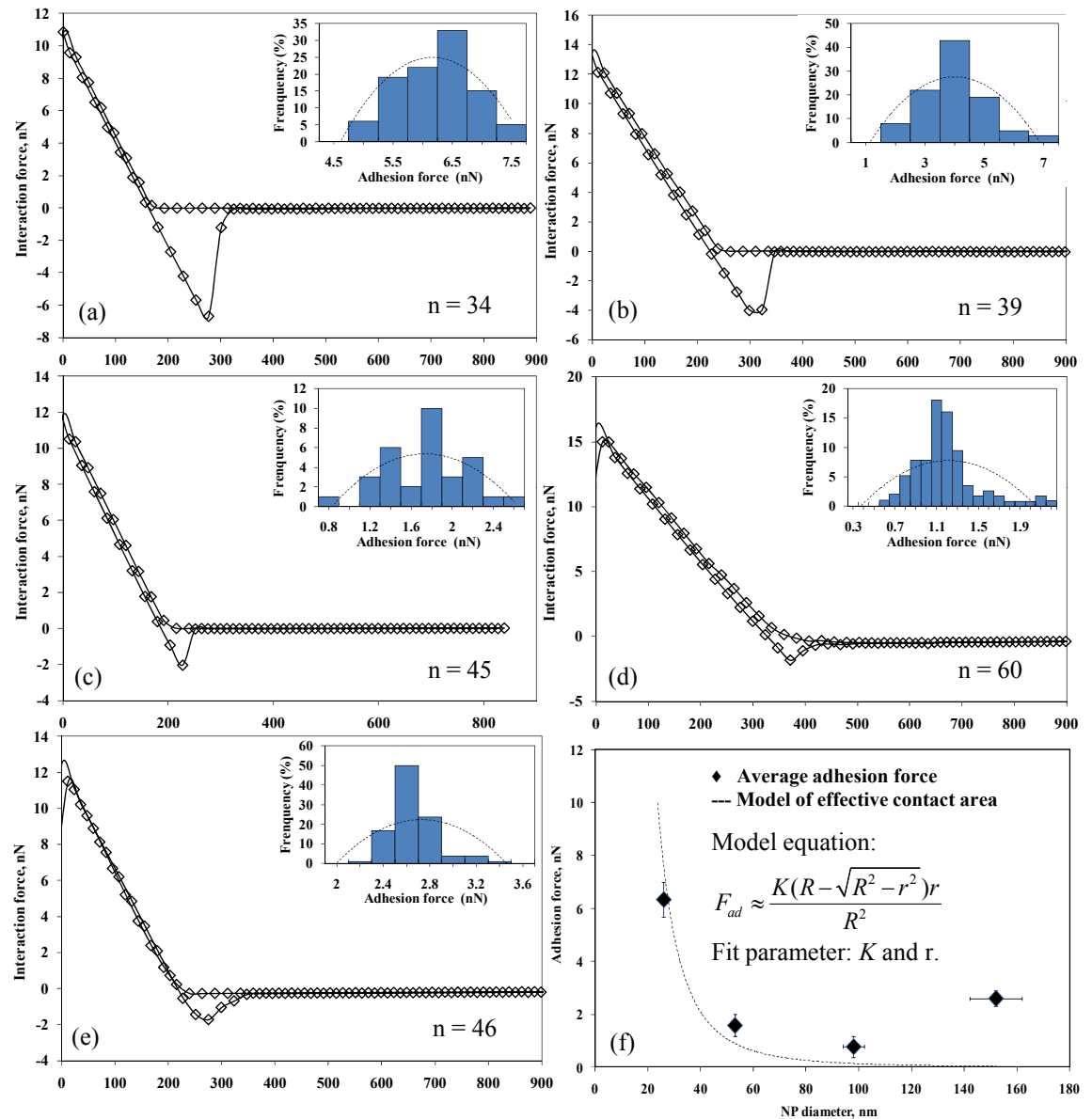


Results and discussion:

1.1 Size effect on Adhesion force between *E. coli* cells and hematite NPs

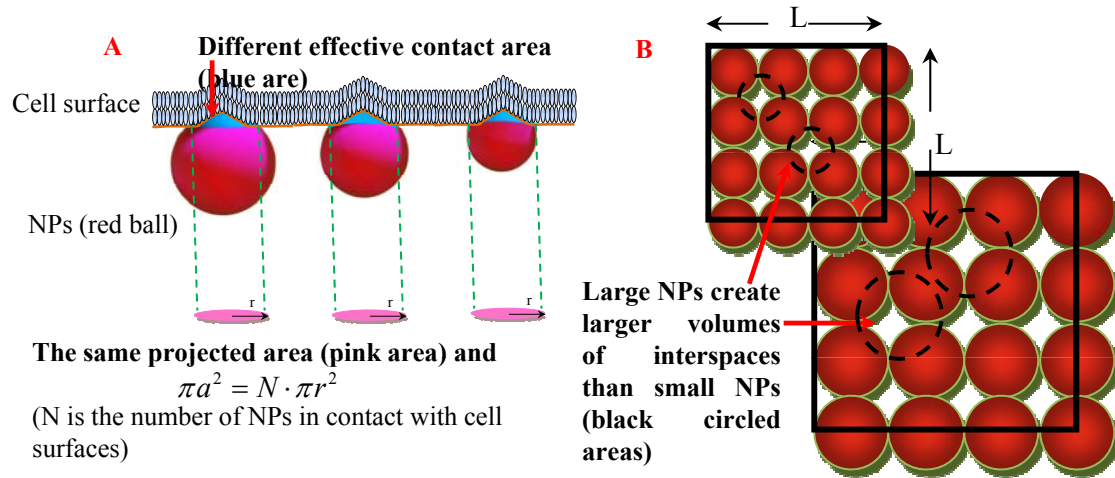
Representative interaction force-distance curves for different sizes of NP array probed by *E. coli* cells. (a) 26 nm. (b) 44 nm. (c) 53 nm. (d) 98 nm. (e) 152 nm. (f) Average adhesion force for different sizes of NPs (horizontal error bars indicate standard deviation of particle diameter and vertical error bars indicate standard deviation of adhesion force). n is the number of force measurements for each sample.

Significance: Adhesion forces between *E. coli* cells and hematite NPs decreased as particle size increased as Figure 3 showed and our model of the effective contact area fitted the trend.



Results and discussion:

1.2 Modeling Size effect on Adhesion force and validation

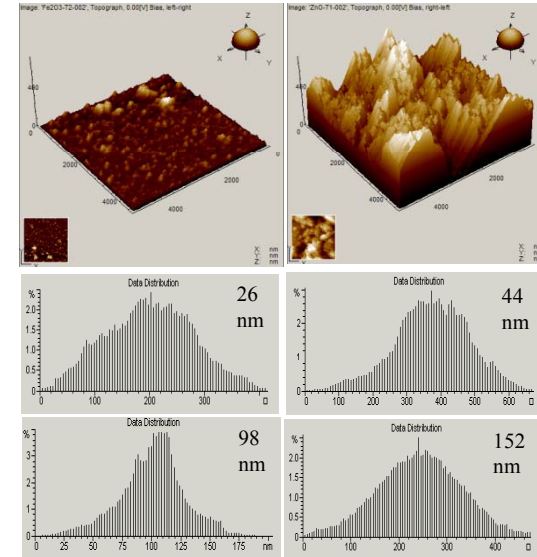


Schematics of modeling the size effect of NPs on adhesion force.

Brief introduction to our proposed model of effective contact area used for explaining the size effect on adhesion force:

$$\left. \begin{aligned}
 F_{ad} &\propto \int_0^{R-\sqrt{R^2-r^2}} 2\pi\sqrt{R^2 - (\sqrt{R^2-r^2} + x)^2} dx \\
 V &= N \times [(2R)^3 - (4\pi R^3/3)]/2 = L \times (4-2\pi/3)R^2 \\
 F_{ad} &\propto 1/V
 \end{aligned} \right\} F_{ad} = K \int_0^{R-\sqrt{R^2-r^2}} \frac{\sqrt{R^2 - (\sqrt{R^2-r^2} + x)^2}}{R^2} dx \approx \frac{K(R-\sqrt{R^2-r^2})r}{R^2} \Rightarrow F_{ad} \propto \frac{Kr}{R}$$

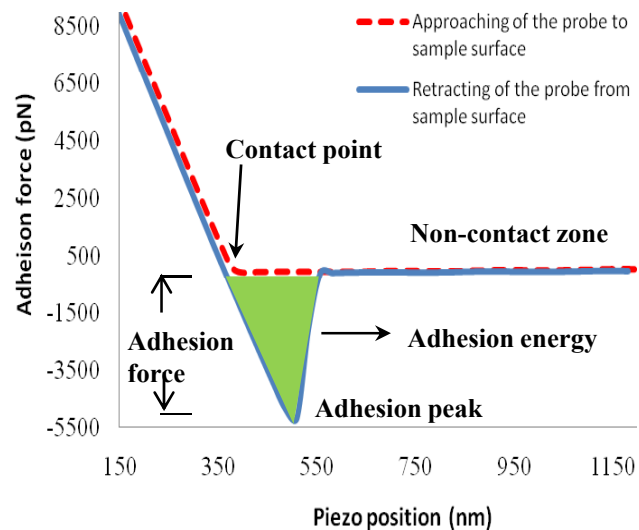
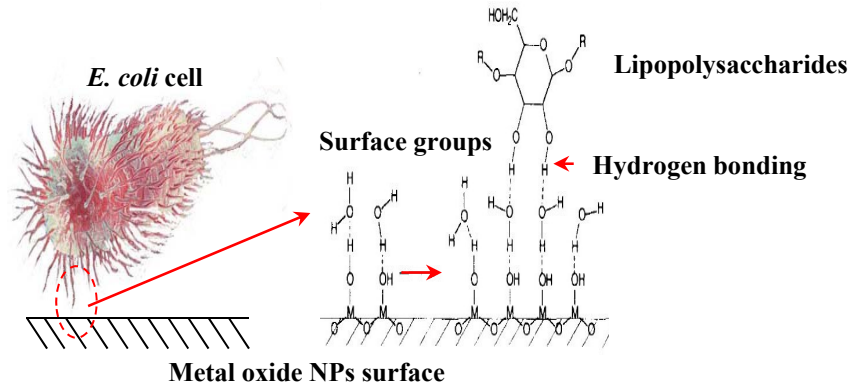
Validations were made between *E. coli* cells and Al₂O₃ NPs, and between Caco-2 cells (human intestinal cells) and hematite NPs. For detailed information, refer to our manuscript.



Surface topography and surface height distribution

Results and discussion:

1.3 Hydrogen bond estimation with force-distance curve and its support of our model of size effect



Adhesion energy and hydrogen bond calculation

Adhesion energy and hydrogen bond number

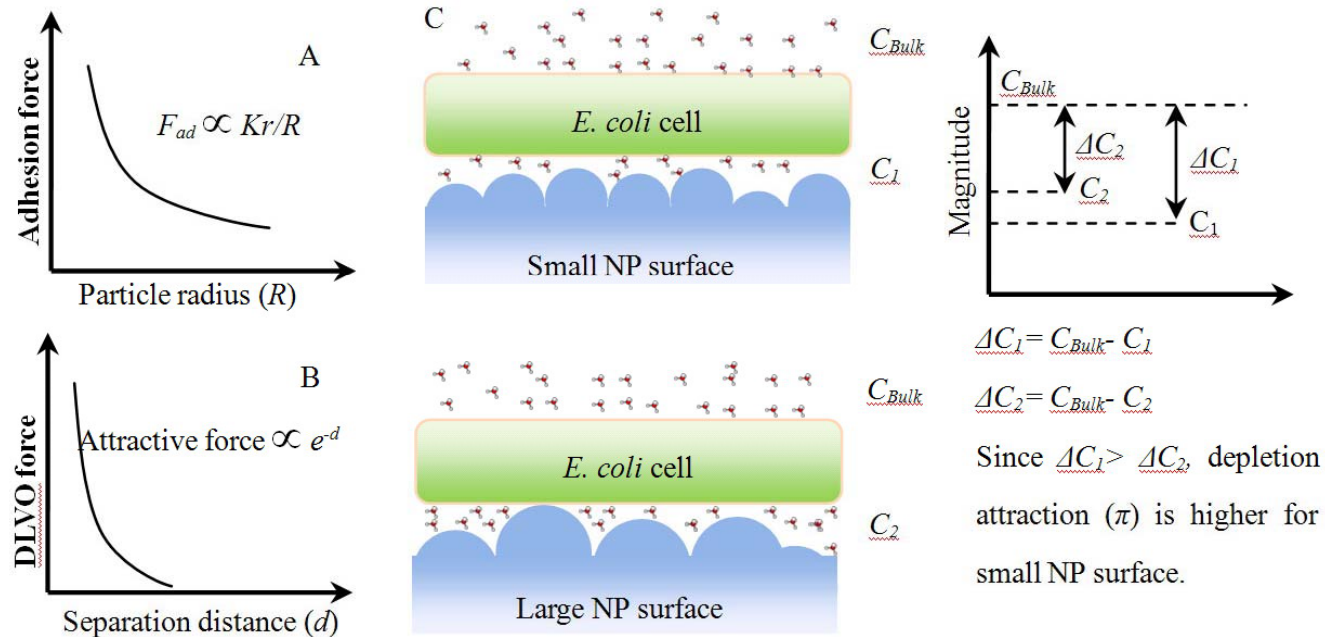
NP diameter (nm)	Adhesion energy (J)	Hydrogen bond number on contact site area
Hematite NPs	23	$(8.5 \pm 1.7) \times 10^4$
	42	$(7.7 \pm 2.2) \times 10^4$
	53	$(1.0 \pm 2.6) \times 10^4$
	98	$(3.7 \pm 2.0) \times 10^3$
	150	$(3.6 \pm 1.2) \times 10^3$
Al ₂ O ₃ NPs	25*	$(6.5 \pm 1.7) \times 10^4$
	30-40*	$(3.2 \pm 1.7) \times 10^4$
	40-80*	$(1.2 \pm 1.7) \times 10^4$
	100-120*	$(7.3 \pm 1.7) \times 10^3$

The surface of an *E. coli* cell (average cell surface area is $6 \times 10^{-12} \text{ m}^2$) contains about 3.5×10^6 LPS molecules that can form hydrogen bonds with a mineral oxide surface. The contact site area between hematite NP array and *E. coli* cells is about 6359 nm^2 ($=\pi \cdot 45^2$, estimated by JKR model). Thus, the average number of hydrogen bonds formed is **3709** ($=6359 \times 10^{-18} \text{ m}^2 \times 3.5 \times 10^6 / 6 \times 10^{-12} \text{ m}^2$).

Implications: NP arrays of small NPs may have a much higher contact area than large NPs.

Results and discussion:

1.4 Other mechanisms involved in adhesion that may explain the size effect

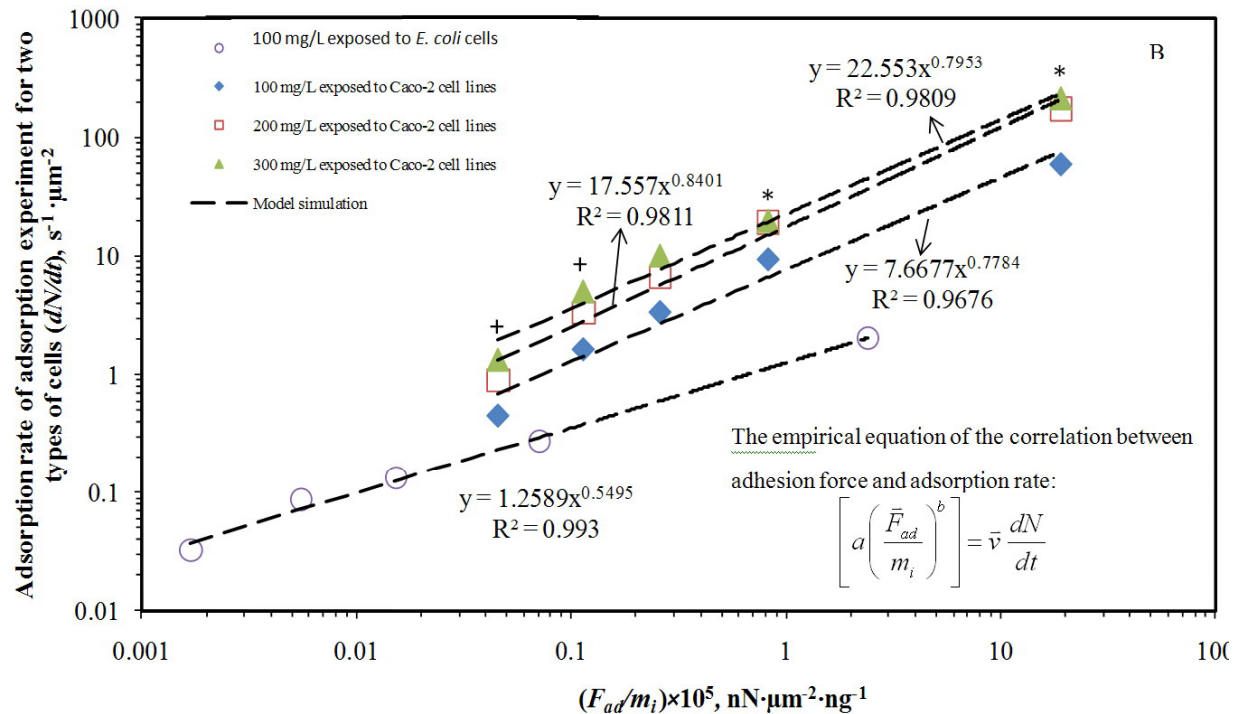


Representation of potential mechanism of size effect on adhesion force. A. Relationship between adhesion force (F_{ad}) and particle radius (R). B. Exponential decay of DLVO forces with distance. C. Depletion attraction (potentially different for cell surface interacting with different sizes of NPs).

Implication: a combined effect of three potential mechanisms were proposed to account for the size effect on adhesion force between NPs and cell surfaces, including the effective contact area, topographical effects on interfacial energy, and depletion attraction.

Results and discussion:

1.5 Correlation between adhesion force and adsorption rate of NPs toward cell surfaces

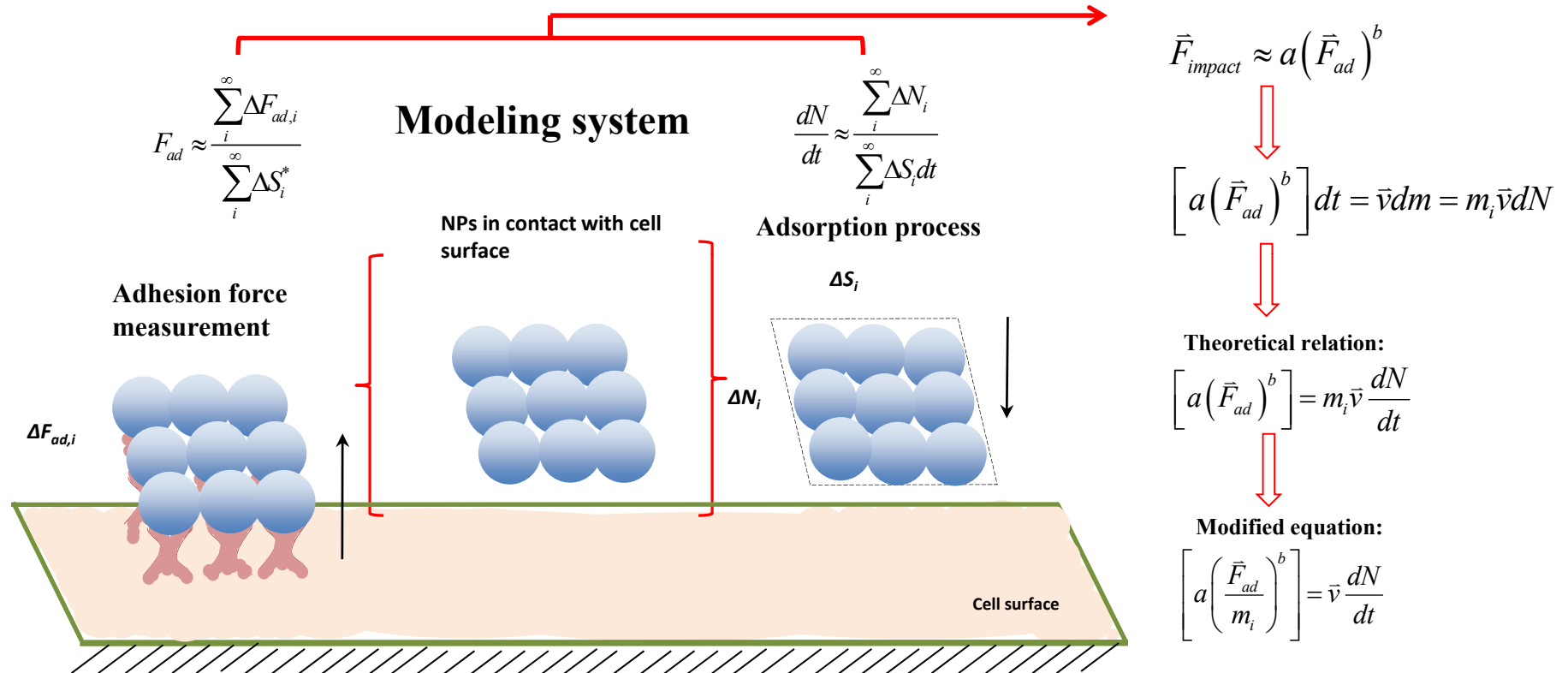


Comparison of the model simulation (dotted line) and experimental data. Symbols (*) and (+) indicate a significant difference ($p < 0.05$) between the groups of three points marked by (+) and those groups marked by (*).

Significance: an important interconnection between adhesion force and adsorption rate of NPs onto the cell surface was established and the theoretical relationship can be derived mathematically from the conceptual model in the next slide.

Results and discussion:

1.5 Correlation between adhesion force and adsorption rate of NPs toward cell surfaces



Conceptual model of the relation between adhesion force and adsorption rate (dN/dt).

This model was derived based on the impulse-momentum theorem and the relationship between the impact force and the resulted adhesion force. The above theoretical relationship between adhesion force and adsorption rate has the following parameters: m_i is the mass of a single NP; \bar{v} is the approach speed of the cantilever tip toward the cells; a and b is the fit parameters.

Method and materials:

2. Cytotoxicity of hematite NPs on Caco-2 cells: size effect

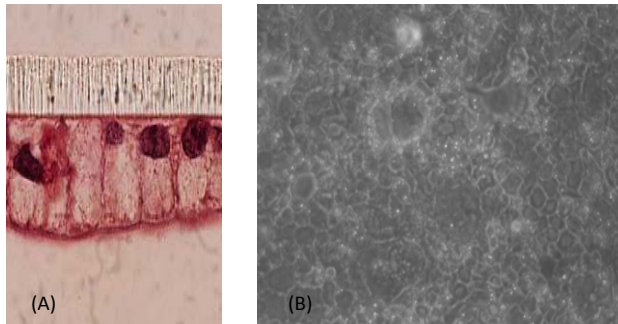


Figure 9 Microscopic images and structures of Caco-2 cells. (a): Side view of the cell lines; (b): phase contrast image for Caco-2 cell lines. The bottom drawing indicates the surface structure (microvilli) of the cell line.

Cytotoxicity was shown by junctional disruption of the cell lines and quantified with transepithelial electrical resistance (TEER). Cell penetration of NPs was visualized by confocal imaging.

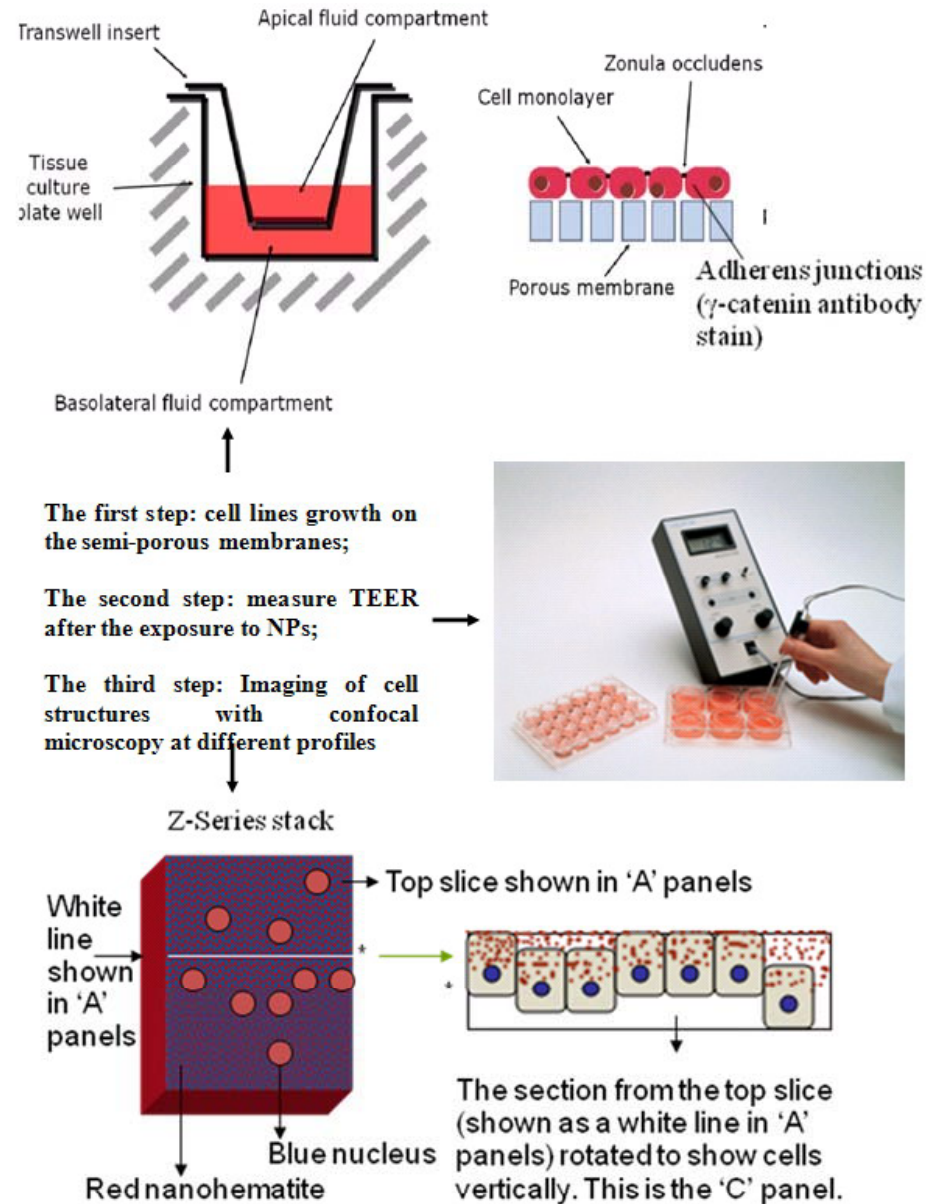


Figure 10 Schematics of cytotoxicity experiments with Caco-2 cells through TEER test and confocal microscopy

Results and discussion: TEER changes and junctional disruption induced by the exposure to NPs

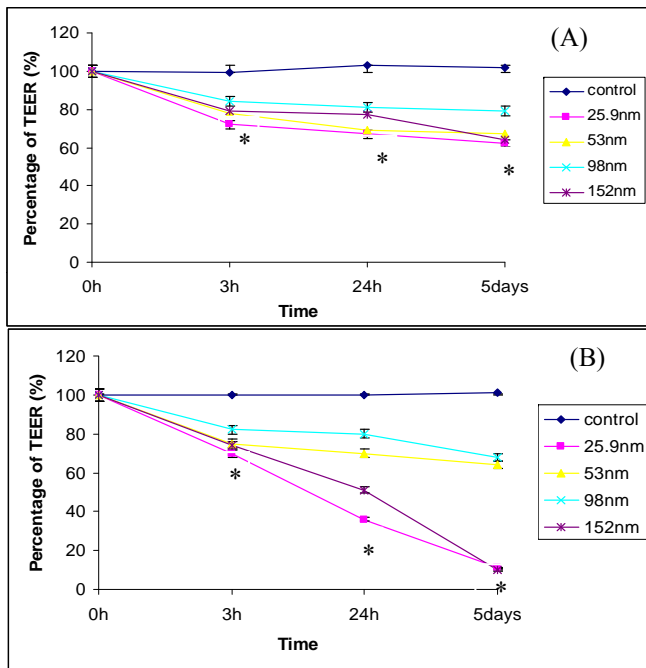


Figure 11 Caco-2 epithelial cells treated with 100 mg/L (A) and 300 mg/L (B) of various sizes of hematite NPs. Error bars represent mean \pm SD (n=3), some of them may be obscured by the data marker; * = $p < 0.002$ when compared to Control (Caco-2 cells without any added hematite NPs).

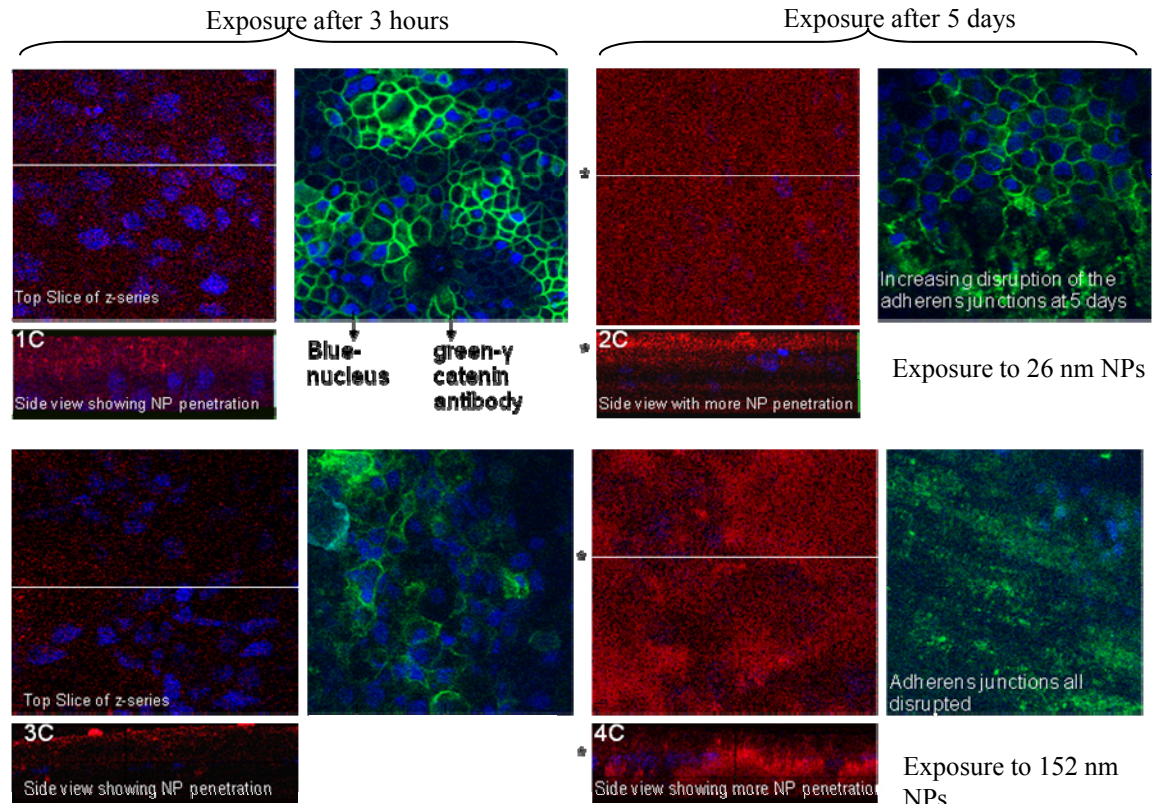


Figure 12 Representative confocal images of junctional changes of Caco-2 cells exposed to 26 nm and 152 nm hematite NPs. The important panels to consider are 3C and 4C. In these panels the red is the hematite NPs and blue color is the nucleus of a Caco-2 cell (refer to the picture of the cell in slide 2). The 3 panels show the penetration of NPs into cells at the specific time point and concentration tested. The nucleus for Caco-2 cells is toward the lower half of a cell, so NPs above the nucleus means NPs are inside the cell.

Future Plans

Next Year Plans

- Cell penetration of NPs and the governing factors
- Interactions between various NPs and representative human proteins such as biotinylated bovine serum albumin(biotin-BSA)
- The effects of environmental parameters (e.g., pH) on the interactions of NPs.

Long-Term Plans

- Build robust QSAR models based on fundamental data of adhesion force and its predicting impact on cells
- Provide information for manufacturing environmental benign NPs for industries.

Publications, Presentations, and Recognitions/Awards

1. Wen Zhang, Madhavi Kalive, David G Capco, and Yongsheng Chen, Effect of Nanoparticle Size on Adsorption onto E. coli and Caco-2 Cells and the Role of Adhesion Force. Environmental Science and Technology, submitted.
2. Wen Zhang and Yongsheng Chen, Effect of Nanoparticle Size on Bacterial Cell Adhesion Force. being prepared.
3. Xiaoshan Zhu, Xuezhi Zhang, Wen Zhang, Yung Chang, Hu Qiang, and Yongsheng Chen. Potential Toxicity of Nanomaterials and their Removal. Proceedings of the Chicago International Environmental Nanotechnology Conference: Applications and Implications Oct. 7-9, 2008
4. Wen Zhang, Xiaoshan Zhu, Xuezhi Zhang, Yongsheng Chen. Potential Toxicity of Nanomaterials and their Removal (oral presentation). International Environmental Nanotechnology conference. Chicago, Michigan, October, 2008
5. Wen Zhang, Yongsheng Chen, et.al., Methodology Development for Adhesion Force Measurement between Nanomaterials and Cells Using AFM (oral presentation). 237th American Chemical Society National Meeting & Exposition, March 22 - 26, 2009 Salt Lake City, UT

Low ESH-impact Gate Stack Fabrication by Selective Surface Chemistry

Project 425.026

Shawn Miller and Anthony Muscat
Department of Chemical and Environmental Engineering
University of Arizona, Tucson, AZ 85721



ERC Review Meeting
Feb 19-20, 2010
Tucson, AZ

Industrial partners:
Sematech
ASM

Low ESH-impact Gate Stack Fabrication **by Selective Surface Chemistry**

(Task Number: 425.026)

PI:

- **Anthony Muscat, Chemical and Environmental Engineering, UA**

Graduate Students:

- **Shawn Miller, MS candidate, Optical Science and Engineering, UA**

Cost Share (other than core ERC funding):

- **ASM**

Industrial Interactions and Technology Transfer

- **Biweekly project updates to ASM**

Mentors

- **Joel M. Barnett, SEMATECH**
- **Willy Rachmady, Intel**

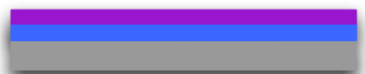
Objectives

- **Simplify multistep subtractive processing used in microelectronic device manufacturing**
 - Develop new processes that can be integrated into current devices flows
 - Minimize water, energy, chemical, and materials consumption
 - Reduce costs
- **Focus on high-k gate stack testbed**
 - Fabricate low defect high-k/semiconductor interfaces


ESH Metrics and Impact: Additive Processing

Subtractive Processing


Deposit material A and imaging layer




Pattern by exposing to light through a mask




Develop pattern in aqueous base




Transfer pattern by plasma etching



Strip imaging layer



Deposit material B with overburden



Planarize



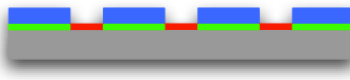
Additive Processing

Chemically activate and deactivate substrate

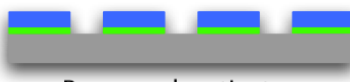


Eliminate photolithography

Selectively deposit material A




Remove deactivator




Eliminate plasma etching

Deactivate material A



Selectively deposit material B



Remove deactivator



Eliminate planarization

Impact

Spin-on imaging layer

Exposure energy
Mask
Solvents
Material A

Etching gas
Plasma energy

Chemicals
Solvents

Material B

Slurry
Water
Chemicals
Planarization energy

ESH Metrics and Impact: Cost Reduction

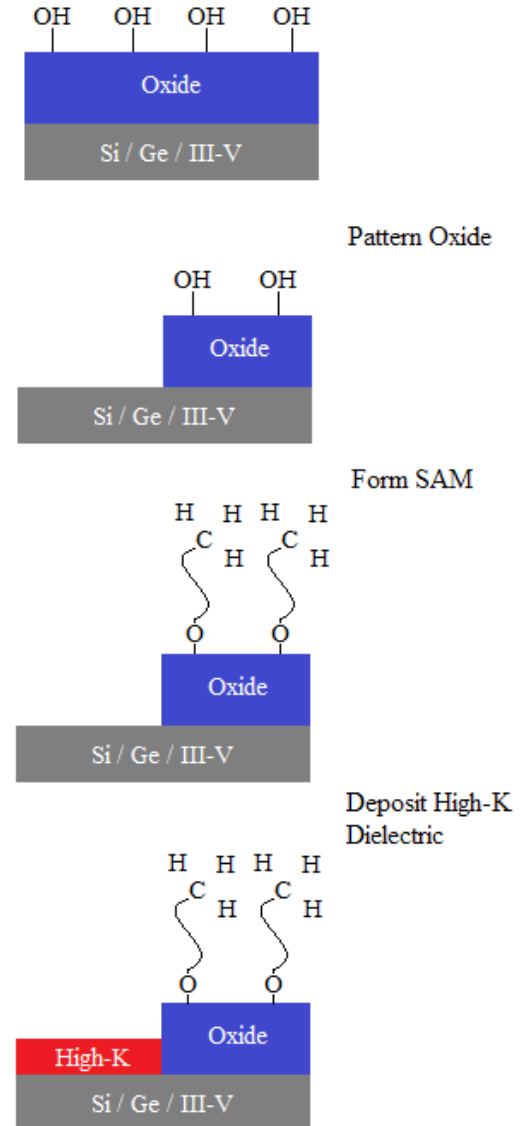
- Integration of selective deposition processes into current front end process flow could reduce ~16% of the processing costs
 - Calculation based on Sematech cost model
 - Eliminate eight processing steps from the gate module
 - Tool depreciation, tool maintenance, direct personnel, indirect personnel, direct space, indirect space, direct material, and indirect material were included
 - Energy, waste disposal, and addition of two selective deposition steps were not included
- There is potential for greater ESH benefit due to minimized cost of raw materials and waste generated

Novelty

- Develop industrially feasible processes to activate and deactivate surfaces
 - Significantly lower time scale
 - Extend to metal and semiconductor surfaces
- Integrate selective deposition steps at carefully chosen points in the CMOS process flow
 - Realize ESH and technical performance gains
- Quantify costs associated with selective deposition steps to refine industry models
 - Account for energy and waste disposal
 - More accurate prediction of the cost model

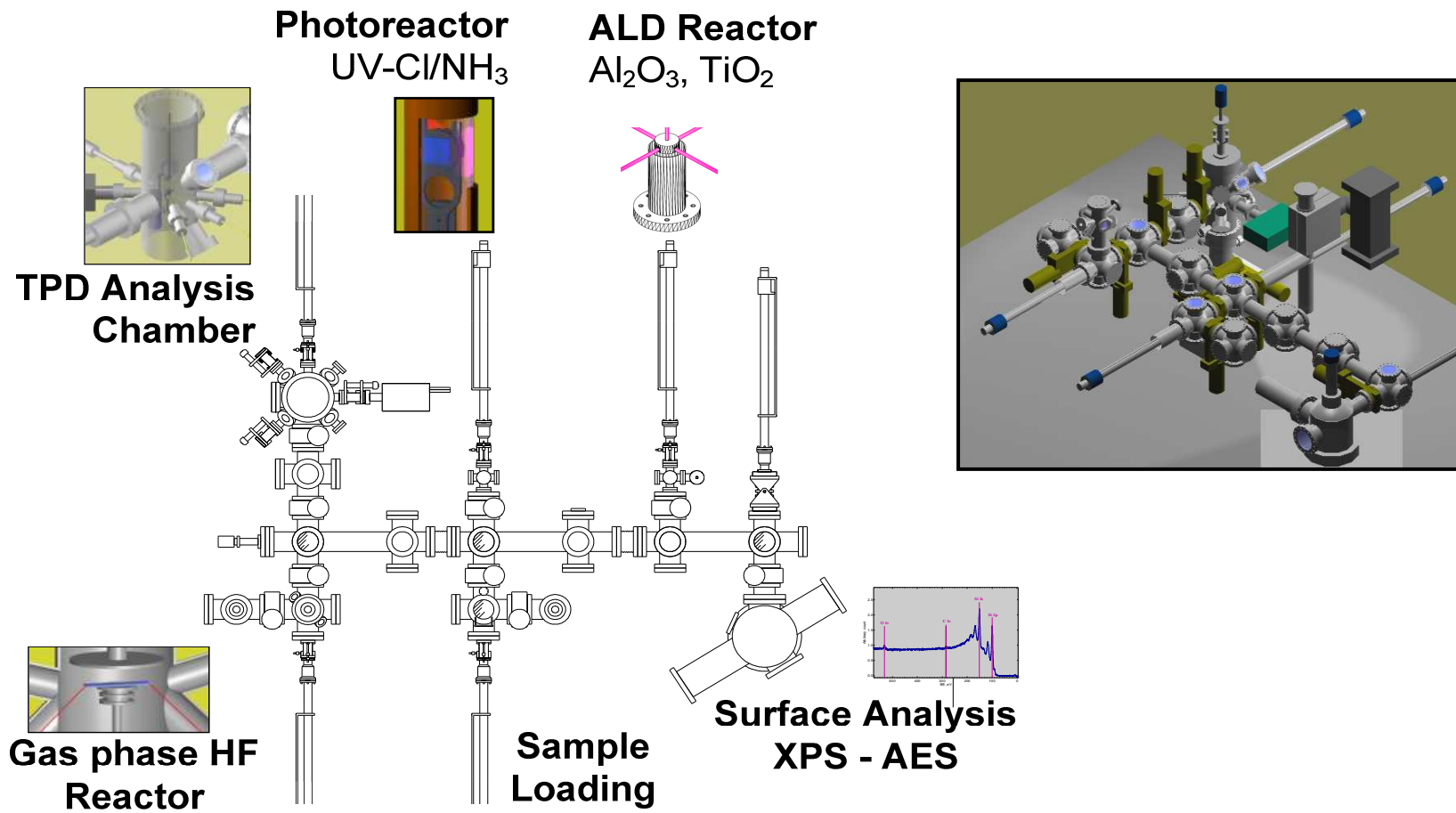
Methods and Approach

- Grow high-k films on semiconductors by activation and deactivation of surface sites
- Activation
 - Utilize surface chemistries to activate substrates for high-k film growth
 - Halogen, amine terminations
- Deactivation
 - Hydrophobic self assembled monolayer (SAM) prevents adsorption of H₂O
- Model systems
 - Si, Ge, and III-V substrates
 - High-k films by atomic layer deposition (ALD)
 - Al₂O₃
 - TiO₂



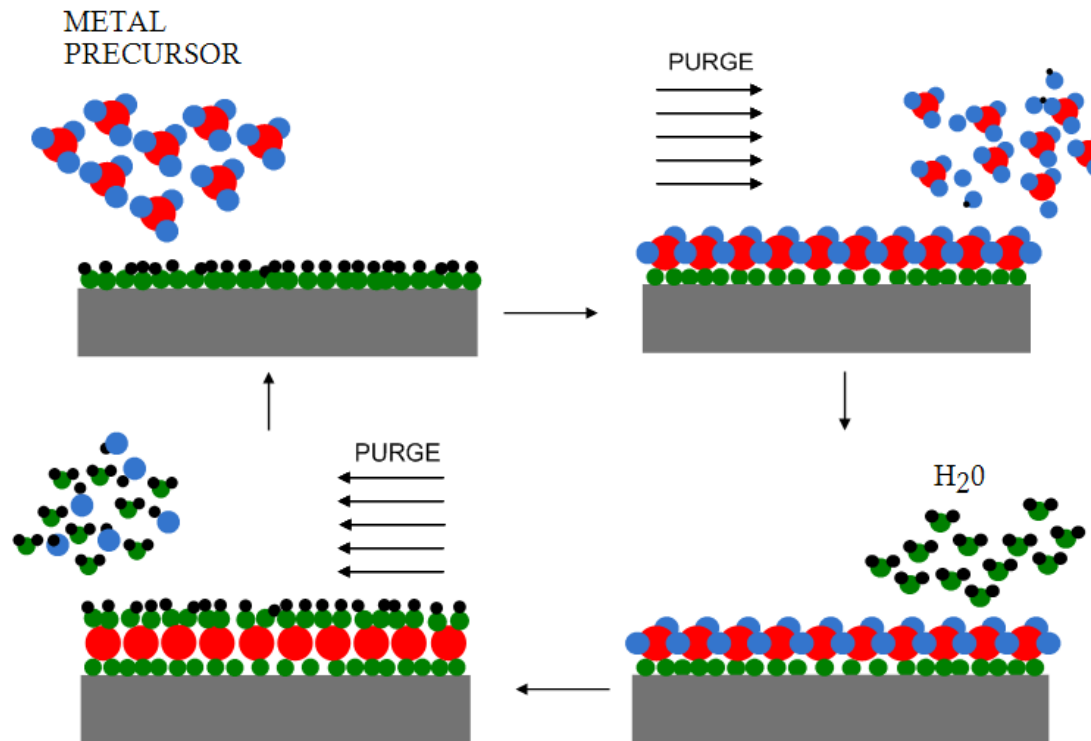
Clustered Reactor Apparatus

- In situ cleaning, high-k deposition, and surface analysis enables studies of surfaces without atmospheric contamination
 - Important for highly reactive substrate such as III-V materials



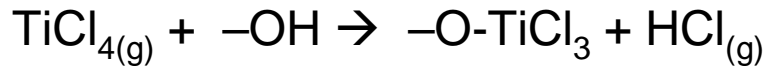
Atomic Layer Deposition of High-k Films

- Break overall reaction into two half reactions and run one at a time to achieve self-limiting growth
 - Surfaces exposed to sequential pulses of metal and oxygen precursors to deposit oxide

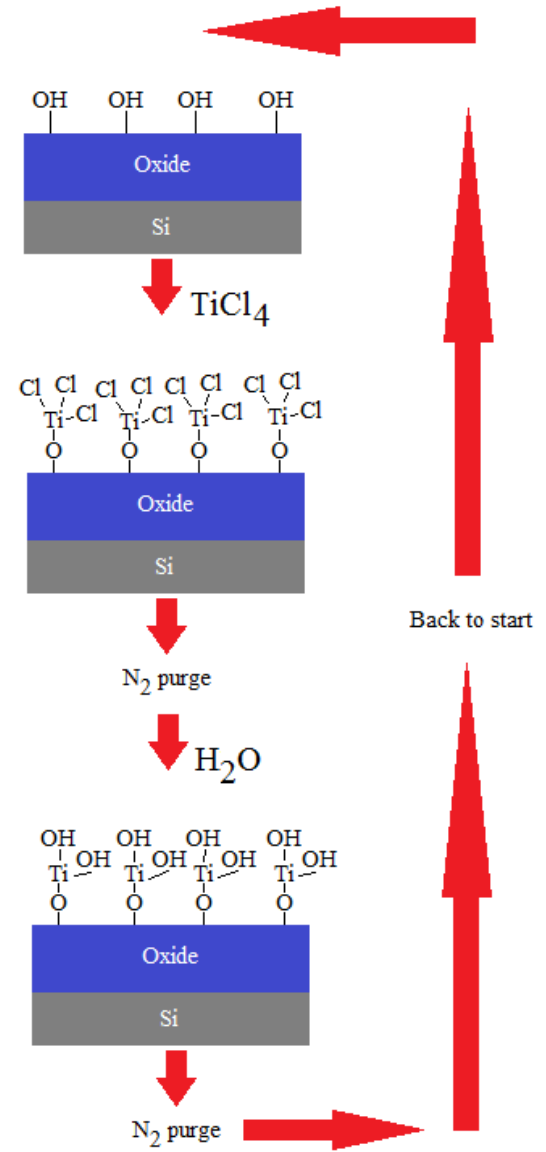


ALD Reaction Mechanism

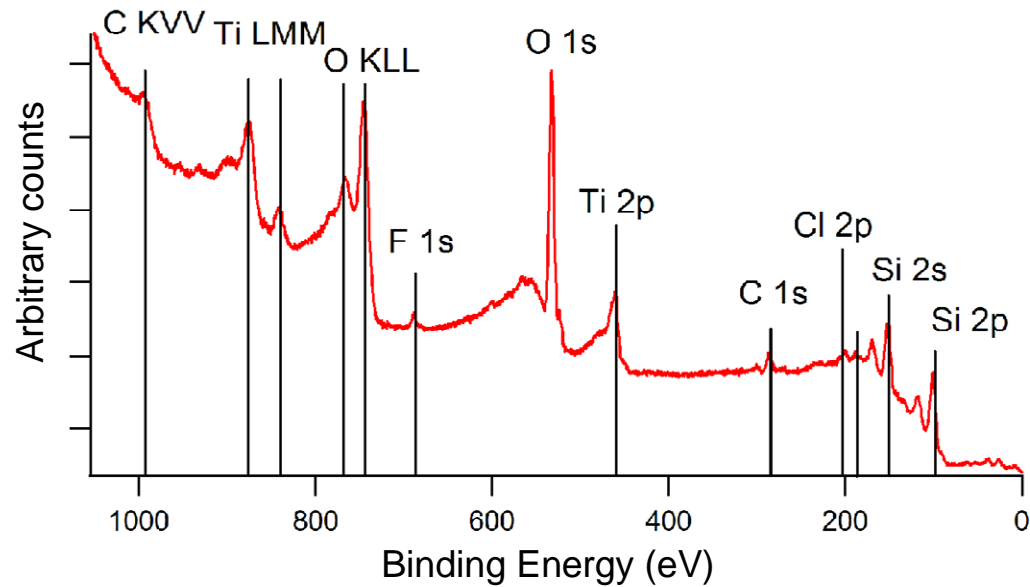
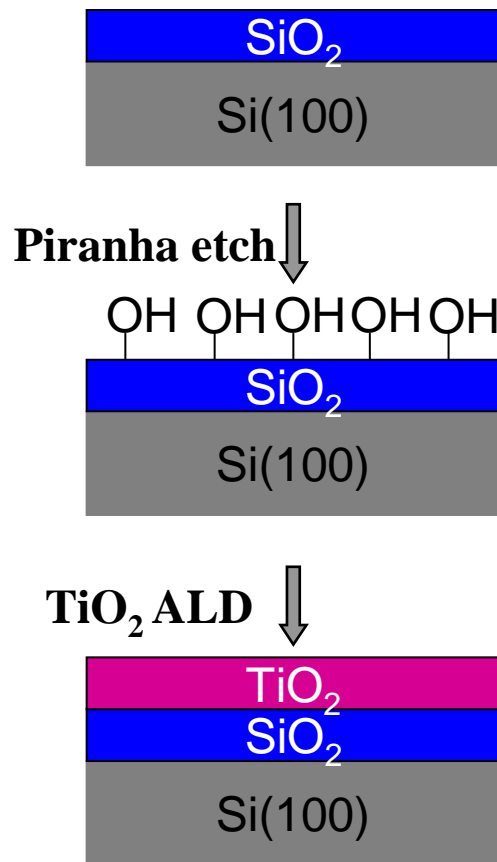
- Factors governing the selective deposition of high-k film
 - Surface conditioning
 - Precursor selection
 - Deposition conditions
- Hydroxylated surface promotes high-k growth on Si
- Two half reaction in TiO₂ deposition



- Deposition mechanism using TiCl₄ precursor could be used as a model for HfCl₄ precursor


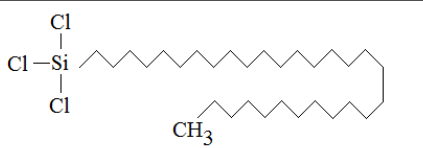
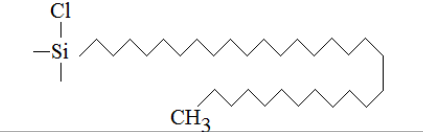
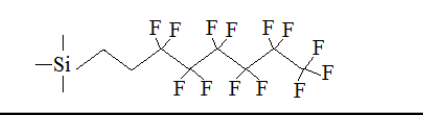
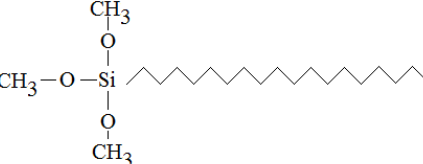
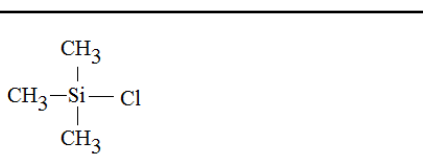
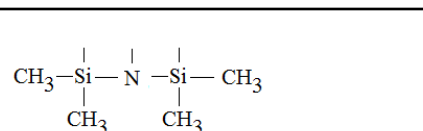


Si(100) high-k deposition: ALD of TiO₂

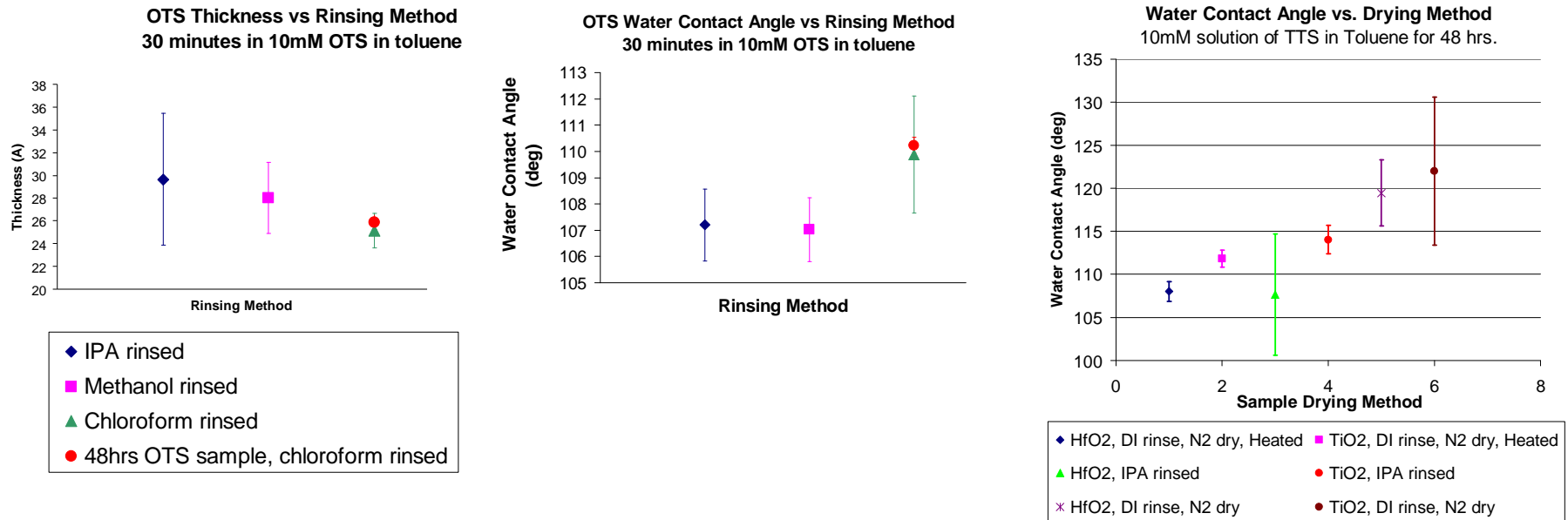


- Demonstrated TiO₂ deposition on hydroxylated Si(100)
 - Residual Cl present on surface
 - Si 2p peak still visible with ~9 Å thick TiO₂ layer

Deactivation using SAM Chemicals

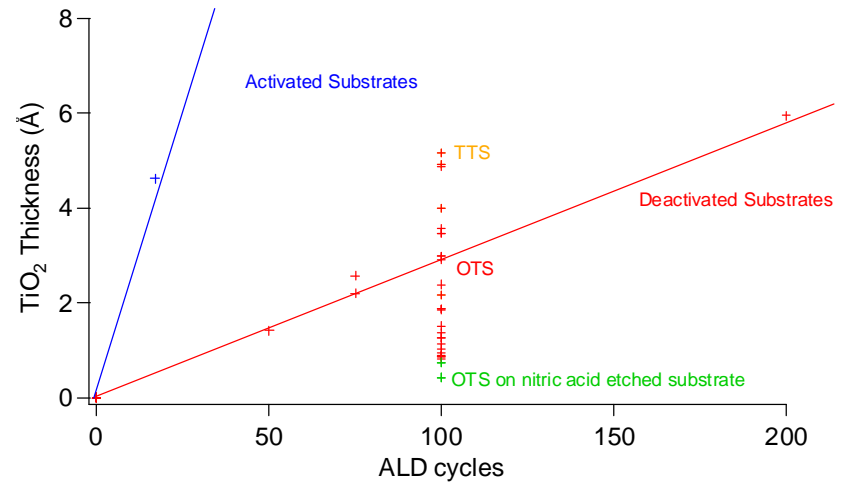
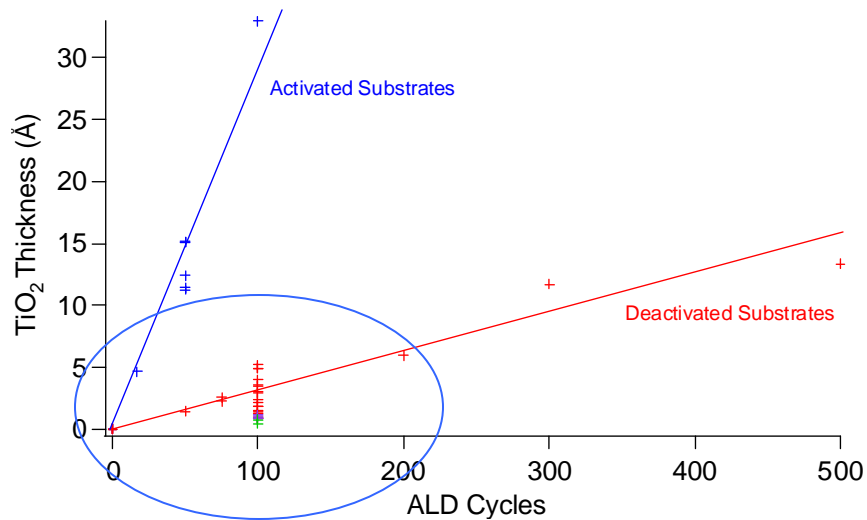
SAM molecules	Formula	Structure
Octadecyltrichlorosilane OTS	$C_{18}H_{37}Cl_3Si$	
Triacontyltrichlorosilane TTS	$C_{30}H_{61}Cl_3Si$	
Triacontyldimethylchlorosilane TDCS	$C_{32}H_{67}ClSi$	
Tridecafluoro-1,1,2,2-tetrahydrooctylsilane FOTS	$C_8H_7F_{13}Si$	
Octadecyldimethoxysilane ODS	$C_{21}H_{43}O_3Si$	
Trimethylchlorosilane TMCS	C_3H_9ClSi	
Tetramethyldisilazane TMDS	$C_4H_{14}NSi_2$	

Surface Deactivation: SAM formation



- High quality OTS layer after only 30 minutes (not 2hrs)
 - 26Å
 - 110° water contact angle
 - Smaller standard deviation after 48hrs in OTS than 30min in OTS
- Chloroform rinse was more effective than IPA and Methanol for OTS and TTS
- Polymerization of the SAM molecule was observed due to reaction with adsorbed water producing large deviation in the water contact angle

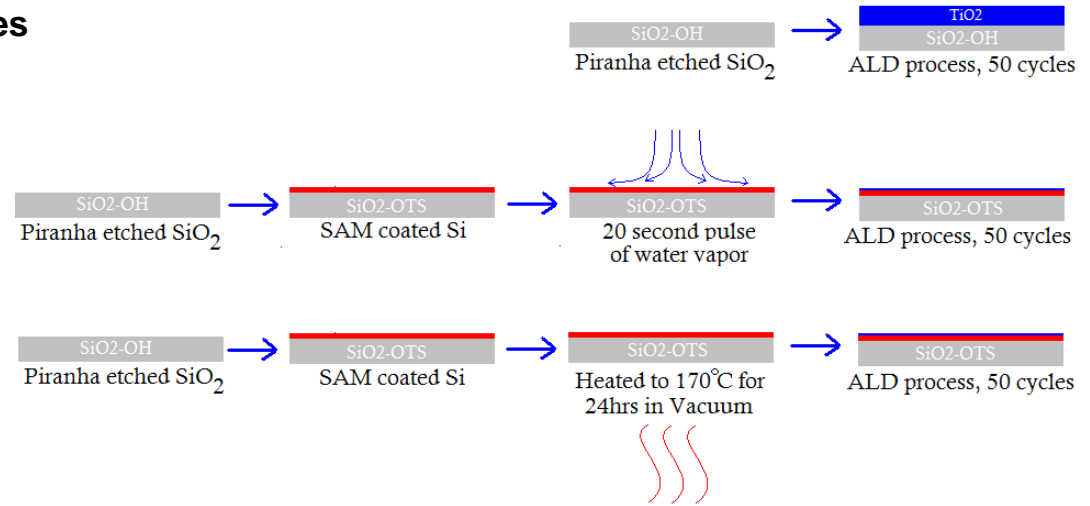
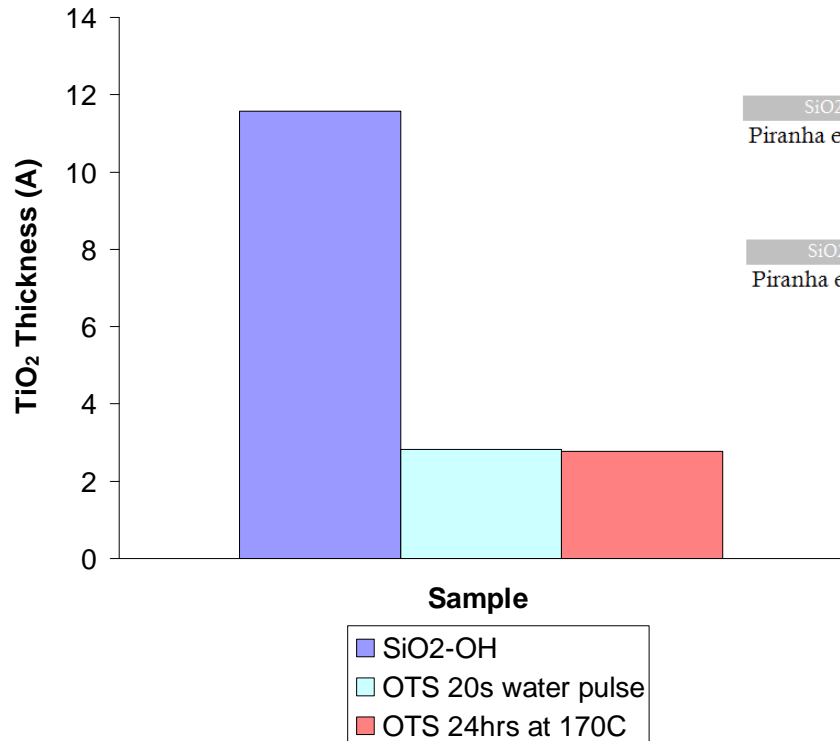
Surface Deactivation: Results



- Reduced TiO₂ growth rate by up to a factor of 50 ± 5
 - Data spread primarily due to sample variation within each solution batch
- Potential SAM defects
 - Water in/on SAM
 - Unblocked hydroxyl groups
 - Exposed Si-O bridges
- Improve deactivation by performing nitric acid etch or SC1 cleaning before SAM formation

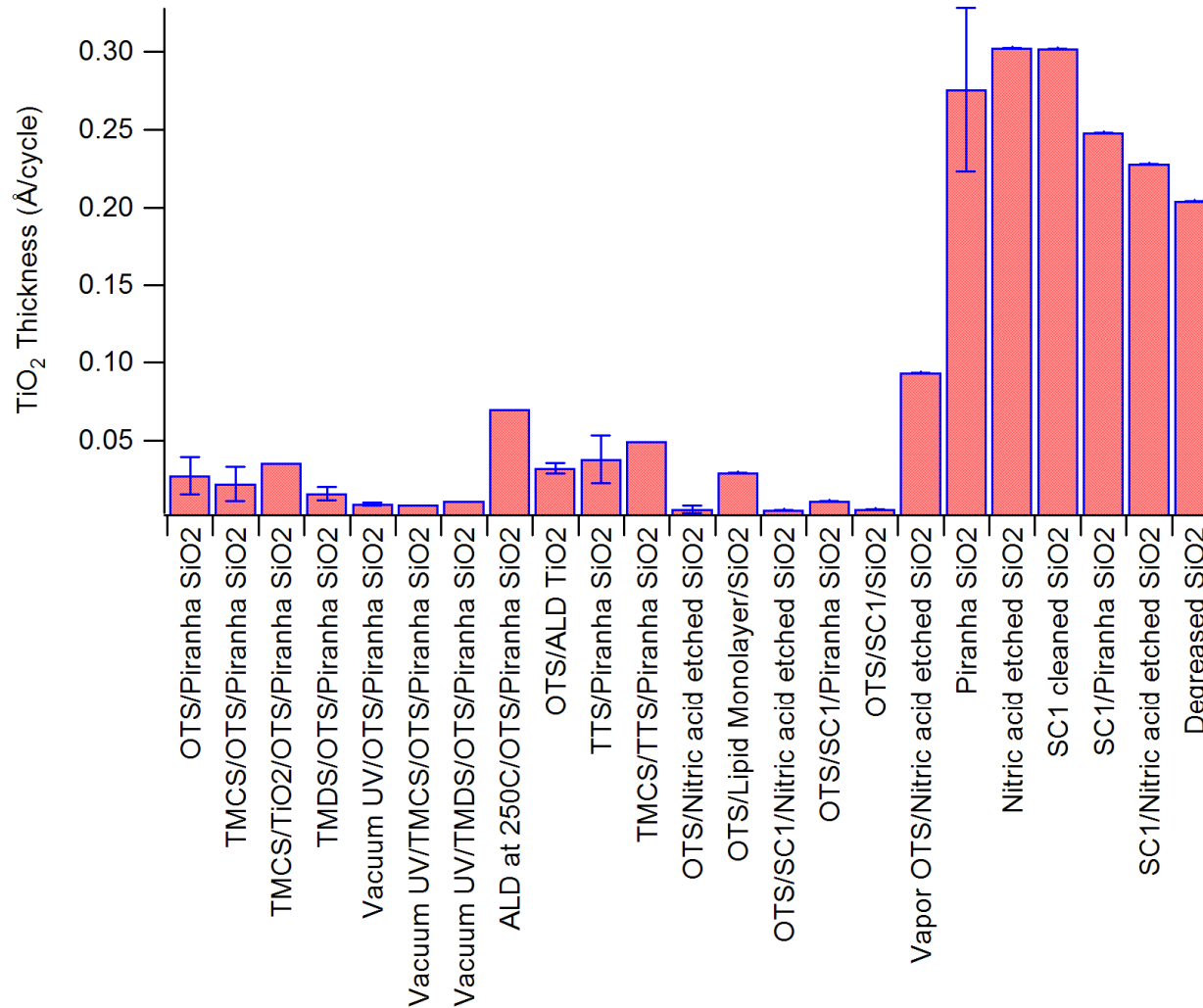
Surface Deactivation: Effect of Water

TiO₂ Thickness After 50 Cycles



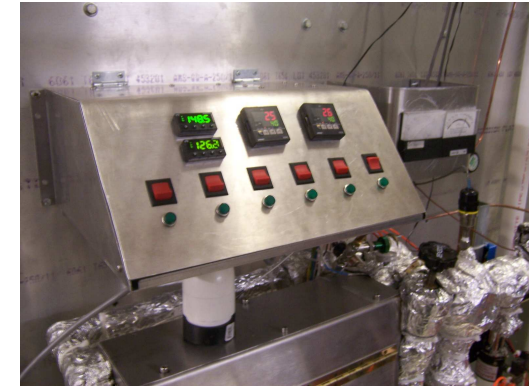
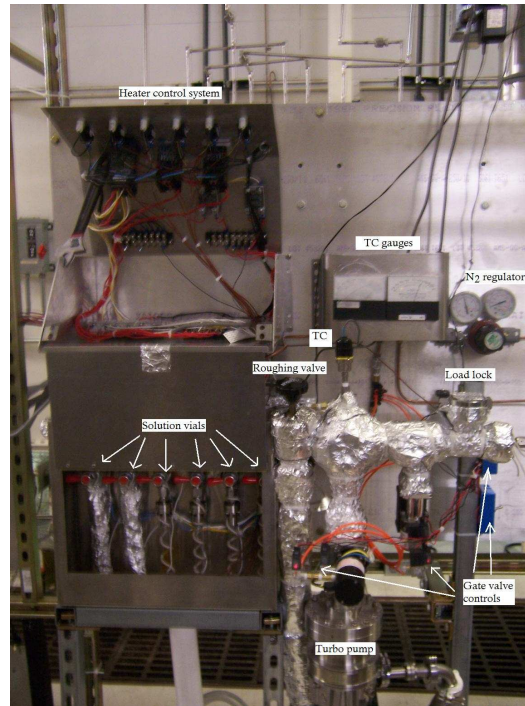
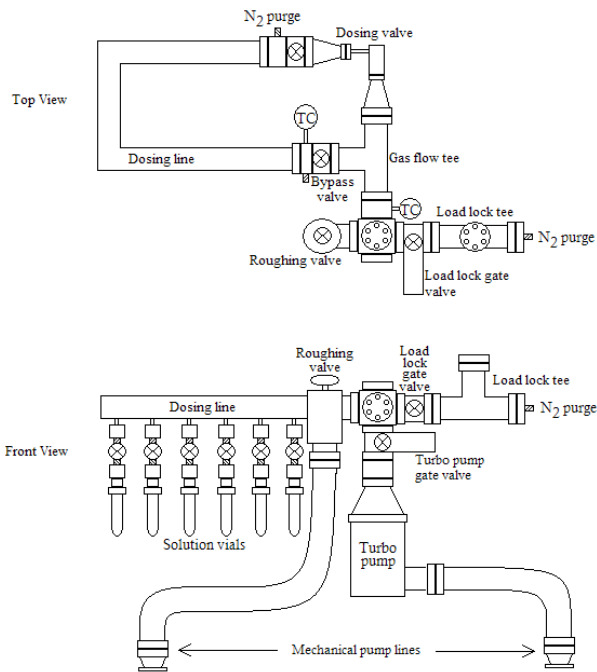
- SAM is equally stable to subsequent water pulses during an ALD process
 - No change in Ti due to additional 20 second water pulse before ALD

Surface Deactivation / Activation



- Improve SAM deactivation capability by
 - Replacing piranha etch step with a nitric acid or SC1 cleaning

SAM Vapor Phase Delivery: Reactor

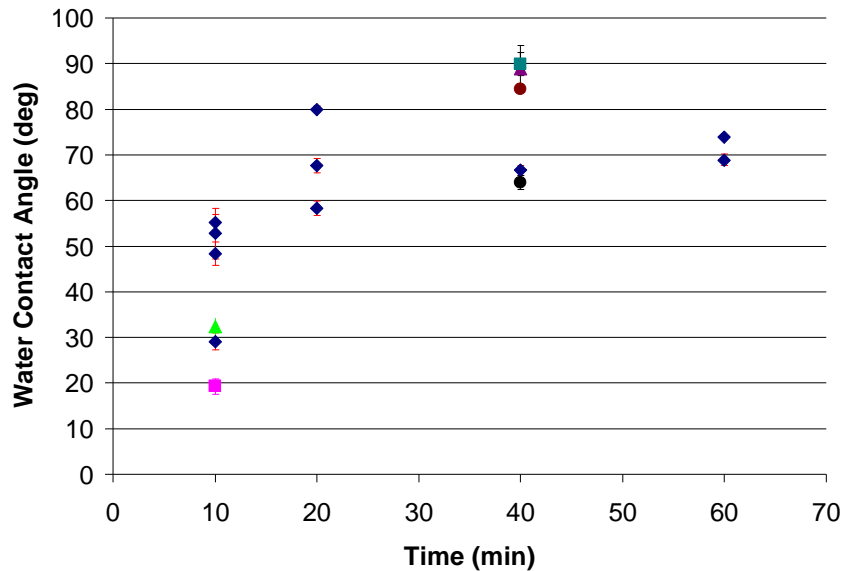


- Vacuum vessel designed to optimize vapor phase delivery of SAM molecules
- Control variables:
 - Vapor pressure
 - Exposure time
 - Temperature of substrate, reactor walls, and SAM solutions
 - SAM and water vapor delivery method
 - Individually
 - Simultaneously
 - Alternately with N₂ purge between pulses

SAM Vapor Phase Delivery: Results

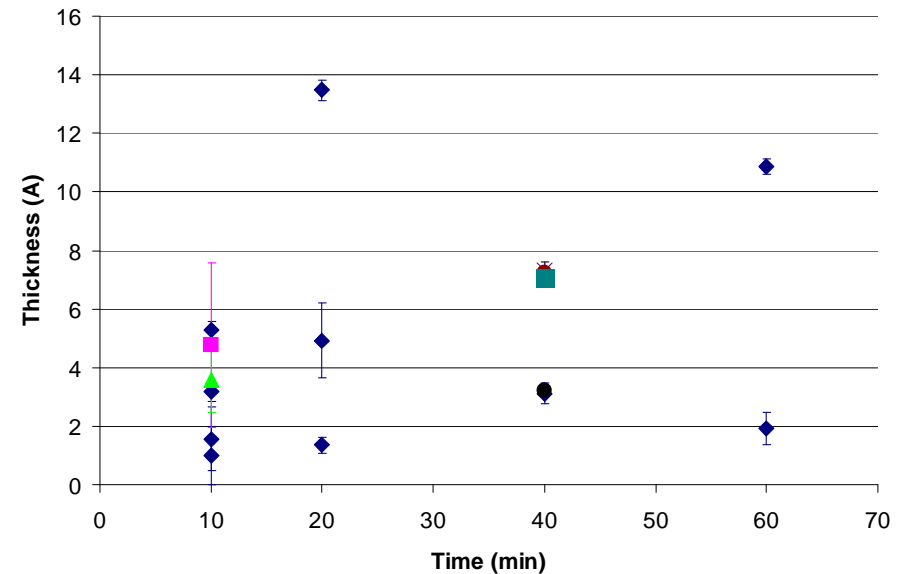
Water Contact Angle vs. Vapor Exposure Time

10min OTS, 30sec H2O...

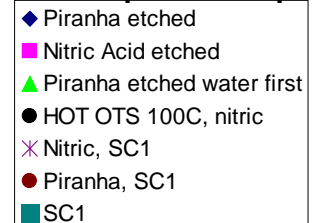


SAM Thickness vs. Vapor Exposure Time

10min OTS, 30sec H2O...



Sample Prep



- 95° water contact angle obtained after only 40 min of vapor OTS exposure
 - 1 cycle = 10min OTS/N₂ purge/pump/30s water/N₂ purge/pump
 - Without water pulses maximum water contact angle was only 65°

Conclusions

- Growing the SAM layer on nitric acid etched and SC1 cleaned samples eliminates many of the defects found in SAM layer formed on piranha etch samples
- 95° water contact angle obtained after only 40 min of vapor OTS exposure
 - SC1 cleaning of the chemical oxide layer has aided in SAM attachment to the surface both in vapor phase and liquid phase
- SAM layer is stable during the ALD water pulse process
 - TiCl_4 is the nucleating precursor

Future Work

- Investigate vapor phase ozone and gas phase HF/vapor treatment to increase and control hydroxylation of oxide surfaces
- Characterize SAM layers
 - Thermal stability for deactivation
 - Durability for large numbers of ALD cycles
 - Chemical bonding between SAMs and surface
 - Degradation and repair of SAMs layers
- Extend deactivation study to Al_2O_3 , TiO_2 , HfO_2 surfaces
- Optimize vapor phase delivery of SAM molecules
 - Pulse and purge both water and SAM molecules as opposed to sealing vapor in a reactor for extended time
- Investigate optimized selective deposition method on III-V semiconductor surfaces

Task Title:

Predicting, Testing, and Neutralizing Nanoparticle Toxicity *(Task Number: 425.027)*

PIs:

- **Steven O. Nielsen (PI), Department of Chemistry (Chemistry) and Alan G. MacDiarmid NanoTech Institute (Nanotech), The University of Texas at Dallas (UTD)**
- **Rockford K. Draper (co-PI), Department of Biology, Chemistry, and Nanotech, UTD**
- **Paul Pantano (co-PI), Chemistry and NanoTech, UTD**
- **Inga H. Musselman (co-PI), Chemistry and NanoTech, UTD**
- **Gregg R. Dieckmann (co-PI), Chemistry and NanoTech, UTD**

Graduate Students:

- **Chi-cheng Chiu: PhD candidate, Department of Chemistry, UTD (100% funded)**
- **David K. Bushdiecker: PhD candidate, Department of Chemistry, UTD (Not funded)**

Undergraduate Students:

- **Laura Lockwood, Kyle Bruner, Nancy Jacobsen, and Prashant Raghavendran, UTD**

Other Researchers:

- **Ruhung Wang: Postdoctoral Fellow, Department of Molecular and Cell Biology, UTD**

Year 1 Cost Share (other than core ERC funding):

- **\$45K from UTD Dean of Science for a zeta potential analyzer**
- **\$25K from UTD Engineering School for RA support**
- **\$20K from UTD Vice President of Research for supplies**

Year 1 Deliverables & Objectives

- **Obtain and validate data on the characterization, fate, and toxicity (tested in model mammalian cells) of carbon nanotube (CNT) nanoparticles.**

ESH Metrics and Impact

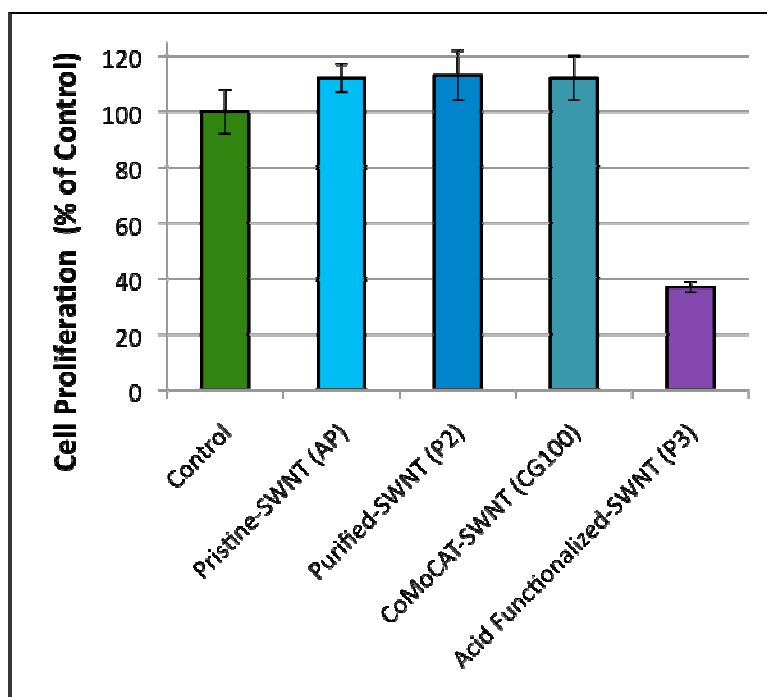
1. *Reduction in emission of ESH problematic material to environment:*
 - Reduce the toxic material associated with commercial preparations of a variety of CNT types to a level such that the final CNT material expresses very little toxicity to cells in a sensitive model cell culture system.
2. *Identification or prediction of inherent material ESH properties and any process by-products:*
 - Assess ESH properties of inherent CNTs and separable by-products.
 - Demonstrate that CNTs themselves have little inherent toxicity in cell culture models and that observed toxicity is due to by-products that can be separated from the CNTs.
3. *Establish dose metrics for pure and oxidized CNTs:*
 - Conduct three day growth assays using cultured mammalian cells to compare any possible effects of CNTs on cell growth with untreated controls.
 - Conduct two-week plating efficiency experiments for a more stringent assay of toxicity.
 - Purified CNTs show little toxicity in either type of assay.
4. *Development of analytical tools to measure trace levels of CNT materials in process effluents:*
 - Detect as little as 5 micrograms of CNTs per milliliter of solution.
 - Develop methods to detect CNTs in process effluents, adhering to tools, or in the air.
 - Develop methods to detect graphene and graphene oxide.
5. *Development of molecular simulation parameters to enable nanoparticle-bio interaction studies:*
 - Develop mesoscopic models for C60 and CNT interactions with cellular membranes.

in vitro Cytotoxicity Comparison of Various SWNTs

Four different single-walled carbon nanotube (SWNT) samples were tested.

Pristine, purified, and CoMoCAT are various un-modified SWNTs from two vendors.

Acid functionalized SWNTs are carboxylated by the vendor to make them more water soluble.



Cultured NRK cells were incubated in media with various SWNT dispersions at the same concentration or in the absence of SWNTs for 3 days.

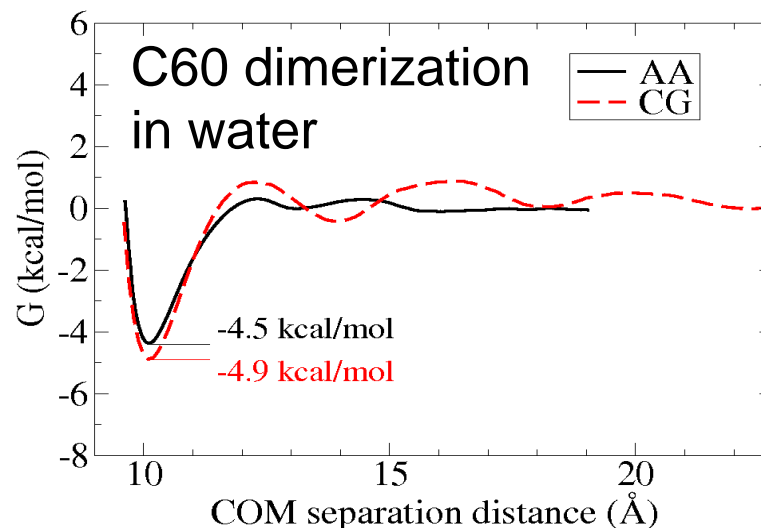
Cytotoxicity was determined by measuring the ability of the cells to proliferate, quantified by comparing the number of cells after 3 days in the presence or absence of the SWNTs.

Significant toxicity was detected only in cells treated with P3 material, carboxylated SWNTs.

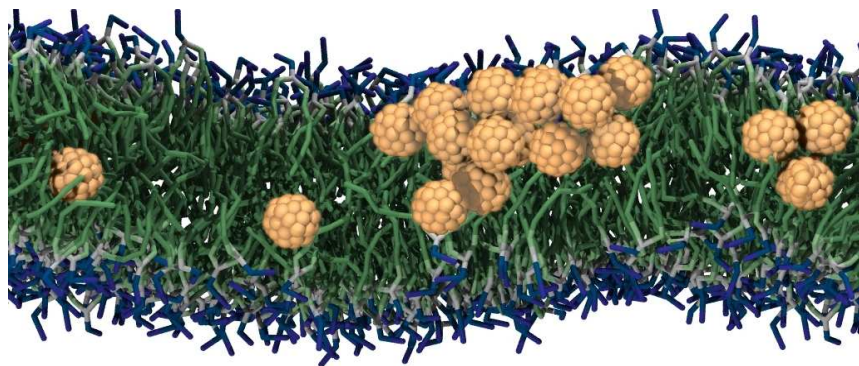
Only the more water-soluble carboxylated P3 SWNTs were cytotoxic. This is surprising given our molecular simulation data (next 4 slides). But the last 3 slides demonstrate that the toxic component could be separated from the SWNTs themselves.

Study the interaction between SWNTs and a cellular membrane

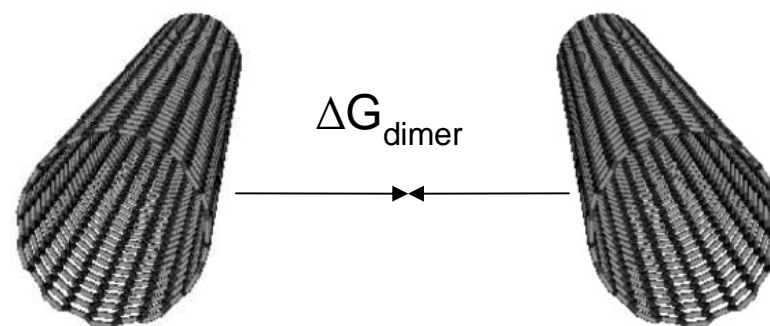
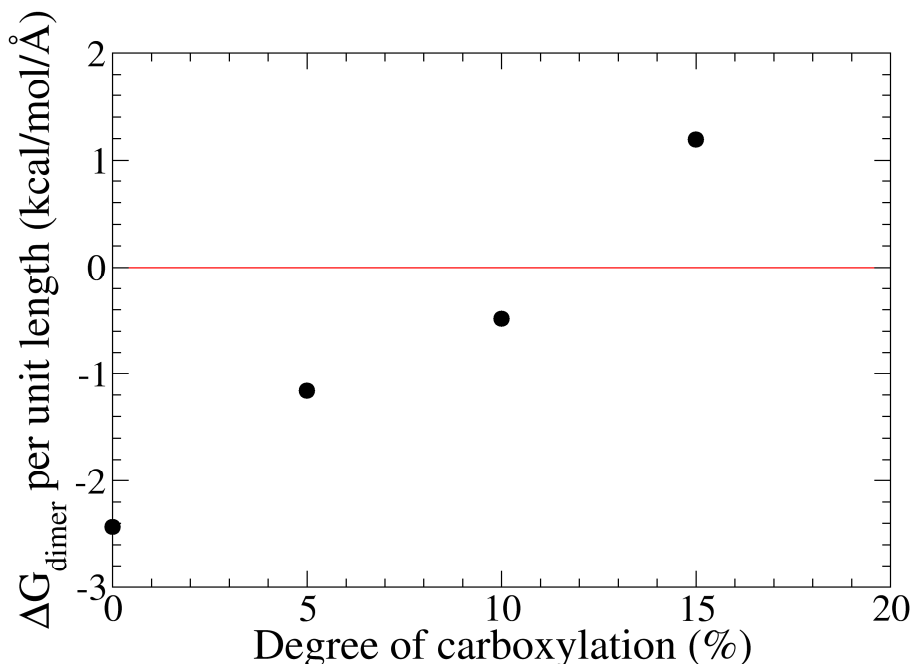
- To interact with living organisms, SWNTs may cross a membrane barrier.
- Molecular simulations can examine this nano-bio interaction.
- Coarse grain (CG) model needed due to required time and size scales.
- We have developed and validated a CG model for C60 and SWNTs: Chiu, C.-c., Nielsen, S. O. *et al.*, submitted to J. Phys. Chem. B
- Validated against surface tension data, transfer free energy data, and aggregation behavior.



Li, L. *et al.* Physical Review E 2005, 71, 011502
 Li, L. *et al.* J. Phys. Chem. B 2007, 111, 4067



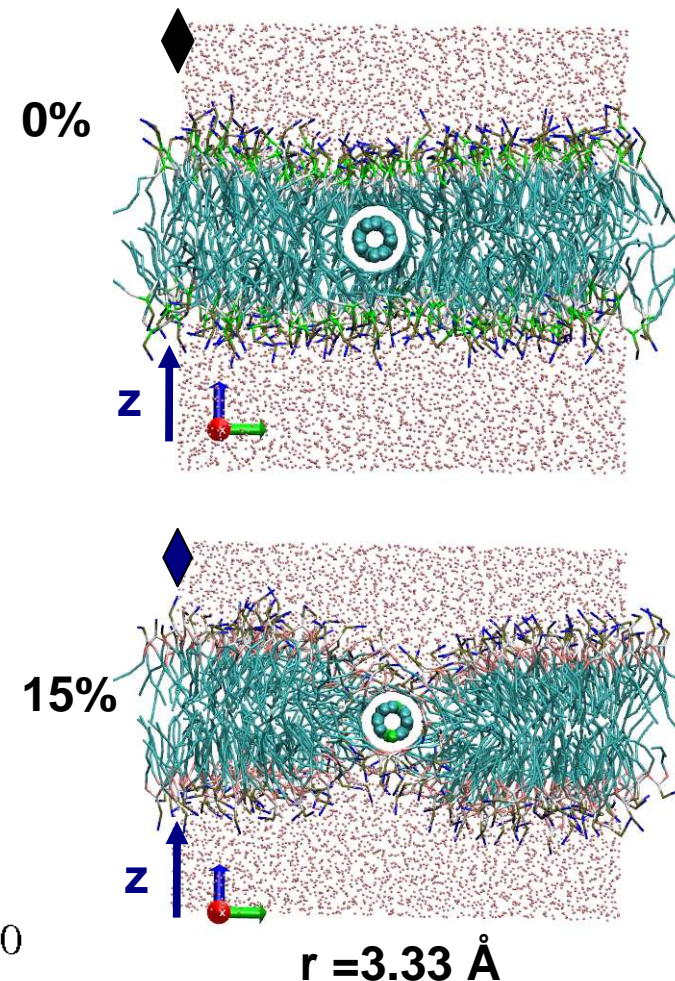
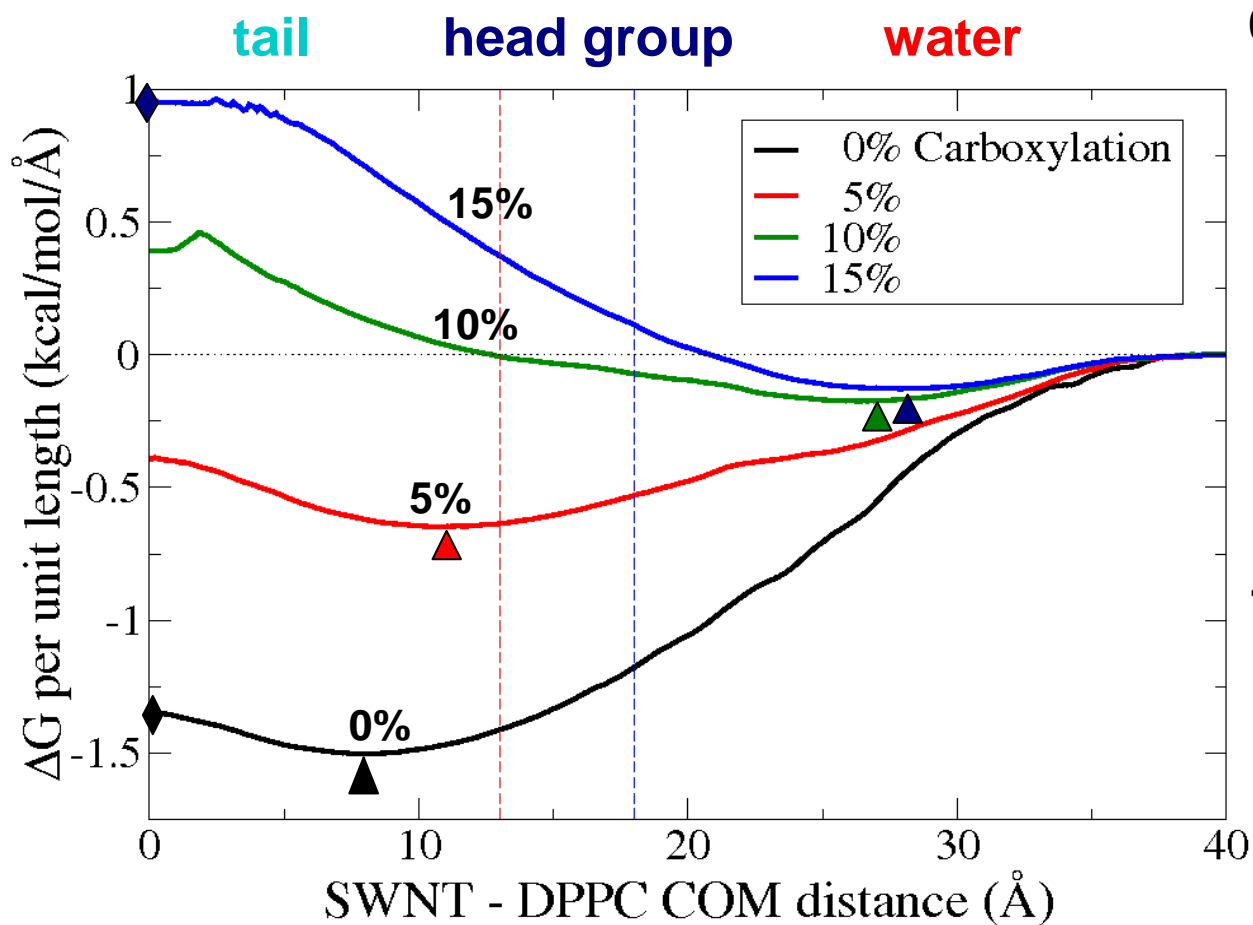
Carboxylated (acid-functionalized) SWNTs: validation of molecular simulation results against experimental data



- SWNT dimerization free energy in water computed from molecular simulation as a function of SWNT % carboxylation.
- $\Delta G_{\text{dimer}} < 0$ indicates that SWNTs will bundle (aggregate) in water.
- $\Delta G_{\text{dimer}} > 0$ indicates that SWNTs will disperse individually in water.
- Crossover % carboxylation agrees with our experimental data: Bajaj, P. M.S. Thesis, The University of Texas at Dallas, Richardson, TX, 2008

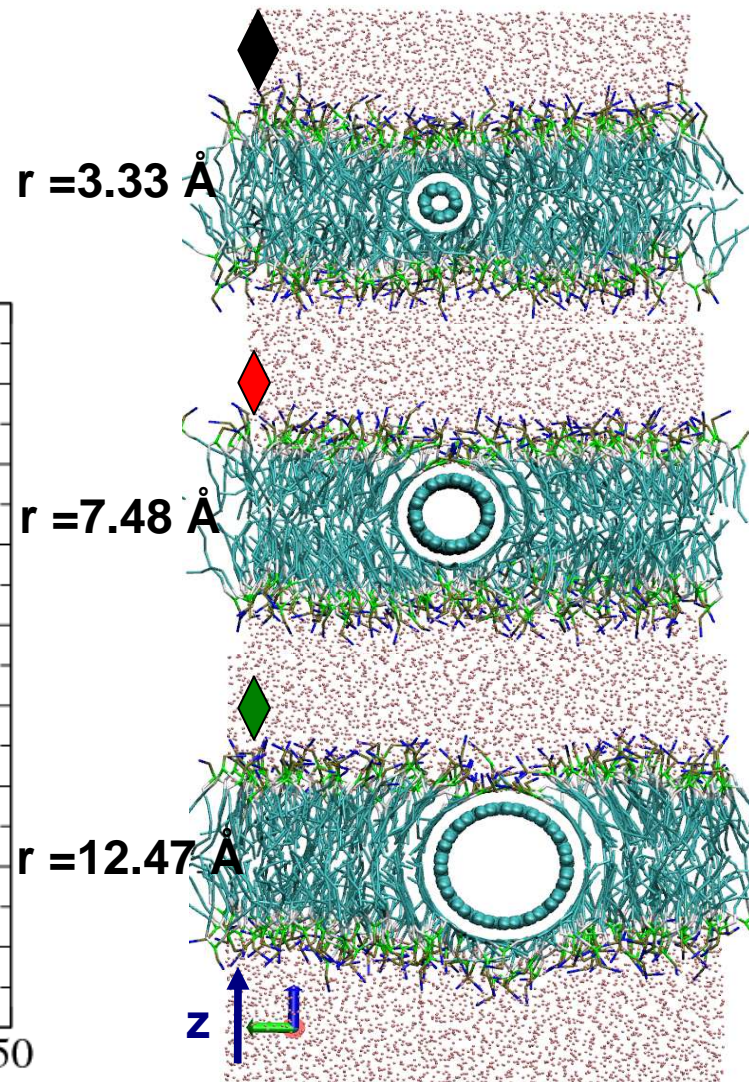
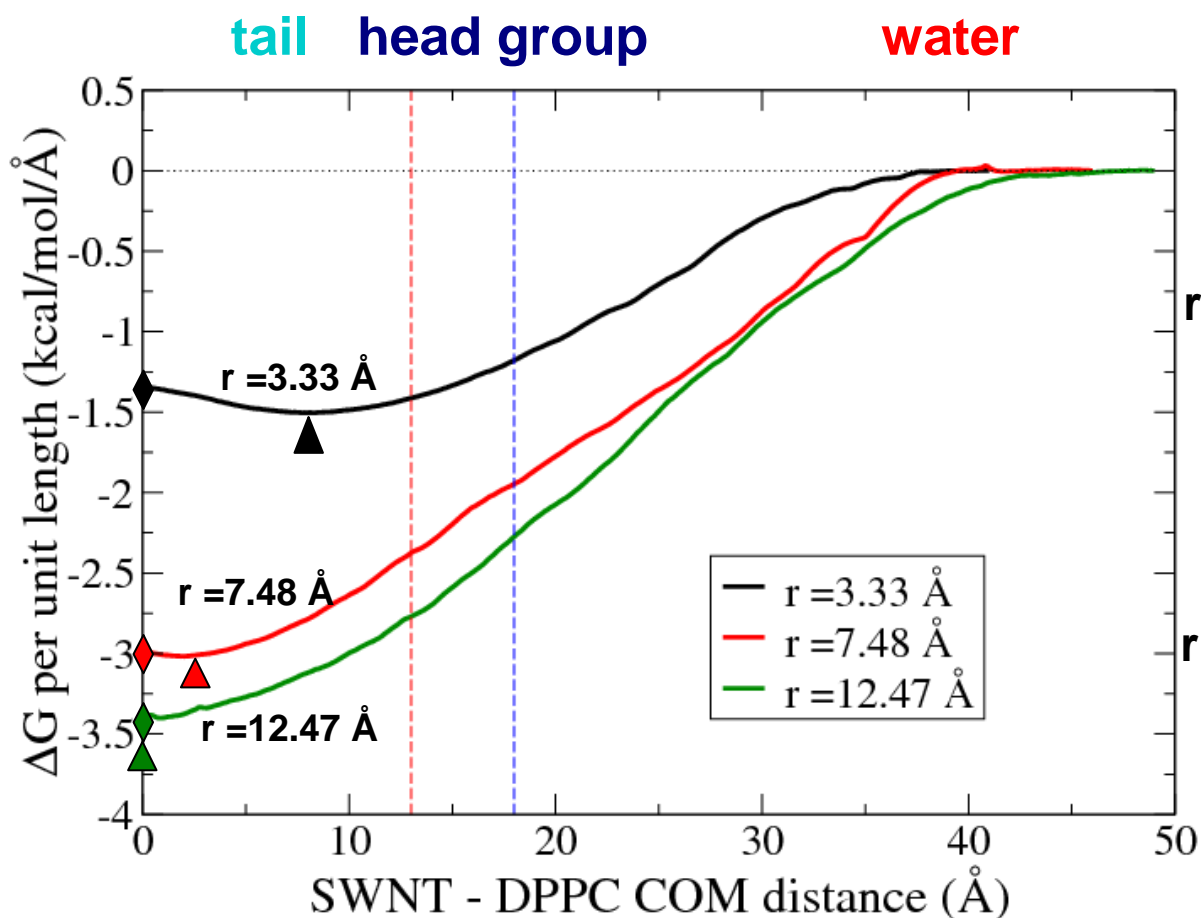
SWNT/Lipid Bilayer Membrane

- Pristine SWNTs spontaneously diffuse into bilayer membrane.
- Above 10% carboxylation, it is no longer favorable for SWNTs to penetrate the bilayer membrane.



SWNT/Lipid Bilayer Membrane

- Pristine SWNTs show expected diameter dependence on bilayer membrane interaction.

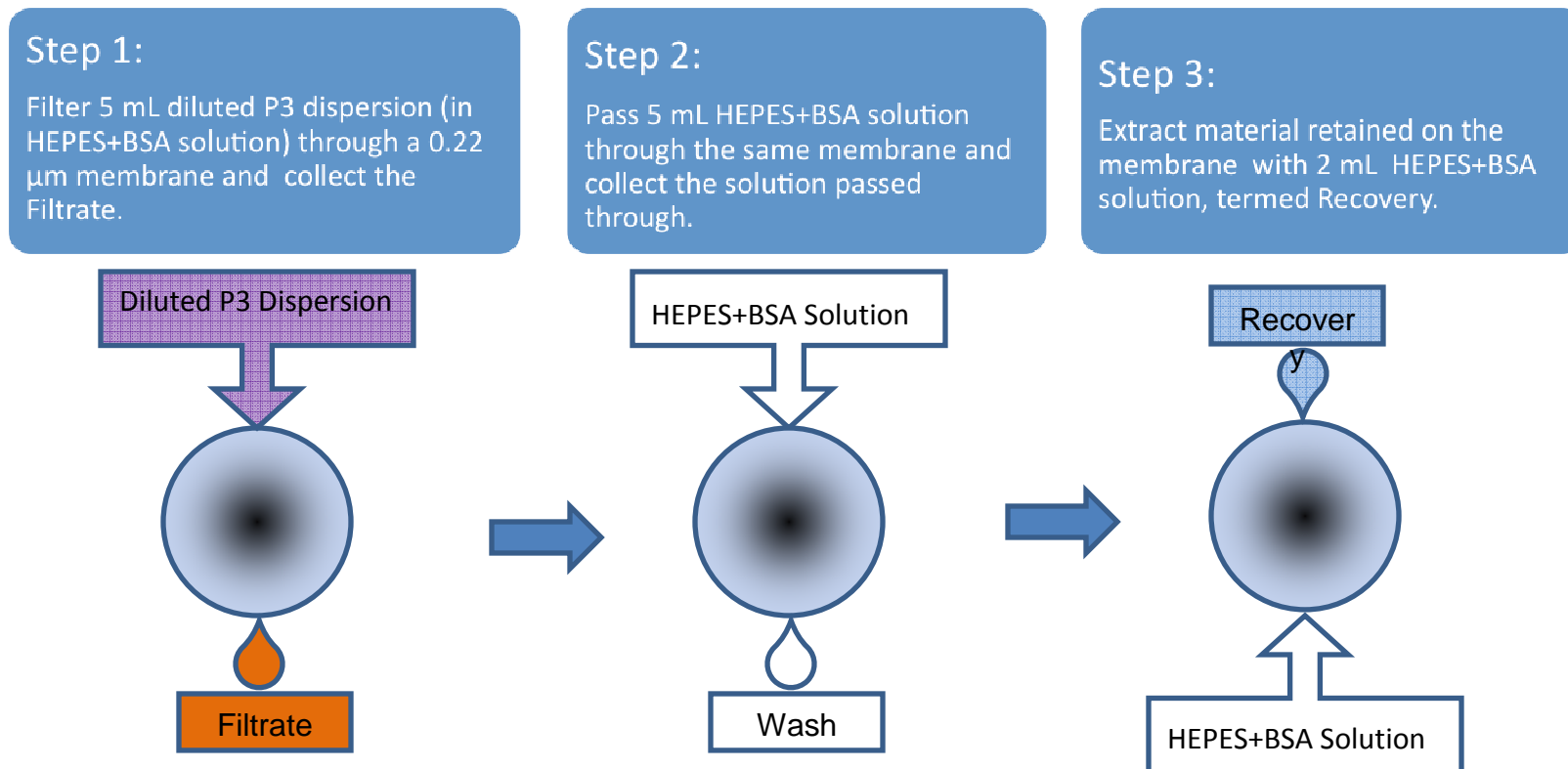


What we learn from comparing the experimental and simulation data

- Simulation studies predict that carboxylated SWNTs should not interact with cellular membranes, suggesting that they would not be cytotoxic.
- However, experimental data in slide 4 showed evidence of a cytotoxic effect.
- In the following 3 slides, we investigate whether the cytotoxic activity was inherent to carboxylated SWNTs, or due to a separable by-product.

Separation of the Toxic Components from P3

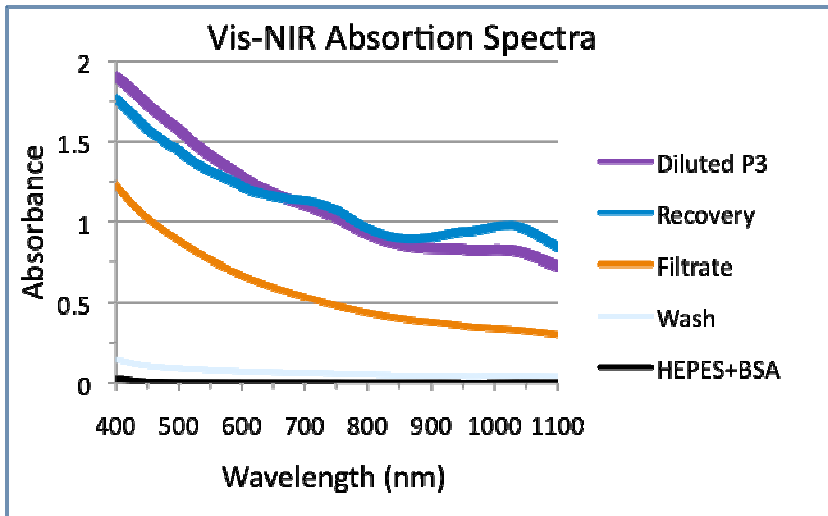
Carboxylated SWNTs



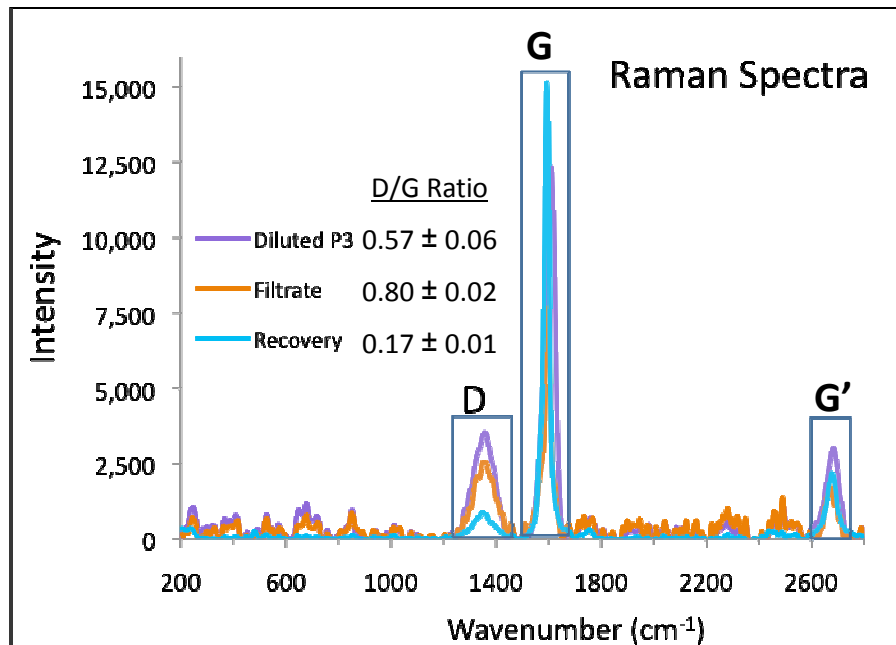
P3 dispersion and samples collected along the filtration process were tested for:

- **Presence of C-SWNTs and amorphous carbons – by Vis-NIR absorption spectroscopy and confocal Raman spectroscopy**
- **Cytotoxicity – by measuring cell proliferation over 3 days**

Majority of P3 Carboxylated SWNTs are Recovered

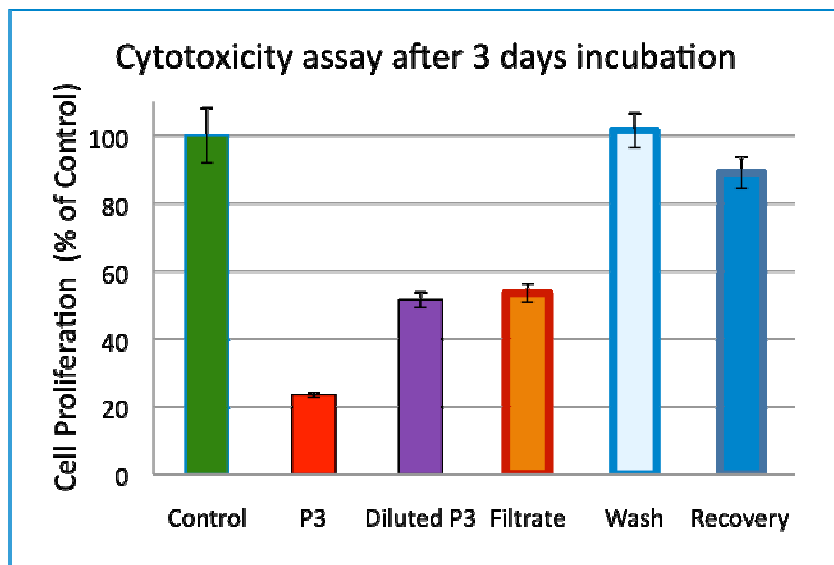


- ✓ The non-filtered P3 dispersion has two broad peaks, ~750 and ~1050 nm.
- ✓ The Filtrate has relatively high background but no peaks.
- ✓ The recovered material has two peaks of higher intensities.
- The filtration membrane retains most SWNTs that can be recovered.



- The D/G ratio is proportional to the amorphous carbon content relative to intact SWNT content.
- ✓ The Filtrate has the highest D/G ratio indicating that it contains mostly amorphous carbon fragments.
 - ✓ The recovered material contains intact SWNTs as indicated by its low D/G ratio.

Filter Purified P3 Carboxylated SWNTs are Not Cytotoxic



✓ The Filtrate is as toxic as the diluted but not filtered P3 dispersion.

✓ The recovered material shows almost no toxicity.

➤ The filtration process efficiently removes toxic component from the P3 carboxylated SWNT dispersion.

Conclusions:

- Commercially purchased carboxylated SWNTs appear to contain carboxylated amorphous carbon fragments.
- These impurities are toxic but can be removed by filtration.
- The carboxylated SWNTs recovered are not toxic, in agreement with predictions of simulation studies, and can be used for various applications with reduced cytotoxic ESH complications.

Industrial Interactions and Technology Transfer

- **Industrial interaction with Marc Heyns, IMEC.**
 - **Analysis of pads used for CMP of CNT's.**
- **Industrial interaction with Don Hooper, Intel.**
 - **ESH of CMP slurries.**
- **Industrial interaction with Mario Bolanos-Avila, TI.**
 - **ESH of packaging.**

Future Plans

Next Year Plans

- **Obtain data on physical and chemical characteristics of CNT and CMP nanoparticles with an initial attempt to correlate with structural modeling, interaction with model mammalian cells, toxicity, and bioactivity. (Deliverables Report, 2011)**
- **Acid-functionalize CNTs using our nitric acid reflux protocol to assess CNT toxicity vs. percent carboxylation.**
- **Preliminary ESH investigation of graphene oxide.**

Long-Term Plans

- **Obtain data on physical and chemical characteristics of CNT and CMP nanoparticles correlated with structural modeling, interaction with model mammalian cells, toxicity, and bioactivity. (Deliverables Final Report, 2012)**
- **Obtain ESH data on graphene and graphene oxide.**
- **ESH of packaging. (Mario Bolanos-Avila, TI: Strategic Packaging Research Manager)**

Presentations

- **ERC Teleseminar, April 16, 2009: “Challenges in Assessing the Potential Cytotoxicity of Carbon Nanotubes” by P. Pantano**
- **ERC Teleseminar, Nov. 12, 2009: “Computer Simulations of the Interaction between Carbon Based Nanoparticles and Biological Systems” by C.-c. Chiu**
- **AIST (Japan) seminar, 2009: “Nanoparticles from a Soft Matter Viewpoint” by S. Nielsen**
- **UT Arlington and TCU seminars, 2009: “Accurately Assessing the Potential Toxicity of Carbon Nanotubes and the Use of Carbon Nanotubes as Cancer Theranostic Agents” by P. Pantano**
- **UTD Institute for Innovation & Entrepreneurship: Conference on “Nanomedicine: Enterprise and Society”, Jan 22, 2010**

Publications

- **Draper, R.K.; Wang, R.; Mikoryak, C.; Chen, E.; Li, S. and Pantano, P. “Gel electrophoresis method to measure the concentration of single-walled carbon nanotubes extracted from biological tissue”. *Anal. Chem.* 81: 2944-2952 (2009).**
- **Katari, S.C.; Wallack, M.; Hubenschmidt, M.; Pantano, P. and Garner, H.R. “Fabrication and evaluation of a near-infrared hyperspectral imaging system”, *J. Microscopy* 236: 11-17 (2009).**
- **Marches, R.; Chakravarty, P.; Bajaj, P.; Musselman, I.H.; Pantano, P.; Draper, R.K. and Vitetta, E.S. “Specific thermal ablation of tumor cells using a monoclonal antibody covalently coupled to a single-walled carbon nanotube”, *Int. J. Cancer* 125: 2970-2977 (2009).**

Awards

- ***2010 Simon Karecki Award: graduate student Chi-cheng Chiu.***

Lowering the Environmental Impact of High-k and Metal Gate-Stack Surface Preparation Processes

(Task Number: 425.028)

PIs:

- **Yoshio Nishi, Electrical Engineering, Stanford University**
- **Srini Raghavan, Materials Science and Engineering, University of Arizona**
- **Bert Vermeire, Electrical Engineering, Arizona State University**
- **Farhang Shadman, Chemical Engineering, University of Arizona**

Graduate Students:

- **Gaurav Thareja, Electrical Engineering, Stanford University**
- **Kedar Dhane, Chemical Engineering, University of Arizona**
- **Davoud Zamani, Chemical Engineering, University of Arizona**
- **Shweta Agrawal, Materials Science and Engineering, University of Arizona**
- **Xu Zhang, Electrical Engineering, Arizona State University**

Research Scientists:

- **Jun Yan, Chemical Engineering, University of Arizona**
- **Junseok Chae, Electrical Engineering, Arizona State University**

Cost Share (other than core ERC funding):

- **\$50k from Stanford CIS**

SRC/SEMATECH Engineering Research Center for Environmentally Benign Semiconductor Manufacturing

Objectives

- **Development of non-fluoride based etch chemistries for hafnium based high-k materials**
- **Elimination of galvanic corrosion between metal gate and polysilicon during wet etching**
- **Significant reduction of water and energy (hot water) usage during rinse**
- **Determination of chemical and electrical characterization methodology for surface preparation of high k dielectric films.**
- **Validation of low resource-usage processes using Metal - high-k device fabrication and electrical characterization**

ESH Metrics and Impact

- **Reduction in the usage of HF and HCl; development of environmentally friendly, non-fluoride based etch chemistries for hafnium-based high-k materials**
- **Significant reduction in water usage during rinse**
- **Significant reduction in energy (hot water) usage during rinse**
- **Reduction of rinse time leading to increase in throughput and decrease in resource usage**

Subtask 1: Environmentally Friendly Chemical Systems for Patterning Silicates and Hafnium Oxide

BACKGROUND

- **In the formation of high k- metal gate structures by the “gate first” process, etching of high k material after ‘P-metal’ removal to prepare the surface for ‘N- metal’ deposition is required. Additionally, selective etching of high k material with respect to SiO₂ is also needed**
- **Currently used chemical system for etching Hf based high-k materials is dilute HF containing HCl; however, these high k materials become very difficult to etch when subjected to a thermal treatment**
- **HF based systems appear to induce galvanic corrosion of polysilicon, which is in contact with metal gate materials; reducing the oxygen level of HF has been recommended to reduce corrosion**

Materials and Experimental Procedures

- Materials

300 mm ALD HfO₂ wafers:

- Provided by ASM
- Film Thickness: ~ 230 Å

300 mm ALD HfSi_{0.74}O_{3.42}

wafers:

- Provided by ASM
- Film Thickness: ~ 240 Å

- Experimental Procedures:

- Wafer was cleaved into 2 x 3 cm pieces for testing
- Cleaned by IPA, rinsed with DI water and dried by N₂
- Etch rate determined from thickness measurements made by spectroscopic ellipsometer (J. A. Woollam Co.) at 5 different locations
- Heat treatment and reduction tests were conducted in a tube furnace;
50% N₂ and 50% H₂ gas mixture was used for reduction tests
- Dilute HF was used for baseline etch rate measurements; ammonium hydroxide was tested as an alternate etchant

Baseline Etch Tests on ALD HfO₂ in Dilute HF Solutions

HF concentration (%)	Temperature (°C)	ER _{HfO₂} (Å/min)	Selectivity ER _{HfO₂} :ER _{SiO₂}
0.01	25	1.5	4.8 : 1
0.1	25	4.1	2.2 : 1
1	25	27.6	0.5 : 1

- **Better etch selectivity of HfO₂ (with respect to SiO₂) at low concentrations of HF---trend in line with literature data for MOCVD HfO₂**

Wet Etching of ALD HfSi_xO_y in Dilute HF Solutions

HF concentration (%)	Temperature (°C)	Reduced in 50%H ₂ /50%N ₂	ER _{HfSi_xO_y} (Å/min)	Selectivity ER _{HfSi_xO_y} :ER _{SiO₂}
0.01	25	No	2.2	7.1 : 1
0.1	25	No	23.2	12.6 : 1
1	25	No	328.4	5.3 : 1
0.1	400	No	23.8	12.9:1
0.1	400	Yes	22.8	12.4:1

- **Hafnium silicate etches at a higher rate than HfO₂ in dilute HF solutions**
- **Heat treatment in hydrogen does no affect the etch rate of hafnium silicate significantly**

Alternative Etch Chemistries for Hafnium Oxide and Silicate

- Literature data indicates that dissolution of metal silicates such as copper silicates is possible in ammoniacal solutions with a pre-reduction treatment in H_2/N_2 or CO/CO_2
- First set of experiments carried out on hafnium oxide and silicate films exposed to $50\%H_2/50\%N_2$ at different temperatures for different duration
- Films subsequently immersed in ammonium hydroxide solutions

Feasibility of Etching of HfO₂ and HfSi_xO_y in Ammonical Solutions Using a Pre-reduction Treatment

Reduction Temperature (°C)	400	200	100
Reduction Time (hr)	0.5	1	3
pH of Ammonium Hydroxide	9.95	13.8	
Time in Ammonium Hydroxide (hr)	1	21	
Etch Rate (HfO ₂ and HfSi _{0.74} O _{3.42})	insignificant		

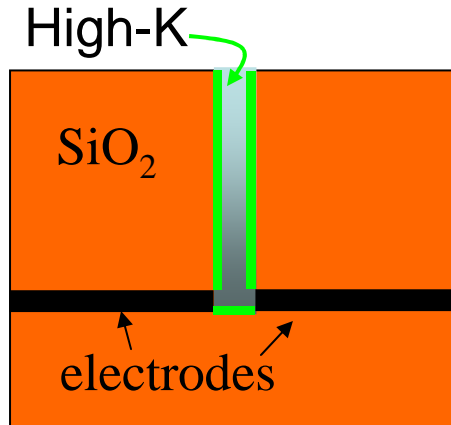
Pre-reduction in H₂/N₂ mixture appears to be ineffective in making HfO₂ and HfSi_{0.74}O_{3.42} soluble in ammoniacal solutions.

Subtask 2: Low-Water and Low-Energy New Rinse and Drying Recipes and Methodologies

BACKGROUND

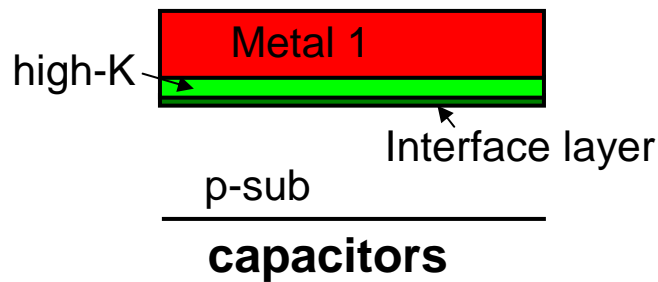
- **Formation of high-k metal gate structures requires cleaning of fine geometries containing materials not traditionally used by the semiconductor industry. Wet etching must be quenched at the appropriate time**
- **More single wafer tools are used for cleaning, rinsing and drying because of better yield. Optimization of cycle time is critical for throughput and reduced resource usage**
- **Elucidating rate-limiting mechanisms to make possible multi-stage, resource-efficient recipes requires in-situ and real-time measurements and accurate simulation capabilities**
- **Validation of low resource-usage processes for high-volume manufacturing using electrical test structures**

Test Structures for Experimental Work

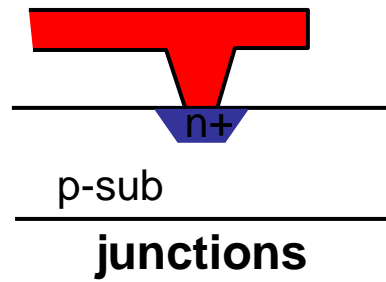


AC impedance of high aspect ratio feature to determine cleaning and drying kinetic parameters in-situ

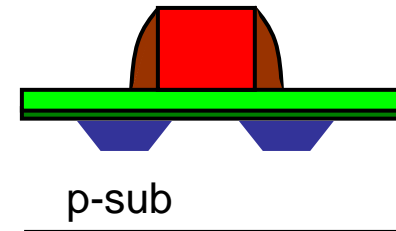
Quartz Crystal Microbalance to determine etch rates and adsorption/desorption rates



capacitors



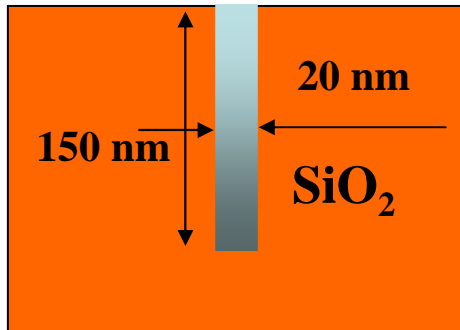
junctions



transistors

Electrical test structures (capacitors, junctions, transistors) to evaluate impact of new recipes on performance

Rinsing/Cleaning of Heterogeneous Nano- Structures



Conventional Structure

The introduction of high-k dielectric makes the surface structure heterogeneous. Rinse must clean both surfaces

A newly developed spin-rinse model was used to parametrically study the heterogeneous structure rinse.

Multi-component transport equations :

$$\frac{\partial C_i}{\partial t} = \nabla \cdot (D_i \nabla C_i + z_i F \mu_i C_i \nabla \phi)$$

Surface adsorption and desorption:

$$\frac{\partial C_S}{\partial t} = k_a C_b (S_0 - C_S) - k_d C_S$$

Poisson equation: $\nabla^2 \phi = -\frac{\rho}{\epsilon}$

Nomenclature

C_i = Liquid Concentration

D_i = Diffusivity

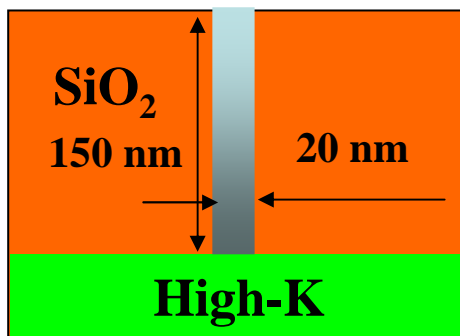
C_s = Surface Concentration

S₀ = Maximum sites available

k_a = Adsorption coefficient

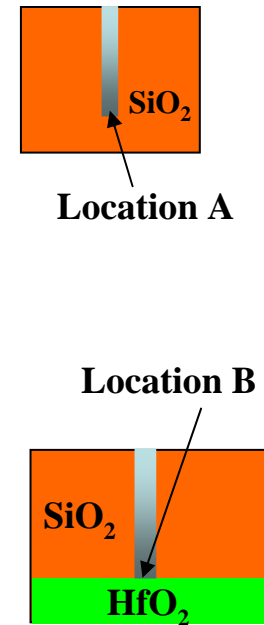
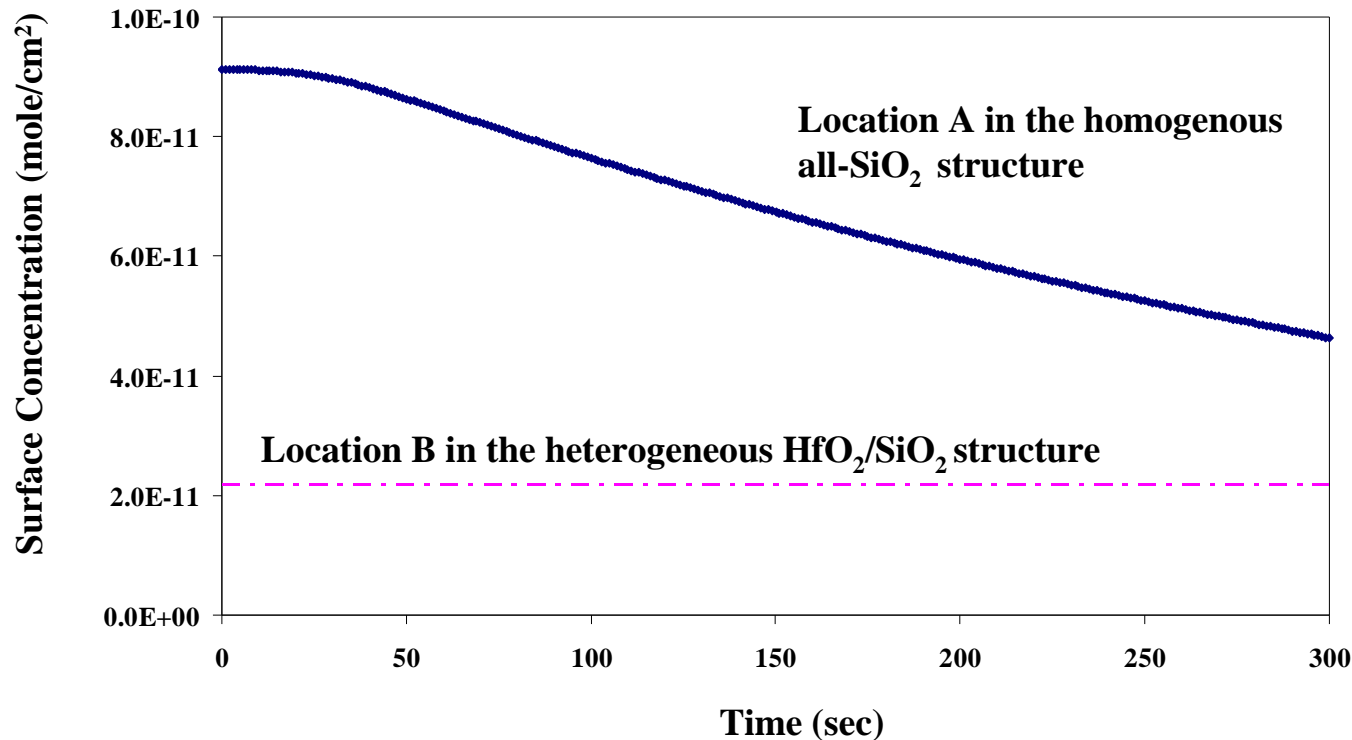
k_d = Desorption coefficient

Φ = Electrostatic Potential



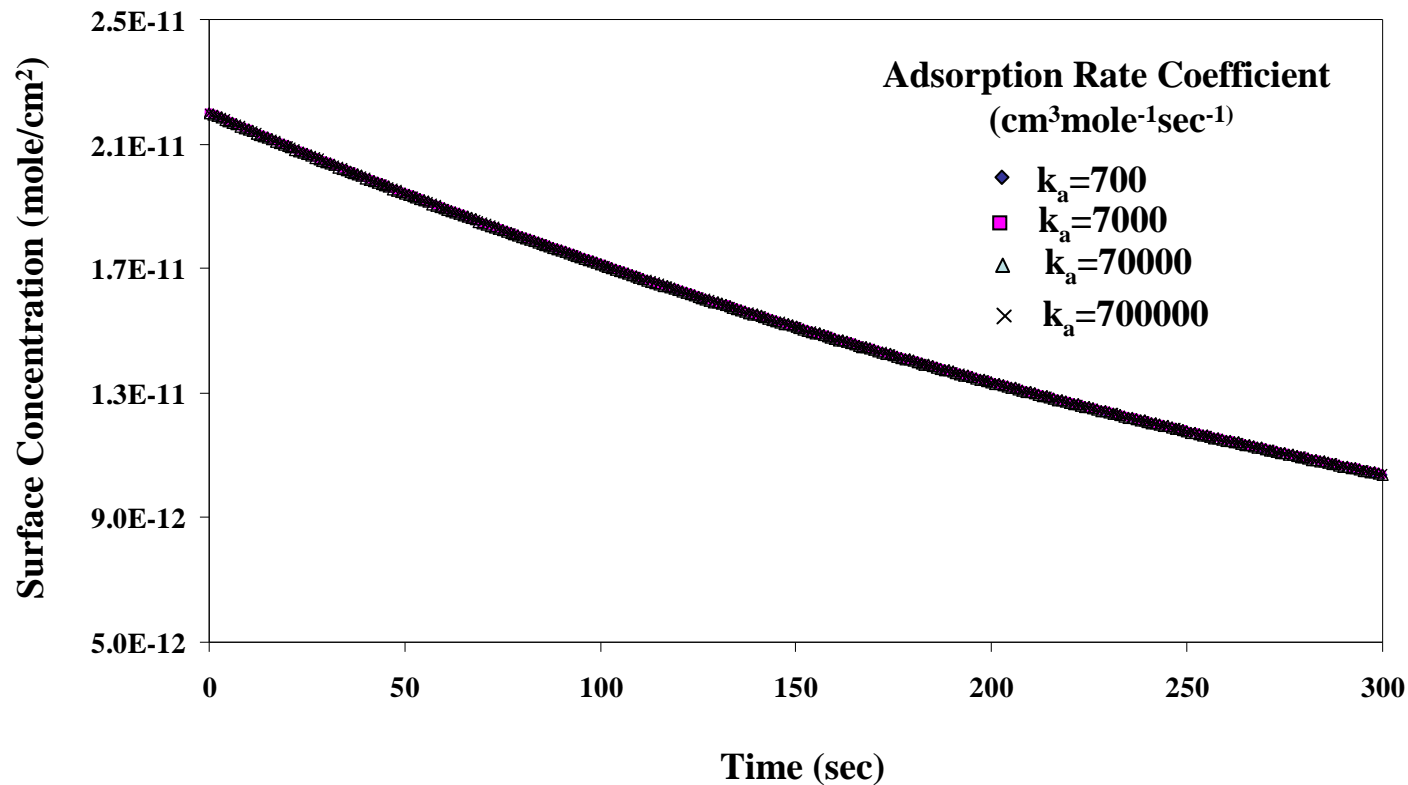
Structure with high-k

Challenges in Rinsing of Nano-Structures that Include HfO₂



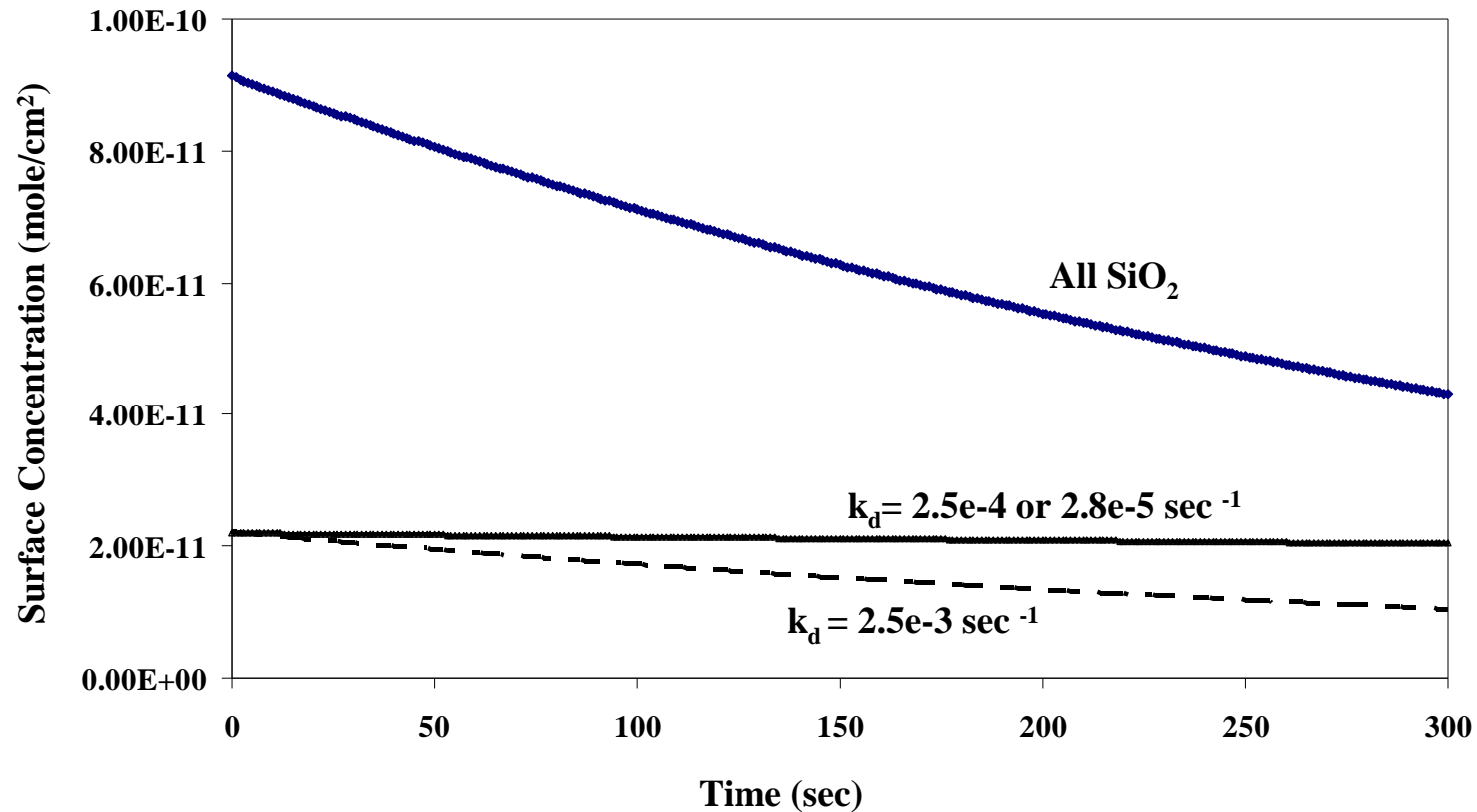
- HfO₂ has lower surface adsorption capacity compared to SiO₂. However, the sites are more energetic and adsorb contaminants more strongly (difficult to clean).
- Current rinse recipes for SiO₂ need to be modified in applications involving heterogeneous structures with Hf-based high-k dielectrics.

Impact of Adsorption Rate on the Cleaning of High-k Dielectric Nano-Structures



Adsorption of contaminants on various dielectrics appears to be thermodynamically favorable; it readily takes place as long as surface is not saturated.

Impact of Desorption Rate on the Cleaning of High-k Dielectric Nano-Structures



The desorption dynamics play a key role in the cleaning of various high-k dielectrics (bottleneck and rate limiting in the overall process)

Electrical Tests Structures

- **Ge as a performance booster and sample novel material**
 - **High electron/hole mobility**
 - **High process compatibility**
 - **Low temperature process**
 - **Possible V_{dd} scaling for reduced power dissipation**

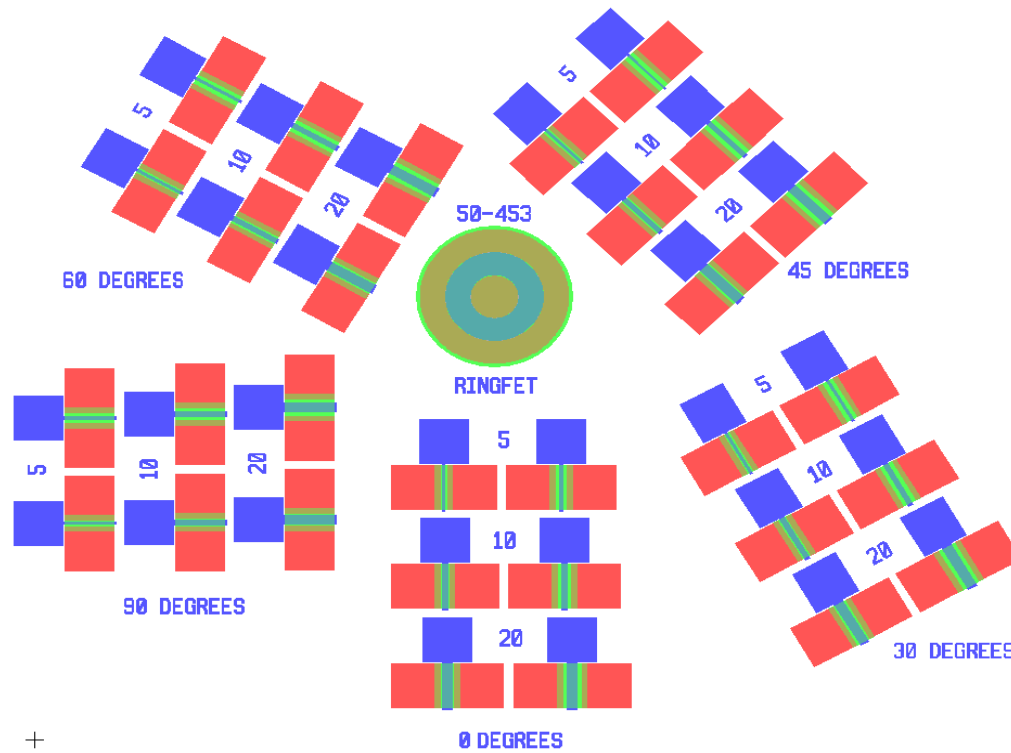
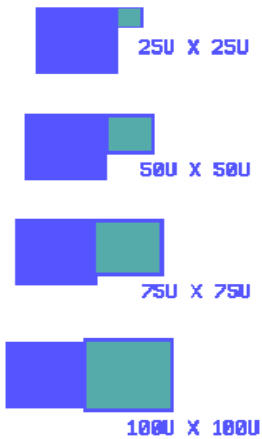
	Si	Ge
Electron m (cm ² /Vs)	1600	3900
Hole m (cm ² /Vs)	430	1900
Band gap (eV, 300K)	1.12	0.66
Dielectric constant	11.9	16
Melting point (°C)	1415	937

- **Key challenges: Interface property of Ge MOS gate stack**
 - **GeO₂ is regarded as a promising interface gate dielectrics***
 - **Since GeO₂ decomposition/GeO evaporation temperature is very low (430°C), low temperature oxidation is needed with high density of oxidant source**

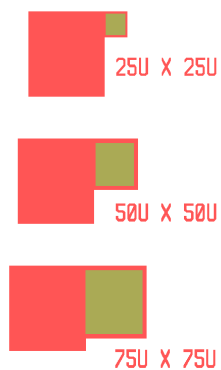
**D. Kuzum, IEDM2007, T. Takahashi, IEDM2007, Y. Nakakita, IEDM2008*

MOSFET Photolithography Mask Design

MOS CAPACITOR

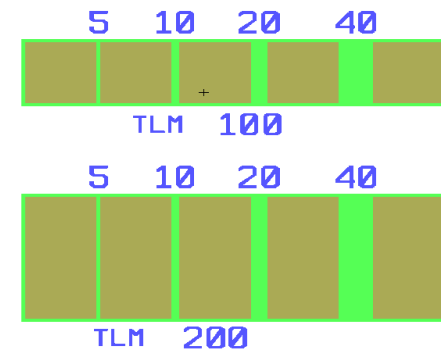
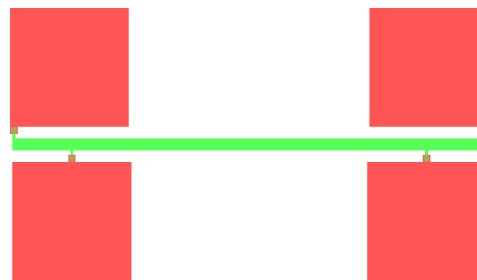


P-N JUNCTION DIODE



+

FOUR POINT PROBE

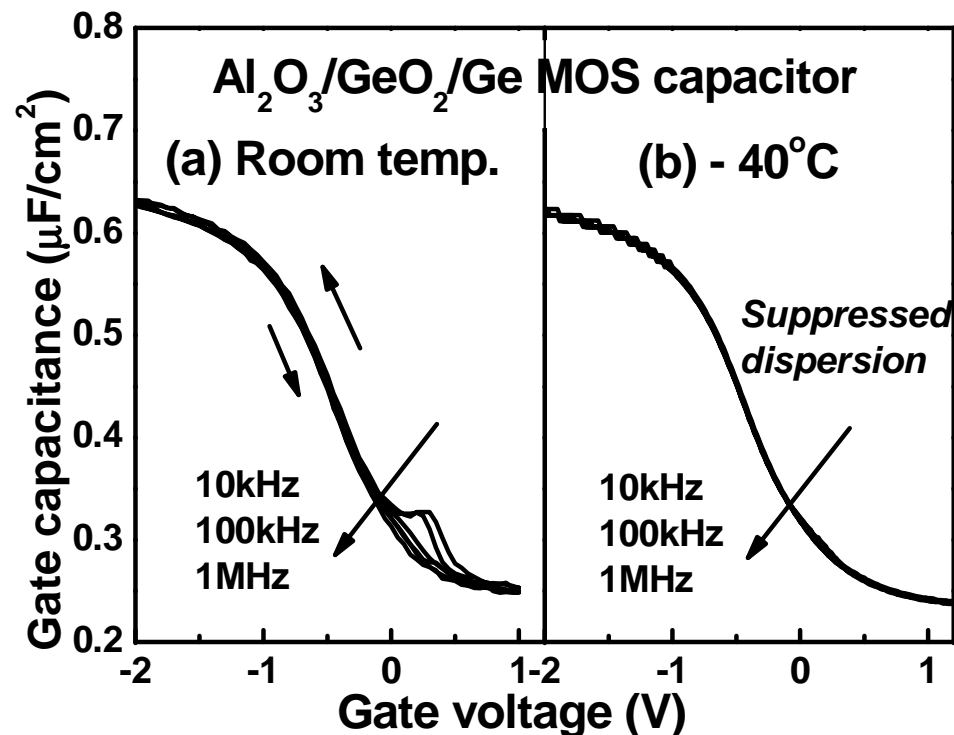


Experiments: Baseline of Cleaning Process using Capacitor Test Structures

- **Sample preparation**
 - (100) and (111) Ge surface was cleaned by PRS100 organic remover and by HCl/HF
 - Surface was oxidized by Slot-Plane-Antennal (SPA) radical oxidation system
 - Thermal oxidation was also done as a reference
- **Electrical property**
 - 5nm ALD Al₂O₃ was deposited on GeO₂/Ge
 - Sputtered Al metal pad
 - 400°C FGA anneal
 - XPS was used to identify surface chemical property
 - Synchrotron radiation photoemission spectroscopy (SRPES) was used for band offset measurement

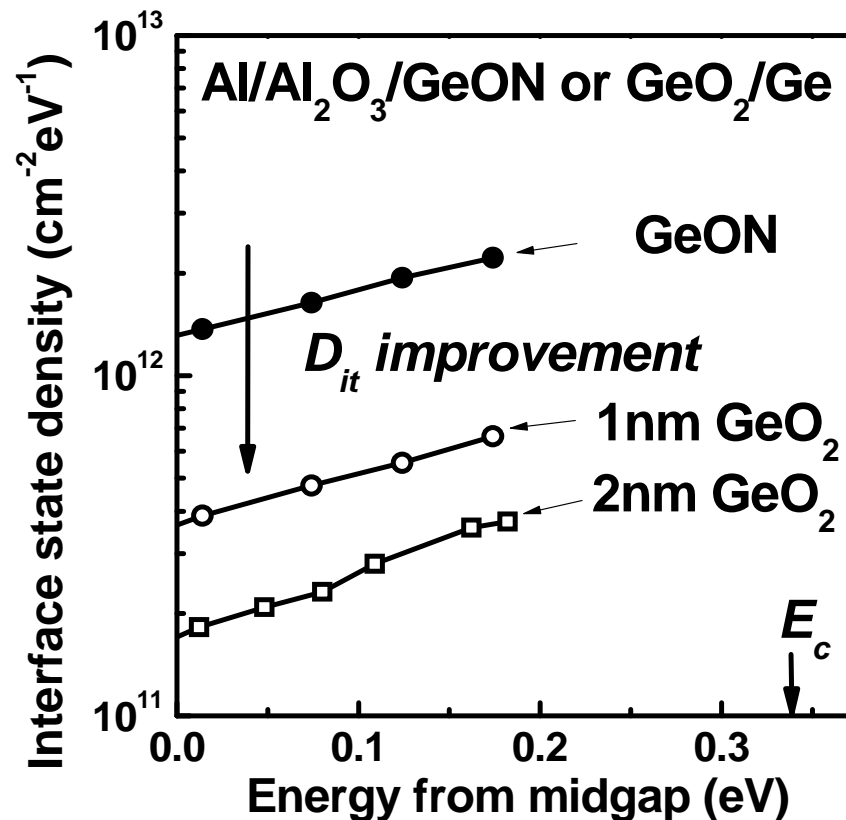
Electrical Properties of GeO₂/Ge Interface

- Al/Al₂O₃/GeO₂/Ge Ge MOS capacitor:
 - 350°C ALD Al₂O₃ deposition + 400°C FGA anneal
 - Very small hysteresis and frequency dispersion
 - Low temperature measurement suppresses frequency dispersion due to minority carrier response



Interface State Density (D_{it}) of GeO_2/Ge

- Comparison between GeON and GeO_2 using capacitor structures
 - D_{it} was measured by conductance method
 - Significant improvement from GeON
 - Achieved $D_{it} = 1.4 \times 10^{11} \text{ cm}^{-2} \text{ eV}^{-1}$ at midgap



Summary

- **Conducted baseline etch tests on ALD HfO₂ and HfSi_xO_y in dilute HF**
- **Investigated the feasibility of etching the materials in ammonium hydroxide solutions after a pre-reduction treatment in H₂/N₂ gas mixtures**
- **Determined the rinse process parameters that are needed and will be used in developing reliable and robust low-water rinse recipes for cleaning of heterogeneous nano-structures**
- **Benchmarked high-k process with electrical characterization using new electrical test structures**

Industrial Interactions and Technology Transfer

- **Collaborative interactions with Initiative for Nanoscale Materials and Processes, INMP, at Stanford which is supported by 7 semiconductor and semiconductor equipment manufacturing companies.**
- **Interactions with ASM (Eric Shero and Eric Liu) for preparation of high-k test samples**

Future Plans

Next Year Plans

- **Pre-reduction of High-k wafers in CO/CO₂ mixtures to improve etching**
- **Use of complexing and chelating agents such as EDTA, and disulfonic acids in ammoniacal solutions to enhance dissolution**
- **Development of methodology and recipes for efficient rinsing and drying of heterogeneous structures using both process simulation and experimental measurements**
- **Ge P/N-MOSFET fabrication and electrical characterization
carrier mobility analysis – substrate orientation and channel anisotropy**
- **Electrical testing methodology applied for comparison of etch and clean/rinse/dry of high-k dielectric using new high aspect ratio features**

Publications, Presentations, and Recognitions/Awards

- Masaharu Kobayashi, Gaurav Thareja, Masato Ishibashi, Yun Sun, Peter Griffin, Jim McVittie, Piero Pianetta, Krishna Saraswat, Yoshio Nishi, “Radical oxidation of germanium for interface gate dielectric GeO₂ formation in metal-insulator-semiconductor gate stack,” *Journal of Applied Physics*, 106, 104117, 2009.
- X. Zhang, J. Yan, B. Vermeire, F. Shadman, J. Chae, “Passive wireless monitoring of wafer cleanliness during rinsing of semiconductor wafers,” *IEEE Sensors* (accepted).

Sugar-Based Photoacid Generators (“Sweet” PAGs): Environmentally Friendly Materials for Next Generation Photolithography

(Task Number: 425.029)

PIs:

- Christopher K. Ober, Materials Science and Engineering, Cornell University
- Reyes Sierra, Chemical and Environmental Engineering, UA

Graduate Students:

- Lila Otero, PhD candidate, Chemical & Environmental Engineering, UA

Undergraduate Students:

- Lily Milner, Chemical & Environmental Engineering, UA

Other Researchers:

- Youngjin Cho, Postdoctoral Fellow, Materials Science & Eng., Cornell University
- Wenjie Sun, Postdoctoral Fellow, Chemical & Environmental Engineering, UA

Cost Share (other than core ERC funding):

- Intel support for laser spike annealing; \$100k (Jing Sha moved to this project)

SRC/SEMATECH Engineering Research Center for Environmentally Benign Semiconductor Manufacturing

Objectives

- **Develop PFOS free and environmentally friendly photoacid generators (PAGs) with sugar-like or other natural structure for chemically amplified resist application**
- **Develop PAGs with superior imaging performance**
- **Evaluate lithographic performance in selected model 193 nm and EUV resists**
- **Evaluate the environmental aspects of new PAGs**

ESH Metrics and Impact

1. *Reduction in the use or replacement of ESH-problematic materials*

Complete replacement of perfluorooctanesulfonate (PFOS) structures including metal salts and photoacid generators in photoresist formulations

2. *Reduction in emission of ESH-problematic material to environment*

Develop new PAGs that can be readily disposed of in ESH friendly manner

3. *Reduction in the use of natural resources (water and energy)*

New PAGs prepared using simple, energy reduced chemistry in high yields and purity to reduce water use and the use of organic solvents.

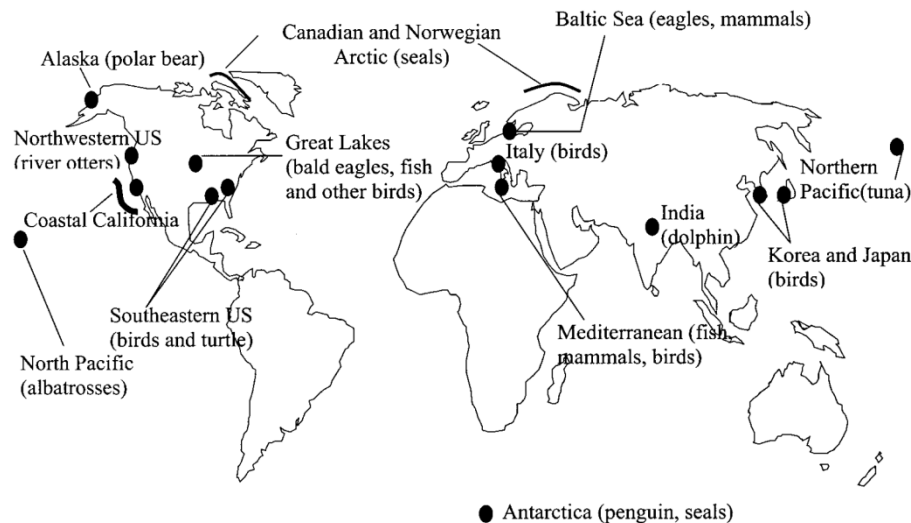
4. *Reduction in the use of chemicals*

Reduce the use of fluorinated chemicals.

Bioaccumulation of PFOS

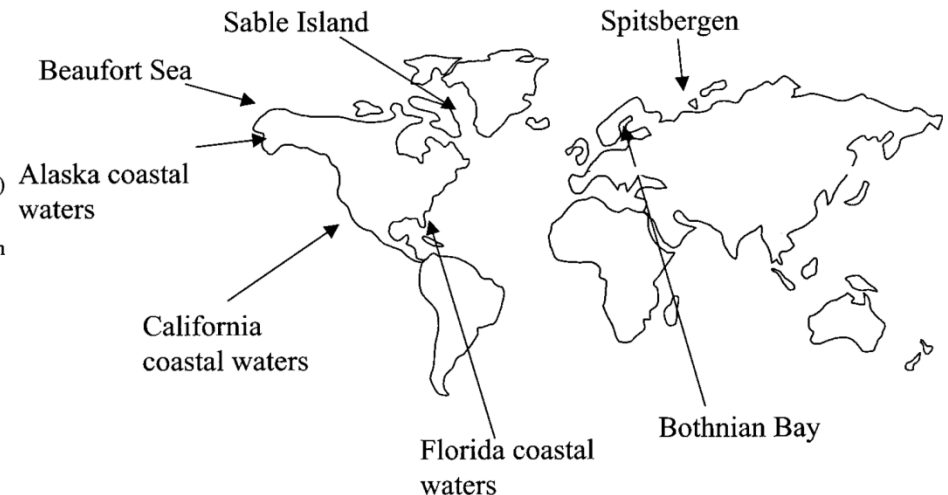
► PFOS and PFOS-related materials are potentially environmentally hazardous

Global Distribution of PFOS in Wildlife



Environ. Sci. Technol. 2001, 35, 1339.

Accumulation of PFOS in Marine Mammals



Environ. Sci. Technol. 2001, 35, 1593.

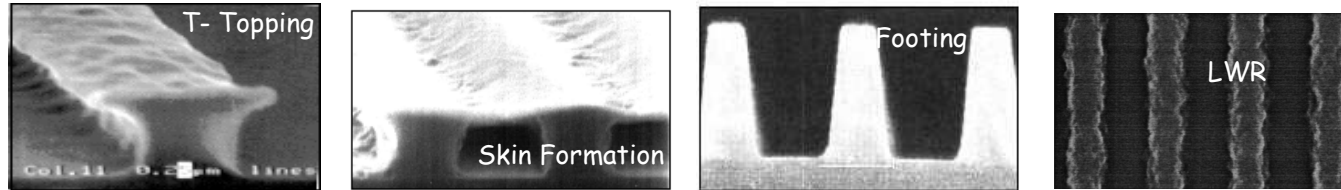
The EPA proposed a significant new use rule (SNUR) for PFOS in 2000

Next Generation PAGs – environmentally friendly, no bioaccumulation

SRC/SEMATECH Engineering Research Center for Environmentally Benign Semiconductor Manufacturing

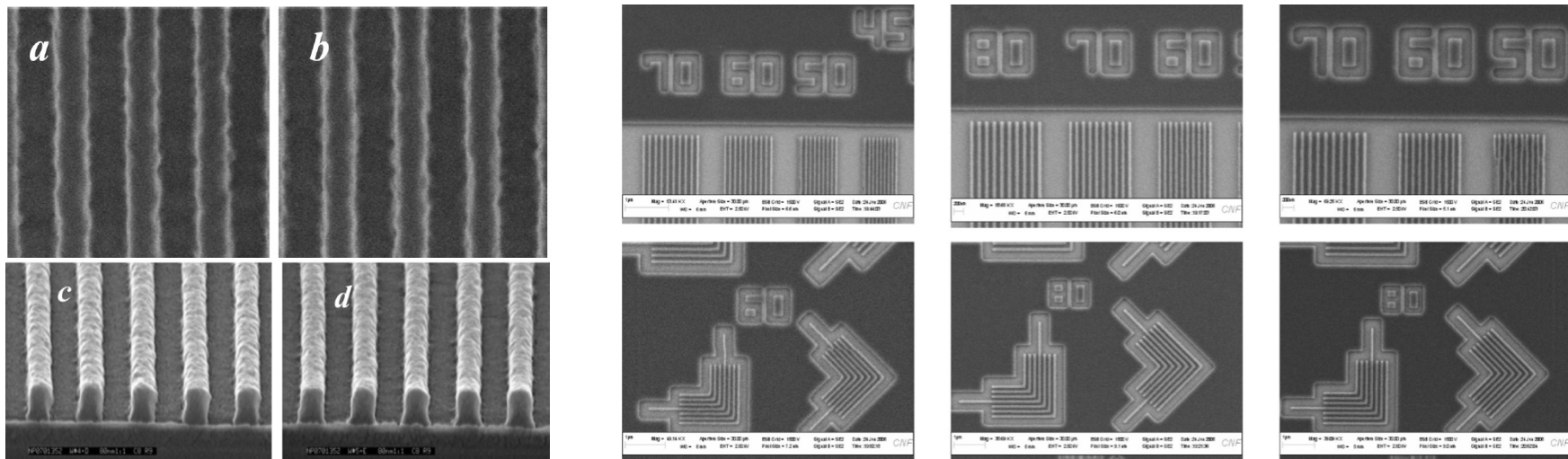
PFOS PAG Performance Issues

“Segregation or non-uniform distribution of PAG”



➔ Surface segregation increases with increase in fluorine content

“PFOS free new PAG”: high resolution patterning



Top-down and cross-sectional SEM images of 90 nm dense lines of resist films of TPS NB (a and c) and the sweet PAG (b and d) patterned by 193 nm lithography. Esize (mJ/cm²): a, 23.8; b, 27.3. LER (nm): a, 5.8; b, 6.5.

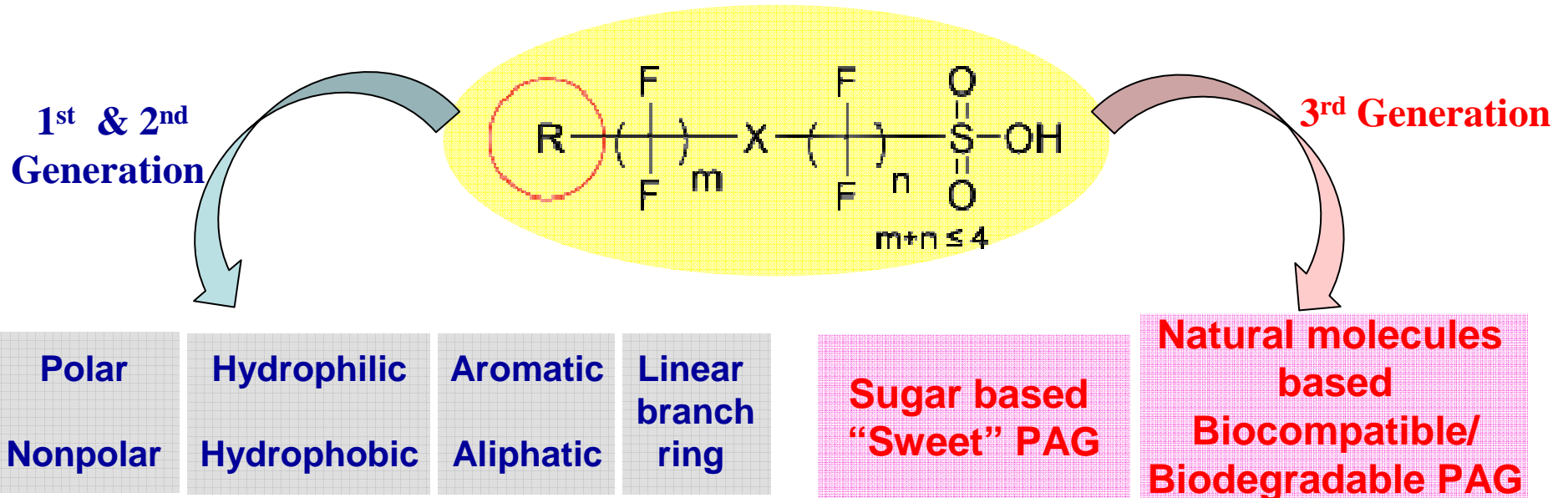
Top-down SEM images of resist films of poly(GBLMA-co-MAdMA) blended separately with TPSGB (left column), TPSNB (middle column), and TPS PFBS (right column) patterned by EUV lithography.

C.K. Ober et al., *Chem. Mater.* (2009); C.K. Ober et al., *JPST* (1999); J. L. Lenhart et al., *Langumir* (2005); W. Hinsberg et al., *SPIE* (2004); M. D. Stewart et al., *JVSTB* (2002)

SRC/SEMATECH Engineering Research Center for Environmentally Benign Semiconductor Manufacturing

Molecular Design of New PAGs: PFOS-free salts

For environmentally friendly and excellent performance:

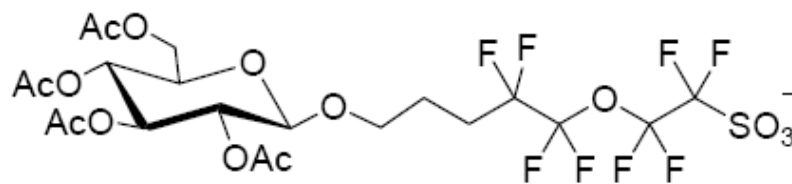
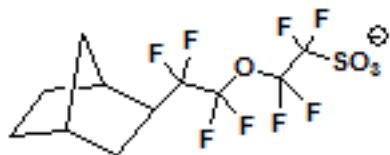
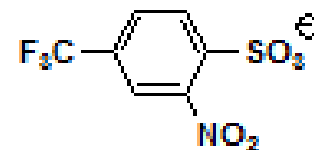
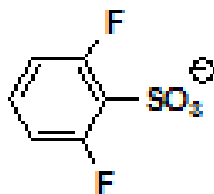
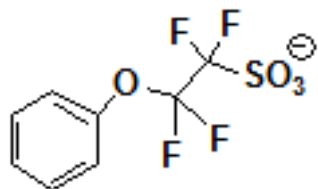


Practical synthetic chemistry considerations:

- Simple chemistry — low cost & less time
- Efficient reactions — high yield & high purity

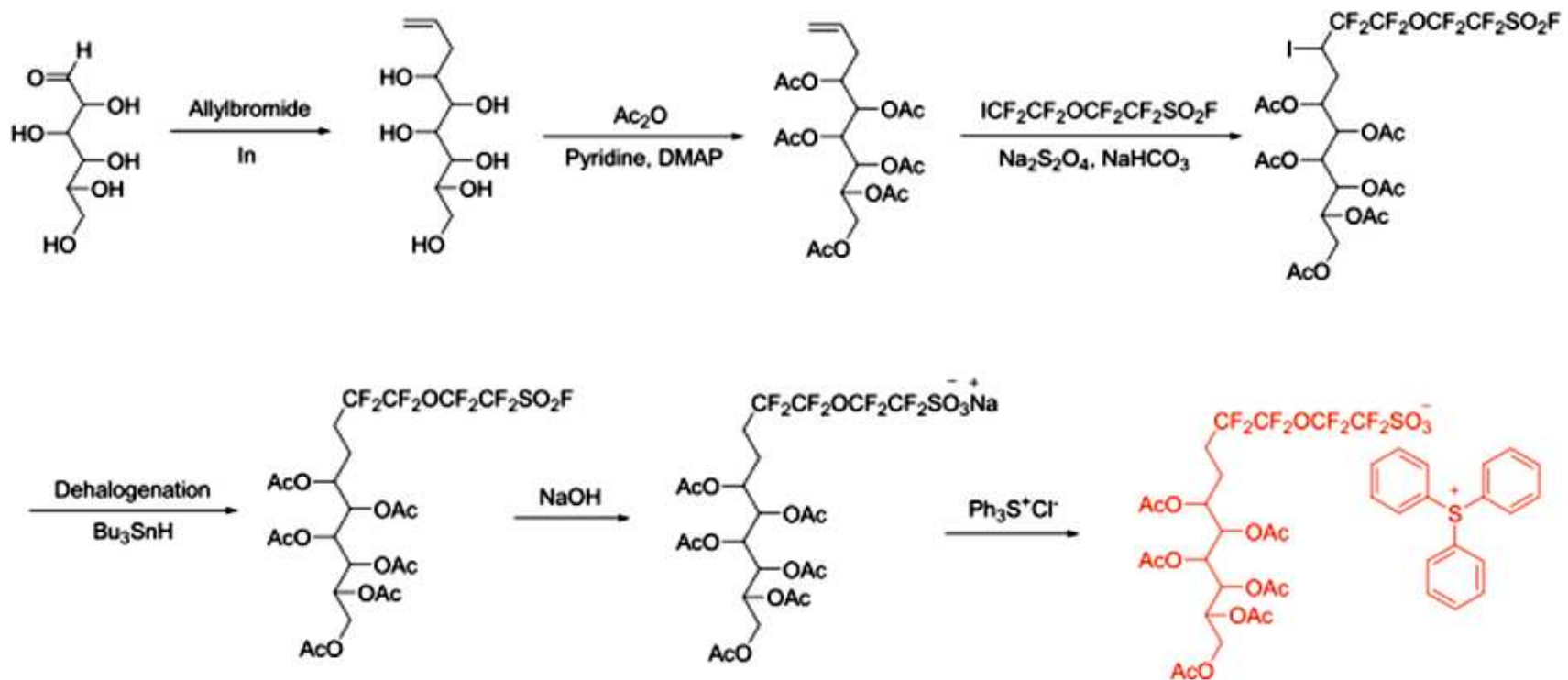
New Non-PFOS PAG Anions

Selected examples:



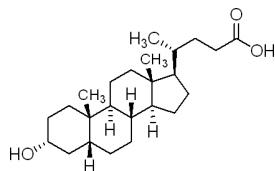
Synthesis of linear type “Sweet” PAG

➤ Synthetic scheme:

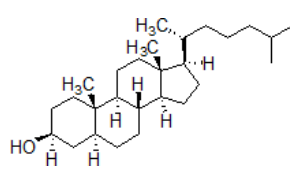


Synthesis of “Biocompatible” PAGs

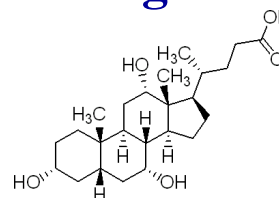
➤ New PAGs based on Steroids and their analogs:



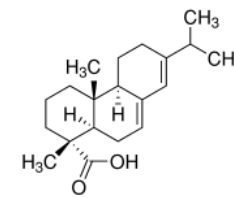
Lithocholic acid



Dihydrocholesterol

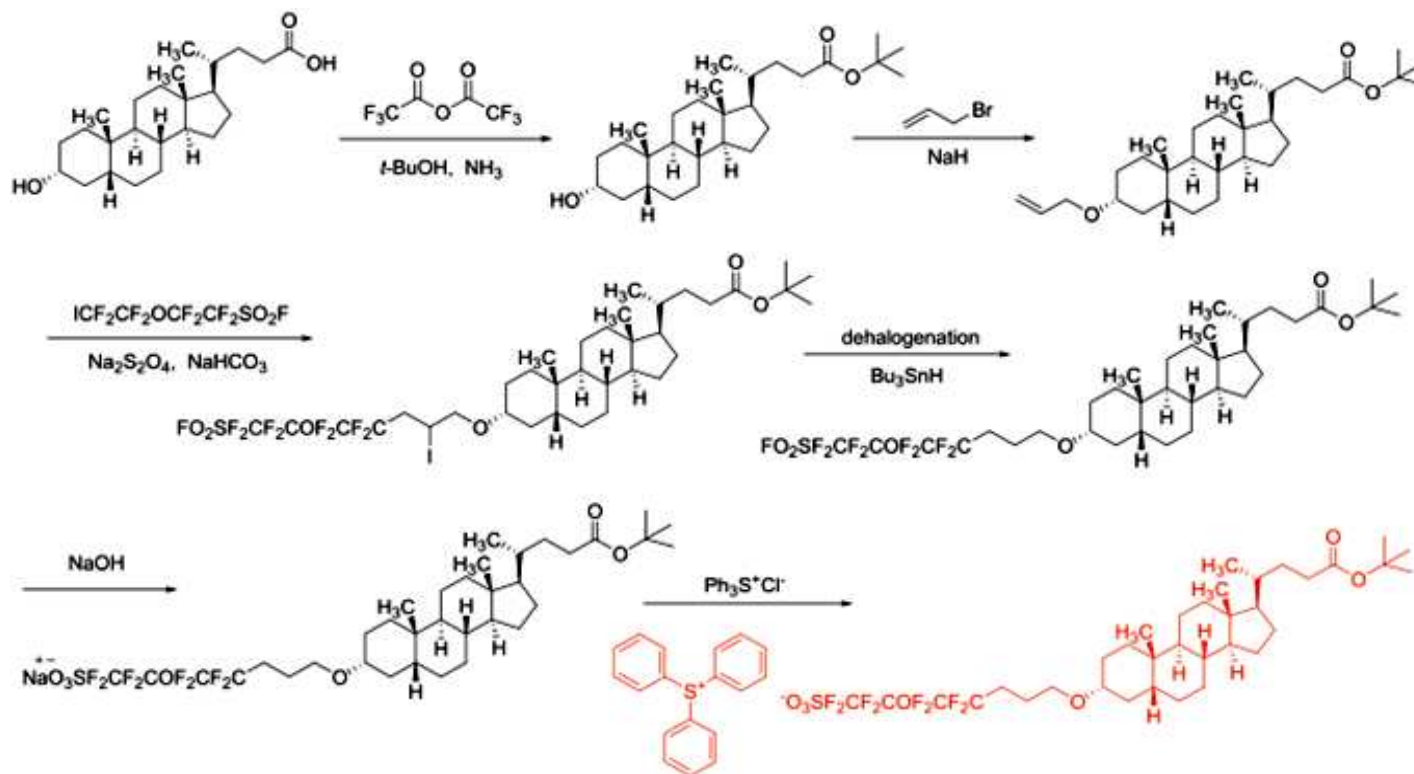


Cholic acid



Abietic acid (Pine resin acid)

➤ Synthetic scheme:



Evaluation of Lithographic Performance

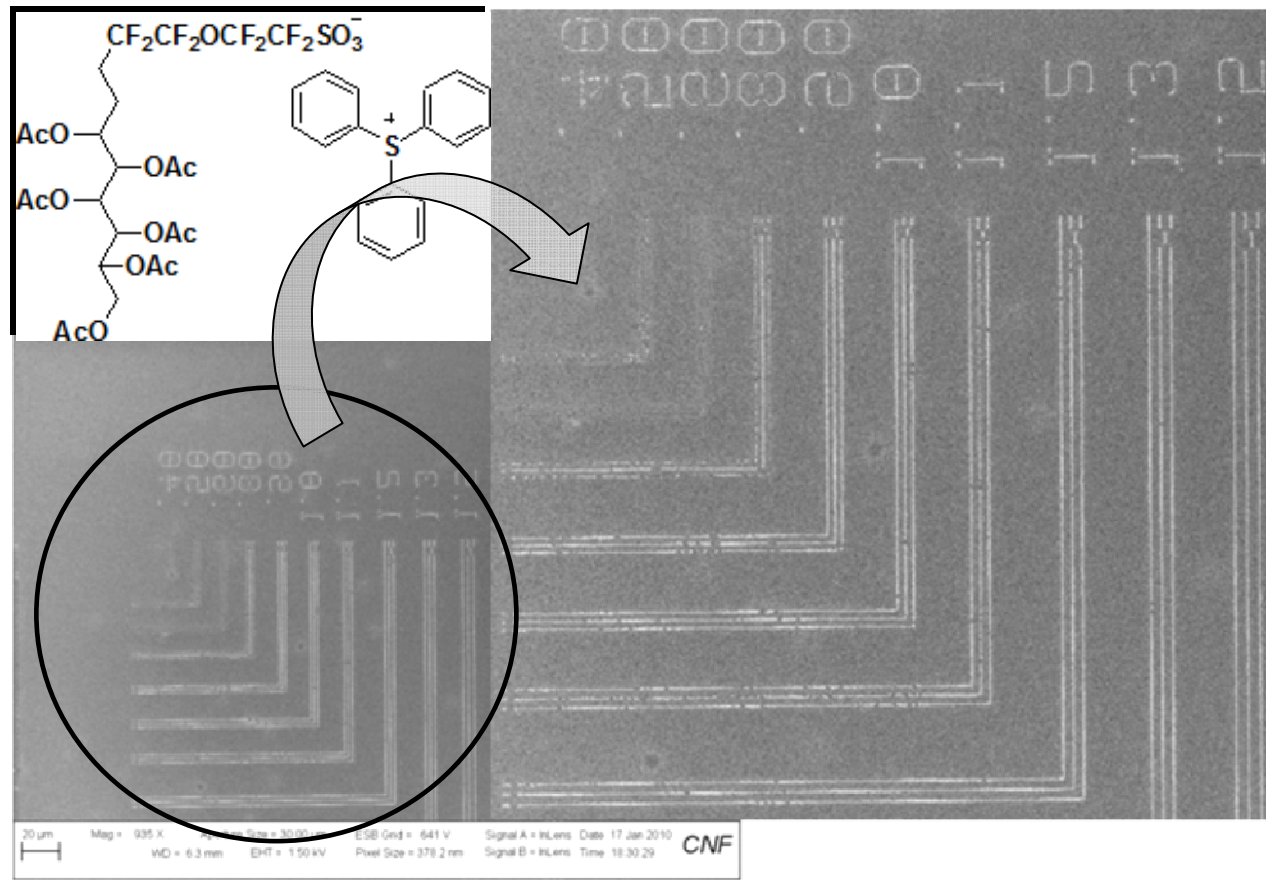
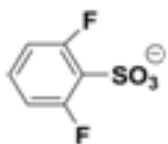


Figure. The SEM images of resist films of ESCAP blended separately with linear type Sweet PAG.

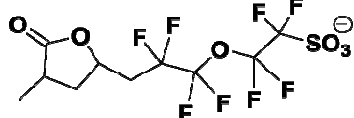
Environmental Compatibility of New Non-PFOS PAG Anions

Selected examples:



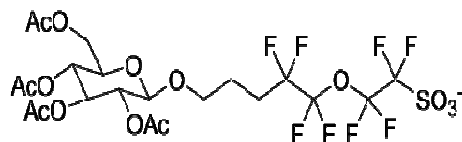
1st generation

(Aromatic structure)



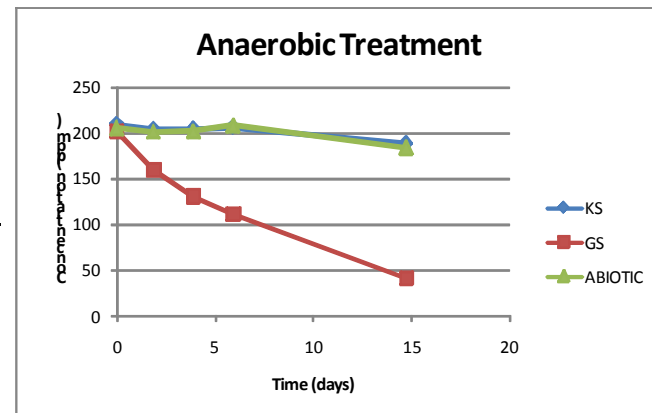
2nd generation

(Aliphatic structure)



3rd generation

(Sugar structure)

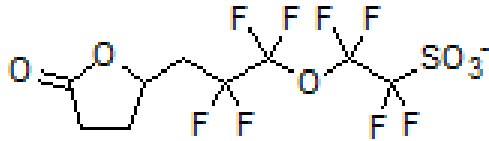


Degradation for 2nd generation PAG in anaerobic batch bioassays. (KS) Abiotic sterilized control; (GS) complete treatment with active sludge; (ABIOTIC) sterile, non-inoculated control.

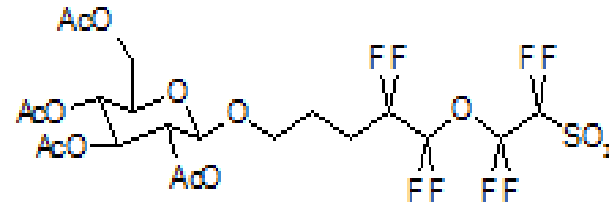
- **1st Generation Non-PFOS PAGs:** Low toxicity and low bioaccumulation potential but relatively persistent to microbial degradation.
- **2nd Generation Non-PFOS PAGs:** Preliminary results show that replacing the phenyl group with a UV-transparent alicyclic moiety increases the susceptibility of the PAG compound to biodegradation.
- **3rd Generation Non-PFOS PAGs:** Replacing with sugar and natural groups is expected to increase biodegradation.

Chemical Degradation of New Generation PAGs

Advanced Oxidation: Fenton's Reaction ($\text{Fe(II)/H}_2\text{O}_2$)



Lactone



Sweet PAG (Sweet)

	Degradation	PAG Removed (%)	Fluoride Released (%)
Lactone PAG	YES	100	5.7
Sweet PAG	YES	100	8.7
PFOS	NO	0.8	0.6
PFBS	NO	0.5	0.4

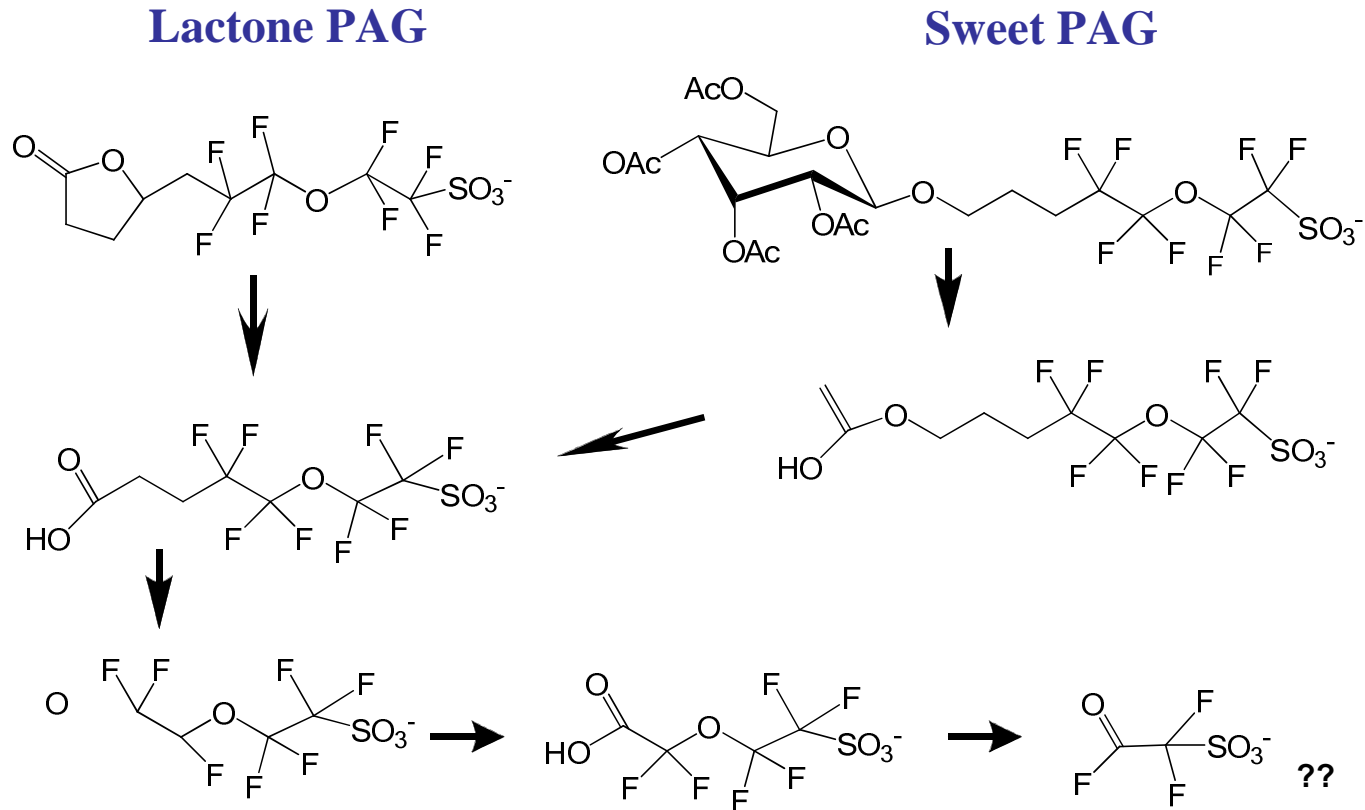
Fenton's reaction: $\text{Fe}^{2+} + \text{H}_2\text{O}_2 \rightarrow \text{Fe}^{3+} + \cdot\text{OH} + \text{OH}^-$, $\text{Fe}^{3+} + \text{H}_2\text{O}_2 \rightarrow \text{Fe}^{2+} + \cdot\text{OOH} + \text{H}^+$

PAG + radicals \rightarrow Oxidized products

Fenton's treatment effective in removing the biomolecule-based non-PFOS PAGs

Chemical Degradation of New Generation PAGs

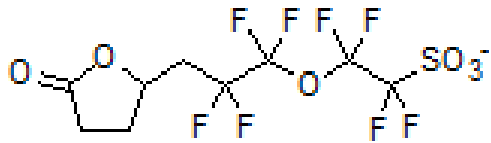
Advanced Oxidation: Fenton's Reaction ($\text{Fe(II)/H}_2\text{O}_2$)



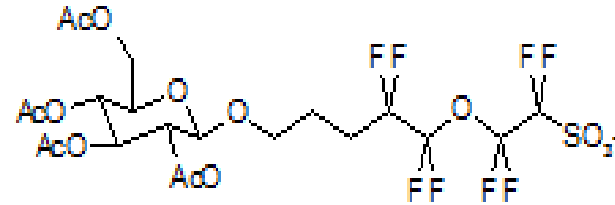
Proposed degradation mechanism based on mass spectrometry (MS) data

Chemical Degradation of New Generation PAGs

Reductive Attack with Zero-Valent Iron (ZVI)



Lactone



Sweet PAG (Sweet)

	Degradation	PAG Removed (%)	Fluoride Released (%)
Lactone PAG	NO	1.0	0.3
Sweet PAG	NO	1.0	0.8
PFOS	NO	0	0
PFBS	NO	0	0

Redox degradation by ZVI: $\text{Fe}^0 \rightarrow \text{Fe}^{2+} + 2\text{e}^-$, $\text{PAG} + 2\text{e}^- \rightarrow \text{Reduced PAG}$

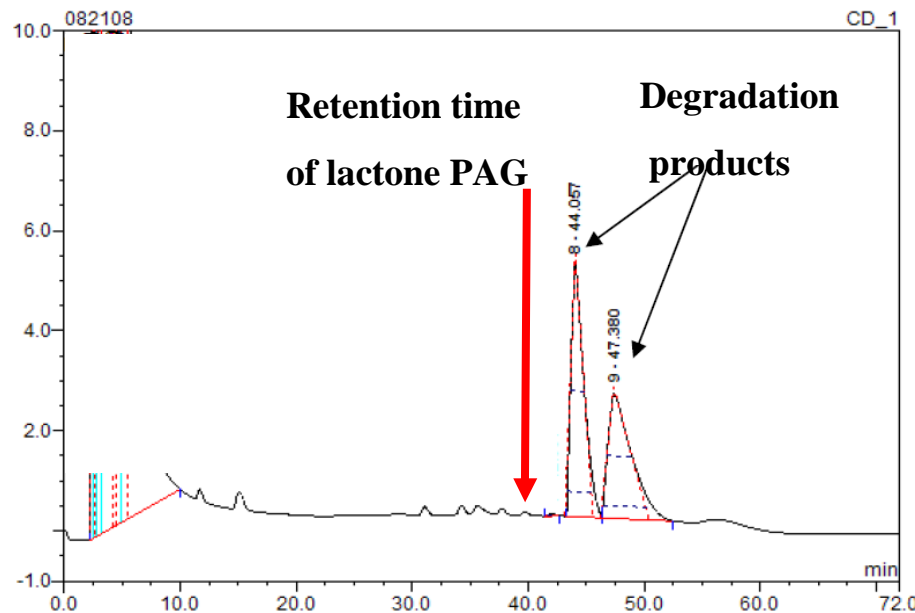
Reductive treatment with ZVI not effective in removing the biomolecule-based non-PFOS PAGs

SRC/SEMATECH Engineering Research Center for Environmentally Benign Semiconductor Manufacturing

Microbial Degradation of New Generation PAGs

Biomolecule-based PAGs are degraded by microorganisms in activated sludge

Compounds	Aerobic Degradation	Anaerobic Degradation
Lactone PAG	YES	NO
Sweet PAG	YES	NO
PFOS	NO	0
PFBS	NO	0



Ion chromatogram obtained for after aerobic incubation of lactone PAG

Formation of several unidentified degradation products by microbial degradation of lactone PAG and sweet PAG was confirmed by ion chromatography and mass spectrometry (MS) analysis

Industrial Interactions and Technology Transfer

- **Collaboration with Rohm & Haas Electronic Materials for photolithography tests of Sweet PAG concluded**
- **Samples provided to Orthogonal, Inc. – a small startup**
- **Performance at 193 nm and EUV evaluated with the assistance of International Sematech**
- **Ongoing interactions with Intel on LER issues**

Future Plans

Next Year's Plans :

- Prepare new generation of linear Sweet PAG and Biocompatible PAG
- Environmental evaluation of the Biocompatible PAGs
- Modification of sulfonium cationic groups
- Reduce synthetic steps and use more environmentally friendly chemicals
- Summarize previous studies and submit manuscripts for transfer of know-how to technical community

Long-Term Plans :

- Establish the relationship between photoacid generators' structure and their environmental properties
- Use advanced analytical tools to evaluate photoacid generators' environmental properties

Publications, Presentations, and Recognitions/Awards

Publications

- Yi Y., Ayothi R., Wang Y., Li M., Barclay G., Sierra-Alvarez R., Ober C. K. “Sulfonium Salts of Alicyclic Group Functionalized Semifluorinated Alkyl Ether Sulfonates As Photoacid Generators” *Chem. Mater.* 2009, 21, 4037.
- Jing Sha, Byungki Jung, Michael O. Thompson, and Christopher K. Ober, “Submillisecond post-exposure bake of chemically amplified resists by CO₂ laser spike annealing”, *J. Vac. Sci. Technol. B*, 27(6), 3020-3024 (2009)
- Ayothi R., Yi Y., Cao H. B., Wang Y., Putna S., Ober C. K. “Arylonium Photoacid Generators Containing Environmentally Compatible Aryloxyperfluoroalkanesulfonate Groups” *Chem. Mater.* 2007, 19, 1434.
- Ober C. K., Yi Y., Ayothi R. “Photoacid generator compounds and compositions” *PCT Application* WO2007124092, April 2007.

Presentations

- Gutenberg Research Prize Award Address, University of Mainz, Mainz, Germany, August 24, 2009. “High Resolution Lithography and the Orthogonal Processing of Organic Semiconductors”, invited talk.
- CAMM Workshop on Flexible Electronics, Traditions at the Glen, Johnson City, NY 13790. “Orthogonal Processing - a new strategy for patterning organic electronics”, invited talk.
- European Polymer Federation Meeting, Graz, Austria, July 12 – 17, 2009. “Self-assembly and directed assembly: Tools for Current Challenges in Nanofabrication”, plenary talk.
- 2009 Lithography Workshop, Coeur d’Alene, Idaho, June 20-July 2, 2009. “Molecular glass resists developed in unconventional solvents”, invited talk.
- Frontiers of Characterization and Metrology for Nanoelectronics, College of Nanoscale Science and Engineering, The University at Albany, Albany, NY, May 11-15, 2009. “The challenges posed to metrology by new approaches to advanced patterning”, invited talk – given by E. Schwartz.

Recognitions/Awards

- 2009 Gutenberg Research Awards for C. K. Ober
- 2009 Fellow of the American Chemical Society for C. K. Ober

Students on Task 425.029

- Graduated Students and Current Affiliation
 - Nelson Felix, AZ Microelectronics, Dec 2007
 - Victor Pham, JSR Microelectronics, May 2004
 - Victor Gamez, CH2M Hill, May 2009
- Internships (Task and related students)
 - Katy Bosworth, IBM
 - Evan Schwartz, Intel
 - Anuja de Silva, IBM
 - Jing Sha, NIST

Supercritical Carbon Dioxide Compatible Additives: Design, Synthesis, and Application of an Environmentally Friendly Development Process to Next Generation Lithography *(Task Number: 425.030)*

PI:

- **Christopher K. Ober, Materials Science and Engineering, Cornell University**

Collaborator:

- **Juan de Pablo, Chemical and Biological Engineering, University of Wisconsin-Madison**

Graduate Student:

- **C. Ouyang: PhD candidate, Materials Science and Engineering, Cornell University**
- **G. N. Toepperwein, PhD candidate, Chemical Engineering, University of Wisconsin**



SRC/SEMATECH Engineering Research Center for Environmentally Benign Semiconductor Manufacturing



Objectives

- **To demonstrate high-resolution patterning capabilities and scCO₂ development of molecular glass resists based on environmentally benign cores**
- **To synthesize and characterize fluorinated quaternary ammonium salts (QAS) as CO₂ compatible additives to develop conventional photoresists in scCO₂**
- **To demonstrate environmentally benign development of conventional photoresists using scCO₂ and silicone fluids using silicon-containing additives**

ESH Metrics and Impact

	Usage Reduction			Emmision Reduction			
Goals/Possibilities	Energy	Water	Chemicals	PFCs	VOCs	HAPs	Other
Reduce organic solvents used in processing materials	No energy used to purify and treat water	Eliminate need for water usage	Up to 100% reduction of organic solvents used	N/A	Minimal use of organic solvents	Up to 100% reduction of HAPs	N/A
Reduce processing time / temperature	Reduce anneal process costs	N/A	N/A	N/A	N/A	N/A	N/A
Additive processing	N/A	N/A	Eliminate waste of costly material	N/A	Minimal use of organic solvents	N/A	N/A



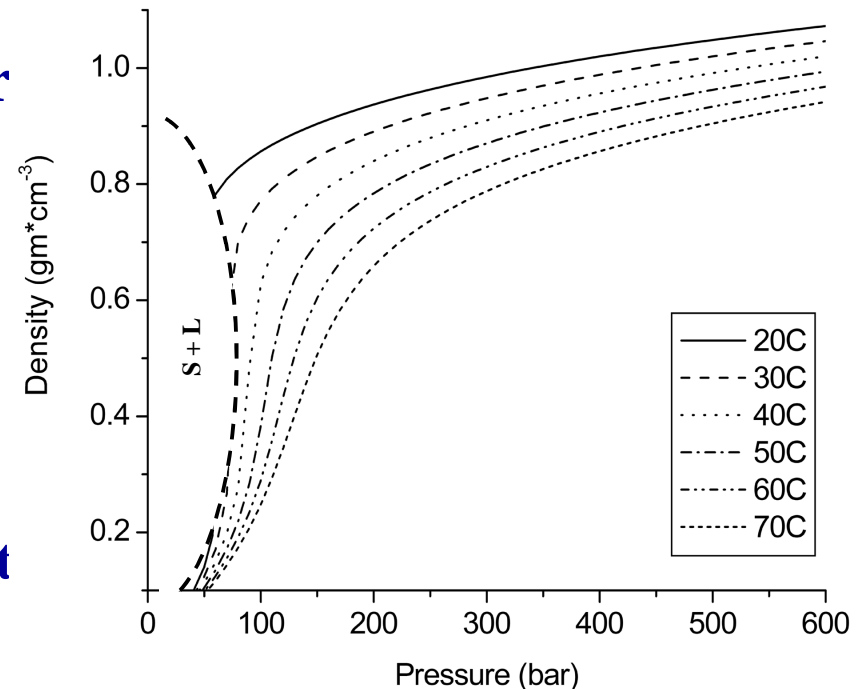
SRC/SEMATECH Engineering Research Center for Environmentally Benign Semiconductor Manufacturing



Why a Non-Aqueous Developer Solvent?

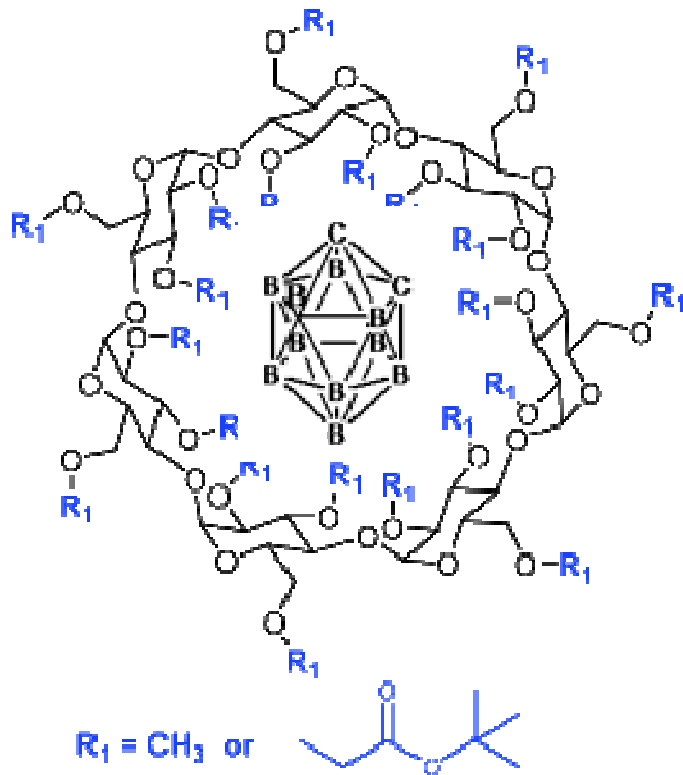
Environmental and Performance Advantages of scCO₂

- Environmentally friendly, zero VOC solvent
- Highly tunable solvating power
 - $\rho(T,P)$
 - Leaves no residue
 - Clean separations
- One-phase fluid
 - Zero surface tension
 - Transport, viscosity between that of liquid and gas
- Nonpolar, inert character
- Potential to reduce LER and eliminate pattern collapse

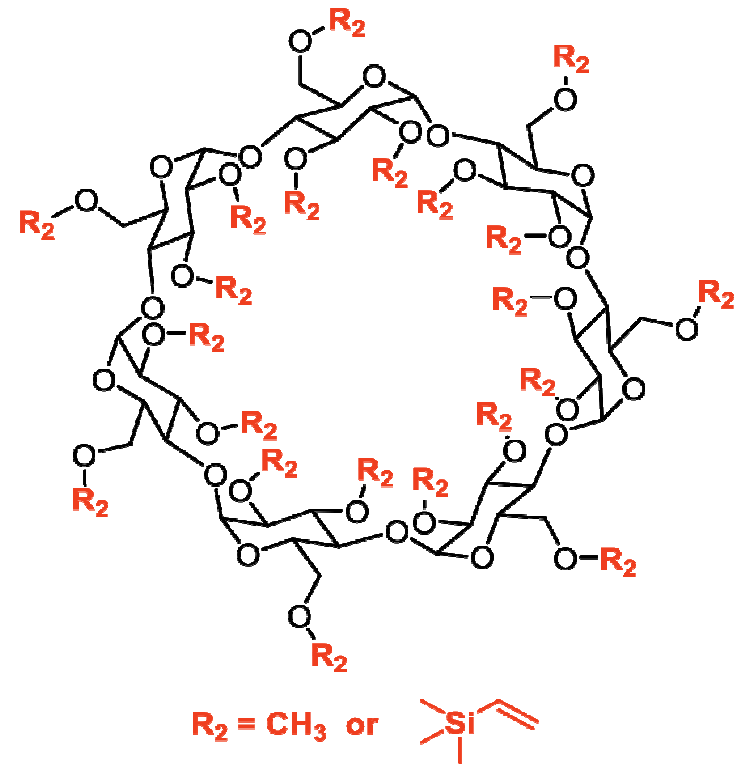


Molecular Glass Resists with Alicyclic Cores

Environmental friendliness and scCO₂ solubility



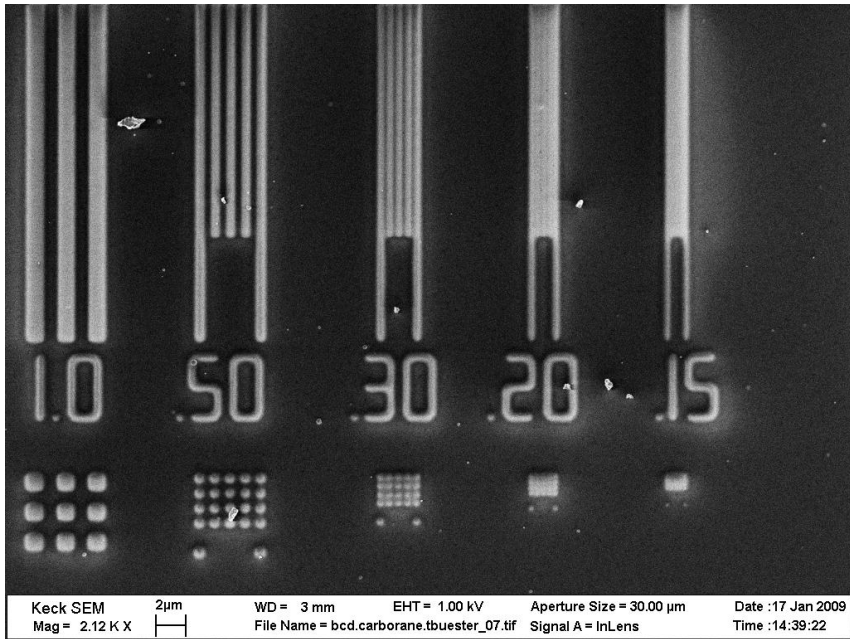
Cyclodextrin-carborane complex



Vinyl silane cyclodextrin

Cyclodextrins are good hosts for inclusion complexes and have potential as molecular resists to hold functional moieties on their periphery

Electron Beam Patterning and scCO₂ Development of Cyclodextrin Resists

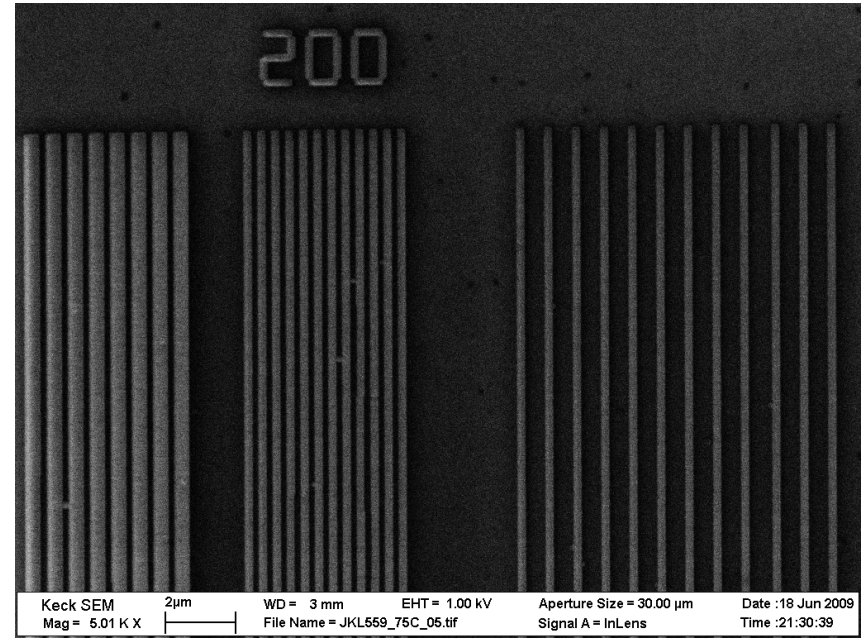


Cyclodextrin-Carborane complex

E-beam dose = $\mu\text{C}/\text{cm}^2$

PEB: 115 °C, 60 sec

scCO₂: 5000 psi, 5 min



Vinyl silane cyclodextrin

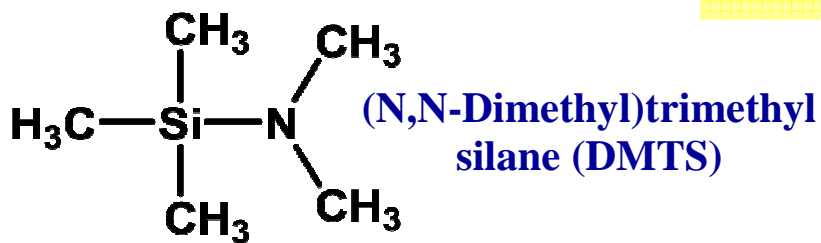
E-beam dose = 44 $\mu\text{C}/\text{cm}^2$

PEB: 75 °C, 60 sec

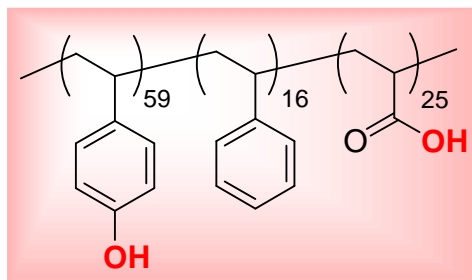
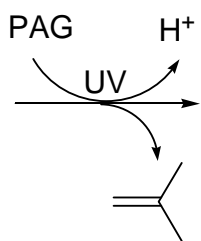
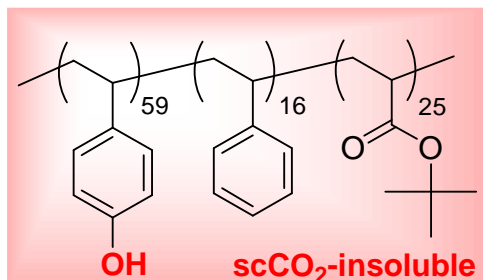
scCO₂: 2000 psi, 2 min

Additives for scCO₂ to Develop Conventional Resists

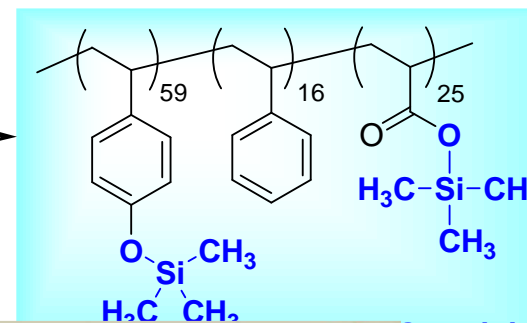
• Silicon-containing Additive



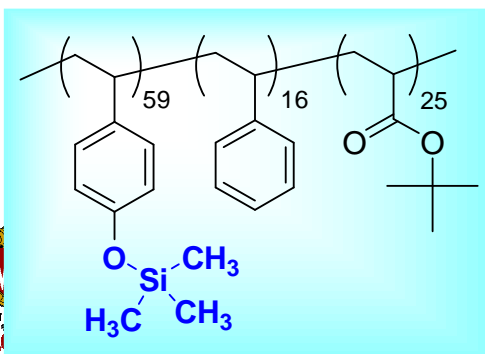
UV exposure



DMTS

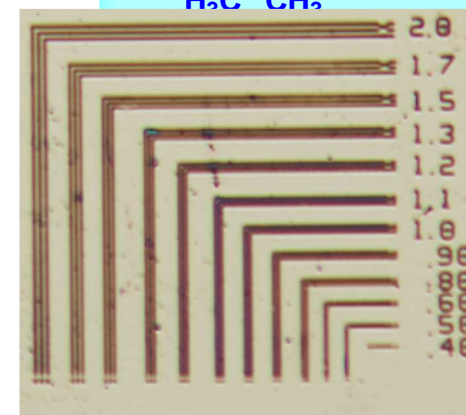


DMTS Development

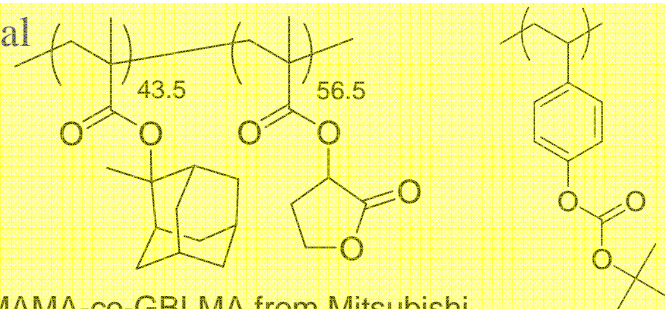


-According to resist materials and lithographic conditions, both positive and negative-tone imaging is possible

Negative image



Other conventional resists tested



PMAMA-co-GBLMA from Mitsubishi Rayon America (PMAMA-co-GBLMA)

Development

PBOCST

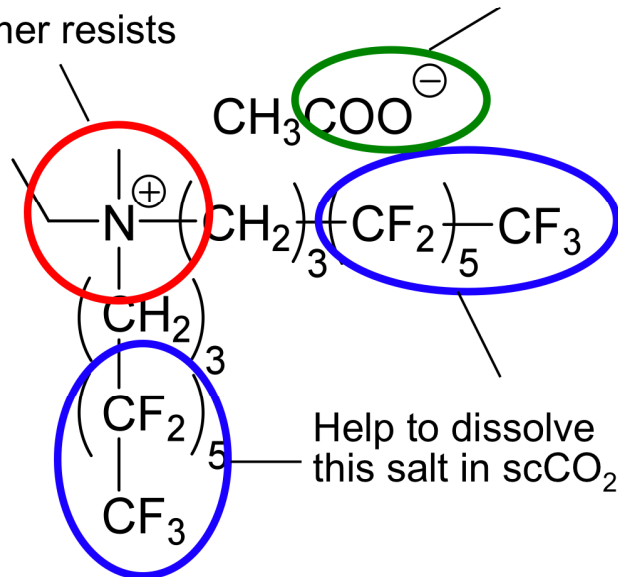
Quaternary Ammonium Salts (QAS)

scCO₂ Compatible Additives:

Fluorinated Quaternary Ammonium Salts (QAS)

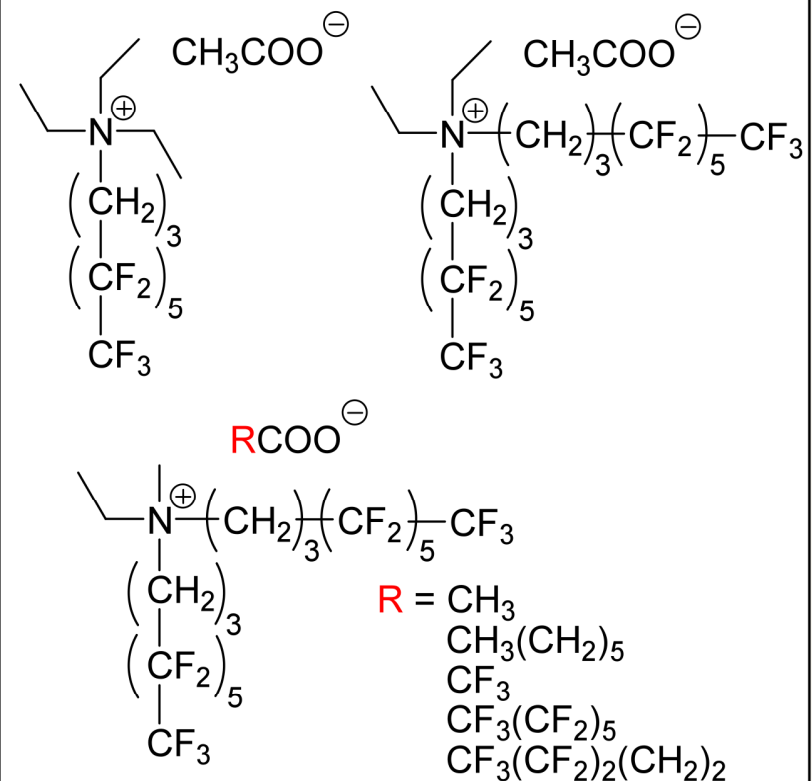
High affinity to phenolate and/or carboxylate moieties in polymer resists

Deprotonate from OH and/or COOH in polymer resists



Some of the fluorinated ammonium salts form **Micelle** in scCO₂.

Examples of fluorinated QAS



Initial Dissolution Results of Resists with QAS

QAS	Resist	Unexposed	Exposed	note
$ \begin{array}{c} \text{CH}_3\text{COO}^\ominus \\ \\ \text{---N}^\oplus\text{---}(\text{CH}_2)_3\text{---}(\text{CF}_2)_5\text{---CF}_3 \\ \\ (\text{CH}_2)_3 \\ \\ (\text{CF}_2)_5 \\ \\ \text{CF}_3 \\ \text{QAS-4} \\ (1.25 \text{ mM}) \end{array} $	PBOCST	Dissolution (40 nm/min)	Slow dissolution (1-4 nm/min)	<i>Negative tone resist</i>
	ESCAP (Du Pont)	Dissolution (25 nm/min)	No dissolution	<i>Negative tone resist</i>
	PMAMA-co- GBLMA (Mitsubishi Rayon)	No dissolution	No dissolution	
	EUV-P568 (TOK)	Dissolution (15 nm/min)	Slow dissolution (1-2 nm/min)	<i>Negative tone resist</i>
$ \begin{array}{c} \text{CF}_3\text{CF}_2\text{COO}^\ominus \\ \\ \text{---N}^\oplus\text{---}(\text{CH}_2)_3\text{---}(\text{CF}_2)_5\text{---CF}_3 \\ \\ (\text{CH}_2)_3 \\ \\ (\text{CF}_2)_5 \\ \\ \text{CF}_3 \\ \text{QAS-7} \\ (1.25 \text{ mM}) \end{array} $	PBOCST	No dissolution	No dissolution	
	ESCAP (Du Pont)	No dissolution	No dissolution	
	PMAMA-co- GBLMA (Mitsubishi Rayon)	No dissolution	No dissolution	
	EUV-P568 (TOK)	Dissolution (45 nm/min)	Slow dissolution (<1 nm/min)	<i>Negative tone resist</i>

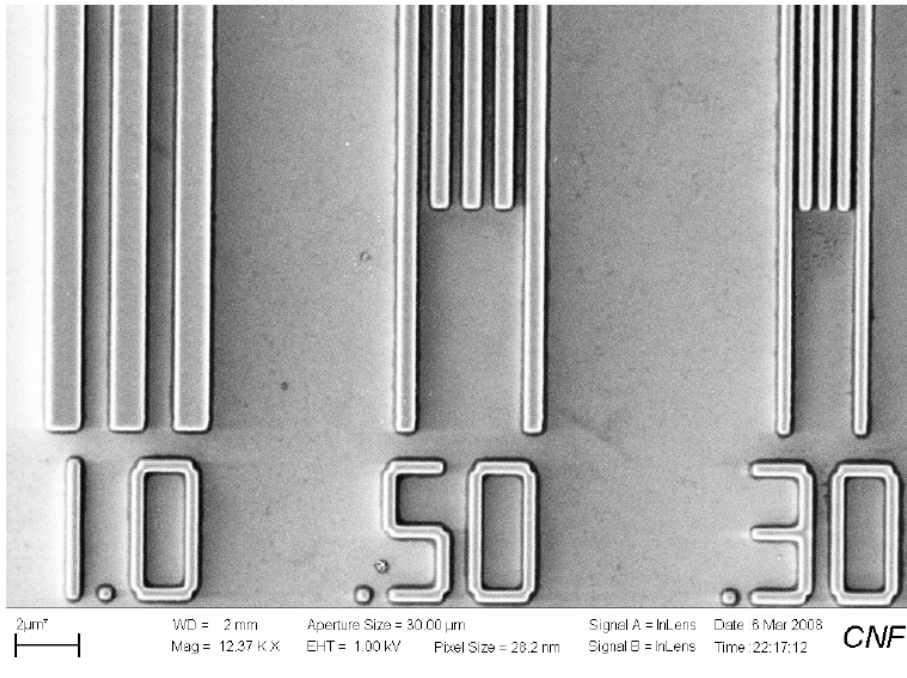
Exposed by UV lamp (254 nm, 24 mC/cm²), developed in scCO₂ at 50°C and 5000 psi.

SRC/SEMATECH Engineering Research Center for Environmentally Benign Semiconductor Manufacturing



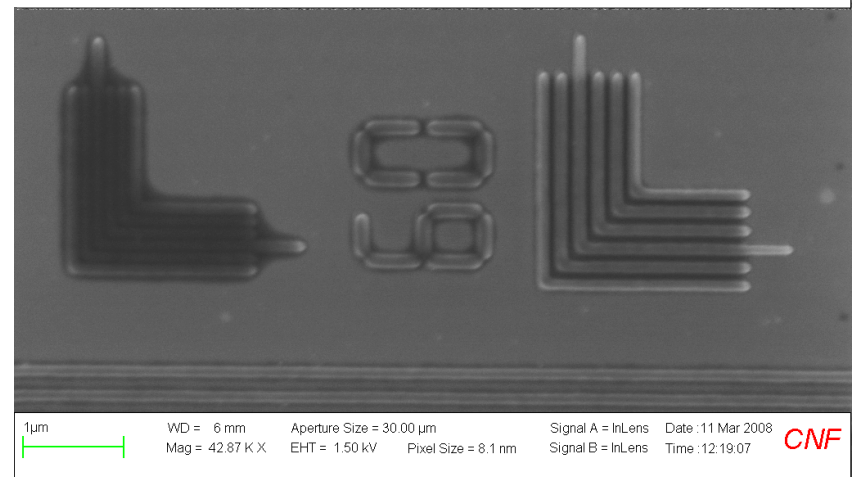
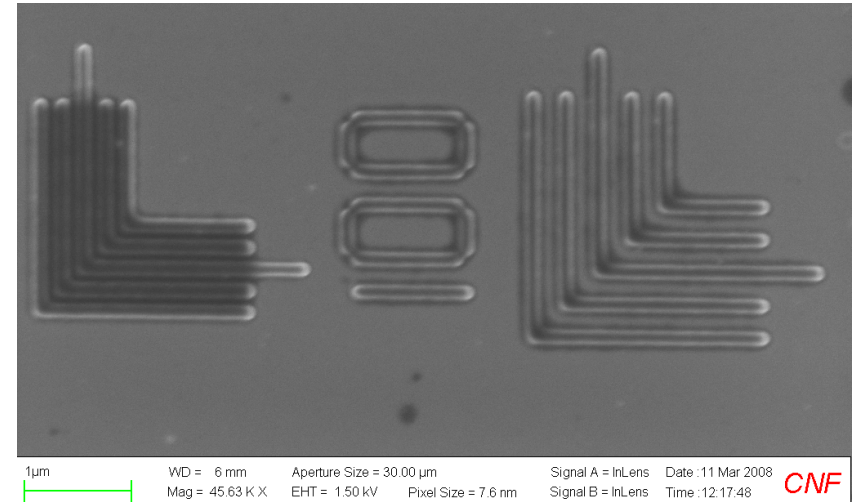
Electron Beam Patterning

Development test of EB-patterned TOK resist (EUV-P568) with QAS-4 or QAS-7



Dose: 107 $\mu\text{C}/\text{cm}^2$, QAS-4 (1.25 mM), dev. for 60 min at 50°C, 5000 psi, flow 30 min

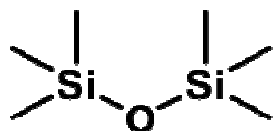
Negative tone patterns with sub-100 nm feature sizes were obtained.



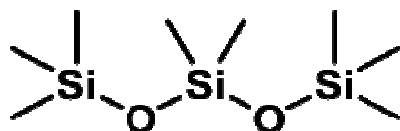
Dose: 20 $\mu\text{C}/\text{cm}^2$, QAS-7 (1.25 mM), dev. for 60 min at 50°C, 5000 psi, flow 30 min

Silicone Fluids-Linear Methyl Siloxanes

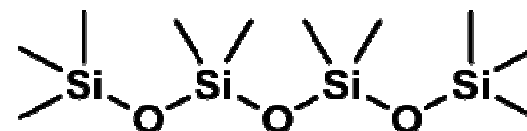
- **Low in toxicity**
 - **Environmentally friendly**
 - **VOC exempt**
- **Contribute little to global warming**
- **Non-ozone depleting**
 - **replacement for Ozone Depleting Substances**
- **Low surface tension**
 - **potential to eliminate patterns collapse**
- **Can be recycled**
 - **degrade to naturally occurring chemical species**



Hexamethyldisiloxane



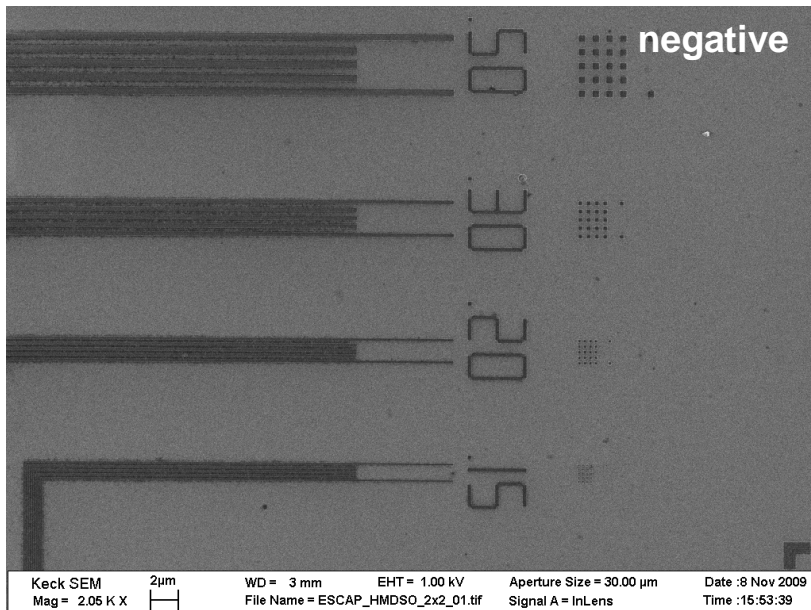
Octamethyltrisiloxane



Decamethyltetrasiloxane

D. E. Williams, ACS Symposium Series, 2000, 767, 244-257.

Electron Beam Patterning and Silicone Fluid Development of Conventional Photoresists



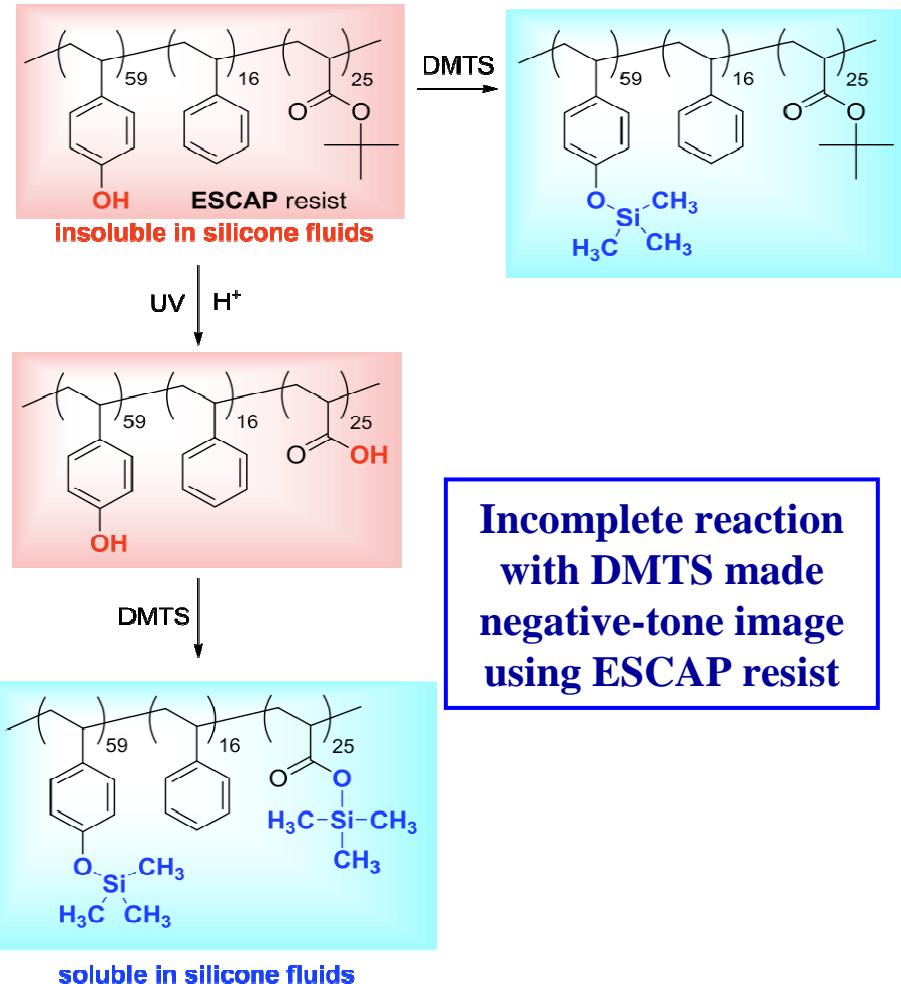
Photoresist: ESCAP

Chemical modifier: DMTS

Solvent: Hexamethyldisiloxane

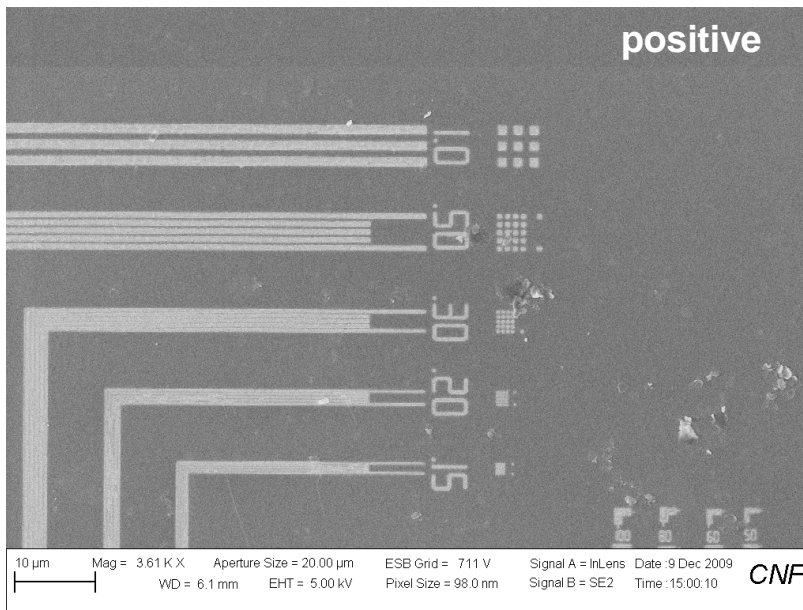
E-beam dose = $\mu\text{C}/\text{cm}^2$

PEB: 115 °C, 60 sec



**Incomplete reaction
with DMTS made
negative-tone image
using ESCAP resist**

Electron Beam Patterning and Silicone Fluid Development of Conventional Photoresists



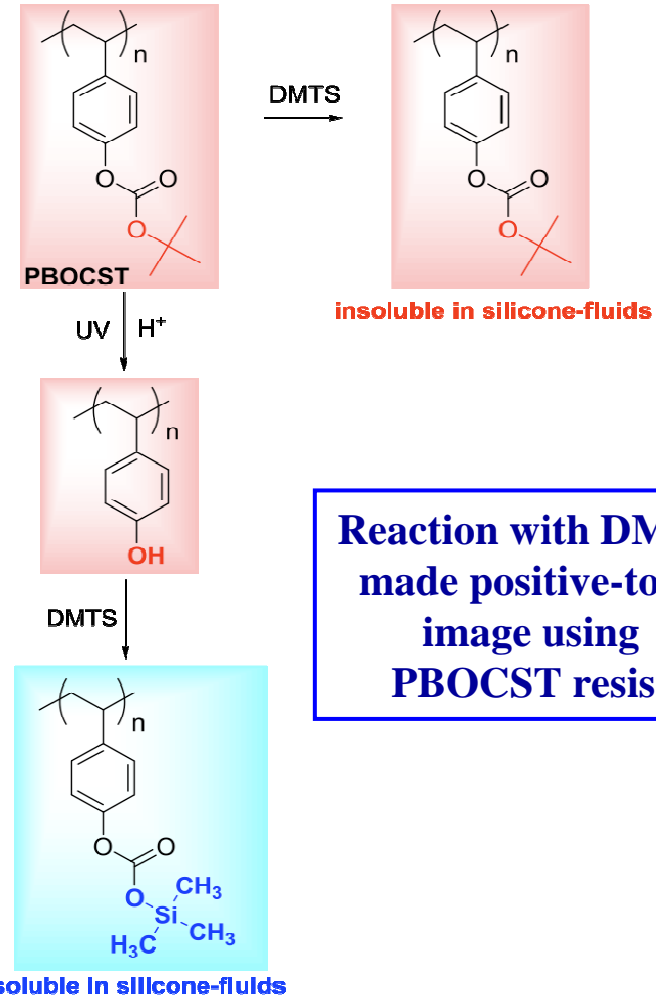
Photoresist: PBOCST

Chemical modifier: DMTS

Solvent: Octamethyldisiloxane

E-beam dose = $\mu\text{C}/\text{cm}^2$

PEB: 90 °C, 60 sec



**Reaction with DMTS
made positive-tone
image using
PBOCST resist**

Industrial Interactions and Technology Transfer

- **Former student (N. Felix) hired by IBM Fishkill Research Center**
- **Jing Sha moved to Intel grant and interned at NIST**
- **Interactions with Intel on this topic have been successful**
- **Collaboration with Albany Nanotech for EUV exposures**



SRC/SEMATECH Engineering Research Center for Environmentally Benign Semiconductor Manufacturing



Task Deliverables

- **Report on the preparation of a series of quaternary ammonium salts for resist development (6/30/2009)**
-completed

Future Plans

Next Year Plans (seed effort)

- To explore more organosilanes and non-fluorinated quaternary ammonium salts (QAS) for faster dissolution of photoresists in silicone fluids and scCO₂ with the help of simulation data from Prof. Juan J de Pablo Group in Univ. of Wisconsin, Madison
- To continue synthesis efforts for scCO₂ processable molecular glass resists with environmentally benign, naturally occurring cores for next generation high-resolution lithography

Long-Term Plans

- To expand use of additives for scCO₂ and environmentally friendly silicone fluids to develop positive tone resists
- To create new chemistries for patterning and functionalizing small, non-polar molecules in scCO₂



SRC/SEMATECH Engineering Research Center for Environmentally Benign Semiconductor Manufacturing



Publications, Presentations, and Recognitions/Awards

Publications

- M. Tanaka, A. Rastogi, N. M. Felix, C. K. Ober, “*Supercritical Carbon Dioxide Compatible Salts: Synthesis and Application to Next Generation Lithography*”, *J. Photopolym. Sci. Technol.* (2008), 21(3), 393-396.
- J. Sha and C. K. Ober, “*Fluorine- and Siloxane-Containing Polymers for Supercritical Carbon Dioxide Lithography*”, *Polymer International* (2009), 58(3), 302-306.
- A. Rastogi, M. Tanaka, G. N. Toepperwein, R. A. Riggleman, J. J. dePablo, C. K. Ober, “*Fluorinated Quaternary Ammonium Salts as Dissolution Aids for Polar Polymers in Environmentally Benign Supercritical Carbon Dioxide*”, *Chem. Mater.* (2009), 21(14), 3121-3135.
- J. Sha, J-K Lee, C. K. Ober, “*Molecular Glass Resists Developable in Supercritical CO₂ for 193-nm Lithography*”, *Proceedings of SPIE* (2009), 7273, 72732T.

Presentations

- 25th International Conference of Photopolymer Science & Technology (June 2008). “*Supercritical Carbon Dioxide Compatible Salts: Synthesis and Application to Next Generation Lithography*”
- US-Japan Polymat 2008 Symposium (Aug 2008). “*Environmentally Benign Development of Polymer Photoresists Using Supercritical Carbon Dioxide*”
- ERC Teleseminar (Oct 2008). “*Environmentally Benign Development of Standard Resists in Supercritical Carbon Dioxide Using CO₂ Compatible Salts*”
- Advances in Resist Materials and Processing Technology XXVI conference (part of the SPIE Symposium on Advanced Lithography) (Feb 2009). “*Environmentally Benign Development of Photoresists in Supercritical Carbon Dioxide Using CO₂ Compatible Additives*”



SRC/SEMATECH Engineering Research Center for Environmentally Benign Semiconductor Manufacturing



Supercritical Carbon Dioxide
Compatible Additives:
Design, Synthesis, and Application of an
Environmentally Friendly Development Process to
Next Generation Lithography
(Task Number: 425.031)

PIs:

- **Juan J. dePablo, Chemical and Biological Engineering, University of Wisconsin**
- **Christopher K. Ober, Materials Science and Engineering, Cornell University**

Graduate Students:

- **Gregory N. Toepperwein: 4th year PhD candidate, Chemical and Biological Engineering, University of Wisconsin**
- **Christine Ouyang: 2nd year PhD candidate, Materials Science and Engineering, Cornell University**

Undergraduate Students:

- **Dan Rynearson, Chemical and Biological Engineering, University of Wisconsin**

SRC/SEMATECH Engineering Research Center for Environmentally Benign Semiconductor Manufacturing

Objectives

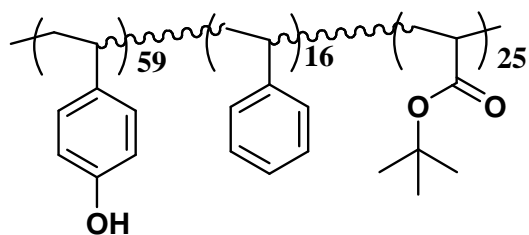
- **Develop chemistry platform for use of scCO₂ as a solvent with traditional photoresists**
 - **Design fluorinated quaternary ammonium salts (QAS) as CO₂ compatible additives**
 - **Elucidate underlying mechanisms of dissolution enhancement**
 - **Apply mechanistic understanding to creation on non-fluorinated additives**
- **Extend scCO₂ methods to molecular glass photoresists**

ESH Metrics and Impact

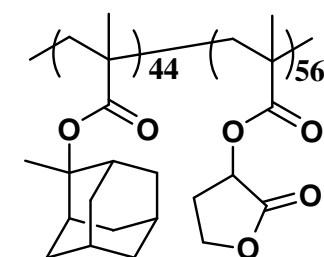
	Usage Reduction			Emmision Reduction			
Goals/Possibilities	Energy	Water	Chemicals	PFCs	VOCs	HAPs	Other
Reduce organic solvents used in processing materials	No energy used to purify and treat water	Eliminate need for water usage	Up to 100% reduction of organic solvents used	N/A	Minimal use of organic solvents	Up to 100% reduction of HAPs	N/A
Reduce processing time / temperature	Reduce anneal process costs	N/A	N/A	N/A	N/A	N/A	N/A
Additive processing	N/A	N/A	Eliminate waste of costly material	N/A	Minimal use of organic solvents	N/A	N/A

Systems of Interest

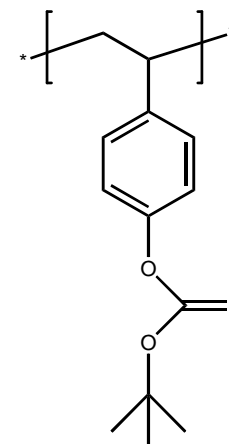
- **Model photoresists in their protected forms**



ESCAP



193nm-resist

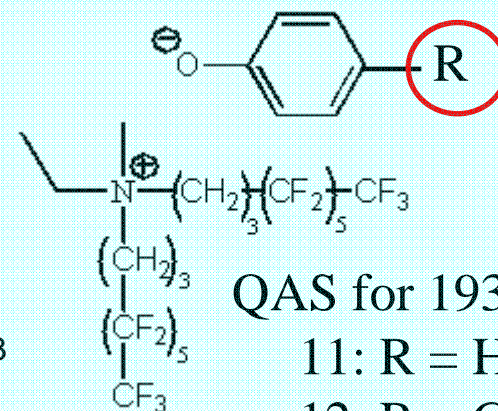
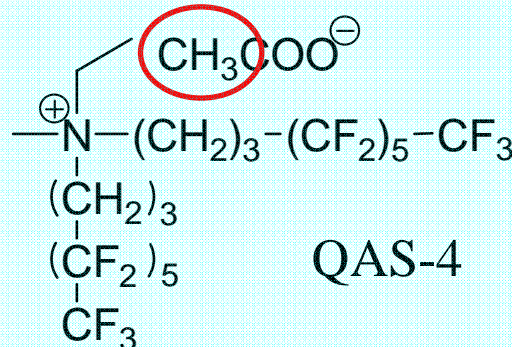
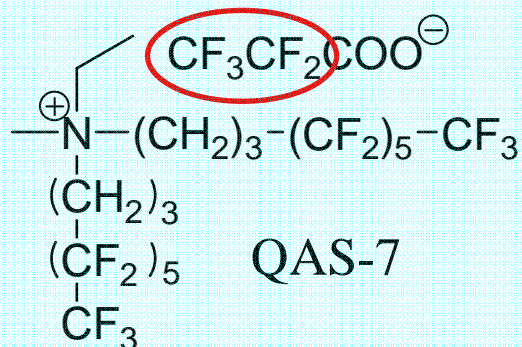


PHOST

- **QAS Additives**

- **Previously shown to be soluble in CO₂**

QAS for ESCAP & PHOST



QAS for 193nm-resist

11: R = H

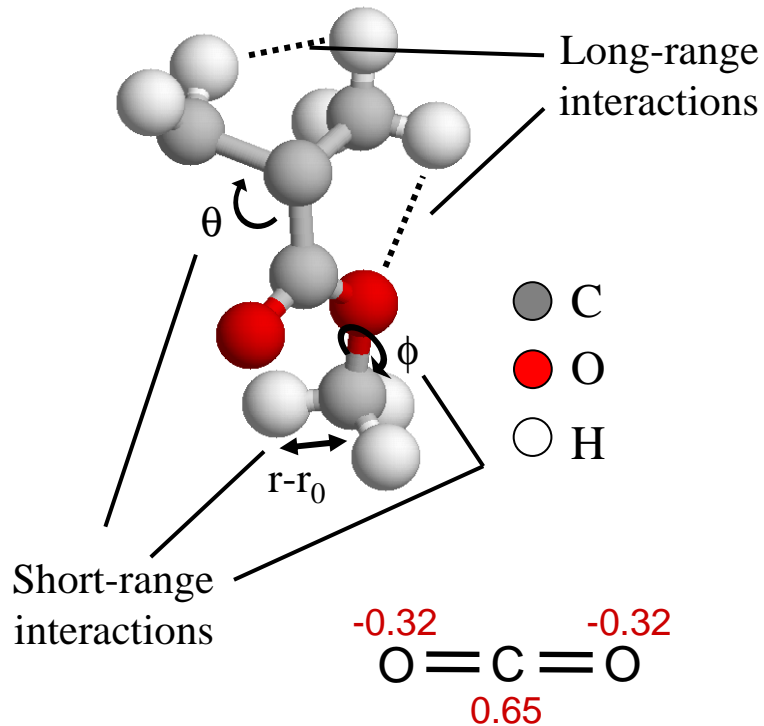
12: R = CH₃

13: R = CF₃

14: R = NO₂

Model

- Simulation allows screening of large numbers of systems and enables direct observation of molecular behavior



charges important: scCO₂ has a large quadrupole moment

OPLS Model:

$$V_{\text{tot}} = \underbrace{V_{\text{LJ}} + V_{\text{coul}}}_{\text{Intermolecular}} + \underbrace{V_{\text{bon}} + V_{\text{ang}} + V_{\text{tors}}}_{\text{Intramolecular}}$$

$$V_{\text{LJ}} = 4 \cdot \epsilon \cdot \left[\left(\frac{\sigma}{r} \right)^{12} - \left(\frac{\sigma}{r} \right)^6 \right]$$

$$V_{\text{coul}} = \frac{q_i \cdot q_j}{4 \cdot \epsilon_0 \cdot \epsilon \cdot r}$$

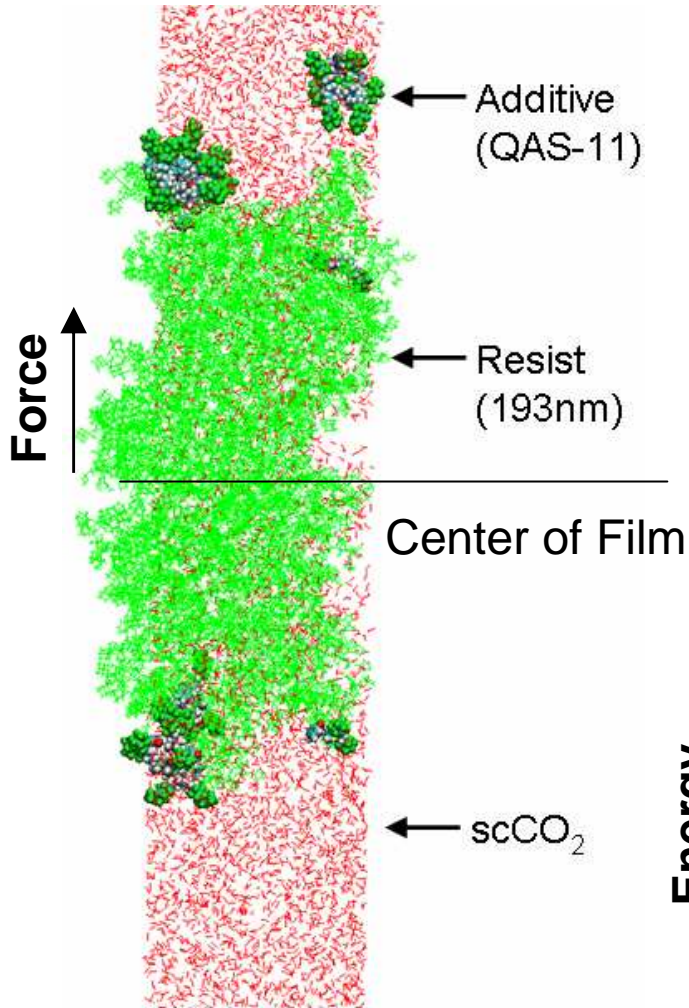
$$V_{\text{bon}} = \frac{1}{2} \cdot k_{\text{bon}} \cdot (r - r_0)^2$$

$$V_{\text{ang}} = \frac{1}{2} \cdot k_{\text{ang}} \cdot (\theta - \theta_0)^2$$

$$V_{\text{tors}} = \sum_n k_n \cdot (1 + \cos(n \cdot \phi - \phi_0))$$

- OPLS force field employed for most parameters
- We calculated charges (q_i) using quantum mechanics
- Process Conditions: $T = 340\text{K}$ ($\sim 67^\circ\text{C}$)
 $P = 345$ bar

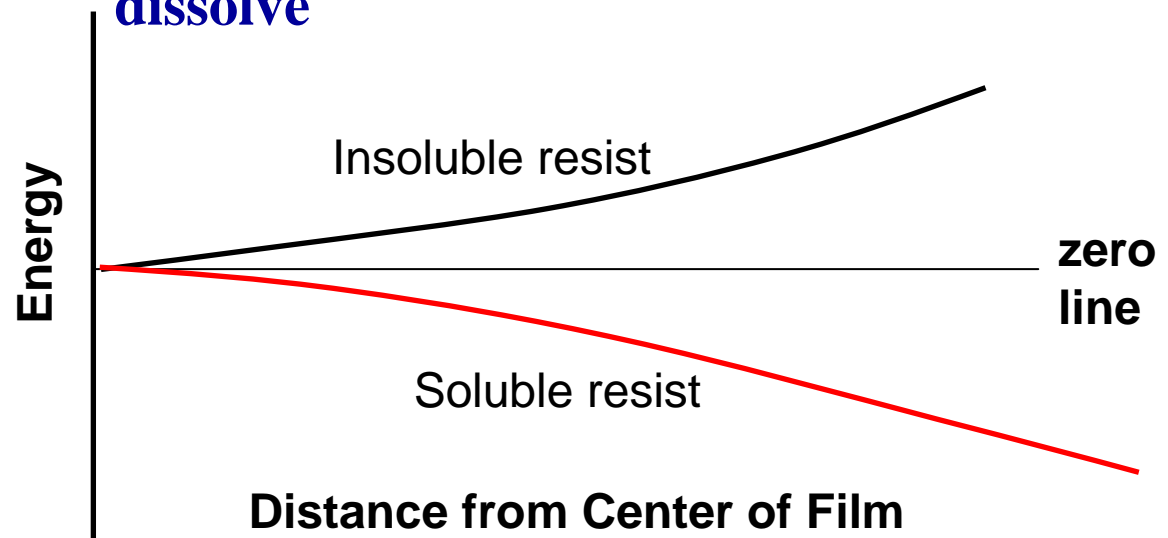
Free Energy Calculation



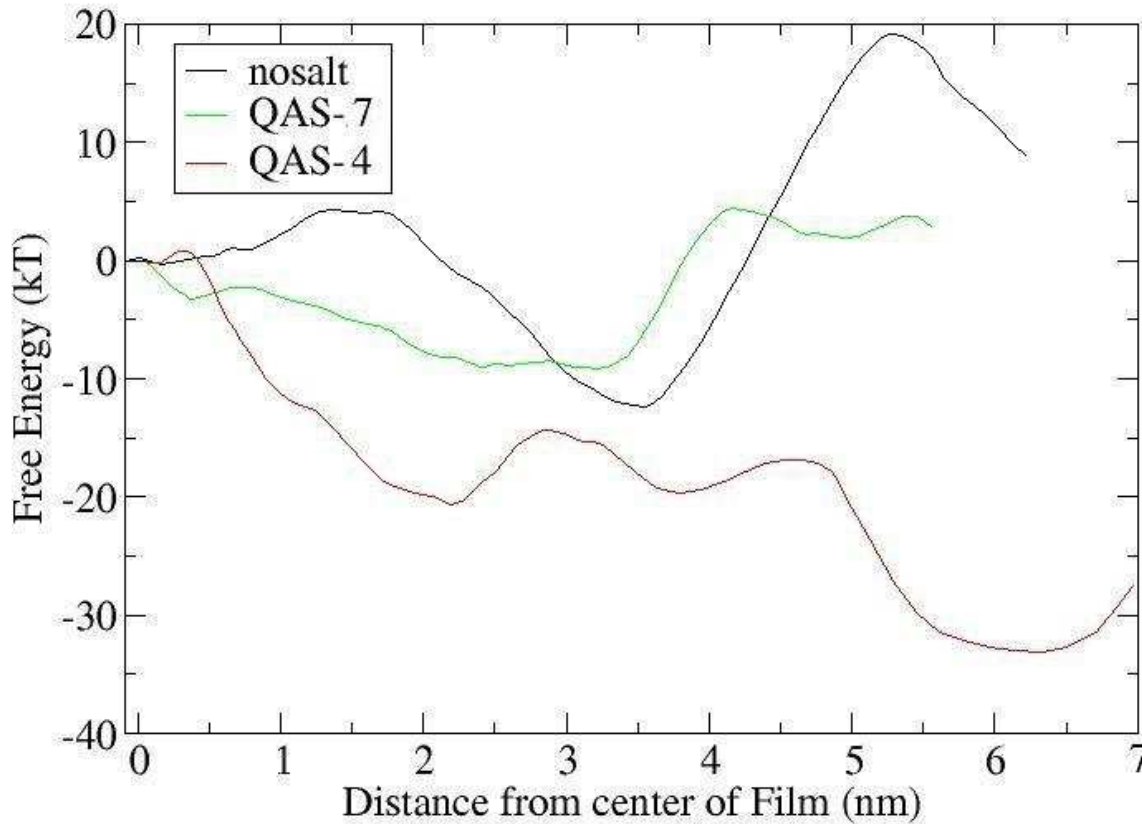
- Thin films of resist are equilibrated in scCO₂ via MD simulation
- Integrating the force on each chain as a function of position provides free energy

$$F(z) = \int_z^{z_\infty} \langle f(z') \rangle dz' + F(z_0)$$

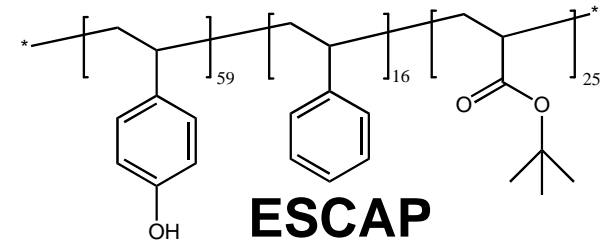
- If the energy is lower at the surface than the center, the film is unstable and will dissolve



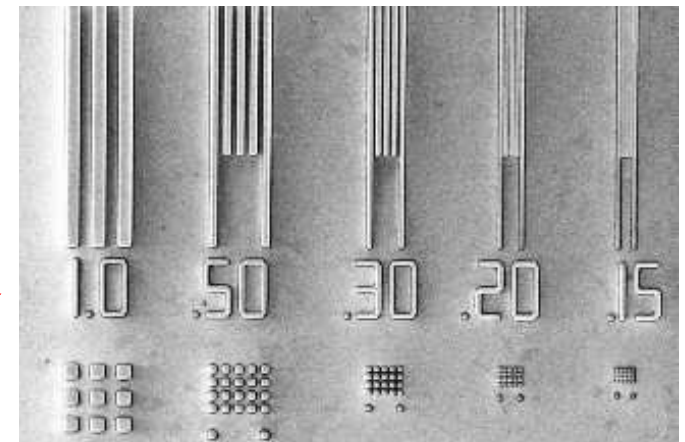
Sample Result: ESCAP Energy Curve



Experimental Results:
No salt – 0 nm/sec
QAS-7 – 0 nm/sec
QAS-4 – 20 nm/sec

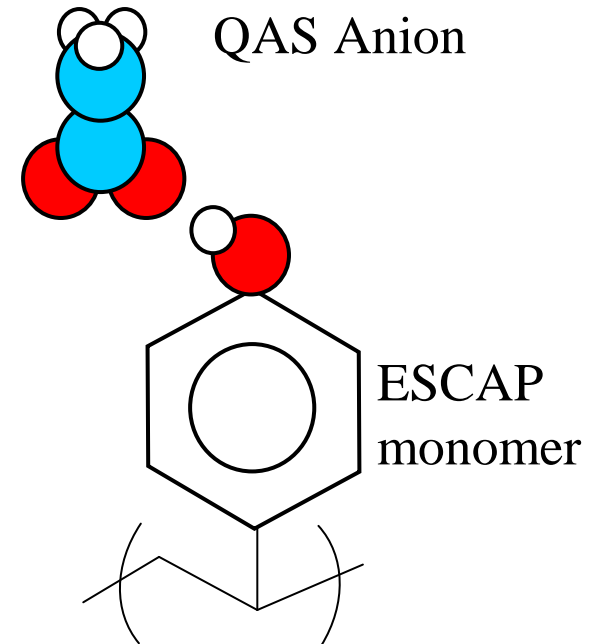
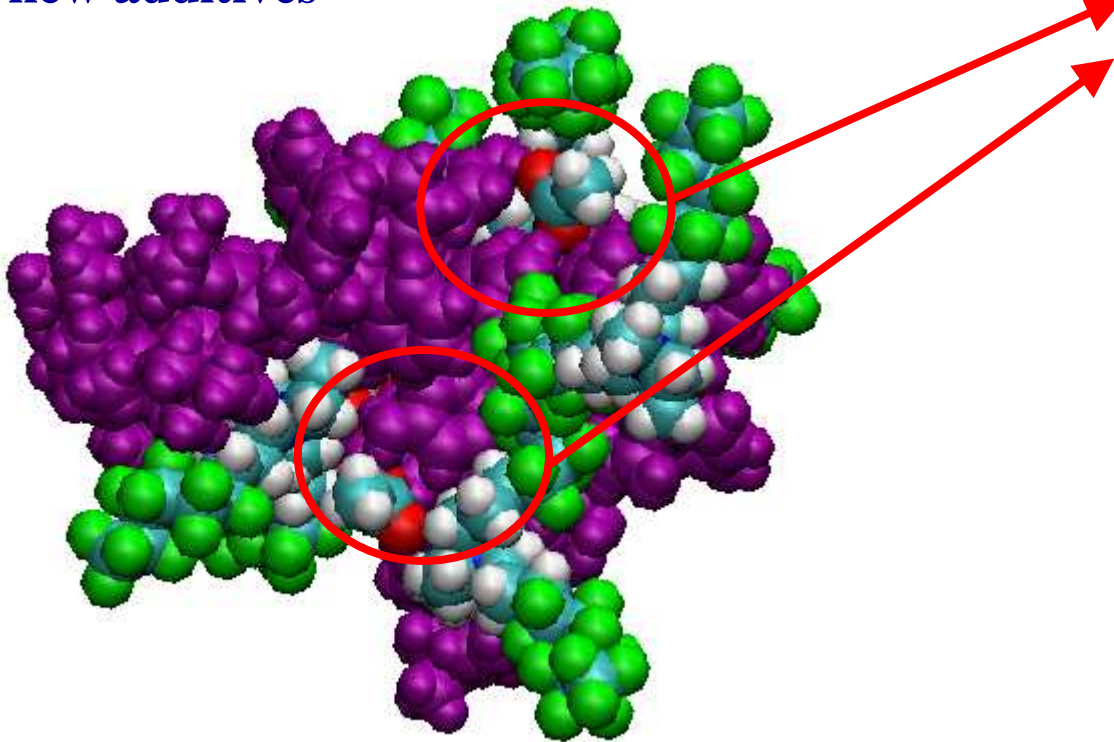


- Only addition of QAS4 to ESCAP results in reduced energy at surface of film (right of plot), indicating eventual dissolution
- Viability confirmed experimentally



ESCAP Mechanism with QAS4

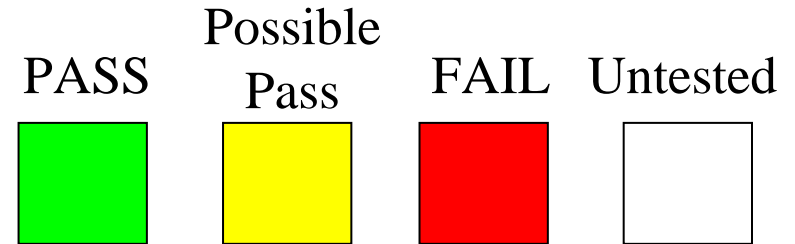
- The -OH group of ESCAP associates with the anions; contacts last >500 ps.
- Reducing available polar regions increases solubility in scCO_2
- Will use understanding of mechanism to develop new additives

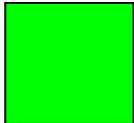
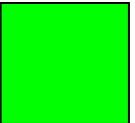



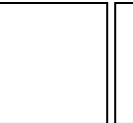

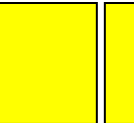
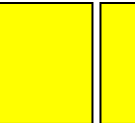
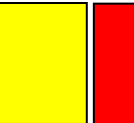





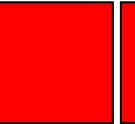
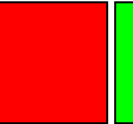
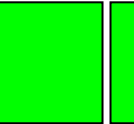
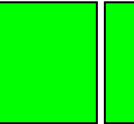
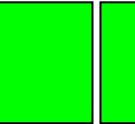
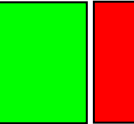
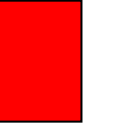
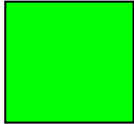






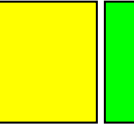
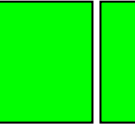
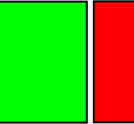
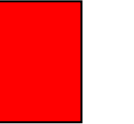
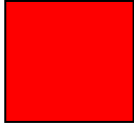
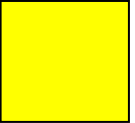







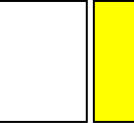
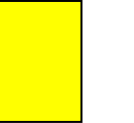


- scCO_2 not shown for clarity
- **Purple** – ESCAP
- **Green** – Fluorine (QAS-4)
- **Cyan** – Carbon (QAS-4)
- **Red** – Oxygen (QAS-4)
- **White** – Hydrogen (QAS-4)

Summary of Fluorinated Additive Results

- We have applied these methods to a range of additive-resist combinations to screen for promising systems
- Excellent agreement with experiment

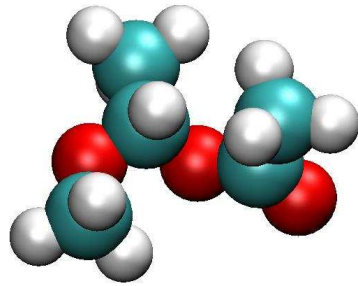


Photoresist	Additive										
	QAS4	QAS6	QAS7	QAS11	QAS12	QAS13	QAS14	Isocyanate	TMDS	HMDS	none
ESCAP											
193nm											
PHOST											
Molecular Glass I											

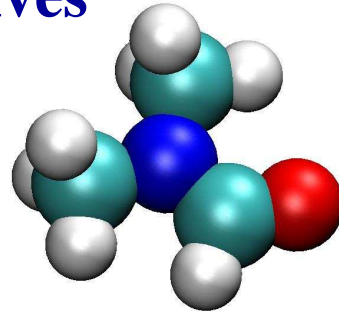
Reactive Additives Not Discussed Today

Non-Fluorinated Systems

- Potential Additives

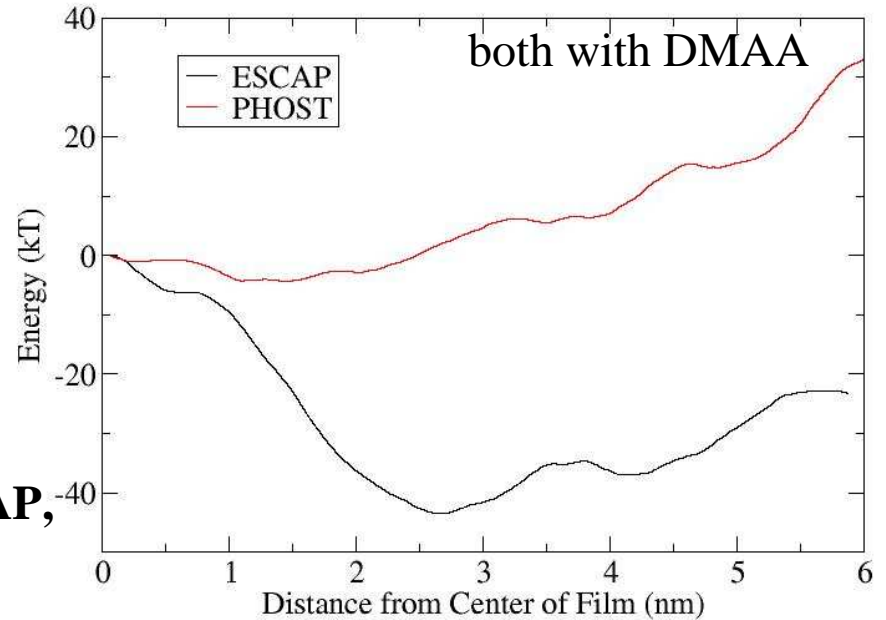


PGMEA

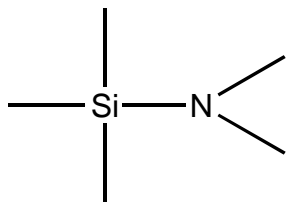


DMAA

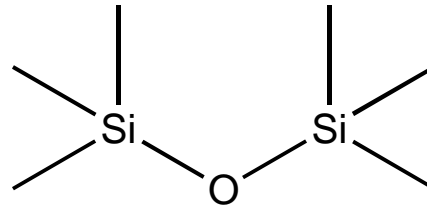
Effective with ESCAP,
but not PHOST



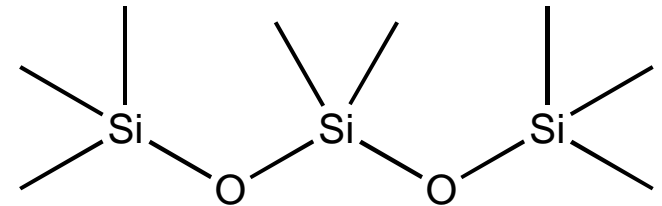
- Alternative solvents not needing fluorinated additives



DMTsilane



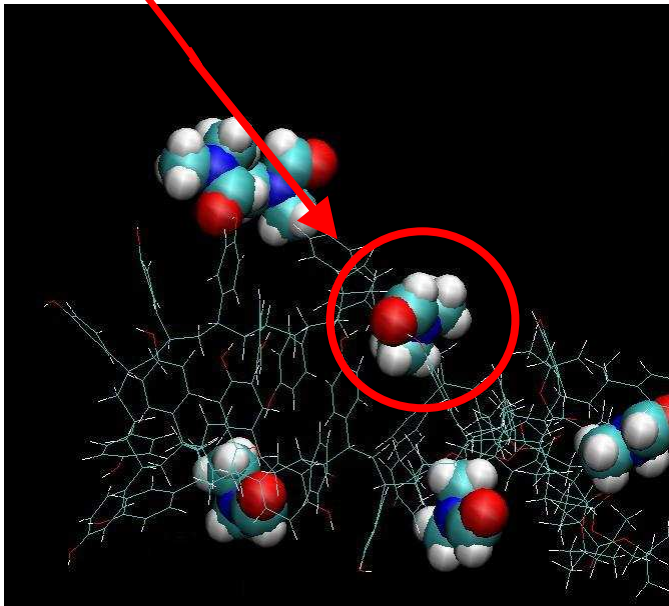
HMDsilane



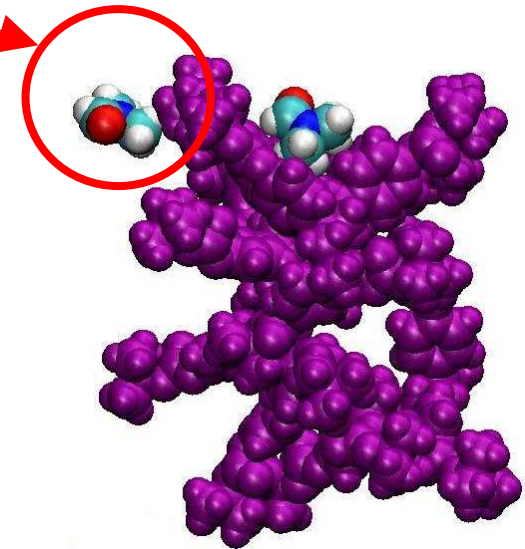
OMTsilane

DMAA Mechanism

- Additive was based on applying our understanding of QAS4 effectiveness on ESCAP
- DMAA demonstrates similar hydrogen bonding
- Ineffective with PHOST; obstructs terminal t-butyl group, instead exposing polar region, reducing scCO₂ solubility

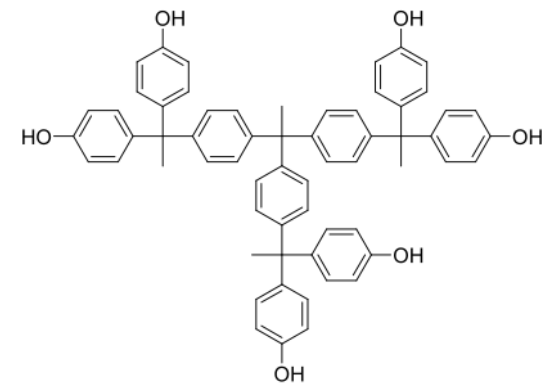
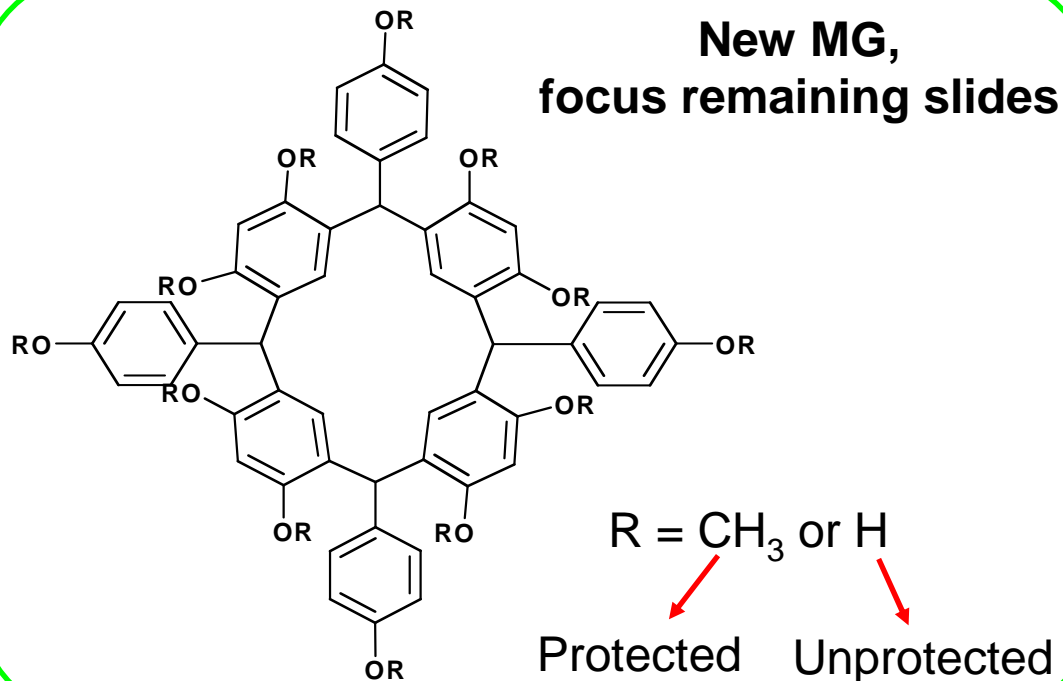


Can develop non-fluorinated additives, but they are more resist-specific



Molecular Glass (MG) Resists

- Molecular Glass have low LER due to small size
- Experimental synthesis and testing is expensive and does not guarantee results; screening via simulation saves resources

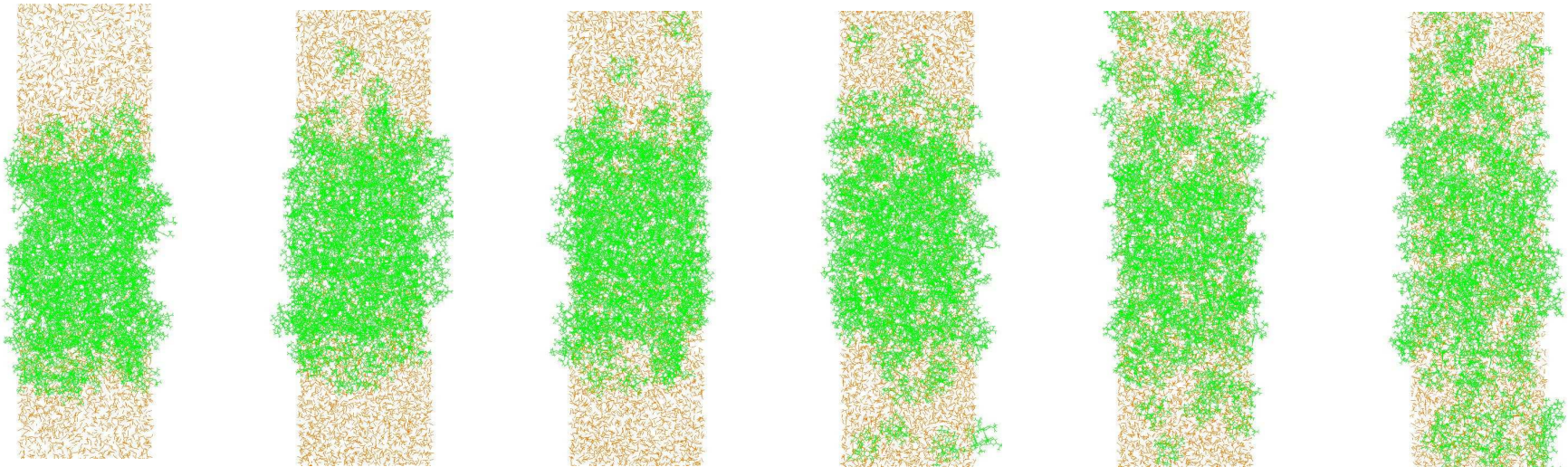


First proposed MG in exposed form. Simulation found viable system, but synthesis yielded a liquid at process conditions

Molecular Glass in scCO₂

- Protected MG dissolved in scCO₂ without additive; unprotected form insoluble
- No testing with additives necessary, system shows most robust dissolution to date; no free-energy curve needed
- Highly promising results to be confirmed experimentally

Time (1-2ns between images)



SRC/SEMATECH Engineering Research Center for Environmentally Benign Semiconductor Manufacturing

Industrial Interactions and Technology Transfer

- **Regular discussions with Intel via Richard Schenker**
- **Interactions with Dario Goldfarb from IBM**
- **Interactions with Kenji Yoshimoto from Global Foundry**



Future Plans

Next Year Plans

- Complete characterization of bulk properties of new potential molecular glass resists and silicone-based solvents
- Verification of new materials via laboratory experiments
- Additional screening of new non-fluorinated additives for use with traditional photoresists

Long-Term Plans

- To expand use of additives for scCO₂ and environmentally friendly silicone fluids for development of positive tone resists
- To create new chemistries for patterning and functionalizing small, non-polar molecules in scCO₂

Publications, Presentations, and Recognitions/Awards

Publications

- **Tanaka M, Rastogi A, Toepperwein GN, Riggleman RA, Felix N, de Pablo JJ, Ober CK. “Fluorinated Quaternary Ammonium Salts as Dissolution Aids for Polar Polymers in Environmentally Benign Supercritical Carbon Dioxide”, Chemistry of Materials (2009), 21(14), 3121-3135**
- **Rastogi A, Toepperwein GN, Tanaka M, Riggleman RA, de Pablo JJ, Ober CK. “Contact Analysis Studies of an ESCAP resist with scCO₂ compatible additives”, Proc. SPIE (2009)**
- **Sha J, Ober CK, “Fluorine- and Siloxane-Containing Polymers for Supercritical Carbon Dioxide Lithography”, Polymer International (2009), 58(3), 302-306**

Presentations

- **ERC Telesminar (Oct 2008). “Environmentally Benign Development of Standard Resists in Supercritical Carbon Dioxide Using CO₂ Compatible Salts”**

Fundamentals of Advanced Planarization: Pad Micro-Texture, Pad Conditioning, Slurry Flow, and Retaining Ring Geometry

(Task 425.032)

Subtask 1: Effect of Retaining Ring Geometry on Slurry Flow and Pad Micro-Texture

PI:

- Ara Philipossian, Chemical and Environment Engineering, UA

Graduate Student:

- Xiaomin Wei, PhD candidate, Chemical and Environment Engineering, UA

Undergraduate Student:

- Adam Rice, Chemical and Environment Engineering, UA

Other Researcher:

- Yasa Sampurno, Postdoctoral Fellow, Chemical and Environment Engineering, UA

Cost Share (other than core ERC funding):

- In-kind donation (pads) from Cabot Microelectronics Corporation
- In-kind donation (retaining rings) from Entegris, Inc.

SRC/SEMATECH Engineering Research Center for Environmentally Benign Semiconductor Manufacturing

Objectives

- **Develop UV enhanced fluorescence system and quantify the extent of fluorescent light emitted by the slurry**
- **Employ the fluorescent light data to rapidly assess slurry flow patterns as a function of retaining ring designs, slurry flow rates, pad groove designs, and tool kinematics**

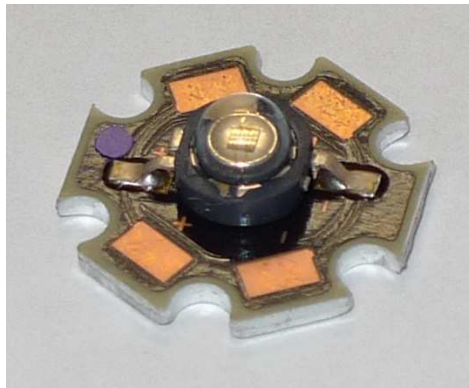
ESH Metrics and Impact

Goal: reduce slurry consumption by 40 %

General Approach

- **Tag slurry with a special set of fluorescent dyes**
- **Use UV – LED as light sources to excite the dyes in the slurry causing them to emit fluorescent light**
- **Employ a high resolution CCD camera to record the emission of fluorescent light**
- **Develop software and quantitatively assess the flow pattern using the movie from CCD camera**

UV – LED and CCD Camera



UV – LED

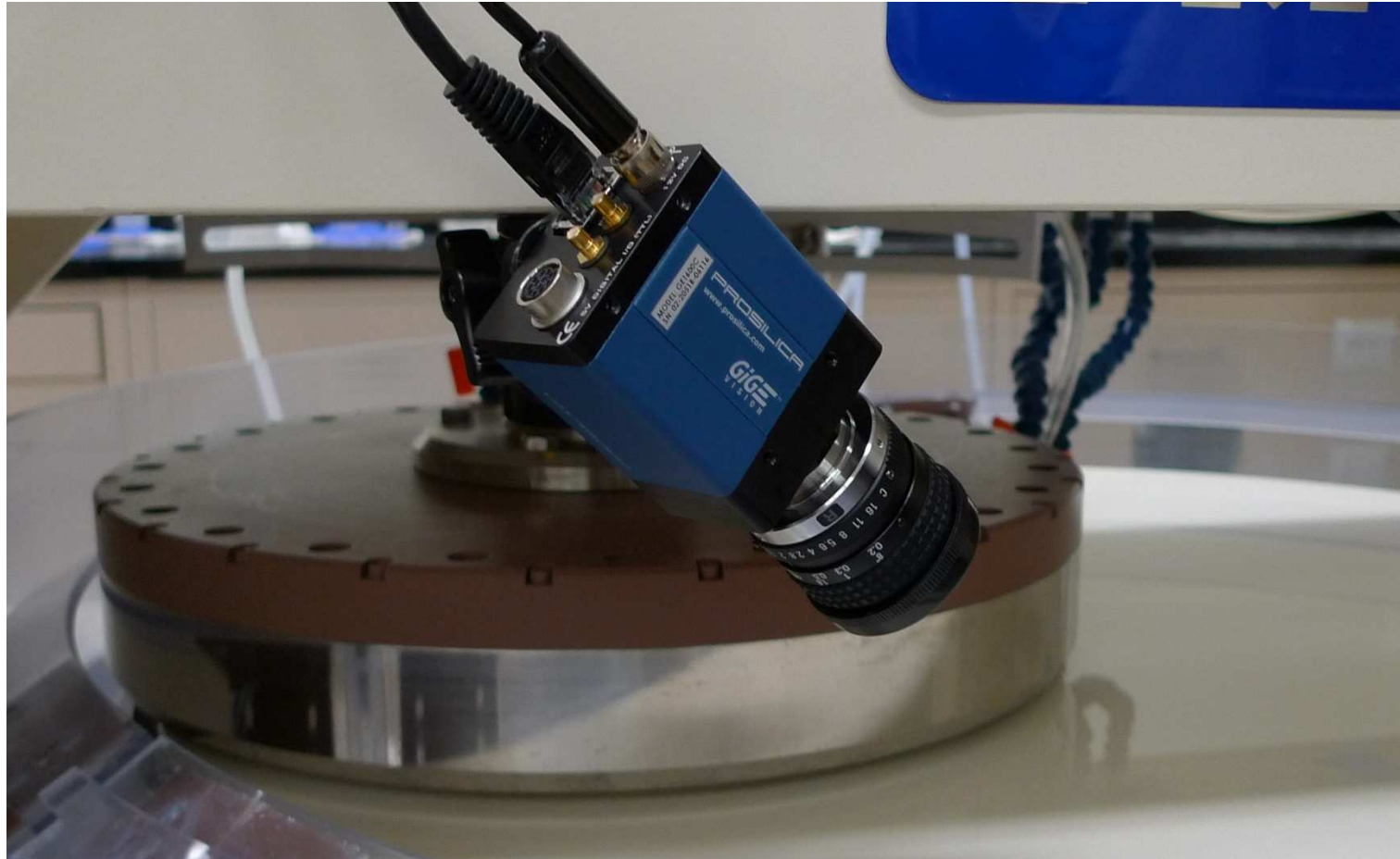


UV – LED Cover



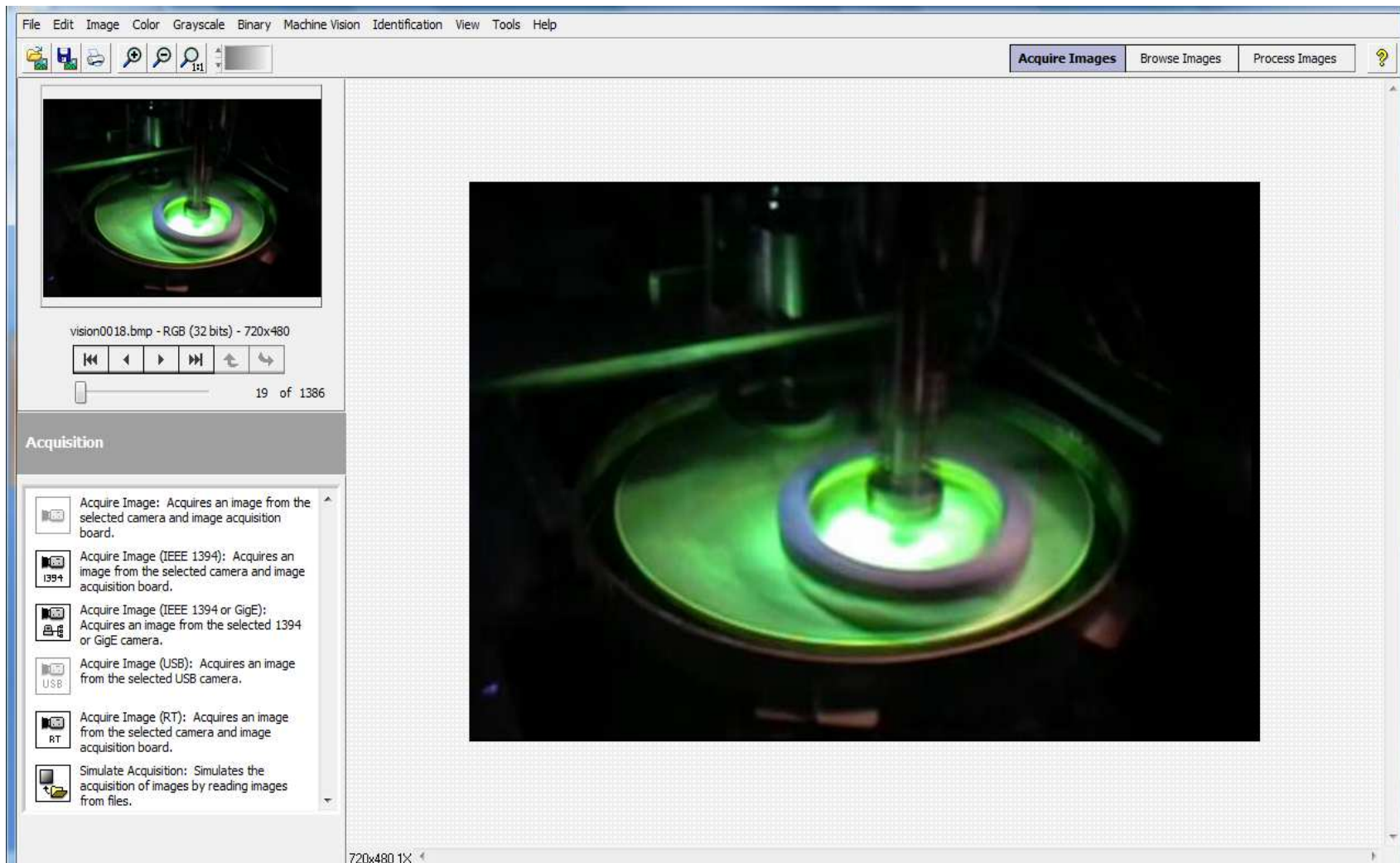
High Resolution CCD Camera

CCD Camera Setup with 300-mm Polisher

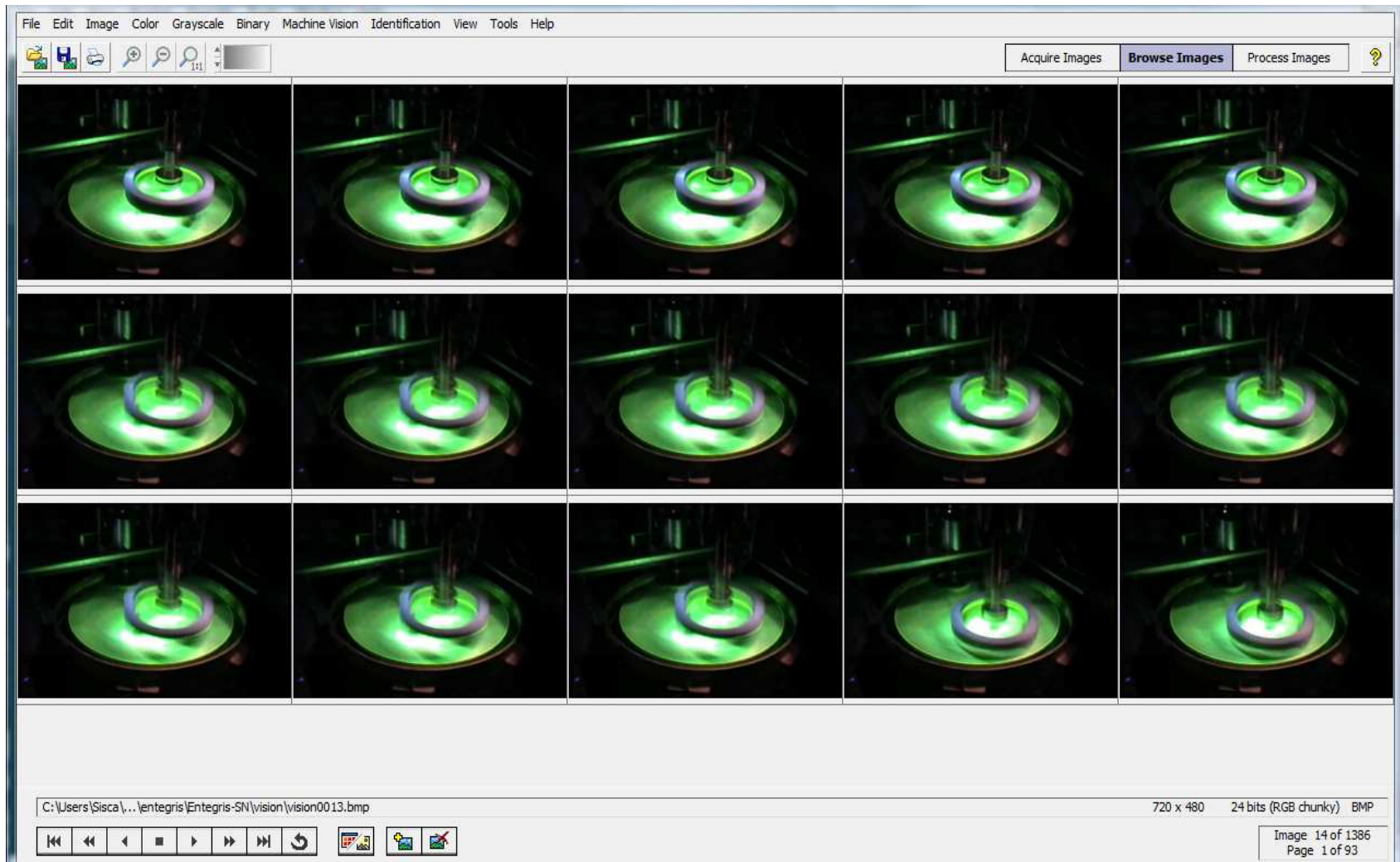


SRC/SEMATECH Engineering Research Center for Environmentally Benign Semiconductor Manufacturing

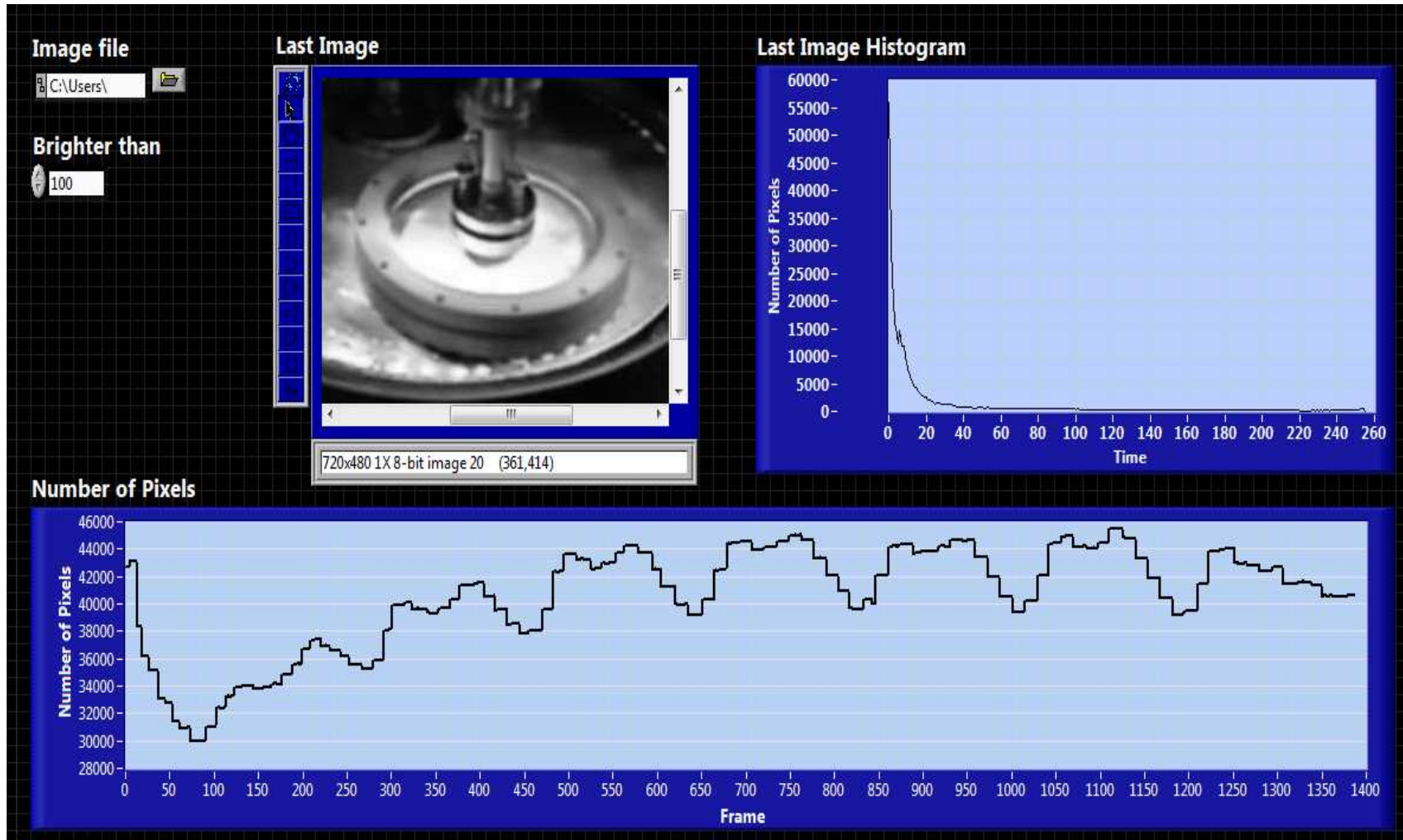
Software Interface for Image Acquisition



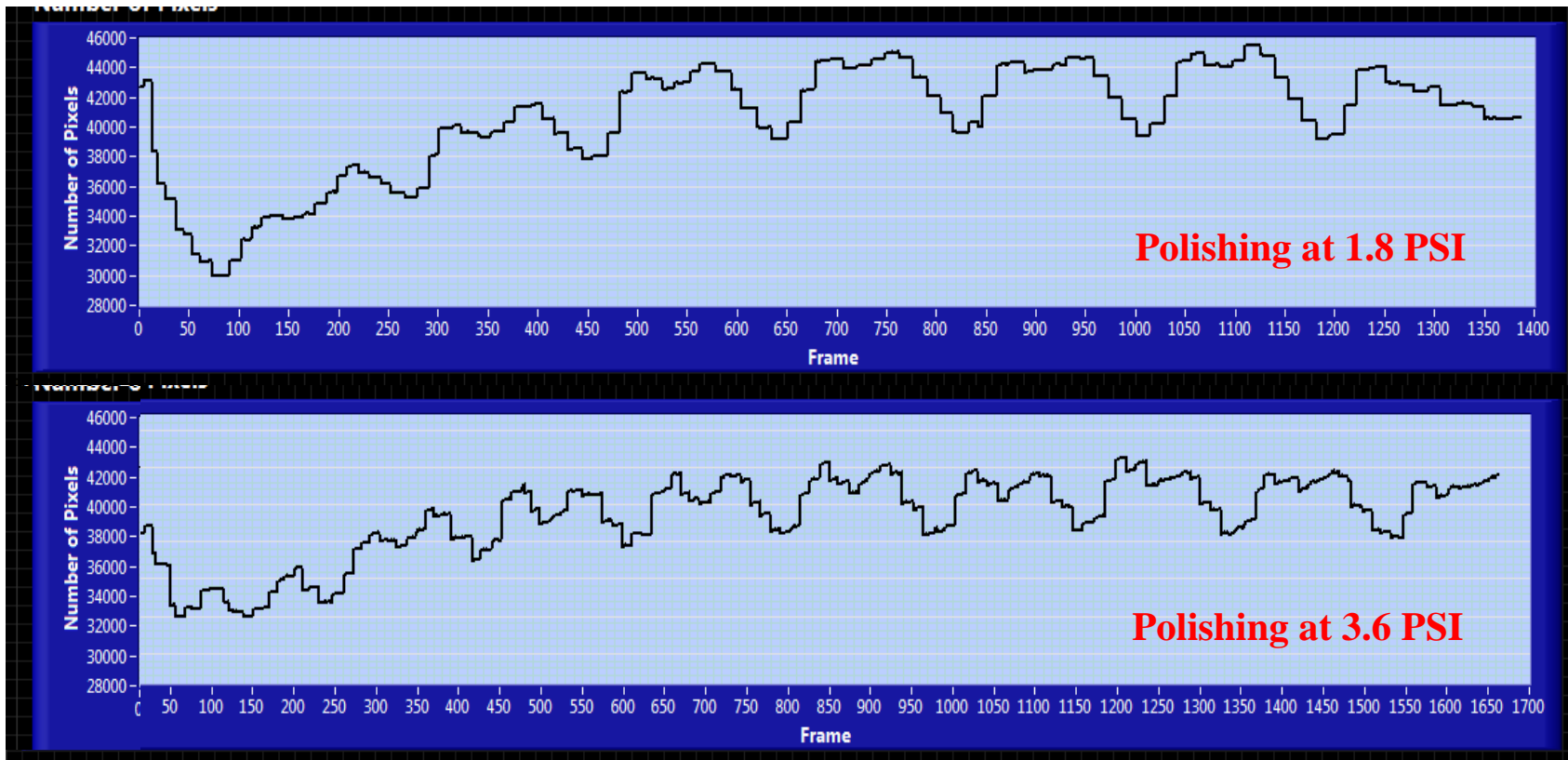
Software Interface for Image Browsing



Software Interface for Image Analysis



Effect of Polishing Pressure



The UV enhanced fluorescence system can be used to assess differences in slurry flow characteristics at two different polishing pressures.

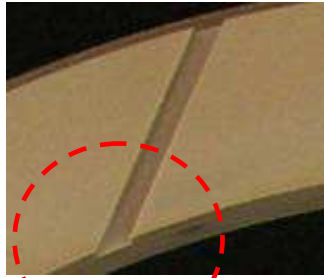
Industrial Interactions and Technology Transfer

Industrial mentors and contacts:

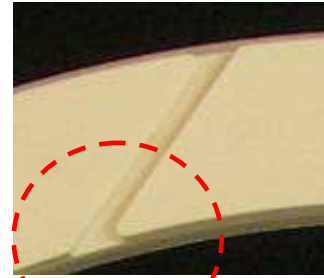
- **Christopher Wargo (Entegris)**
- **Cliff Spiro (Cabot Microelectronics)**

Future Plans

- **Next year plan: investigate the effect of retaining ring geometry and material (PPS vs. PEEK) on slurry flow and pad micro-texture**



Slot Design #1



Slot Design #2

- **Long-term plan: develop fundamental understanding of retaining ring's effects on slurry flow and polishing performance to overcome difficult challenges in environmental and manufacturing efficiency.**

Fundamentals of Advanced Planarization: Pad Micro-Texture, Pad Conditioning, Slurry Flow, and Retaining Ring Geometry

(Task 425.032)

Subtask 2: Effect of Pad Conditioning on Pad Micro-Texture and Polishing Performance

PI:

- Ara Philipossian, Chemical and Environment Engineering, UA
- Duane Boning, Electrical Engineering and Computer Science, MIT

Graduate Students:

- Ting Sun, Chemical and Environmental Engineering, UA, graduated with Ph. D. degree in May 2009
- Xiaoyan Liao, Ph. D. candidate, Chemical and Environment Engineering, UA
- Yubo Jiao, Ph. D. candidate, Chemical and Environment Engineering, UA
- Zhenxing Han, Ph. D. candidate, Chemical and Environment Engineering, UA
- Anand Meled, Ph. D. candidate, Chemical and Environment Engineering, UA
- Wei Fan, Ph. D. candidate, Electrical Engineering and Computer Science, MIT

Fundamentals of Advanced Planarization: Pad Micro-Texture, Pad Conditioning, Slurry Flow, and Retaining Ring Geometry

(Task 425.032)

Subtask 2: Effect of Pad Conditioning on Pad Micro-Texture and Polishing Performance

Other Researchers:

- Yun Zhuang, Postdoctoral Fellow, Chemical and Environment Engineering, UA
- Yasa Sampurno, Postdoctoral Fellow, Chemical and Environment Engineering, UA
- Jiang Cheng, Visiting Scholar, Chemical and Environment Engineering, UA

Cost Share (other than core ERC funding):

- In-kind donation (slurry) from Hitachi Chemical
- In-kind support from Araca, Inc.

Objectives

- Investigate the effect of pad conditioning on pad surface micro-texture, as well as frictional force, removal rate, and wafer topography (dishing/erosion) during ILD/STI CMP processes
- Investigate the origin of pad surface contact in CMP processes
- Characterize pad asperity height using stylus micro profilometry

ESH Metrics and Impact

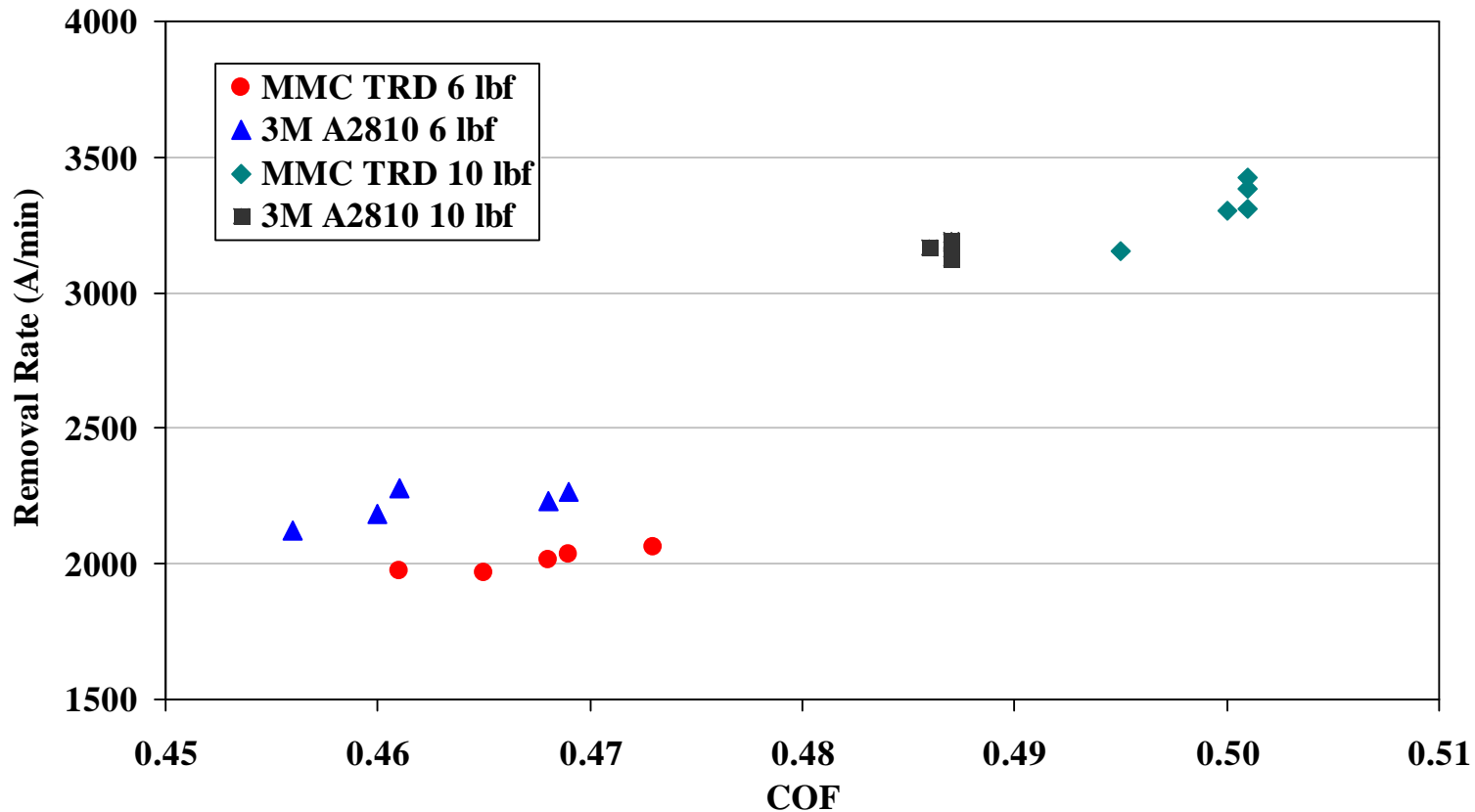
- 1. Reduce CMP consumable consumption (pad, slurry, UPW, chemicals, pad conditioner, and retaining ring) by increasing yield through 1-3X dishing and erosion reduction*

General Approach

Polish 200-mm blanket TEOS and SKW3-2 STI wafers under 6 and 10 lb conditioning forces with a 3M A2810 disc and a Mitsubishi Materials Corporation 100-grit TRD disc, and analyze pad micro-texture through laser confocal microscopy:

- Blanket wafer polishing: frictional force and removal rate**
- Patterned wafer polishing: dishing and erosion**
- Pad micro-texture analyses: contact area, surface abruptness, and summit curvature**

Removal Rate vs. COF



The removal rate increased much more significantly with the conditioning force (65% for the MMC TRD disc and 43% for the 3M A2810 disc) than the COF (7% for the MMC TRD disc and 5% for the 3M A2810 disc).

Dishing and Erosion Analysis

Center Die, 100 Micron Pitch

Conditioning Force (lb)	Diamond Disc	Dishing (A)					Erosion (A)				
		Pattern Density					Pattern Density				
		10%	30%	50%	70%	90%	10%	30%	50%	70%	90%
6	3M A2810	125	1200	300	300	275	110	134	125	113	117
	MMC TRD	325	2800	500	500	325	330	215	406	129	172
10	3M A2810	275	600	200	125	175	34	22	49	11	4
	MMC TRD	750	1400	300	225	275	103	23	86	24	18

At both conditioning forces, $\text{Dishing/Erosion}_{3M\ A2810\ disc} < \text{Dishing/Erosion}_{MMC\ TRD\ disc}$

Laser Confocal Microscopy

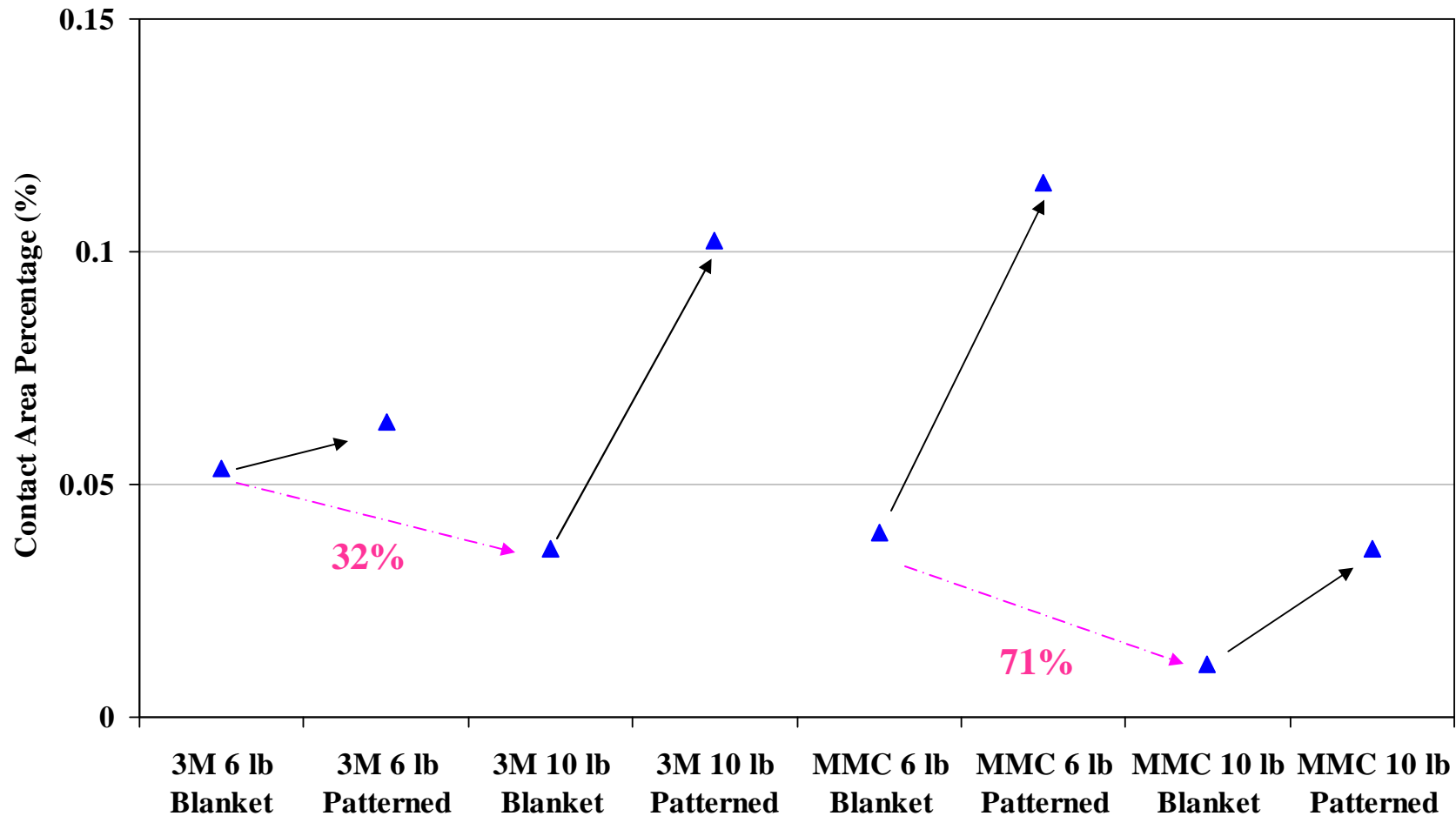


Zeiss LSM 510 Meta NLO

Pad surface contact area and topography analyses were performed through laser confocal microscopy.

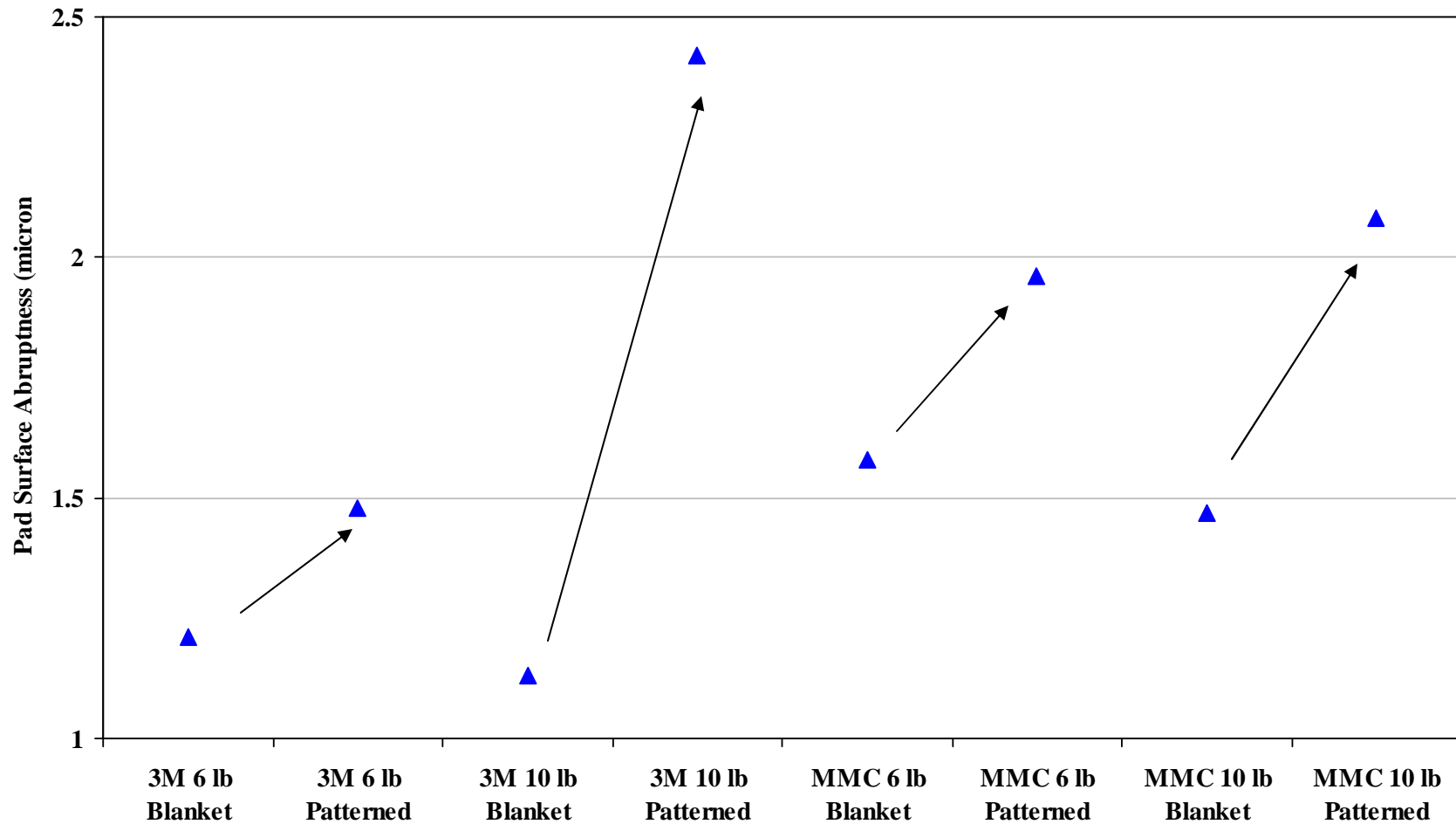
SRC/SEMATECH Engineering Research Center for Environmentally Benign Semiconductor Manufacturing

Contact Area Percentage



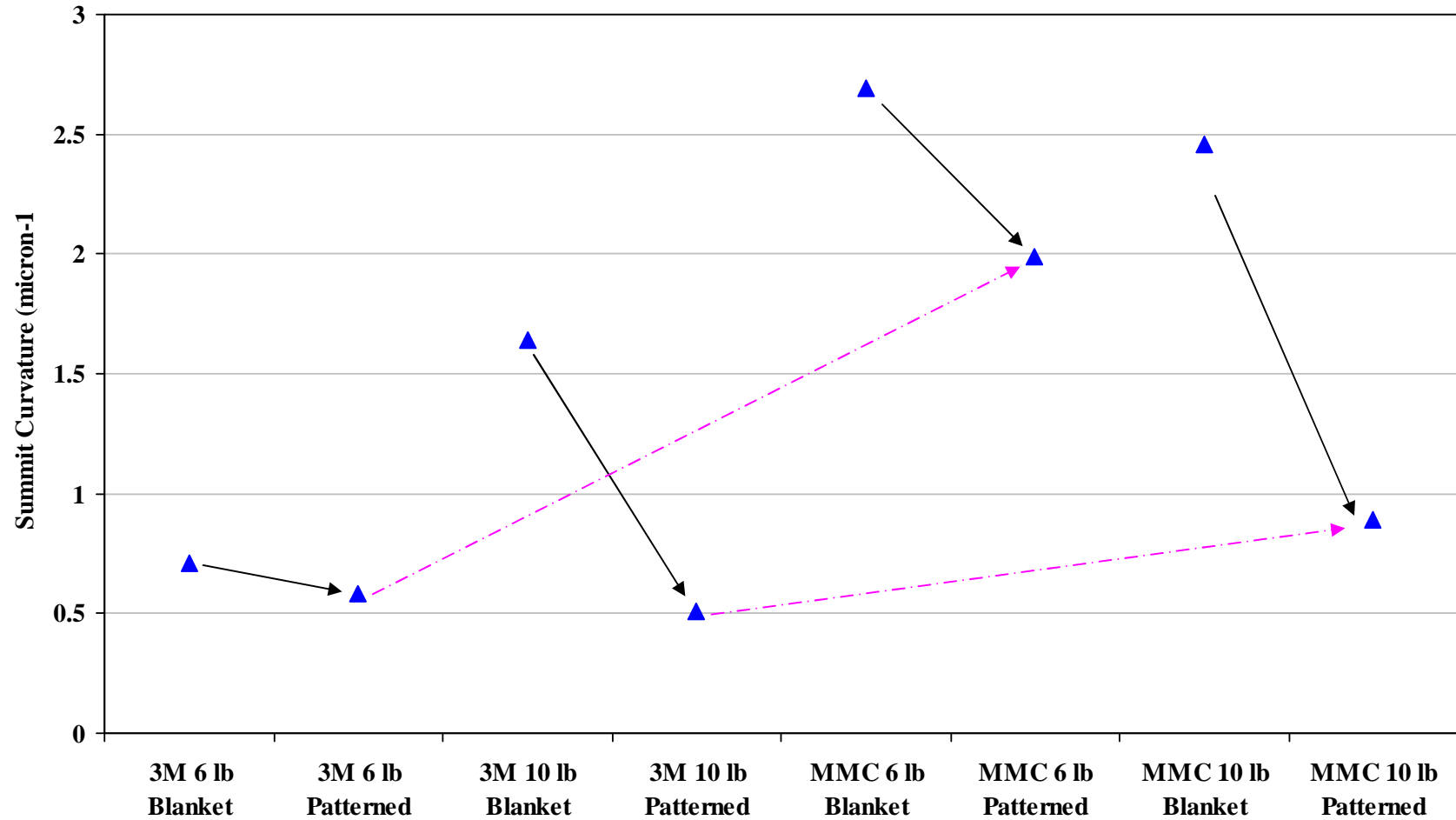
Contact area percentage decreased significantly when the conditioning force increased from 6 to 10 lb for both diamond discs during blanket wafer polishing, resulting in significantly smaller contact area, larger mean contact pressure, and higher removal rate.

Pad Surface Abruptness



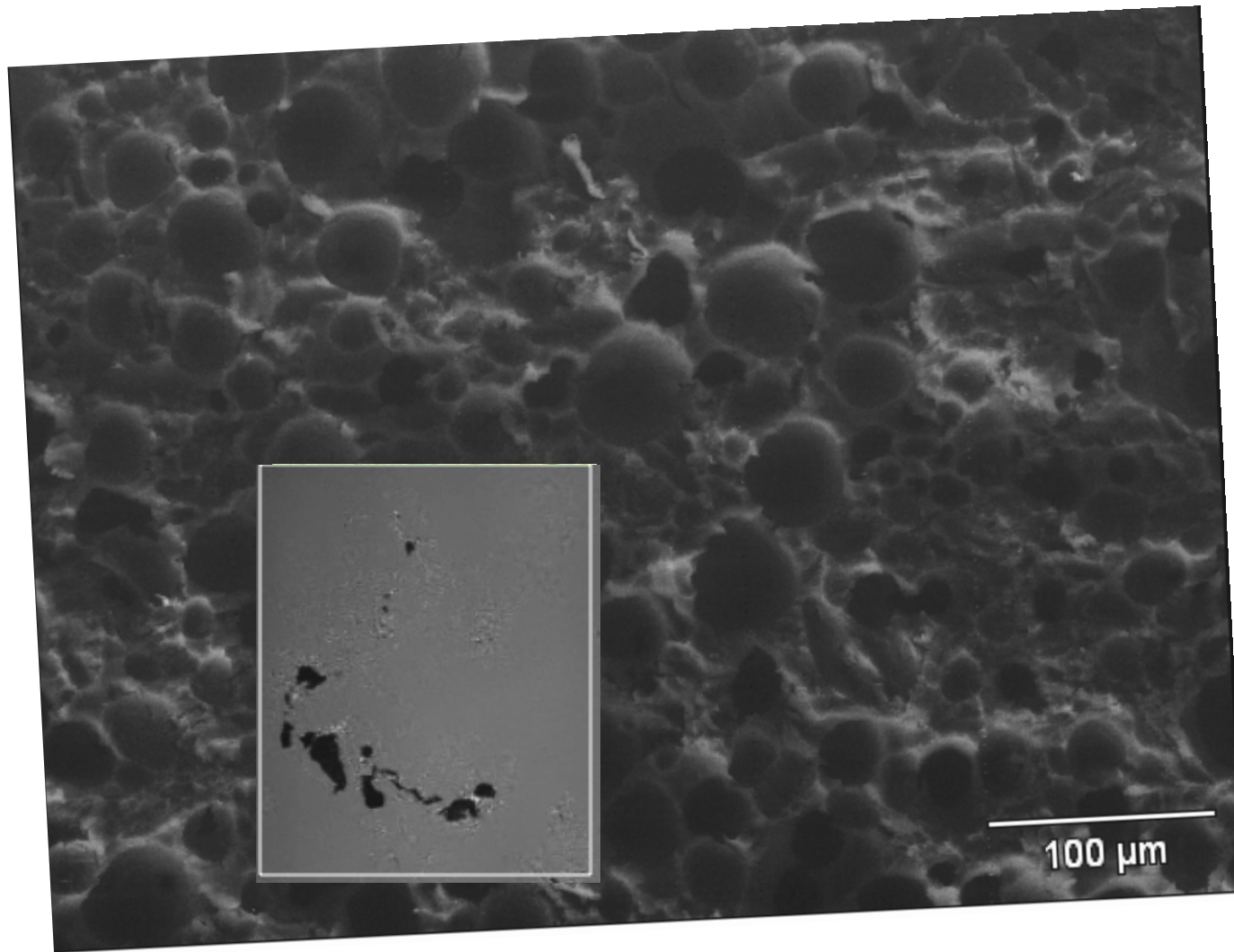
The topography on the patterned wafer surface created extra collisions with pad summits, resulting in less abrupt pad surface compared with blanket wafer polishing.

Mean Summit Curvature

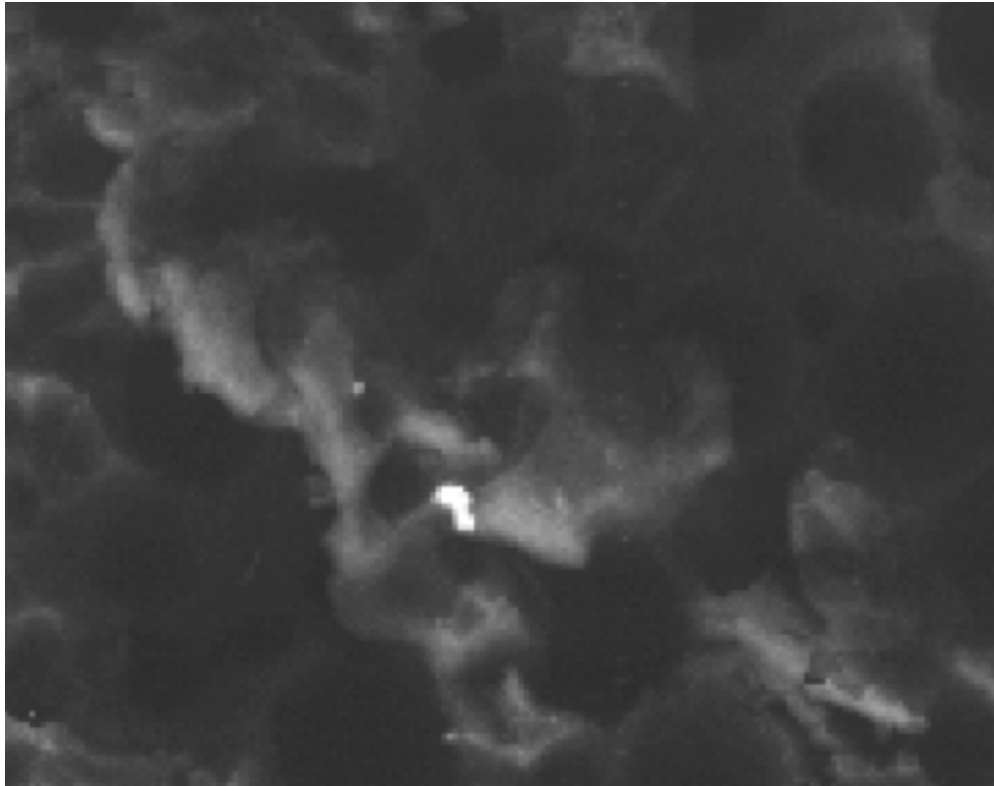


Sharper pad summits (larger summit curvature) contributed to higher dishing and erosion.

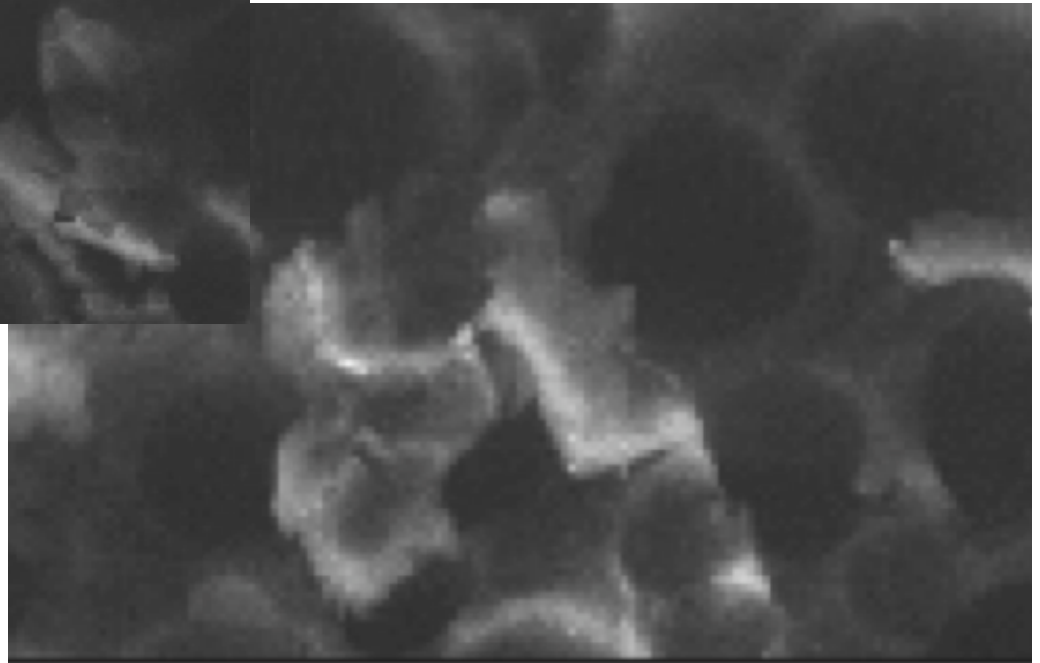
SEM, Topography and Contact Image



More Examples of Contact

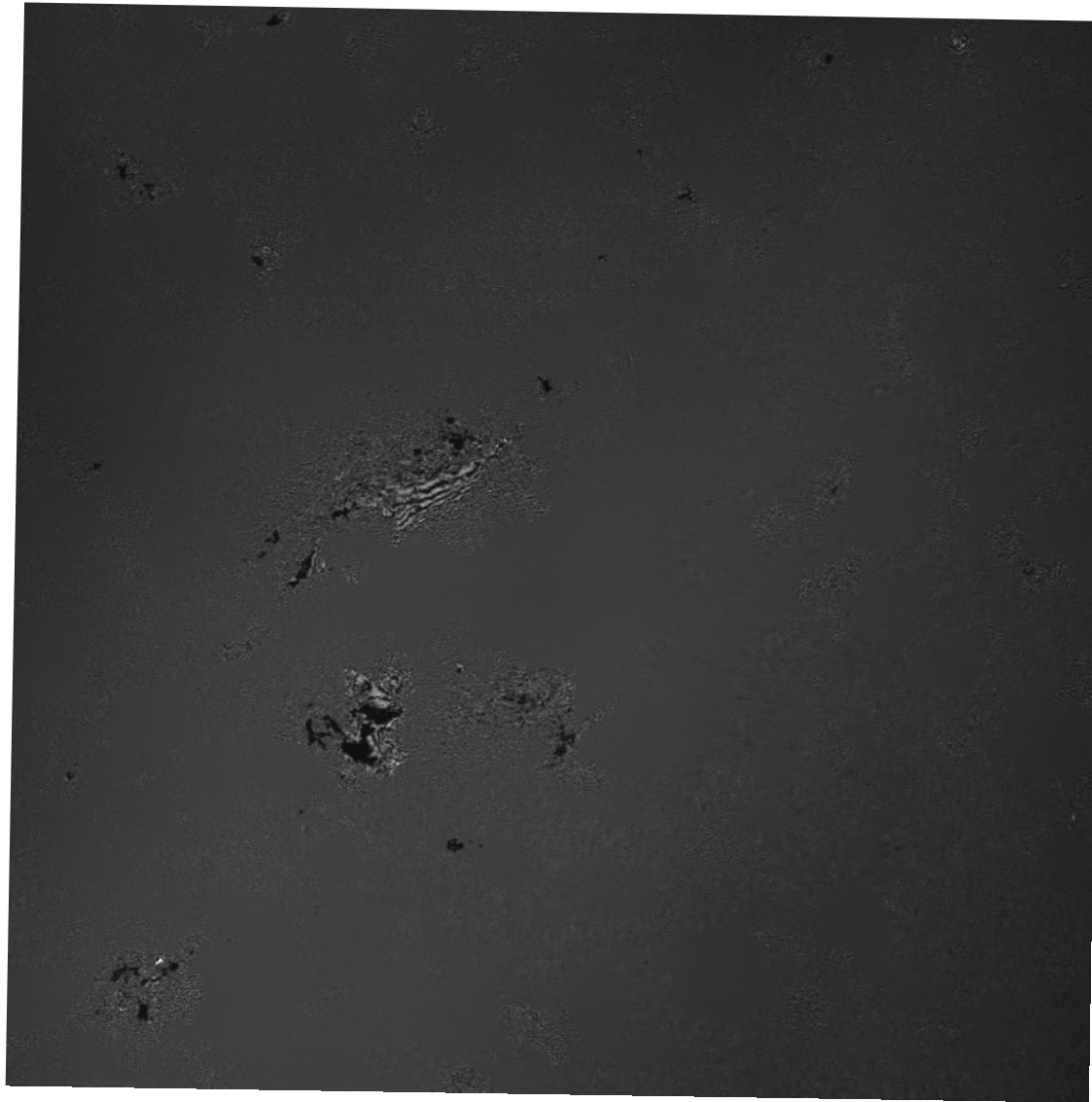


Contacting material appears to consist of fractured and collapsed pore walls.

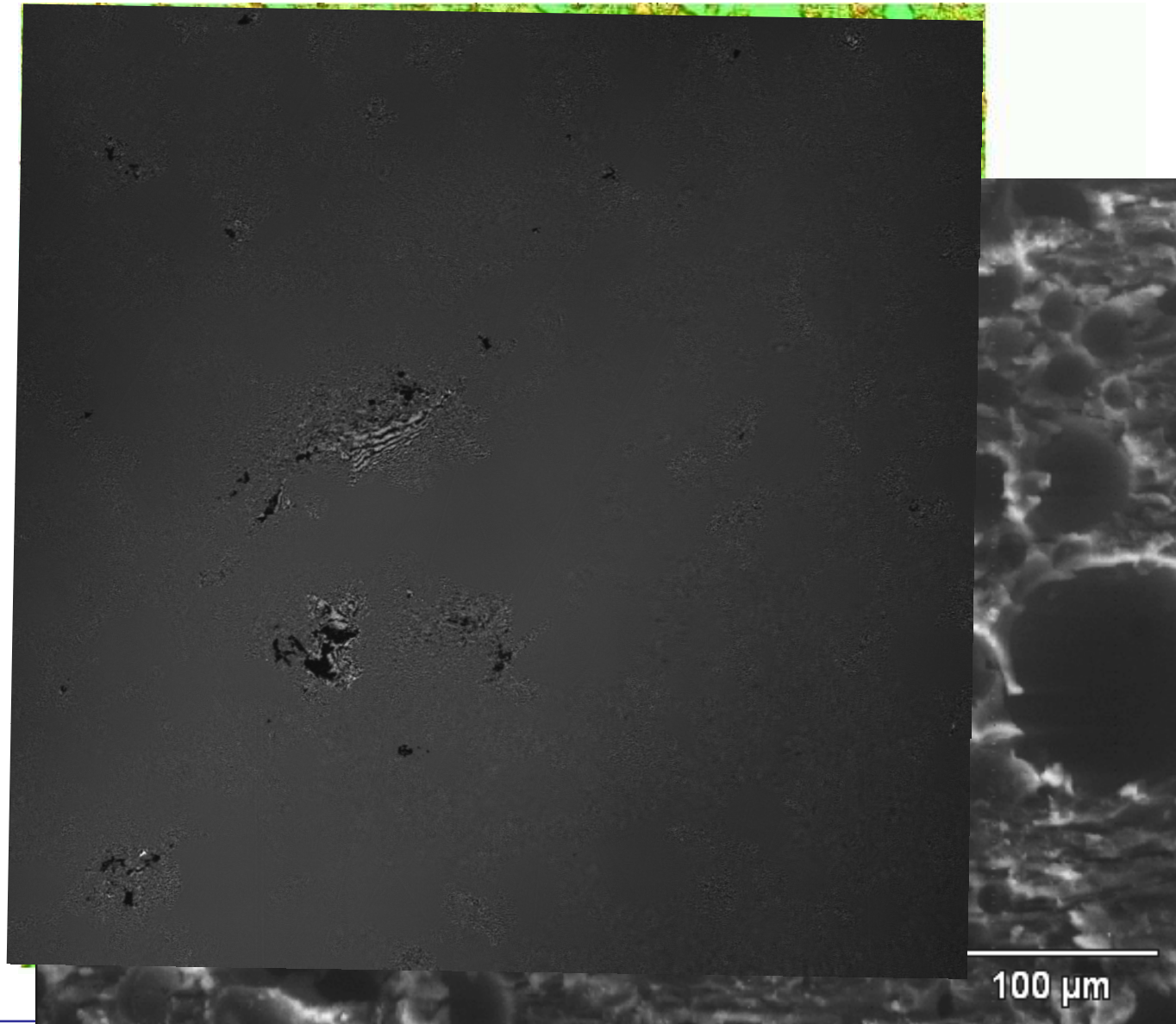


Large Contacts with Fringed Areas

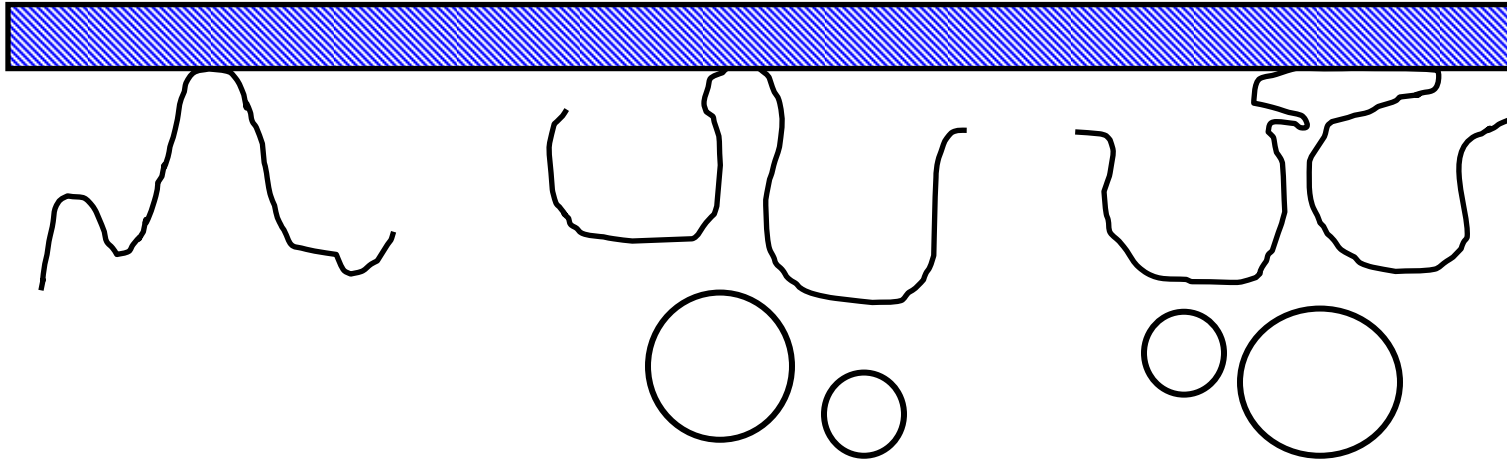
50 μm



Topography and SEM Comparison



Contacting Summit Types



Fully supported contacting summit, solid underlying pad material.

Applied force produces a small deflection and a small contact area.

Assumed in most rough surface contact theories.

May be rare in CMP

Less well-supported contacting summit, pore-filled bulk.

Applied force produces a larger deflection but a small contact area.

Fractured, poorly supported contacting summit.

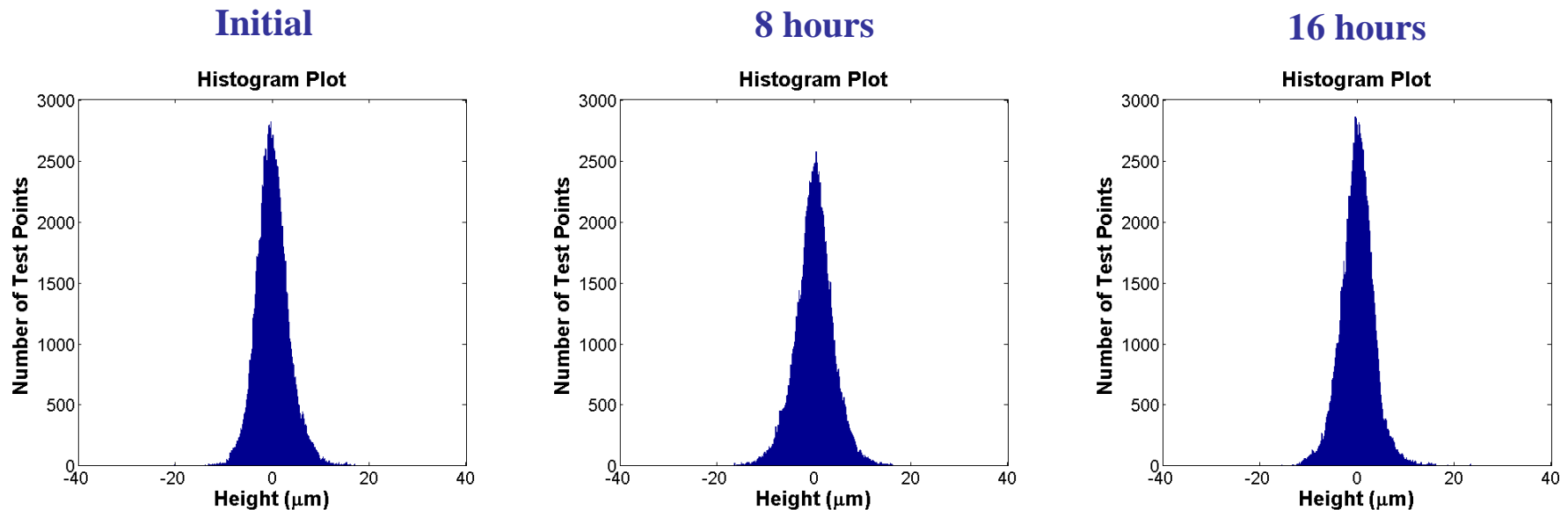
Applied force produces a large, low pressure contact area.

Contact behaves like a compliant, flexible plate.

Very common in CMP

Pad Asperity Height Distribution

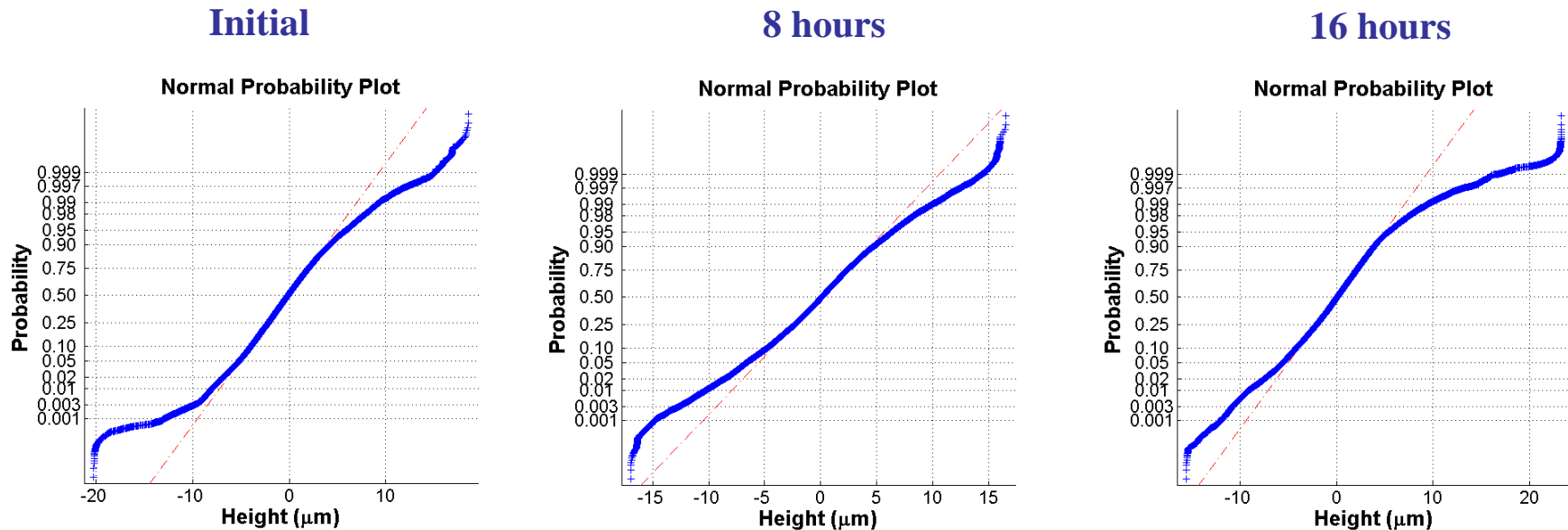
- Take pad samples during 16-hour polishing process
 - Initial, 8 hours and 16 hours
- Scan a 500 μm by 500 μm area on pad sample surface with a stylus micro profilometer



W. Fan (MIT)

Pad Asperity Height Distribution

- Pad asperity height range does not change significantly during 16-hour polishing
- Pad asperity height distribution changes during 16-hour polishing
 - The height distribution is symmetric on normal plot at 8 hours, but not at initial and 16 hours
- Asperity height distribution goes out of normal above 5 μm



W. Fan (MIT)

Pad Asperity Height Distribution

- Exponential distribution fits medium high asperities (5~15 μm) well

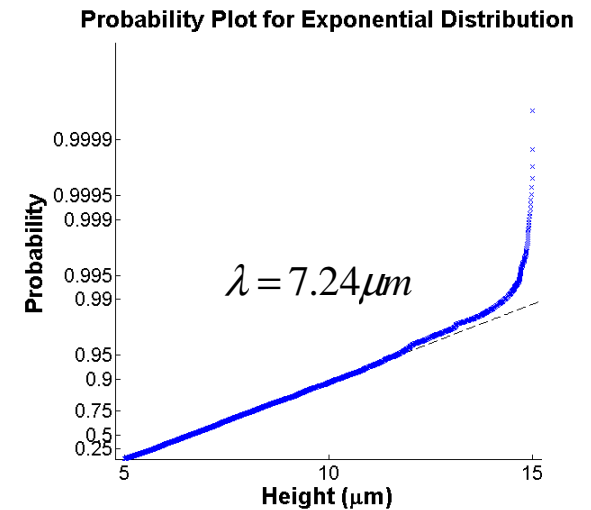
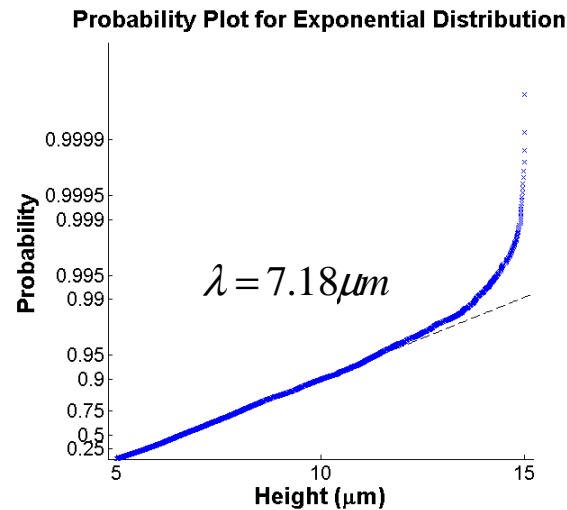
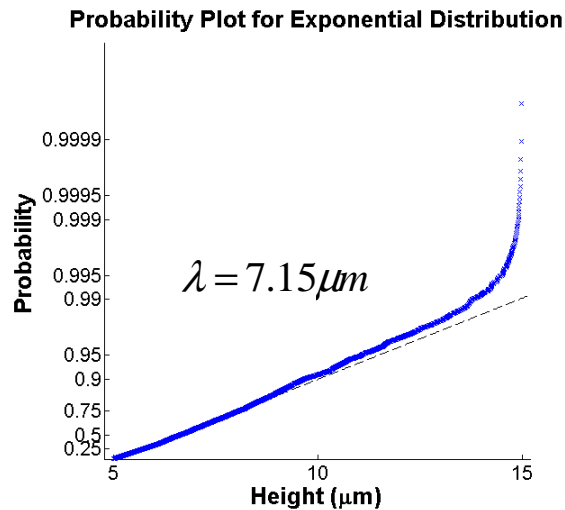
$$l(h) = \frac{1}{\lambda} e^{-\frac{h}{\lambda}} \quad \lambda : \text{characteristic asperity height}$$

- Characteristic asperity height does not change significantly in medium high region during 16-hour polishing

Initial

8 hours

16 hours



W. Fan (MIT)

Industrial Interactions and Technology Transfer

Industrial mentors and contacts:

- **Lenoard Borucki (Araca)**
- **Mansour Moinpour (Intel)**

Future Plans

- **Next year plan:** investigate the effect of pad conditioning on pad surface micro-texture, as well as frictional force, removal rate, and wafer topography (dishing/erosion) during copper CMP processes.
- **Long-term plan:** develop fundamental understanding of the effect of pad conditioning and pad-wafer contact in CMP processes.

Publications

- **Theoretical and Experimental Investigation of Conditioner Design Factors on Tribology and Removal Rate in Copper Chemical Mechanical Planarization. L. Borucki, H. Lee, Y. Zhuang, N. Nikita, R. Kikuma and A. Philipossian. Japanese Journal of Applied Physics, 48(11), 115502 (2009).**
- **Investigating the effect of diamond size and conditioning force on chemical mechanical planarization pad topography. T. Sun, L. Borucki, Y. Zhuang and A. Philipossian. Microelectronic Engineering, in press.**
- **Investigating the Effect of Conditioner Aggressiveness on Removal Rate during Inter-Layer Dielectric CMP through Confocal Microscopy and Dual Emission UV Enhanced Fluorescence Imaging. T. Sun, L. Borucki, Y. Zhuang, Y. Sampurno, F. Sudargho, X. Wei, S. Anjur and A. Philipossian. Japanese Journal of Applied Physics, in press.**
- **Effect of Pad Micro-Texture on Frictional Force, Removal Rate, and Wafer Topography during ILD/STI CMP Processes. Y. Zhuang, X. Liao, L. Borucki, J. Cheng, S. Theng, T. Ashizawa and A. Philipossian. International Conference on Planarization/CMP Technology Proceedings, 85-90 (2009).**
- **Pad Topography, Contact Area and Hydrodynamic Lubrication in Chemical-Mechanical Polishing. L. Borucki, T. Sun, Y. Zhuang, D. Slutz and A. Philipossian. Materials Research Society Symposium Proceedings, Vol. 1157, E01-02 (2009).**

Presentations

- **Effect of Pad Micro-Texture on Frictional Force, Removal Rate, and Wafer Topography during ILD/STI CMP Processes.** Y. Zhuang, X. Liao, L. Borucki, J. Cheng, S. Theng, T. Ashizawa and A. Philipossian. International Conference on Planarization/CMP Technology, Fukuoka, Japan, November 19-21 (2009).
- **The Origin and Mechanics of Large Pad-Wafer Contact Areas.** L. Borucki, Y. Sampurno, Y. Zhuang and A. Philipossian. The Fourteenth International Symposium on Chemical-mechanical Planarization, Lake Placid, New York, August 9-12 (2009).
- **Pad Topography, Contact Area and Hydrodynamic Lubrication in Chemical Mechanical Polishing.** L. Borucki, T. Sun, Y. Zhuang, D. Slutz and A. Philipossian. Materials Research Society Spring Meeting, San Francisco, California, April 13-17 (2009).

Fundamentals of Advanced Planarization: Pad Micro-Texture, Pad Conditioning, Slurry Flow, and Retaining Ring Geometry

(Task 425.032)

Subtask 3: Implementation of an Extended Die-Level and Wafer-Level CMP Model

PI:

- Duane Boning, Electrical Engineering and Computer Science, MIT

Graduate Students:

- Wei Fan, Ph.D. candidate, EECS, MIT
- Joy Johnson, Ph.D. candidate, EECS, MIT

Cost Share (other than core ERC funding):

- Experimental data, Intel
- Experimental support, National Semiconductor Corporation

Objectives

Goal: Improve fundamental understanding of CMP to

- Reduce use of high-cost engineered consumables
- Reduce generation of by-product wastes
- Save processing times requiring significant energy

1. Retaining ring/wafer-level CMP modeling:

- Evaluate within-wafer nonuniformity as function of process and tool design
- Retaining ring geometry: affect on edge polish uniformity

2. Slurry agglomeration/wafer-level CMP modeling:

- Understand how slurry abrasive particles, pad debris, and wafer debris affect agglomeration
- Understand how agglomeration relates to the *planarization* capability of CMP processes as well as defectivity

ESH Metrics and Impact

Driving principle and goals: Joint improvement in CMP performance and ESH performance

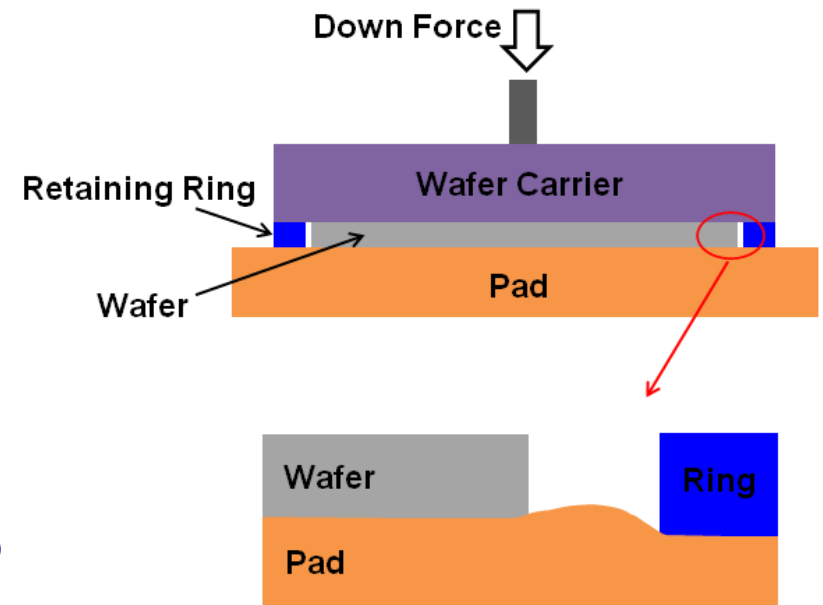
- 1. Reduction in the use or replacement of ESH-problematic materials***
- 2. Reduction in emission of ESH-problematic material to environment***
 - Reduce slurry particle use and Cu solid waste by 20-50%**
- 3. Reduction in the use of natural resources (water and energy)***
 - Shorten CMP polish times (copper, barrier) by 20-50%**
 - Improve yield (multiplication over all inputs/outputs) by 1-2%**
- 4. Reduction in the use of chemicals***
 - Reduce slurry usage by 20%**
 - Improve pad lifetime by 20-50%**

1. Retaining Ring/Wafer-Level CMP Model

- **Evaluate Within-Wafer Polish Non-Uniformity**
 - Pressure distribution is highly non-uniform near the wafer edge
 - The non-uniform removal rate causes a roll-off profile at wafer edge
- **Investigate the Impact of CMP Tool System**
 - Retaining ring geometry and design
 - Relative velocity affected by wafer speed, pad speed and polishing head position

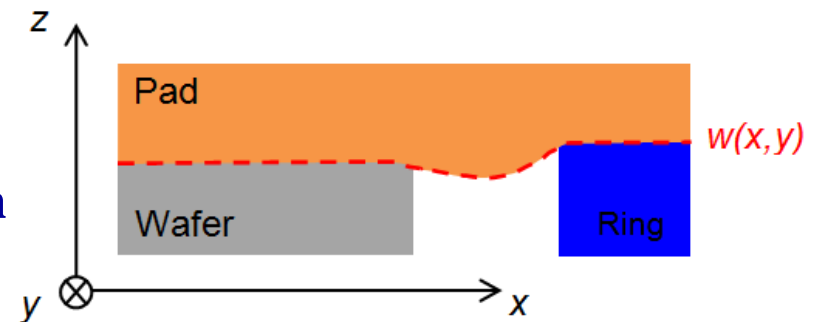
Modeling of Pressure Distribution

- **Non-uniform pressure distribution results from the discontinuities of the process tool geometry at the wafer edge**
- **The retaining ring is usually under higher pressure to prevent the wafer from slipping out**
- **The pad bends around the wafer edge due to the existence of the gap and retaining ring**
- **Wafer edge pressure can be tuned by the ring pressure**



Modeling of Pressure Distribution Cont'd

- The pad can be treated as an elastic body
- Wafer and retaining are both rigid
- The relationship between pad deformation and wafer/ring surface topography can be calculated using a contact wear model



Pad Surface Displacement

$$w(x, y) - w_0 = F(x, y) \otimes P(x, y)$$

Point Pressure Response

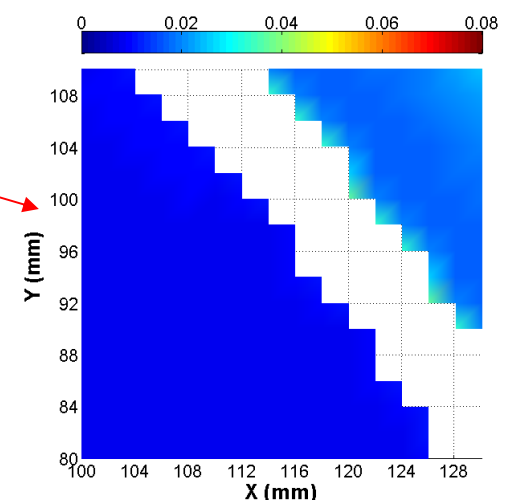
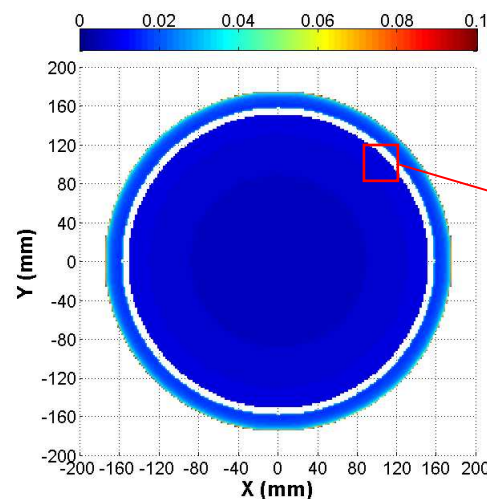
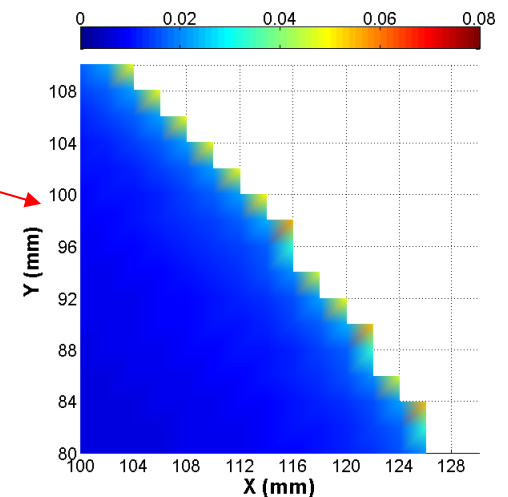
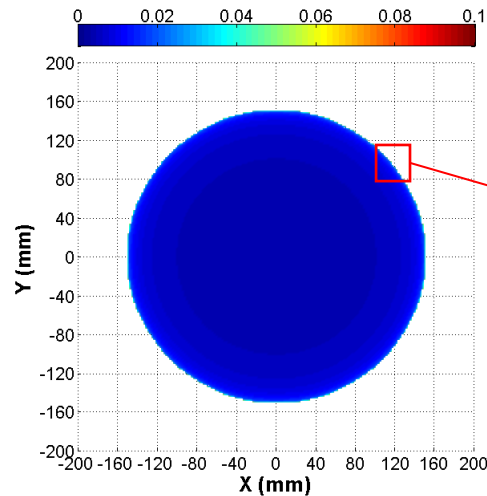
$$F(x, y) = \frac{1}{\pi E} \int d\xi \int d\eta \frac{1}{\sqrt{(x-\xi)^2 + (y-\eta)^2}} \quad E: \text{pad effective modulus}$$

Boundary Conditions

$$\left\{ \begin{array}{l} P(x, y) \geq 0 \\ \frac{1}{S_0} \int_{\text{wafer}} P(x, y) \cdot dx \cdot dy = P_0 \\ \frac{1}{S_r} \int_{\text{ring}} P(x, y) \cdot dx \cdot dy = P_r \\ w(x, y) \geq z(x, y) \end{array} \right. \quad \begin{array}{l} \text{Pressure can not be negative} \\ \text{Average wafer pressure equals to wafer reference pressure} \\ \text{Average ring pressure equals to ring reference pressure} \\ z(x, y): \text{ surface of wafer and ring structure} \end{array}$$

Retaining Ring Effect on Wafer Edge Pressure

- 300mm flat wafer surface pressure (MPa) without and with retaining ring
- Assumptions of the simulation:
 - Pad effective modulus: 100MPa
 - Wafer reference pressure: 1psi
 - Ring reference pressure: 4psi
 - Ring width: 20mm
 - Gap between ring and wafer: 4mm
- Wafer edge pressure is tuned by the retaining ring
 - No pressure concentration at wafer edge when retaining ring is applied



Modeling of Relative Velocity

- **The instantaneous velocity distribution is a function of the configuration of the CMP machine**

$$\vec{V}(p) = -\omega_p (\vec{k} \times \vec{r}_0) + (\omega_w - \omega_p) (\vec{k} \times \vec{r}_w)$$

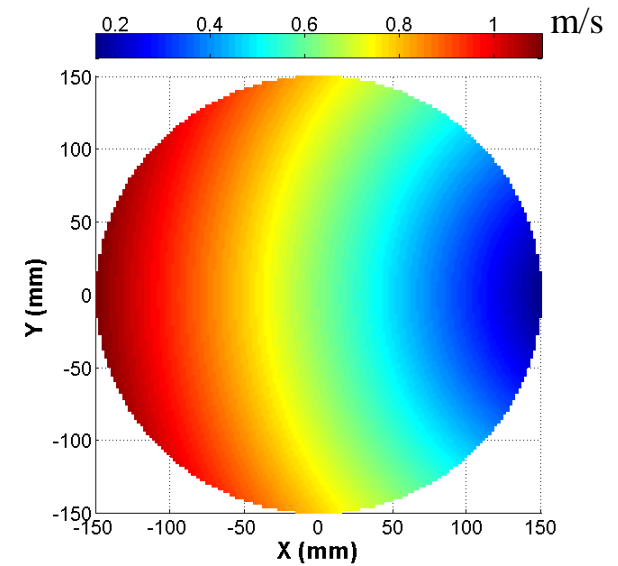
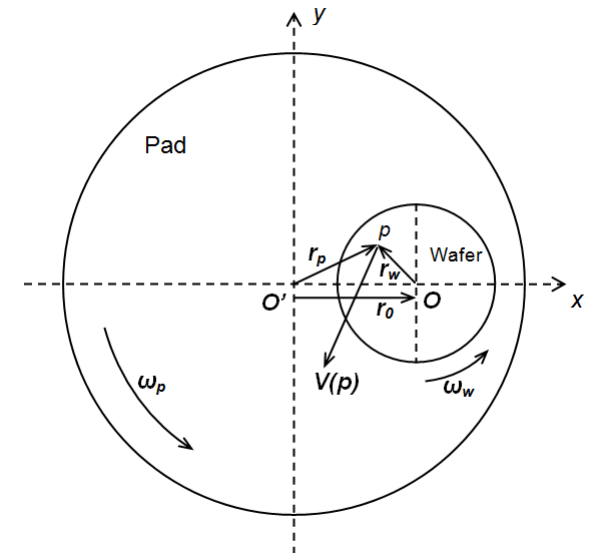
ω_w : wafer angular velocity

ω_p : pad angular velocity

\vec{k} : unit vector perpendicular to the rotation plane

- **Assumptions of the simulation:**

- 300mm wafer
- Pad rotation speed: 30rpm
- Wafer rotation speed: 60rpm
- Offset distance between pad and wafer centers: 200mm



Next Steps – Wafer-level CMP Model

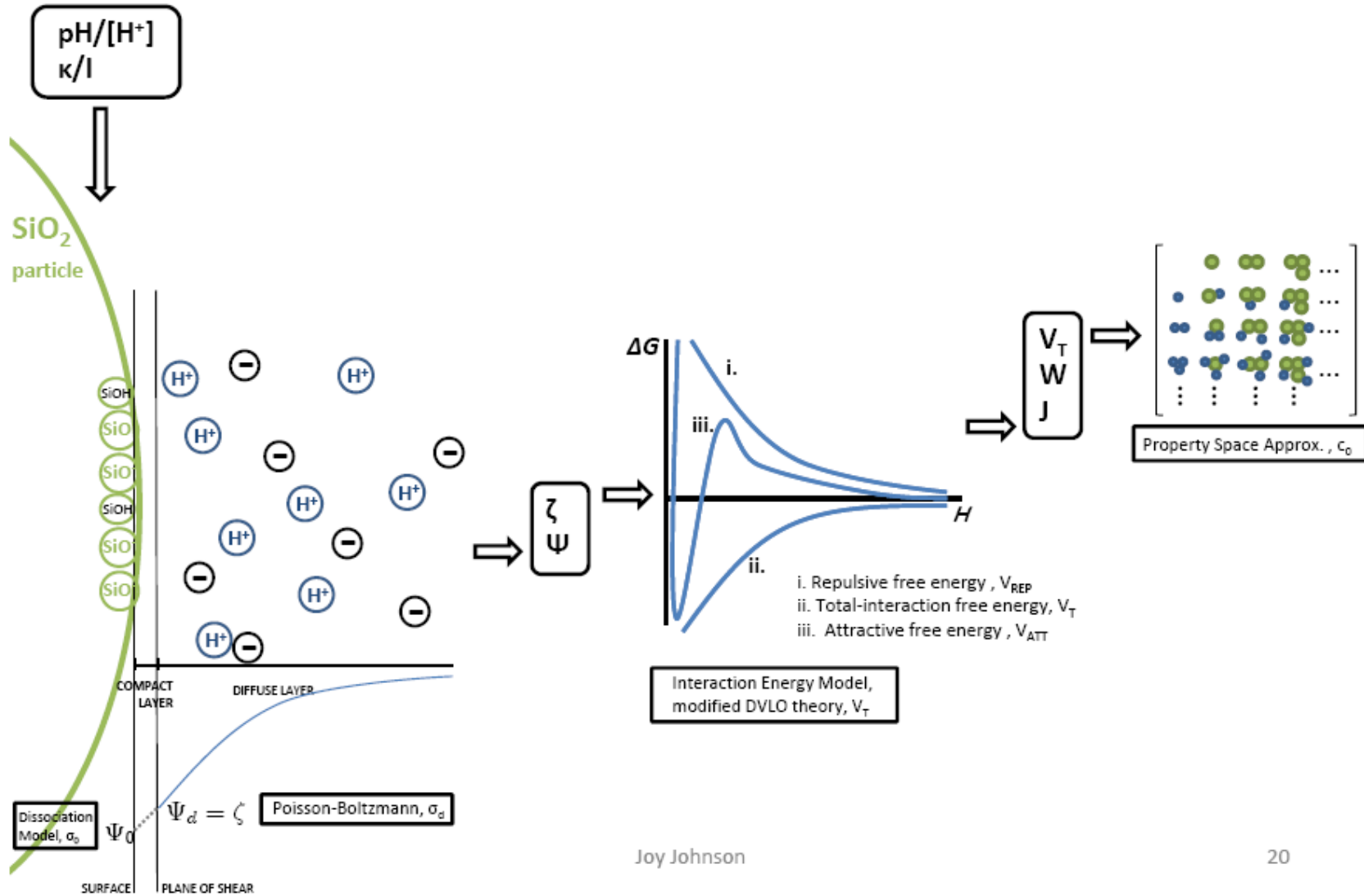
- **Integrate wafer-level model for conditioning**
 - Geometric dependencies in pad surface microtexture generation/modification based on conditioning kinematics
- **Model slurry dynamics**
 - Based on wafer edge and across-wafer pressure profiles, relative velocity kinetics, and pad microtexture
- **Integrate wafer-level with die-level CMP model**
 - Understand and capture wafer level polish rate and slurry/pad-surface nonuniformity impacts on chip uniformity and feature planarization
 - Optimization studies: pad/process/tool to reduce consumables, time, cost and improve performance

2. Slurry Agglomeration/Wafer-Level CMP Modeling:

Issue: Slurry chemistry, process conditions, and tool design affect slurry particle size and agglomeration

- **Model how/when slurry abrasive particles form agglomerates**
- **Understand how agglomeration relates to the *planarization* capability of CMP processes as well as defectivity**
 - agglomerate (particle) size distribution, slurry stability
 - dependency of wafer-scale uniformity (pattern density)
- **Integrate with *wafer- and die-scale* models:**
 - Pressure/velocity (shear) impact on slurry
 - Pad microstructure and slurry interactions

Initial Agglomeration Model



Joy Johnson

20

Next Steps – Slurry Agglomeration Model

- **Agglomeration model verification/improvement:**
 - Account for slurry particles, pad and wafer debris in the creation of agglomerates (respective of size and composition)
 - Account for slurry stability based on agglomerates, chemical composition, and shear forces during CMP
 - Calculate probability of agglomerate size distribution and corresponding stability
- **CMP model/experimental investigations:**
 - Slurry particle size distribution and stability
- **CMP wafer-scale model application**
 - Studies of planarization and defectivity as a function of slurry agglomerates
 - Possible integration of agglomeration model metrics in planarization model on wafer scale

Industrial Interactions and Technology Transfer

- **Intel**
 - **Conducting experiments for agglomeration model metrics and verification**

- **National Semiconductor**
 - **Experimental support for die-level CMP model improvements**

Publications, Presentations, and Recognitions/Awards

1. **Fan, W., D. Boning, L. Charns, H. Miyauchi, H. Tano, and S. Tsuji, “Study on Hardness and Conditioning Effects of CMP Pad Based on Physical Die-level CMP Model,” accepted in Journal of the Electrochemical Society, Dec. 2009.**
2. **D. Boning and J. Johnson, “Slurry Particle Agglomeration Model for Chemical Mechanical Planarization (CMP),” to be presented, CMP Symposium, MRS Spring Meeting, April 2010.**

Students on Task 425.032

- **Graduated Students and Current Affiliation**
- **Current Students and Anticipated Grad Date**
 - Wei Fan (Ph.D.), June 2011
 - Joy Johnson (Ph.D.), June 2012
- **Internships**
 - Joy Johnson, summer 2009, Intel Corporation (Hillsboro, Oregon)

Development of an All-Wet Benign Process for Stripping of Implanted State- of-the-Art Deep UV Resists

(Task number: 425.033)

Experimental Investigation of Catalyzed Hydrogen Peroxide(CHP) System For HDIS

PI:

- **Srini Raghavan, Department of Materials Science and Engineering, UA**

Graduate Students:

- **R. Govindarajan: PhD candidate, Department of Materials Science and Engineering, UA**

Cost Share (other than core ERC funding):

- **In-kind donation (wafers) from Sematech(~ \$ 5,000)**

Objectives

- Investigate the use of Catalyzed Hydrogen Peroxide (CHP) chemical system for disrupting the carbonized crust on deep UV resist layers exposed to high dose of ions ($\geq 10^{15}$ /cm²)
- Identify the effectiveness of CHP system using amorphous carbon as model compound

ESH Metrics and Impact

➤ SPM solution

- Requires high temperature (~180°C) for stripping high dose implanted resists

➤ Low toxicity of CHP system

Compound	LD ₅₀ (mouse)	Carcinogenic
Peroxide	2000 mg/kg	NO
Sulfuric acid	90 ml/kg (rat)	Yes
Ferrous sulfate	1520mg/kg	NO

➤ ESH Impact

- Safety issues related to the use of very hot SPM can be significantly reduced

Current Year Activities

- **Explored the use of Catalyzed Hydrogen Peroxide (CHP) system for disrupting carbonized crust that typically forms on high dose implanted resists using amorphous carbon films as model compound**
- **Tested CHP system on ion-implanted resists**
- **Removal of the resist after disruption of crust was investigated using conventional SPM solutions at temperatures less than 80°C.**

Experimental Approach

➤ **Methods**

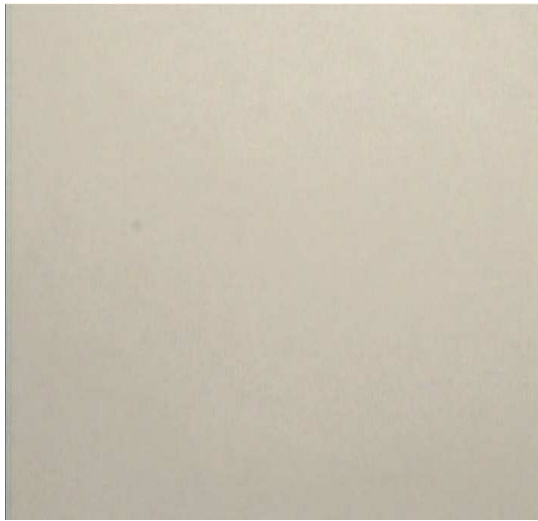
- **Morphological changes after CHP treatment were characterized using Leica DM4000B microscope operated using QCapture Pro 5.0 software, Leeds Confocal microscope, AFM and FESEM**

➤ **Materials**

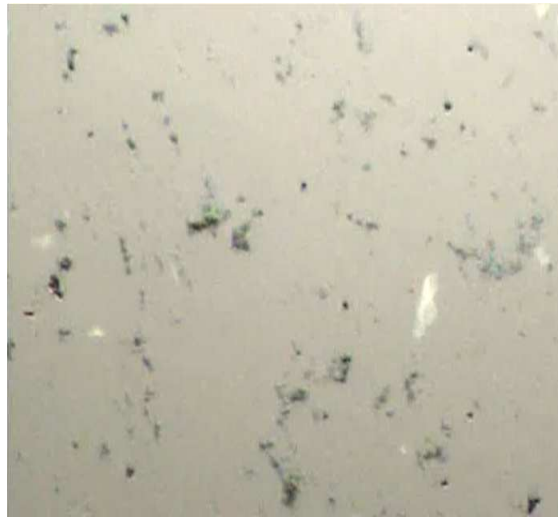
- **Amorphous carbon films ($\sim 900 \text{ \AA}$) donated by Applied Materials , Implanted resist films ($1\text{E}16 \text{ As /cm}^2$; $\sim 1.5 \text{ \mu m}$) donated by Sematech**
- **Ferrous Sulfate, 99.998% pure**
- **Hydrogen Peroxide (Semiconductor grade)**

Attack of Amorphous Carbon (a-C) Films

Optical Microscope Magnification : 1000x



Blanket a-C



a-C in 10% H₂O₂ CHP system

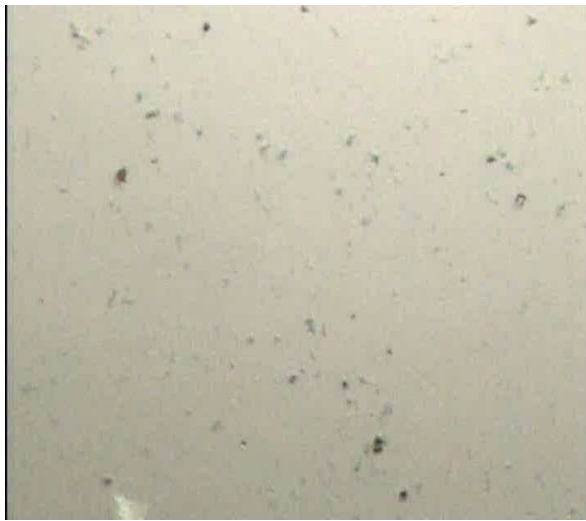


a-C in 20% H₂O₂ CHP system

- **CHP system: Hydrogen peroxide plus 1mM Fe²⁺; pH: 2.8; room temperature**
- **Optical micrographs show disruption for one hour exposure**
- **Even after 15 minutes exposure, disruption was evident**

Effect of Fe^{2+} level in CHP on a-C disruption

Optical Microscope Magnification : 1000x



a-C in 1mM Fe^{2+} CHP system



a-C in 5mM Fe^{2+} CHP system

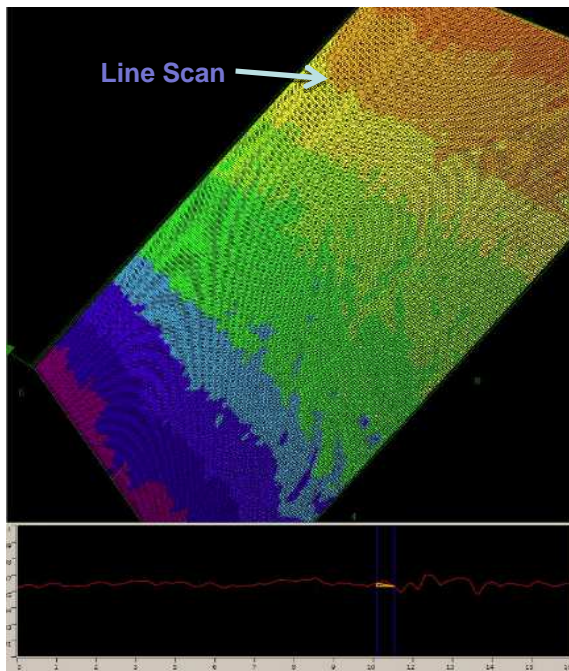


a-C in 10mM Fe^{2+} CHP system

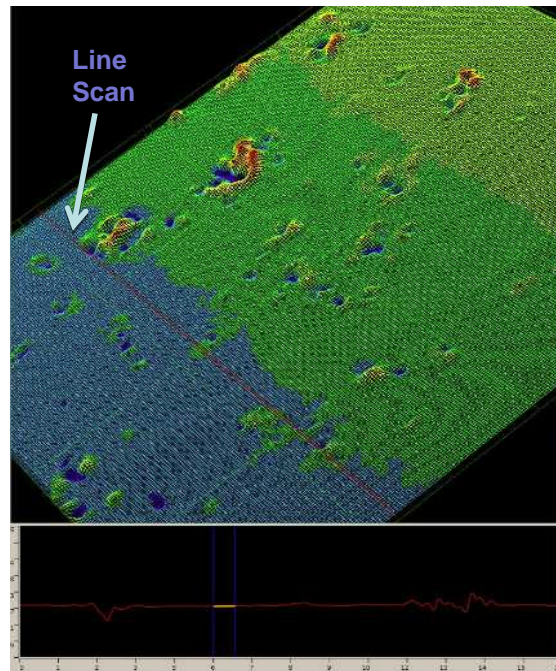
- Experiments conducted for 30 minutes
- H_2O_2 concentration fixed at 20%
- **Higher Disruption observed at 5mM Fe^{2+} level**
- **Poor attack in 10mM Fe^{2+} level CHP system may be due to faster decomposition of H_2O_2**

Confocal Microscopic Study of Changes in a-C film and High Dose Implanted Photoresist Film When Exposed to CHP

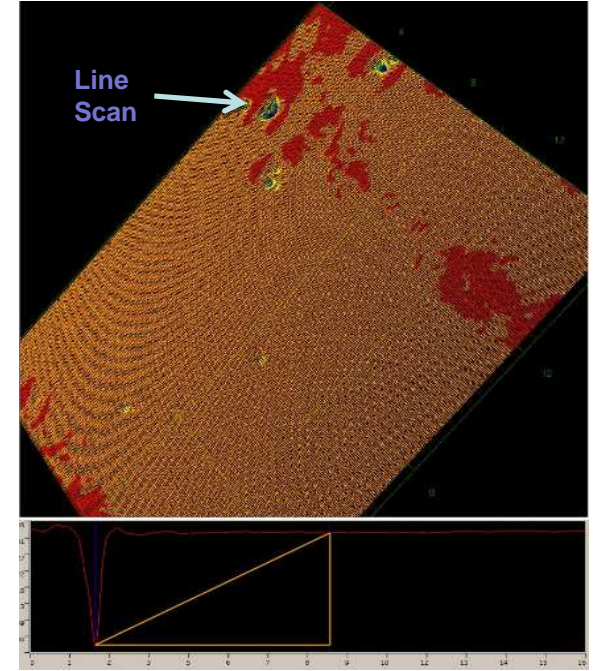
Confocal Microscope Magnification : 17Kx



Blanket a-C



a-C in 5mM Fe²⁺, 20%H₂O₂



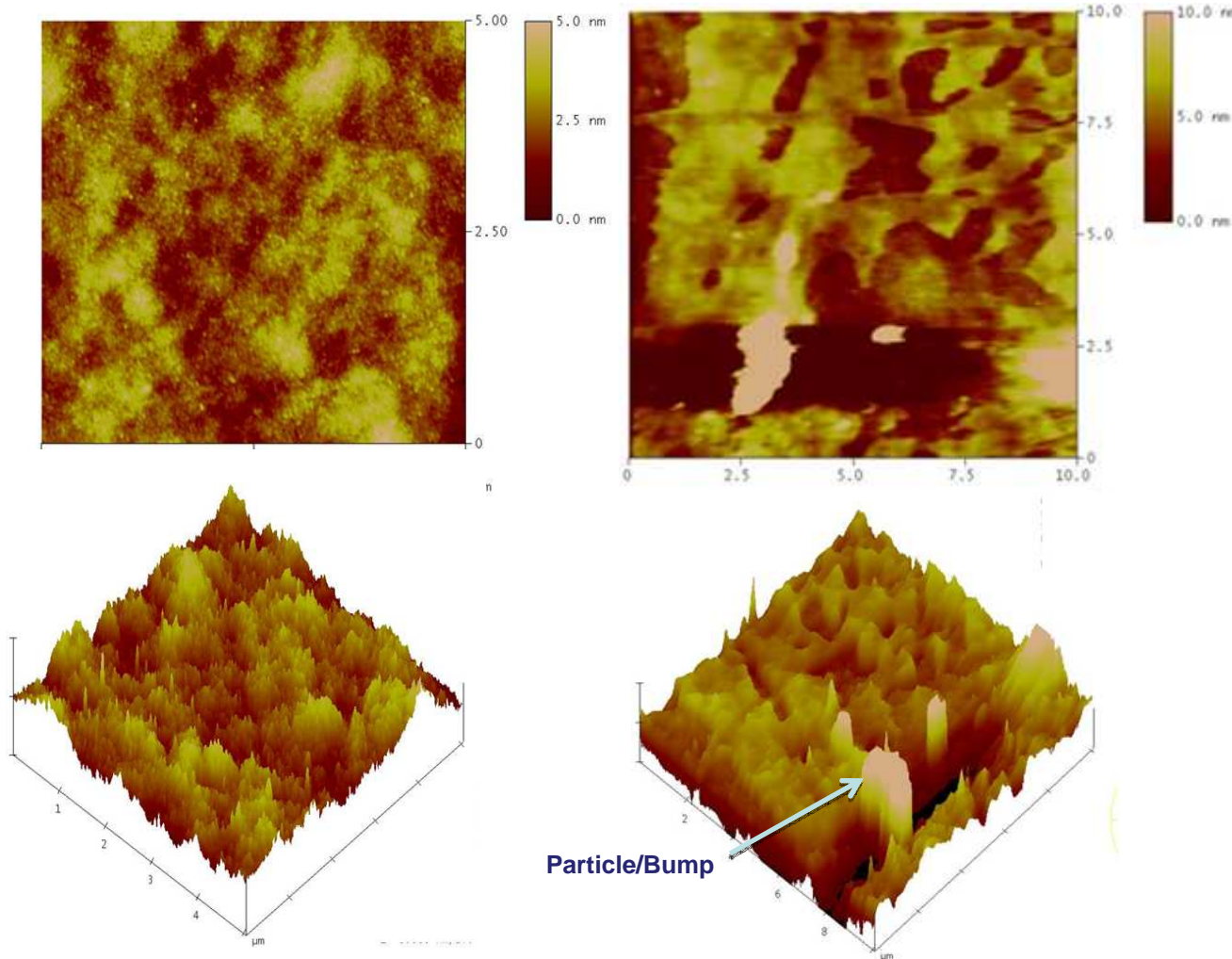
PR in 5mM Fe²⁺, 20%H₂O₂

- Effect of CHP on a-C and PR studied for 15 minutes
- Blanket a-C is smooth without pores
- CHP treated a-C shows disruption with depth up to 90 nm (~ film thickness)
- In high dose implanted PR (1E16 As/cm²) pores of depth ~ 300 nm are seen

SRC/SEMATECH Engineering Research Center for Environmentally Benign Semiconductor Manufacturing

AFM Analysis of Model a-C film

AFM Contact mode



Blanket a-C

a-C in 5mM Fe²⁺, 20%H₂O₂

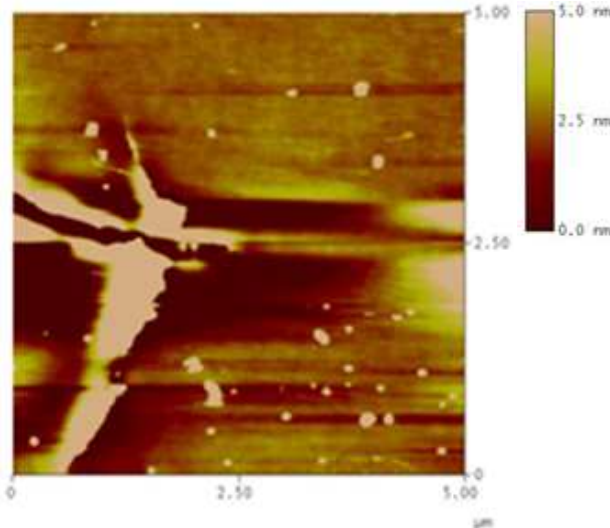
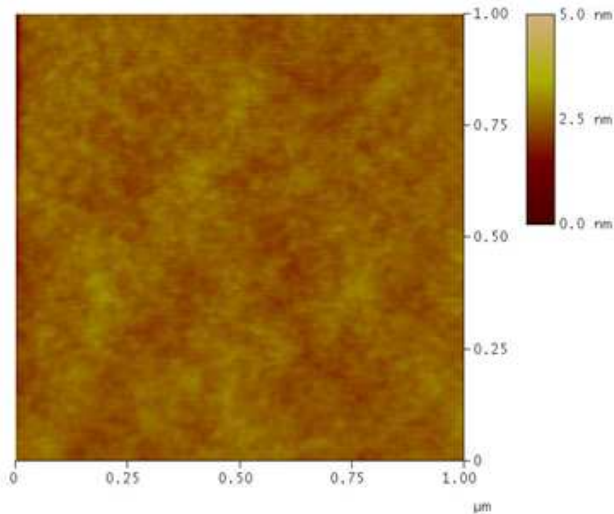
➤ Effect of CHP on a-C studied for a contact time of 15 minutes

➤ Blanket a-C surface is smooth with $RMS_{\text{roughness}} \sim 0.8\text{nm}$

➤ CHP treated a-C shows modification of surface with $RMS_{\text{roughness}} \sim 10\text{nm}$

AFM Analysis of High Dose Implanted PR film

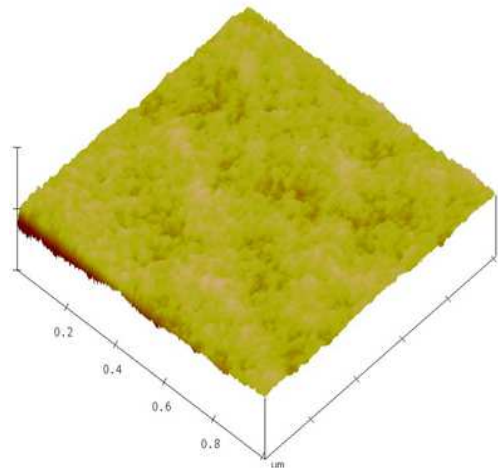
AFM Contact mode



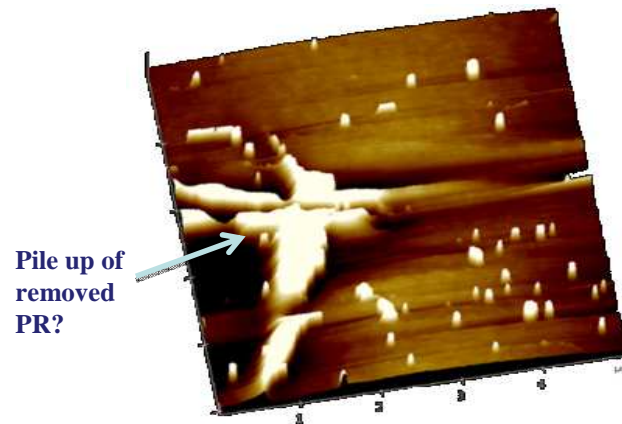
➤ Effect of CHP on 1E16 As/cm² implanted PR studied for a contact time of 15 minutes

➤ Blanket PR surface is smooth with RMS ~ 0.2 nm

➤ CHP treated PR shows disruption on surface with RMS ~ 8 nm

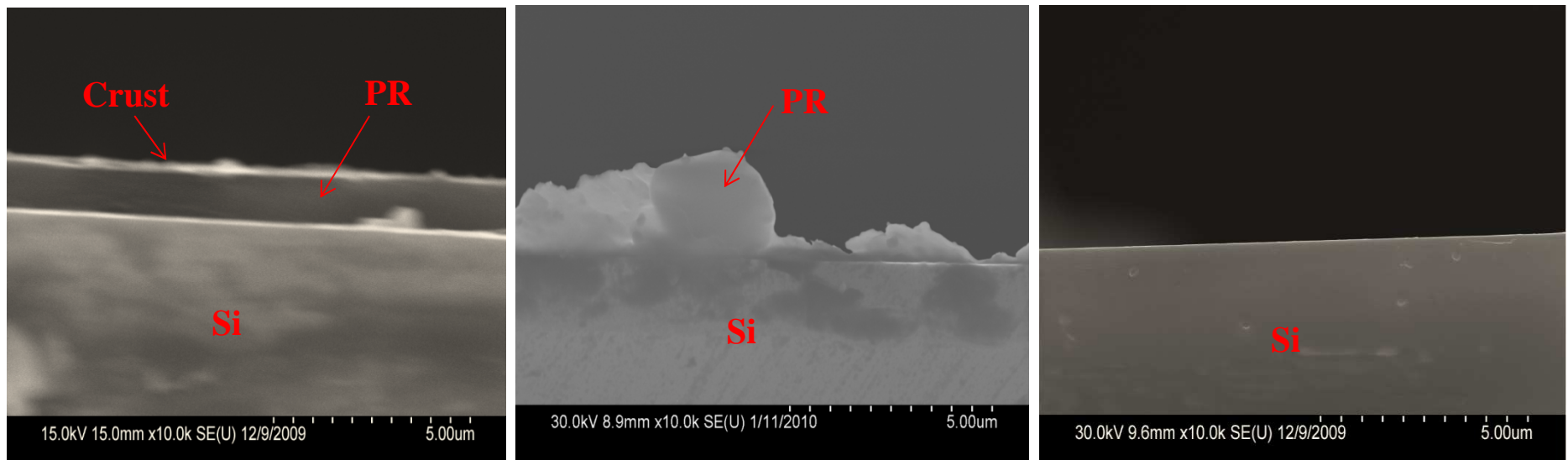


Blanket PR 1E16 As/cm²



PR 1E16 As/cm² in 5mM Fe²⁺, 20%H₂O₂

Effect of CHP on High Dose Implanted PR film



Blanket PR

PR in 2:1 SPM

PR in CHP + SPM

- **1E16 As/cm² implanted PR shows crust layer**
- **Discontinuous PR residue film observed after 2:1 SPM treatment for 5 minutes at 80°C**
- **CHP (5mM Fe^{II}, 20% H₂O₂; Time: 30min; room temperature) treated PR was completely removed in 2:1 SPM @ 80°C in 5minutes**

Summary

- **Effectiveness of Catalyzed Hydrogen Peroxide system in disrupting crust layer was investigated using a-C film as model compound**
- **Disruption of a-C film surface was observed in CHP system containing 5mM Fe^{II}, 20% H₂O₂ at room temperature**
- **Confocal microscopy has revealed surface disruption with depth ~90 nm and ~300 nm for a-C film and high dose implanted PR respectively**
- *Complete removal of high dose implanted PR is possible by first exposing the resist in CHP solution for 30 minutes and then in 2:1 SPM at 80°C for 5minutes*

Future Plans

Next Year Plans

- **Optimization of CHP system to decrease the exposure time prior to conventional SPM treatment**
 - **Variables: H₂O₂/Metal ion level, Time, Temperature, pH**
- **Measure metal levels after cleaning**
- **Work with a tool maker to test the chemical system on full wafers**

Long Term Plans

- **Development of CHP system for one step removal of implanted photoresists**

Industrial Interactions and Technology Transfer

- **Technical discussions with Joel Barnett of Sematech and Hsi-An Kwong of Freescale**
- **Interactions with Dr. Renhe Jia and Dr. Chiu Chan of **Applied Materials** to decide on a-C films as model films**

Improvement of ESH Impact of Back End of Line (BEOL) Cleaning Formulations Using Ionic Liquids to Replace Traditional Solvents *(Task Number: 425.034)*

PI:

- **Srini Raghavan, Materials Science and Engineering, University of Arizona**

Graduate Student:

- **Dinesh P R Thanu, PhD candidate, Materials Science and Engineering, University of Arizona**

Objectives

OVERALL OBJECTIVE

- **Develop cleaning formulations based on ionic liquids to replace traditional organic solvent based formulations for BEOL cleaning**

SPECIFIC OBJECTIVE FOR THE CURRENT CONTRACT YEAR

- **Investigate the use of deep eutectic solvents (DES) based on choline chloride and urea for the removal of post etch residues**

ESH Metrics and Impact

- ESH objective:* Replacement of organic solvents from BEOL cleaning formulations which generate a waste stream that is difficult to treat

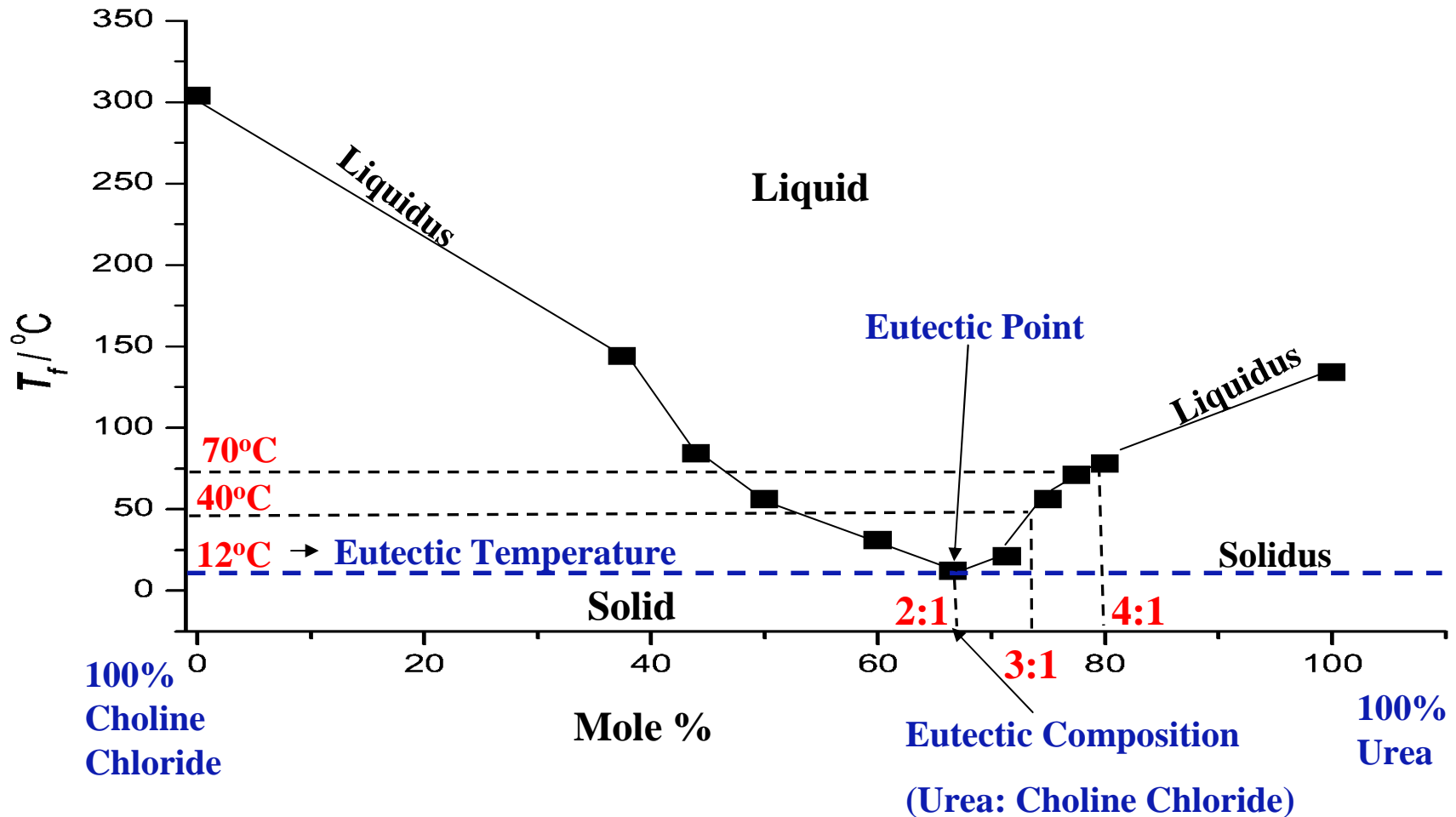
Solution components	Weight % in typical formulations	Formulation used in this study
Traditional organic Solvent	> 60%	Eutectic composition of two benign compounds 100%
Water	< 40%	0%
Fluoride	~ 1-2%	0%

Ingredients	LD ₅₀ (Oral Rat) mg/kg
Urea	8471
Choline Chloride	5000

Components	Vapor Pressure (@20 ⁰ C) mm Hg
<u>Deep Eutectic Solvents:</u>	
Choline Chloride	4.93 E-10 @25°C
Urea	6.75 E-3
<u>Conventional Solvents:</u>	
DMSO	0.42
N-Methyl Pyrrolidone	0.29
Sulfolane	0.01

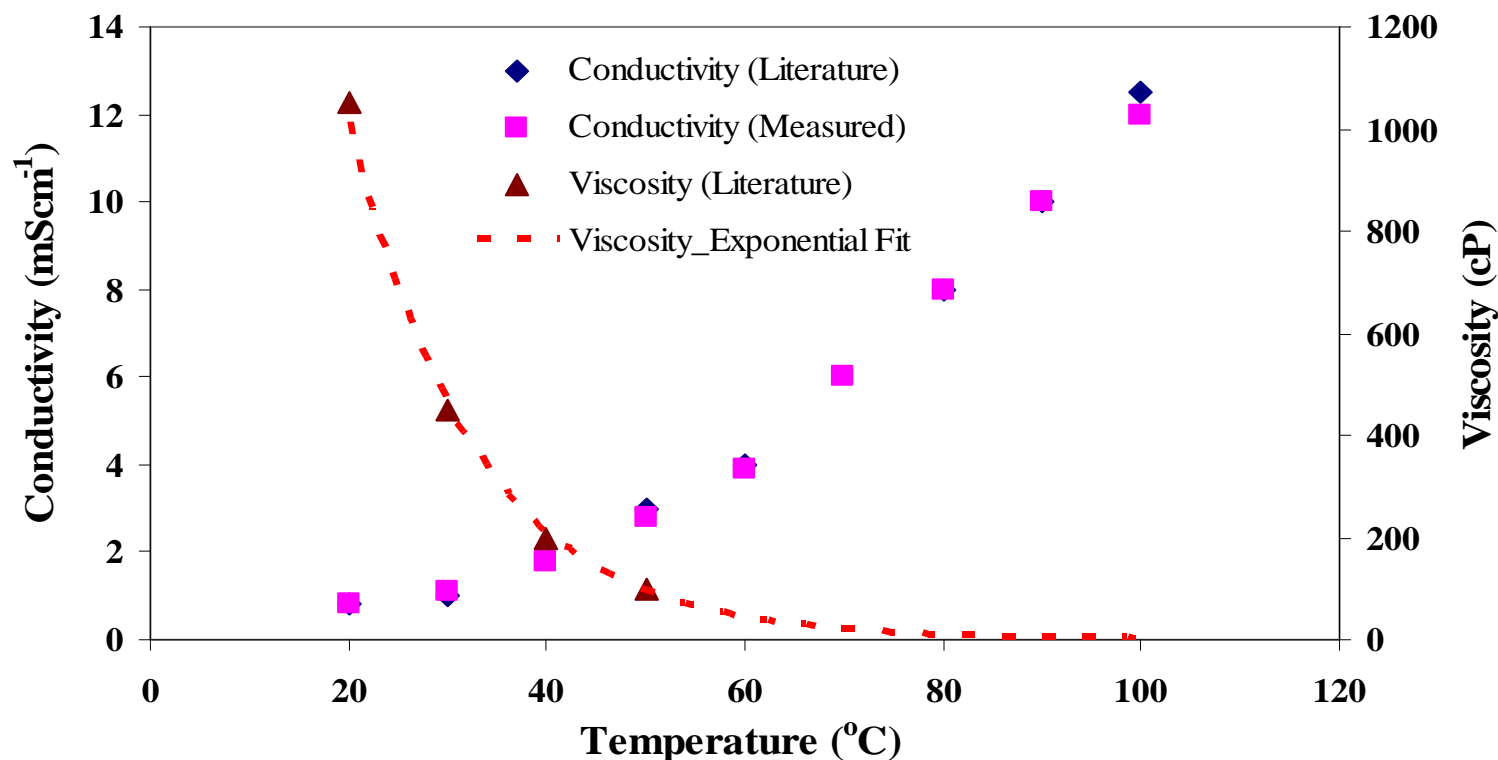
Deep Eutectic Solvents (DES)

(e.g.) Urea-Choline Chloride Binary Phase Diagram



- 2:1, 3:1 and 4:1 (urea:choline chloride) chosen for investigation

Conductivity and Viscosity of Urea:Choline Chloride (2:1) as a Function of Temperature



- Good conductivity (1mScm^{-1} @ 20°C), low vapor pressure and toxicity
- Conductivity increases with temperature (2mScm^{-1} @ 40°C , 6mScm^{-1} @ 70°C)
- High viscosity at room temperature and it decreases with increase in temperature
- Good solubility for copper oxides at elevated temperatures [1]

1. A. Abbott, et al., *Journal of Chemical Engineering Data*, Volume 51, p. 1280-1282 (2006)

SRC/SEMATECH Engineering Research Center for Environmentally Benign Semiconductor Manufacturing

Experimental Approach

Preparation of Residue Film

Photoresist coating:

- Photoresist AZ 3312 (g line) spin coated on copper wafers to a thickness of 1.2 μ m at a spin speed of 4000 rpm for 30 seconds; Baking: 90°C for 90 seconds

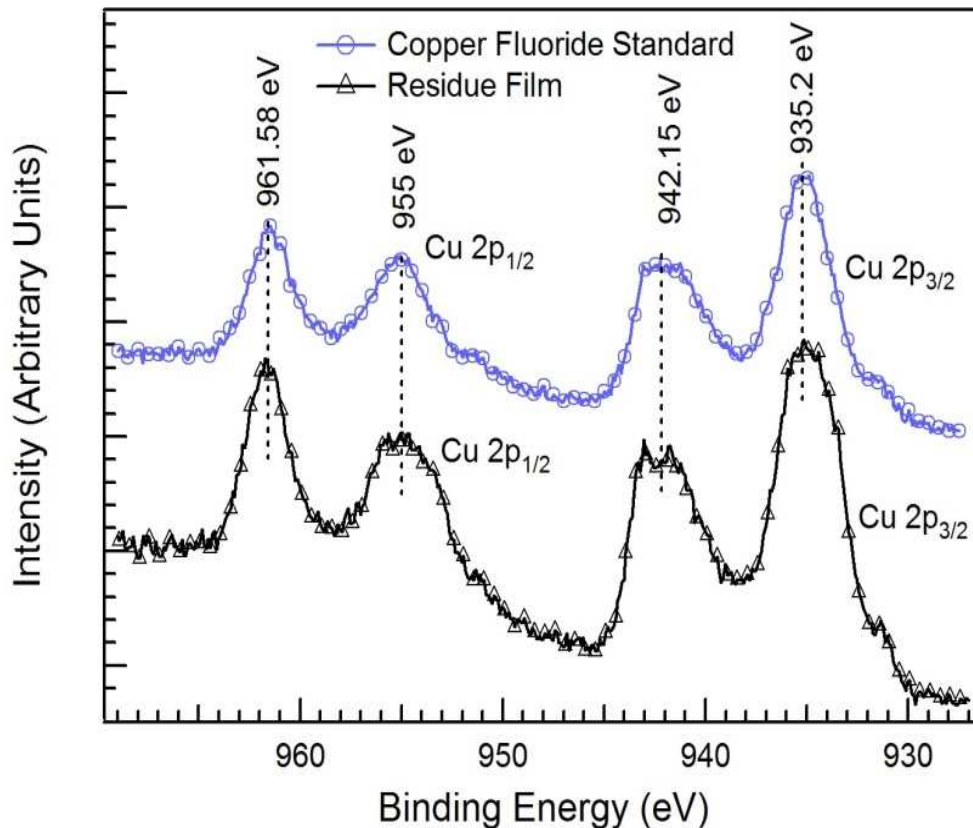
Photoresist ashing :

- Ashed in Reactive Ion Etcher (RIE) tool at a rate of 1580 Å/min using CF₄/O₂ plasma at 50 mTorr pressure and 250W of plasma power; Ashing time: ~7min
- Thickness: ~30nm measured by Atomic Force Microscope step height measurements
- Contains mainly CuF₂ as determined from X-ray Photoelectron Spectroscopy (XPS)

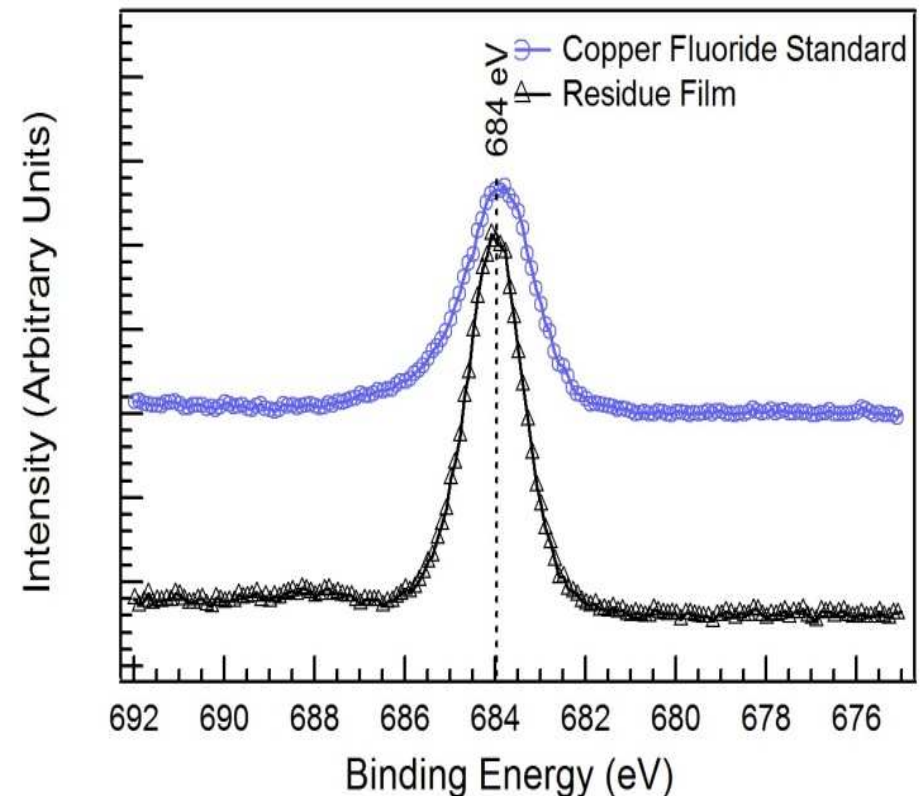
Methods

- Residue removal investigated using Scanning Electron Microscopy (SEM) and confirmed using XPS and open circuit potential measurements

Oxidation State and Bonding of Elements in Residue Film- Comparison with CuF_2 Standard



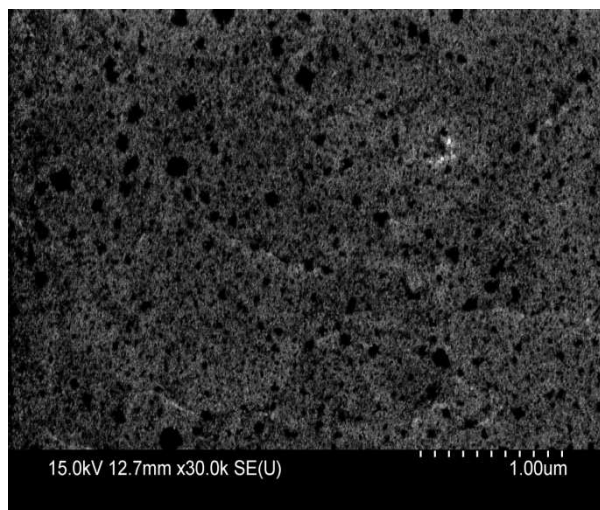
Cu 2p spectrum



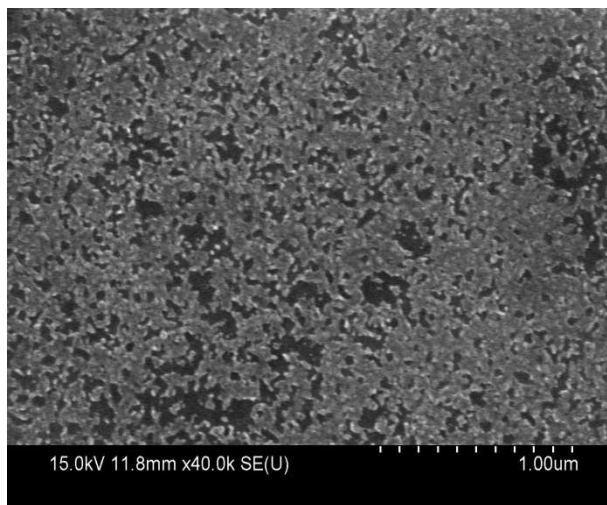
F 1s spectrum

- Copper exists in +2 oxidation state
- Residue film mainly contains CuF_2

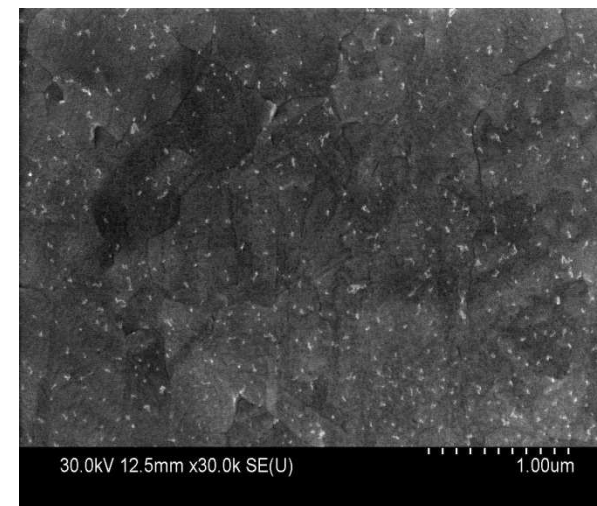
Residue Removal using 2:1 DES (Urea:Choline Chloride) at 40°C



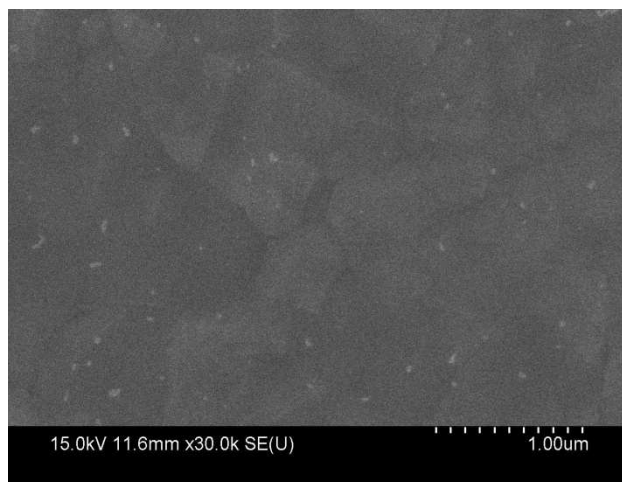
0 min



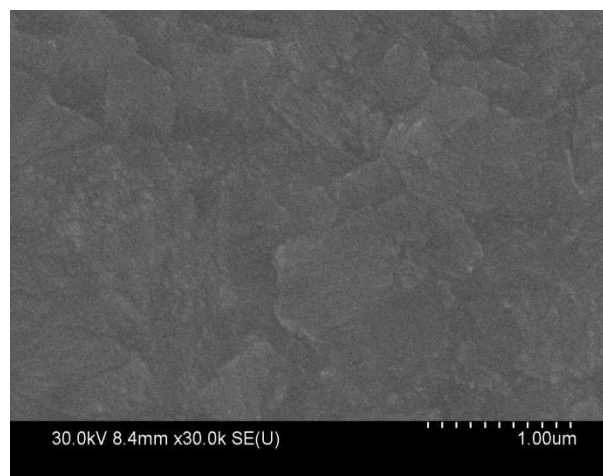
5 min



10 min



30 min

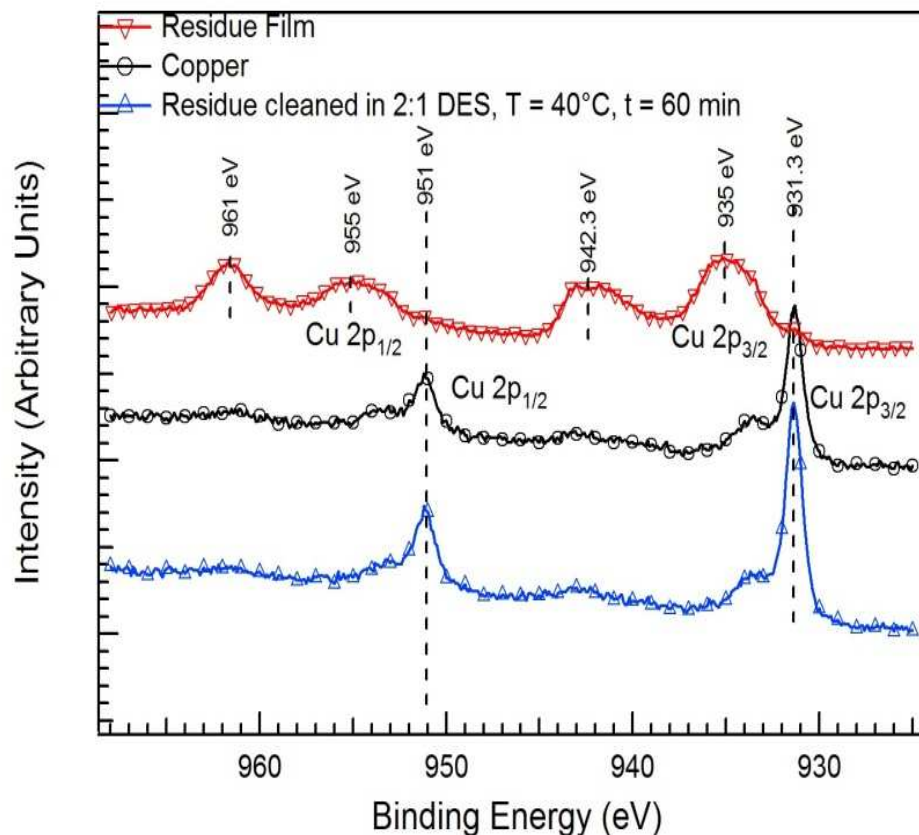


60 min

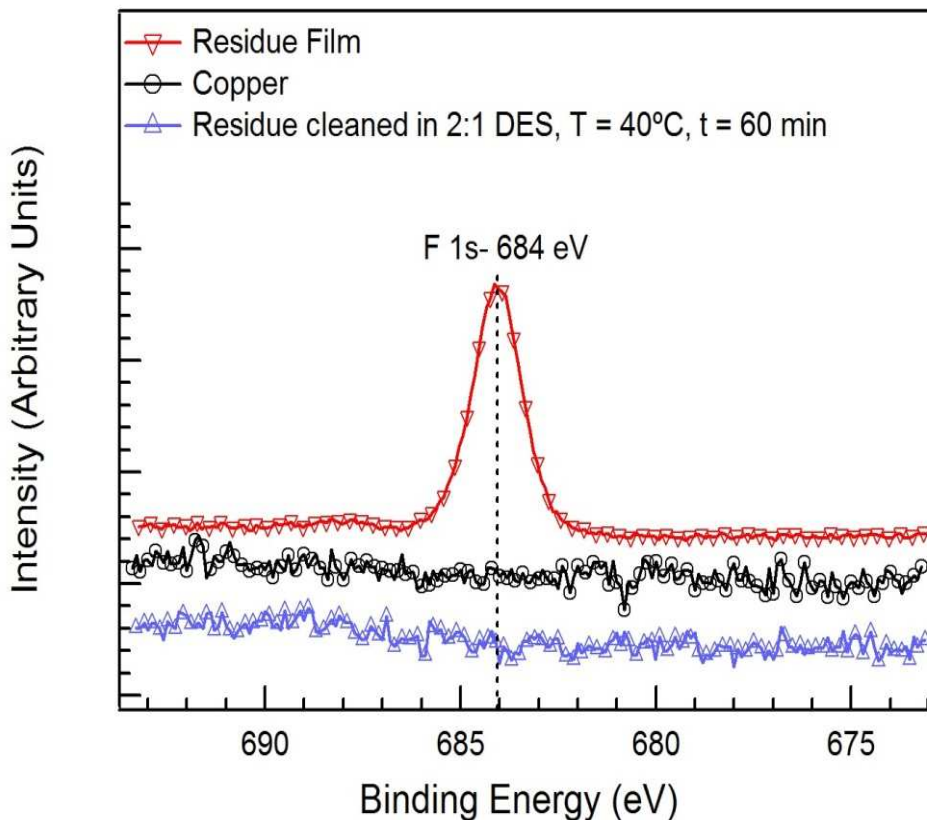
- Residue removal monitored using SEM imaging
- Complete removal of residue film observed within 60 minutes of cleaning

Confirmation of Residue Removal in 2:1 DES using XPS Analysis

Cu 2p spectrum



F 1s spectrum



- Residue removal exposes bare copper surface after cleaning

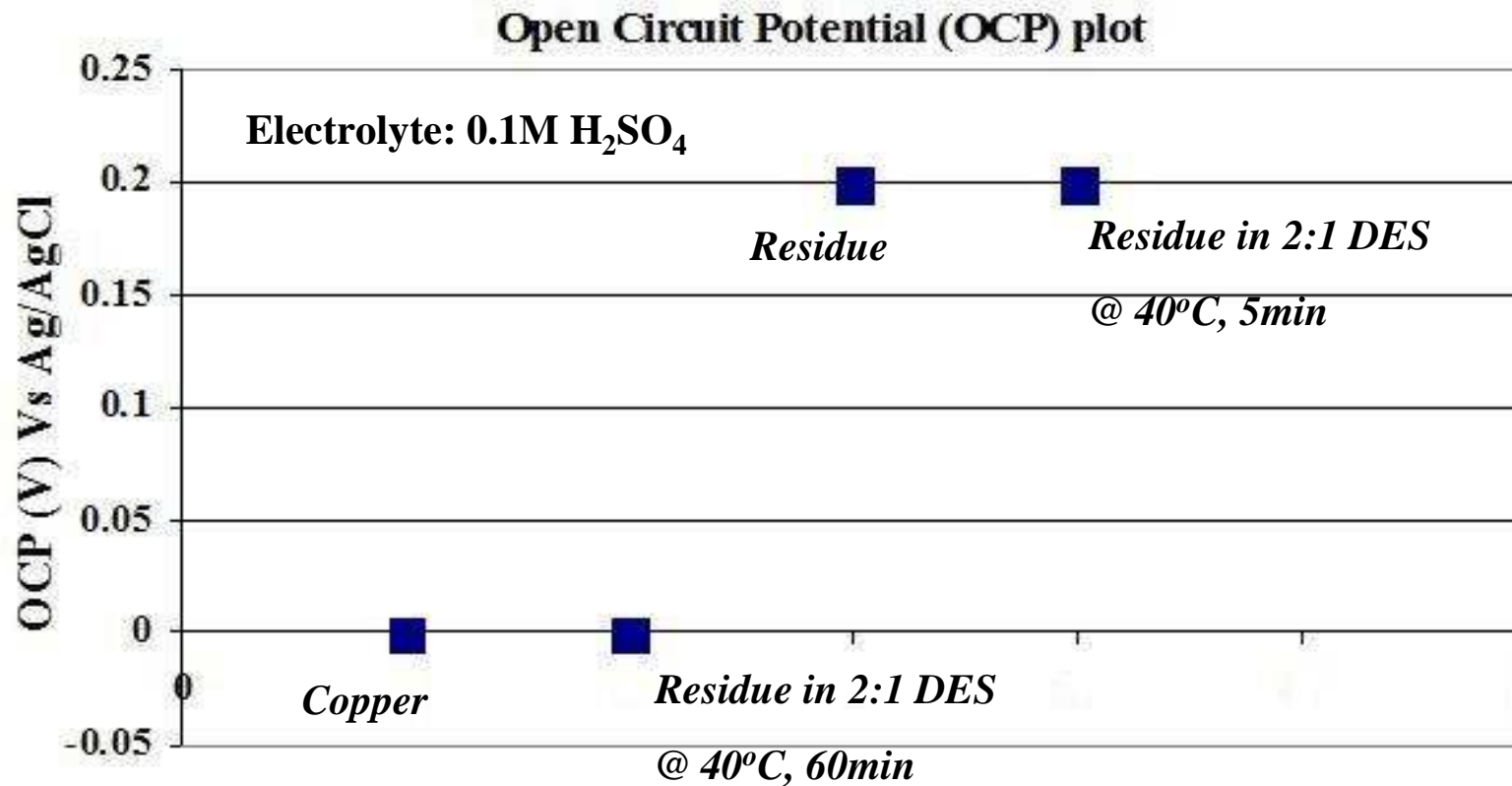
Cu 2p Spectrum

- Binding energies in sample cleaned in 2:1 DES at 40°C are identical to those for bare Cu

F 1s Spectrum

- Absence of fluorine peak in sample cleaned in 2:1 DES at 40°C –complete residue removal

Electrochemical Study to Confirm Residue Removal in DES



- Complete Removal

OCP of bare copper and sample cleaned in 2:1 DES at 40° for 60 min is same

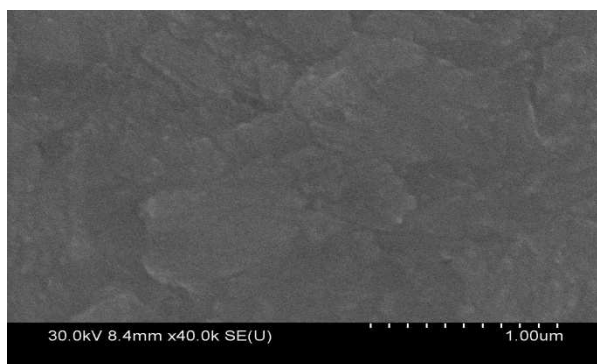
- Incomplete Removal

Higher OCP of residue film coated Cu exposed to 2:1 DES at 40° for 5 min indicates incomplete film removal

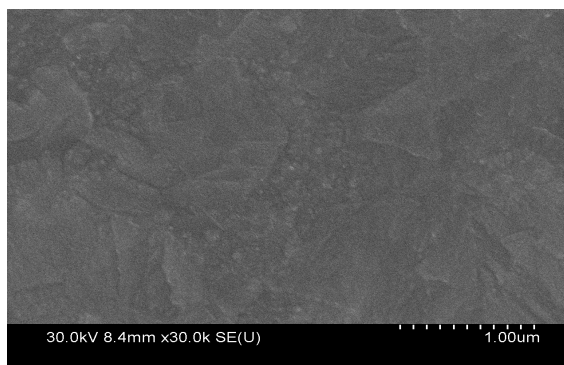
Comparison of Residue Removal in DES and Conventional Cleaning Formulations

- Cleaning Time: 30 min
- DES and conventional cleaning formulations are comparable—DES provides very low etch rate of dielectric

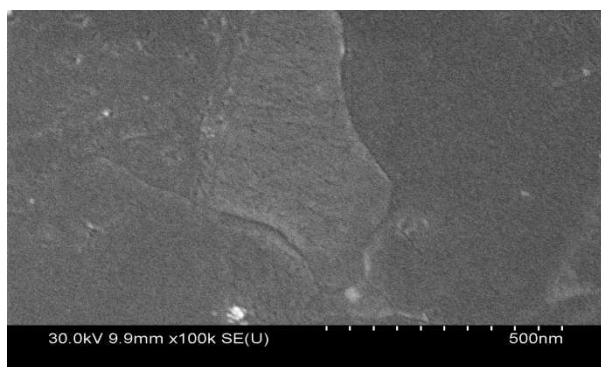
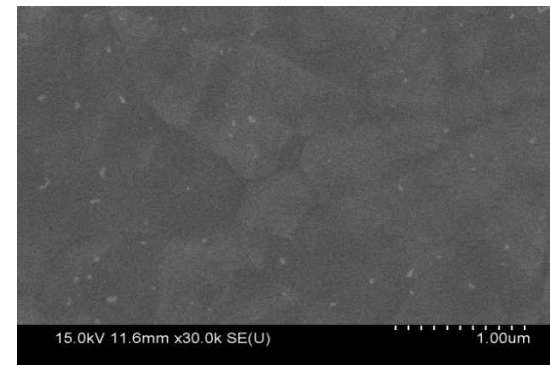
29% DMSO+1% NH₄F+70% H₂O



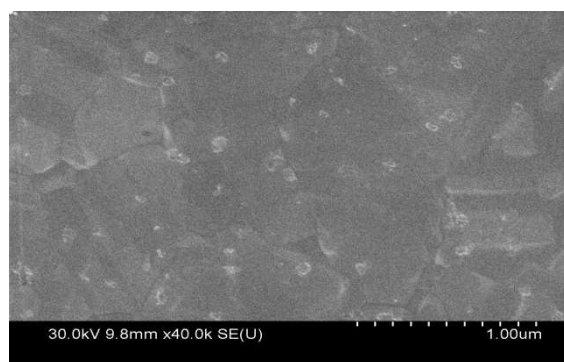
250:1 HF



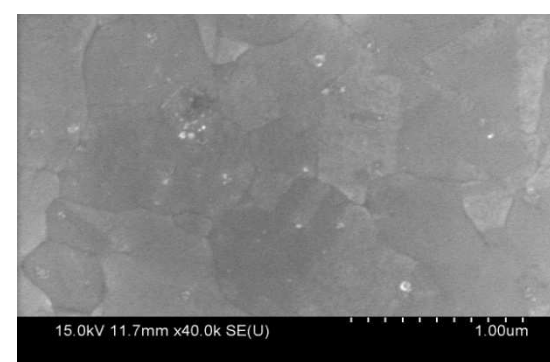
2:1 DES @ 40°C



2:1 DES @ 70°C



3:1 DES @ 40°C



4:1 DES @ 70°C

Highlight of Results

- Deep eutectic solvent (DES) containing benign chemicals, choline chloride and urea, shows promise as a BEOL cleaning formulation
 - 2:1 DES at 40°C and 70°C effectively removed post etch residues on copper
 - Removal of post etch residues confirmed using X-ray Photoelectron Spectroscopy (XPS) and electrochemical techniques

Industrial Interactions

- Discussions with Dr. Robert Small, *R.S. Associates, Tucson*
- Teleconference with Dr. Mansour Moinpour, Intel, to discuss results and seek advice on future direction

Acknowledgements

- Shariq Siddiqui, PhD, Materials Science and Engineering, University of Arizona
- Nandini Venkataraman, PhD, Materials Science and Engineering, University of Arizona

Future Plans

Next Year Plans

- Reduction of cleaning time, DES carry over, and operating temperature
- Rinsing of cleaned substrates—address any corrosion issues during rinsing
- Optimize formulation for the selective removal of post etch residue created from DUV resists
- Investigate cleaning of patterned test structures and determine the end point removal using electrochemical techniques

Long-term Plans

- Investigation of choline chloride/malonic acid as a cleaning formulation for post etch residue removal
 - Eutectic mixture of choline chloride with malonic acid possess a high solubility of copper oxides

Publications, Presentations, and Recognitions/Awards

Publication

- D. P. R. Thanu, N. Venkataraman, S. Raghavan and O. Mahdavi, “Dilute HF Solutions for Copper Cleaning During BEOL Processes: Effect of Aeration on Selectivity and Copper Corrosion”, ECS Transactions, Volume 25, Issue 5, Page: 109-116 (2009)

Presentation

- D. P. R. Thanu, N. Venkataraman, S. Raghavan and O. Mahdavi, “Dilute HF Solutions for Copper Cleaning During BEOL Processes: Effect of Aeration on Selectivity and Copper Corrosion”, 216th ECS Fall Meeting, Vienna, Austria, October 4-9 (2009)

High-Throughput Cellular-Based Toxicity Assays for Manufactured Nanoparticles and Nanostructure-Toxicity Relationship Models

(Task Number: 425.035)

Subtask 1: “High Throughput Screening”

Subtask 2: “Computational Models”

PIs:

- **Subtask 1 Leader: Dr. Russell J. Mumper, Center for Nanotechnology in Drug Delivery, UNC Eshelman School of Pharmacy, UNC-Chapel Hill**
- **Subtask 2 Leader: Dr. Alexander Tropsha, Division of Medicinal Chemistry and Natural Products, UNC Eshelman School of Pharmacy, UNC-Chapel Hill**

Graduate Students and Postdoctoral Fellows:

- **Shalini Minocha, PhD Candidate, Center for Nanotechnology in Drug Delivery, UNC Eshelman School of Pharmacy, UNC-Chapel Hill**
- **John Pu, PhD Candidate, Laboratory for Molecular Modeling, UNC Eshelman School of Pharmacy, UNC-Chapel Hill**
- **Denis Fourches, Postdoctoral Fellow, Laboratory for Molecular Modeling, UNC Eshelman School of Pharmacy, UNC-Chapel Hill**

SRC/SEMATECH Engineering Research Center for Environmentally Benign Semiconductor Manufacturing

Objectives

Subtask 1:

- **Validation of high-throughput cellular-based toxicity assays for MNP assessment.**
- **Test QNTR (Quantitative Nanostructure Toxicity Relationship) model using the predictive models developed in subtask 2.**

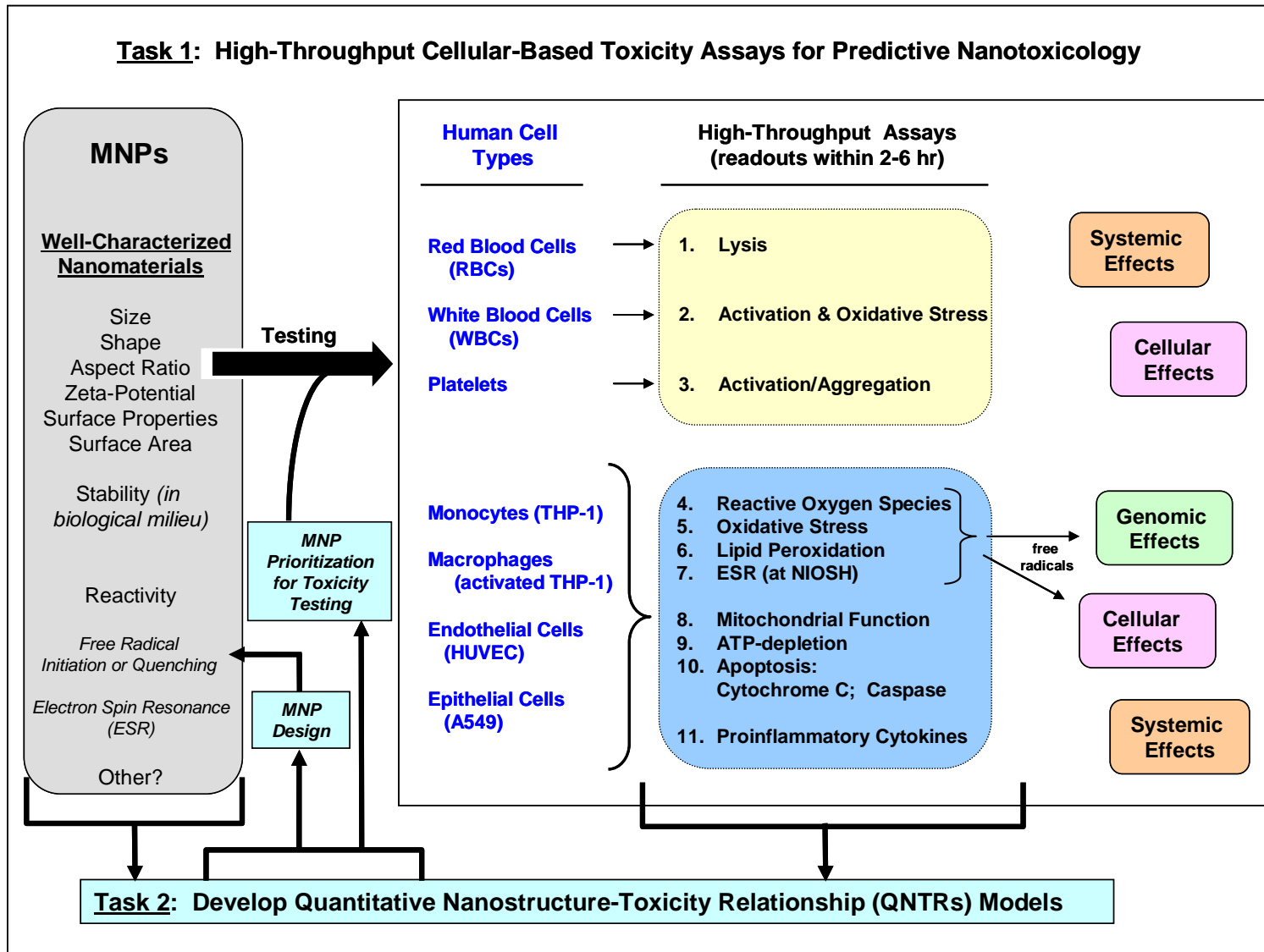
Subtask 2:

- **Develop QNTR models that correlate the compositional/physical/chemical/geometrical and biological descriptors of MNPs with known toxicological endpoints.**
- **Improve the prediction performance of QNTR models with the availability of new experimental data from subtask 1.**

ESH Metrics and Impact

- 1. Obtain predictive knowledge of the physical and chemical properties of manufactured nanoparticles.*
 - 2. Develop relevant in-vitro assays utilizing human cells to predict the toxicity of manufactured nanoparticles.*
 - 3. Develop predictive computational models that correlate physical-chemical descriptors of MNPs with their toxic effects.*
- Impact: Utilize the knowledge gained through above three metrics for improved MNP experimental design and prioritized toxicity testing toward the manufacturing of safe nanomaterials.*

General Framework of the Proposed Approach

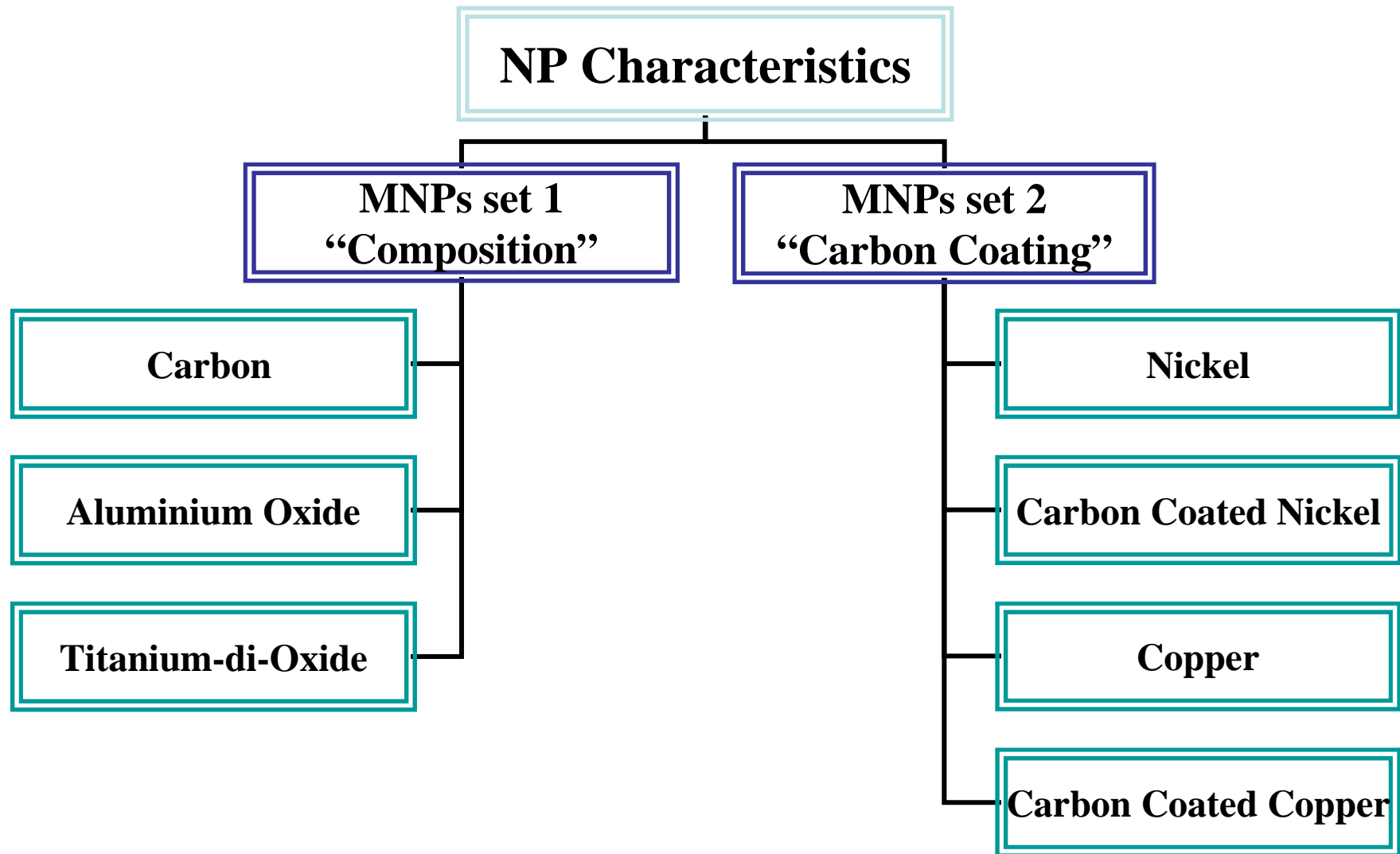


Subtask 1: Potential Cellular-based Assays

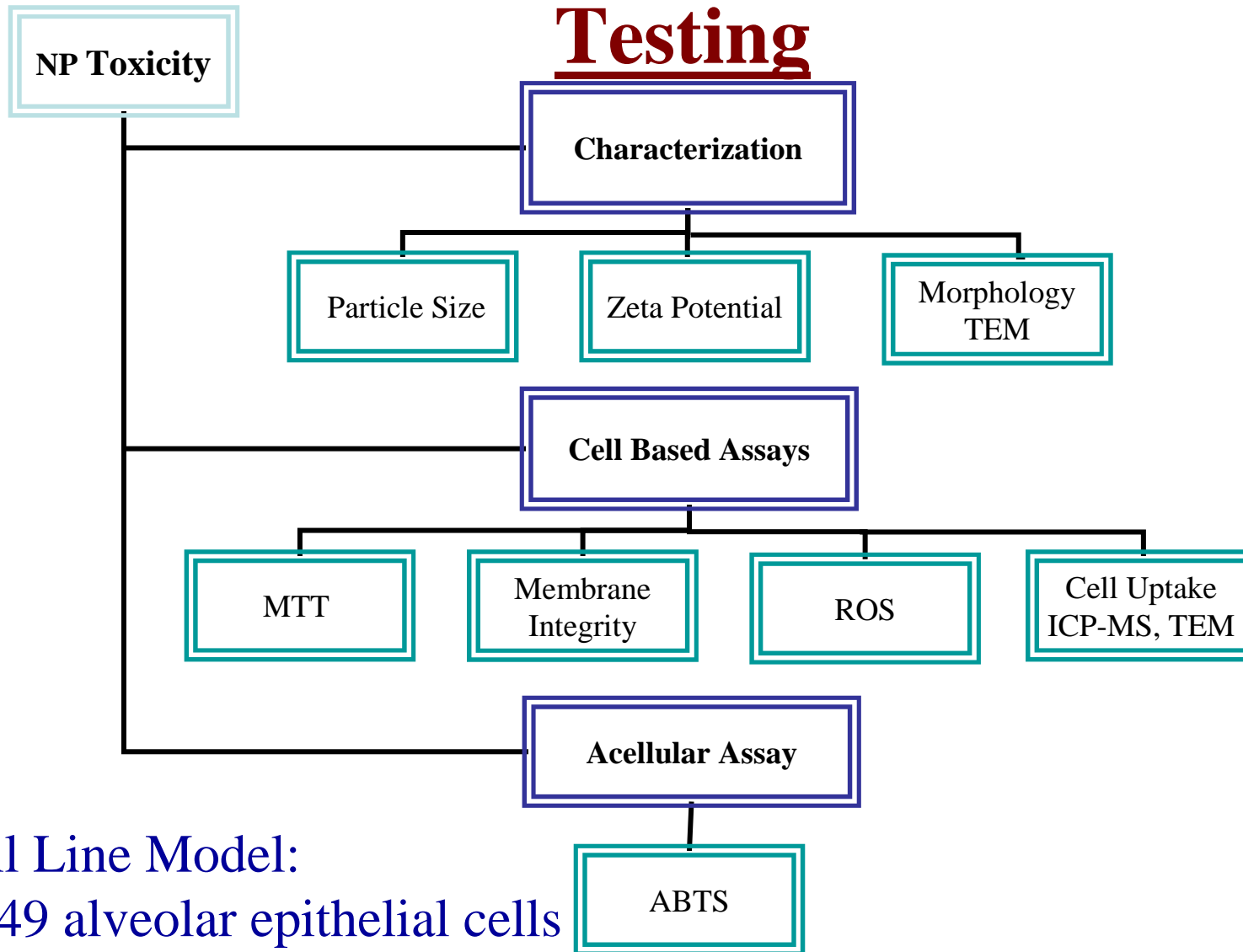
Human Cells	Assay	Description
Red Blood Cells (RBCs)	Lysis	Measure oxyhemoglobin at 540 nm
White Blood Cells (WBCs)	Activation	Measure reduction of ferricytochrome c caused by produced superoxide anions
	Oxidative Stress	Measure intracellular GSSG/GSH ratio; where GSSG is oxidized glutathione and GSH is reduced glutathione
Platelets	Activation	Flow cytometry to measure PAC-1-FITC binding to activated platelets
	Aggregation	Whole Blood Impedance Aggregometry

Human Cells	Assay	Description
Monocytes (THP-1) Macrophages (activated THP-1) Endothelial Cells (HUVEC) Epithelial Cells (A549)	Reactive Oxygen Species	1) Measure intracellular fluorescence produced with H ₂ DCFDA or carboxy-H ₂ DCFDA loaded cells; 2) Measure (a) cellular ESR
	Oxidative Stress	Measure intracellular GSSG/GSH ratio; where GSSG is oxidized glutathione and GSH is reduced glutathione
	Lipid Peroxidation	Lipid Hydroperoxide (LPO) Assay
	Mitochondrial Function	MTT assay & JC-1 assay
	ATP-depletion	ATPlite 1step® Assay Kit (PerkinElmer)
	Apoptosis:	
	Cytochrome C	Cytochrome C immunoassay
	Caspase-3	Caspase-3 Fluorometric Assay (R&D Systems); Quantify caspase-3 activation by cleavage of DEVD-AFC substrate
	Proinflammatory Cytokines	Cytokine assays by ELISA; NFκB, IL-1β, TNF-α, IFN-γ, IL-8

Subtask 1: Current Method Approach



Subtask 1: Current Scheme for Toxicity



Cell Line Model:
A549 alveolar epithelial cells

Characterization: MNPs Set 1 and 2

NP Type	Manufacturer	Particle Size* Range (nm)	Particle Size in DI water (nm)	Zeta Potential (mV)
Carbon	American Elements	55-100	611.7 ± 510.5	-21.1 ± 4.6
Aluminum oxide	Alfa-Aesar	40-50	488.8 ± 318.7	-17.7 ± 7.4
Titanium-di-oxide	NanoAmor	30-40	511.7 ± 336.7	-25.3 ± 5.2
Nickel	NanoAmor	20	834.6 ± 495.1	2.76 ± 0.7
Carbon coated Nickel	NanoAmor	20	466.6 ± 179.6	-16.4 ± 1.8
Copper	NanoAmor	25	662.2 ± 139.3	-9.0 ± 2.4
Carbon coated Copper	NanoAmor	25	412.1 ± 210.9	-6.21 ± 0.7

* Provided by Manufacturer

Sample preparation: 1 mg/ml suspensions in DI water; bath sonicated for 6 x30 sec

SRC/SEMATECH Engineering Research Center for Environmentally Benign Semiconductor Manufacturing

MNPs Set 1

ABTS and ROS Assay

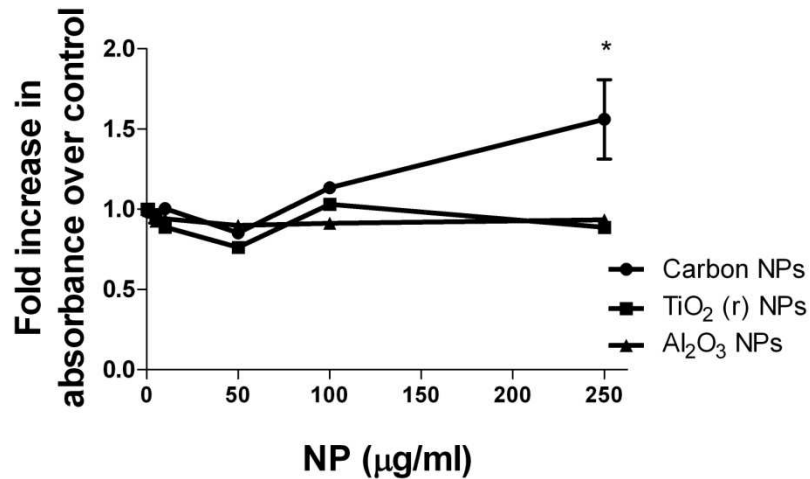


Fig. 1 ABTS assay is an *in-vitro* acellular assay that gives an indication about reactivity of MNPs. ABTS conversion to ABTS radical is observed by measuring increase in absorbance at 734 nm (characteristic of ABTS radical). MNPs in various concentrations were incubated with ABTS, 60 mM solution in a 96 well plate for 24 hr. Data are corrected for absorbance from blank NPs. (* $p < 0.05$ as compared to control)

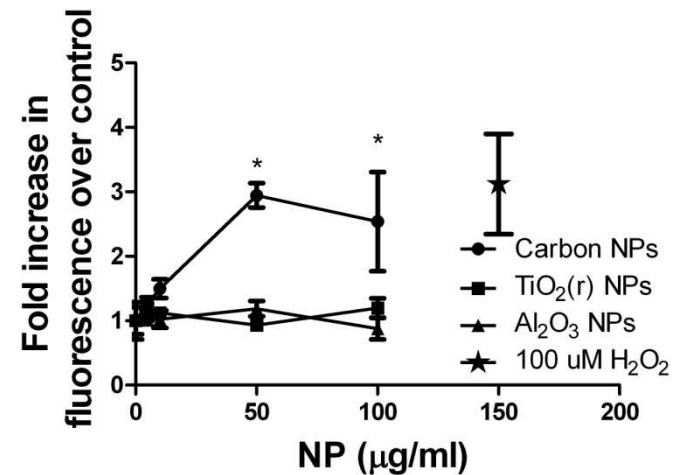


Fig. 2 ROS or Reactive Oxygen Species assay gives an indication of the ability of MNPs to induce oxidative damage in cells. A549, human alveolar epithelial cells (25,000 per well), were incubated with NPs for 4 hr. Observed fluorescence is due to cleavage of carboxy H₂DCFDA to fluorescein inside cells. Data corrected for fluorescence from blank NPs. H₂O₂ was used as positive control. (* $p < 0.05$ as compared to control)

ABTS = 2,2'-Azinobis (3-ethylbenzothiazoline-6-sulfonic acid diammonium salt)

MNPs Set 1

Mitochondrial Function

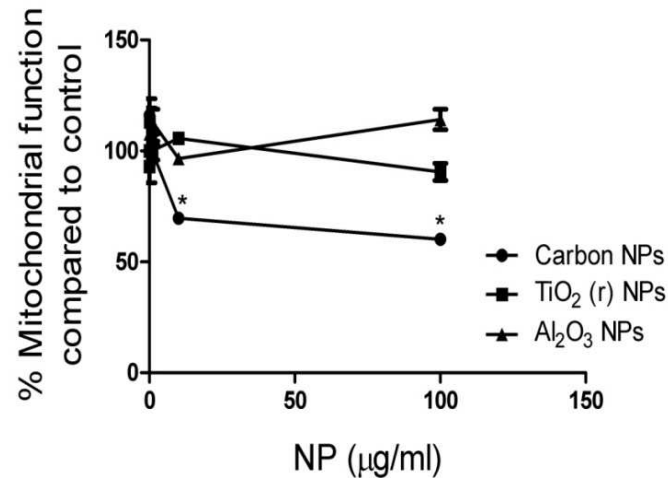


Fig. 3 MTT dye reduction assay measures ability of MNPs to alter with the mitochondrial function. A549, human alveolar epithelial cells (25,000 per well), were incubated with NPs for 24 hr. Observed absorbance is due to reduction of MTT dye inside viable cells. Data corrected for absorbance from blank NPs.

(* p < 0.05 as compared to control)

Note : Carbon NPs are 98% pure. Impurities include, among a few others: Si (0.1%), Fe (0.08%), Cr (0.06%), Ni (0.05%). Among carbon, TiO₂, Al₂O₃ NPs; Only carbon NPs have transition metal impurities.

Conclusions: MNPs Set 1

- Particle size measurement by dynamic light scattering shows that NP sizes are different from those provided by the manufacturer.
- ABTS assay was successfully developed as an *in-vitro* acellular assay to assess the free radical forming potential of NPs. The assay is simple, adaptable to 96 well plate and cost effective.
- Carbon NPs appear to be more toxic as compared to other NPs as shown by *in-vitro* MTT and ROS data.
- Carbon nanoparticles probably act as a vehicle to carry iron/nickel in cells. This is a very plausible scenario as hydrophobicity provided by carbon NPs facilitate iron entry in cells.
- Results from ABTS assay correlates well with ROS and MTT cytotoxicity data.

MNPs Set 2

MTT and Membrane Integrity Assay

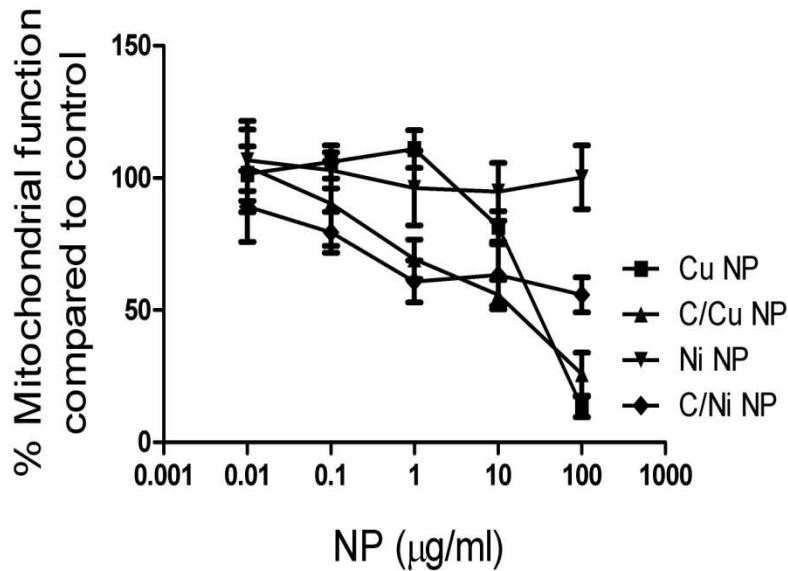


Fig. 4 MTT dye reduction assay measures the ability of MNPs to alter with the mitochondrial function. A549, human alveolar epithelial cells (25,000 per well), were incubated with NPs for 24 hr. Observed absorbance is due to reduction of MTT dye inside viable cells. Data corrected for absorbance from blank NPs. Ni NPs significantly differ from C/Ni NPs at all doses and Cu NPs significantly differ from C/Cu NPs at 0.1, 1 and 10 µg/ml.

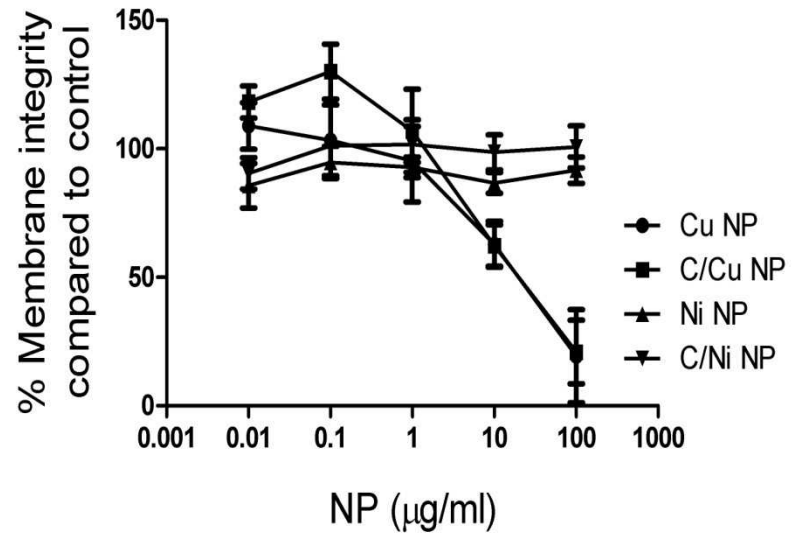


Fig. 5 Membrane Integrity assay measures the ability of MNPs to alter with the plasma membrane integrity. A549, human alveolar epithelial cells (25,000 per well), were incubated with NPs for 24 hr. Neutral red dye absorbs at 540 nm in lysosomes of cells with intact plasma membrane. Data corrected for absorbance from blank NPs. Ni NPs and C/Ni NPs do not appear to alter membrane integrity whereas Cu NPs and C/Cu NPs are equally toxic.

MNPs Set 2

TEM Characterization of MNPs

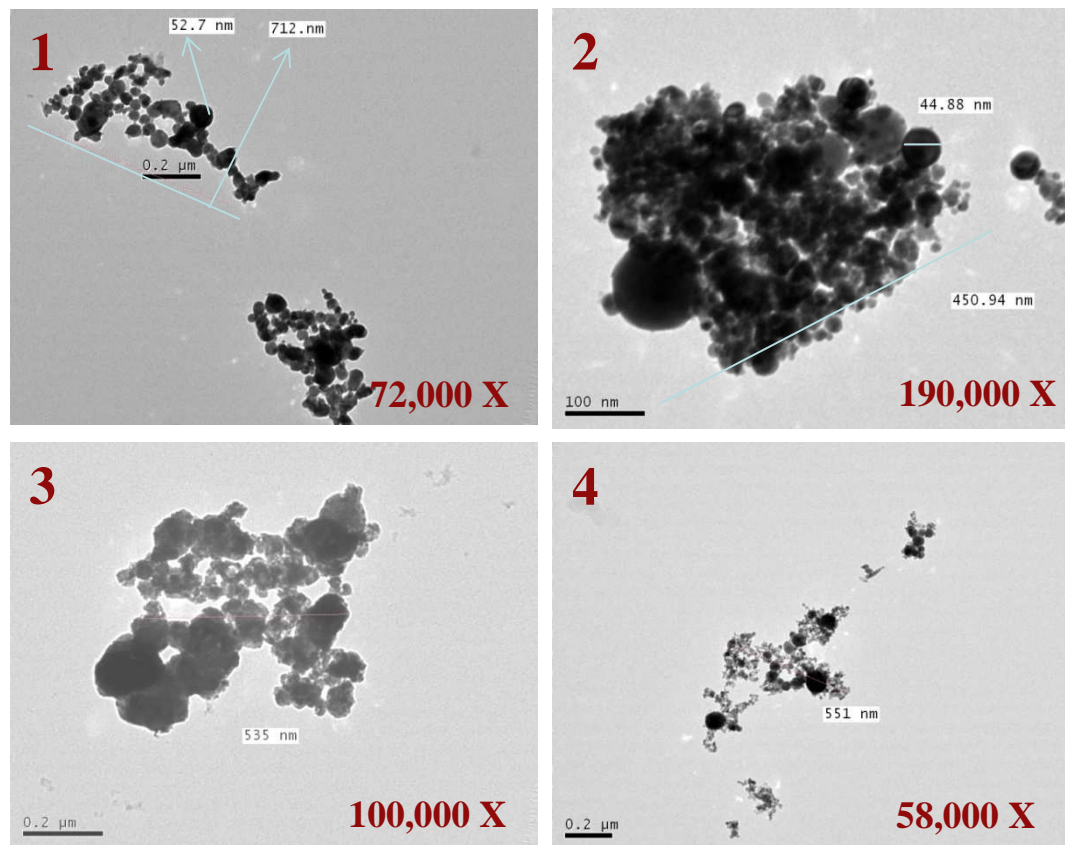


Fig. 6 TEM Images of 1. Ni , 2. C/Ni, 3. Cu and 4. C/Cu MNPs. Nanoparticles were suspended at concentration of 10 μg/ml in DI water for this analysis. The average particle sizes measured by TEM correlates with the dynamic light scattering data.

MNPs Set 2

Cell Uptake Analysis by TEM

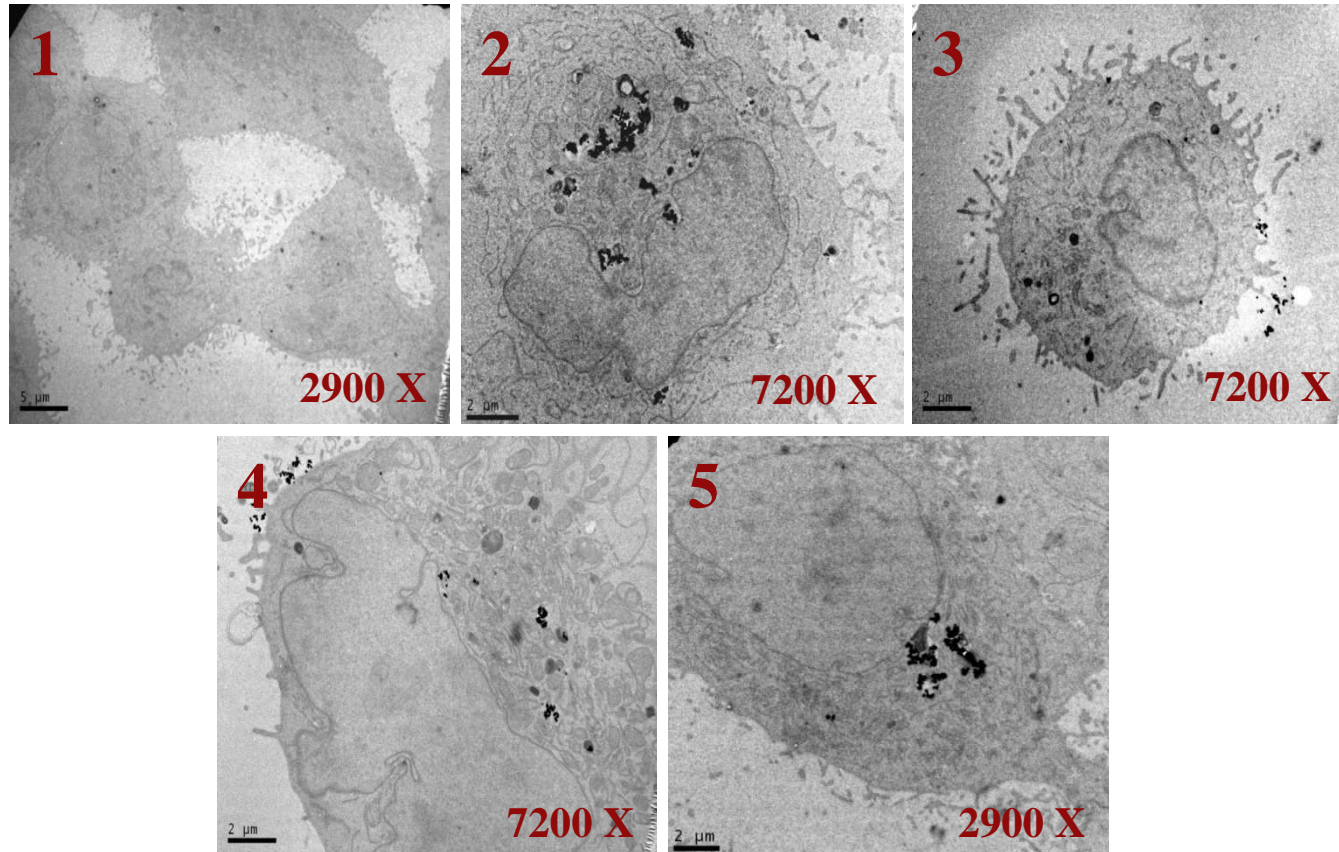


Fig. 7 TEM Images of 1. Control A549 cells , 2. Cu treated , 3. C/Cu treated , 4. Ni treated and 5. C/Ni treated A549 cells. Cells were treated with nanoparticles at concentration of 10 μ g/ml for 8hr.

MNPs Set 2

Cell Uptake Analysis by ICP-MS

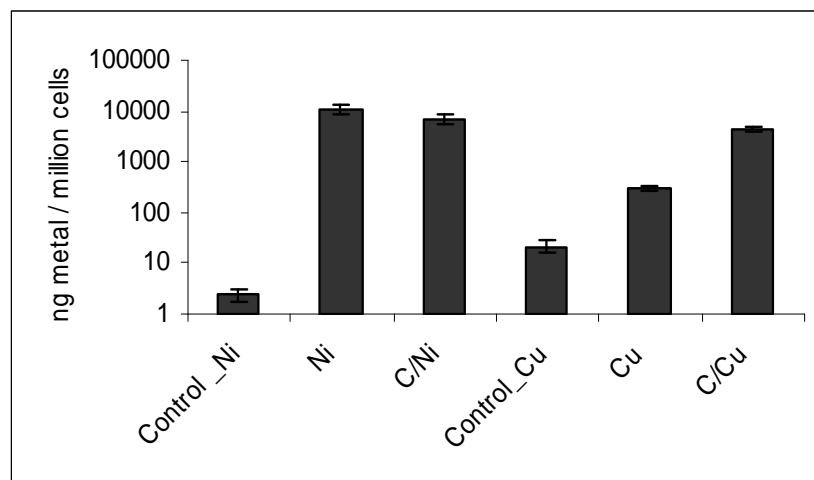


Fig. 8 Preliminary data on Cell uptake analysis of Ni and Cu from Ni, C/Ni and Cu and C/Cu NPs respectively. Control_Ni and Control_Cu signify the amount of respective metal content in untreated control A549 cells. Nanoparticles were tested at concentrations of 10 μ g/ml for 8 hr in A549 cells. Ni uptake from Ni and C/Ni NPs is comparable but Cu uptake from C/Cu NPs is an order of magnitude higher than uptake from Cu NPs. Correlation of uptake data with observed toxicity in cell based assays awaits data on detailed physico-chemical characterization.

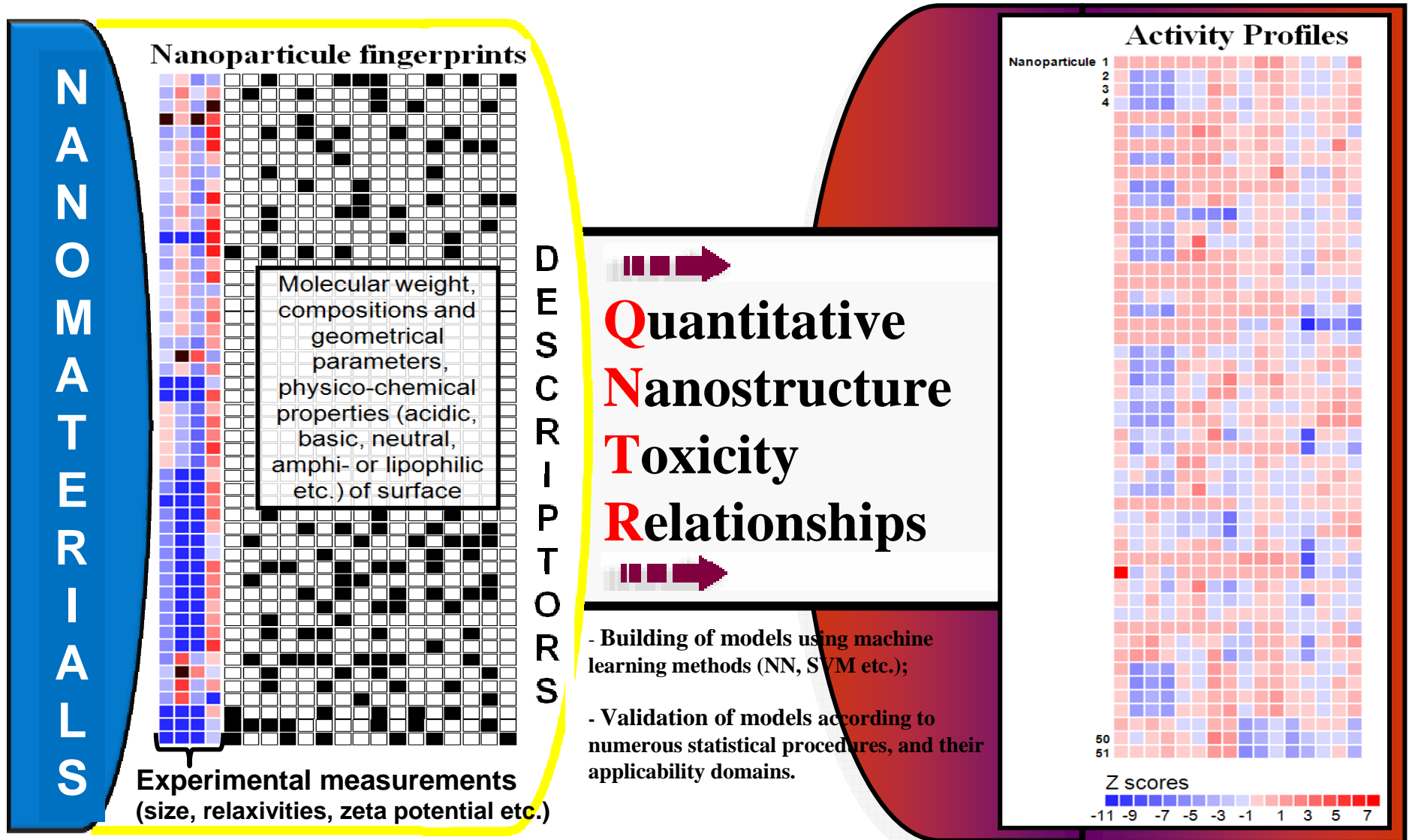
Conclusions: MNPs Set 2

- Average particle size measured by DLS of all MNPs in Set 2 are on an average 20-fold higher than provided by the manufacturers.
- Ni NPs do not alter mitochondrial function and membrane integrity although their uptake by cells is comparable to C/Ni NPs.
- C/Ni NPs alter the mitochondrial function but not membrane integrity.
- Cu NPs alter mitochondrial function at 100 $\mu\text{g/ml}$ but can alter membrane integrity even at 10 $\mu\text{g/ml}$ dose.
- Rounded morphology of Cu NP treated cells and results from membrane integrity and ICP-MS suggest that Cu NPs might act on cell surface at lower dose, possibility of alterations with cell adhesion.
- C/Cu NPs alter mitochondrial function and membrane integrity to the same extent.
- Cu and C/Cu NPs appear to be more toxic than Ni and C/Ni NPs.
- Correlation of uptake data with observed toxicity in cell based assays awaits data on detailed physico-chemical characterization.

Subtask 2: Research Hypothesis

- The effects of MNPs on different types of human cells depend on the compositional/physical/chemical/geometrical properties of the MNPs.
- High-throughput cellular-based assays with endpoints within 2-6 hr provide useful and predictive information about long-term biological properties of NPs.
- Toxicological data obtained from *in-vitro* cellular-based toxicity assays will correlate reasonably with *in-vivo* findings.
- Using physical/chemical characterization and toxicological screens for an ensemble of MNPs, it will be possible to develop **predictive Quantitative Nanostructure – Toxicity (QNTR) models**.

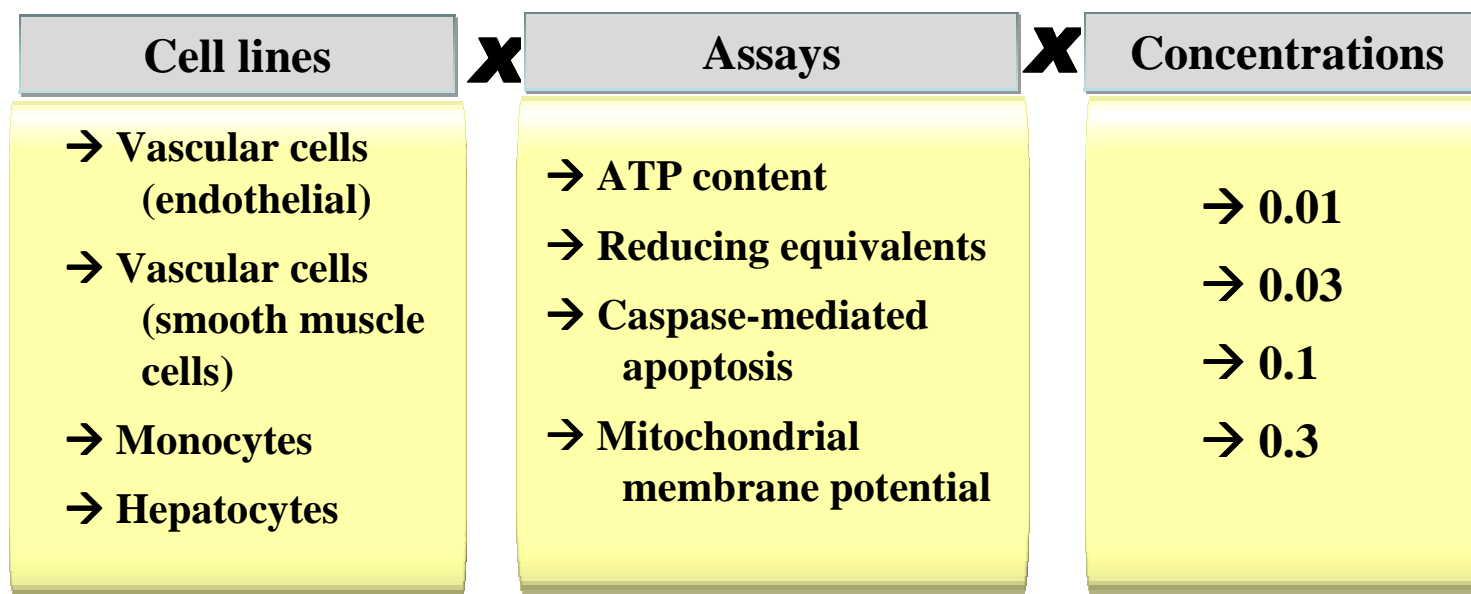
Subtask 2: QNTR Scheme



Case Study 1: QNTR of Whole NPs

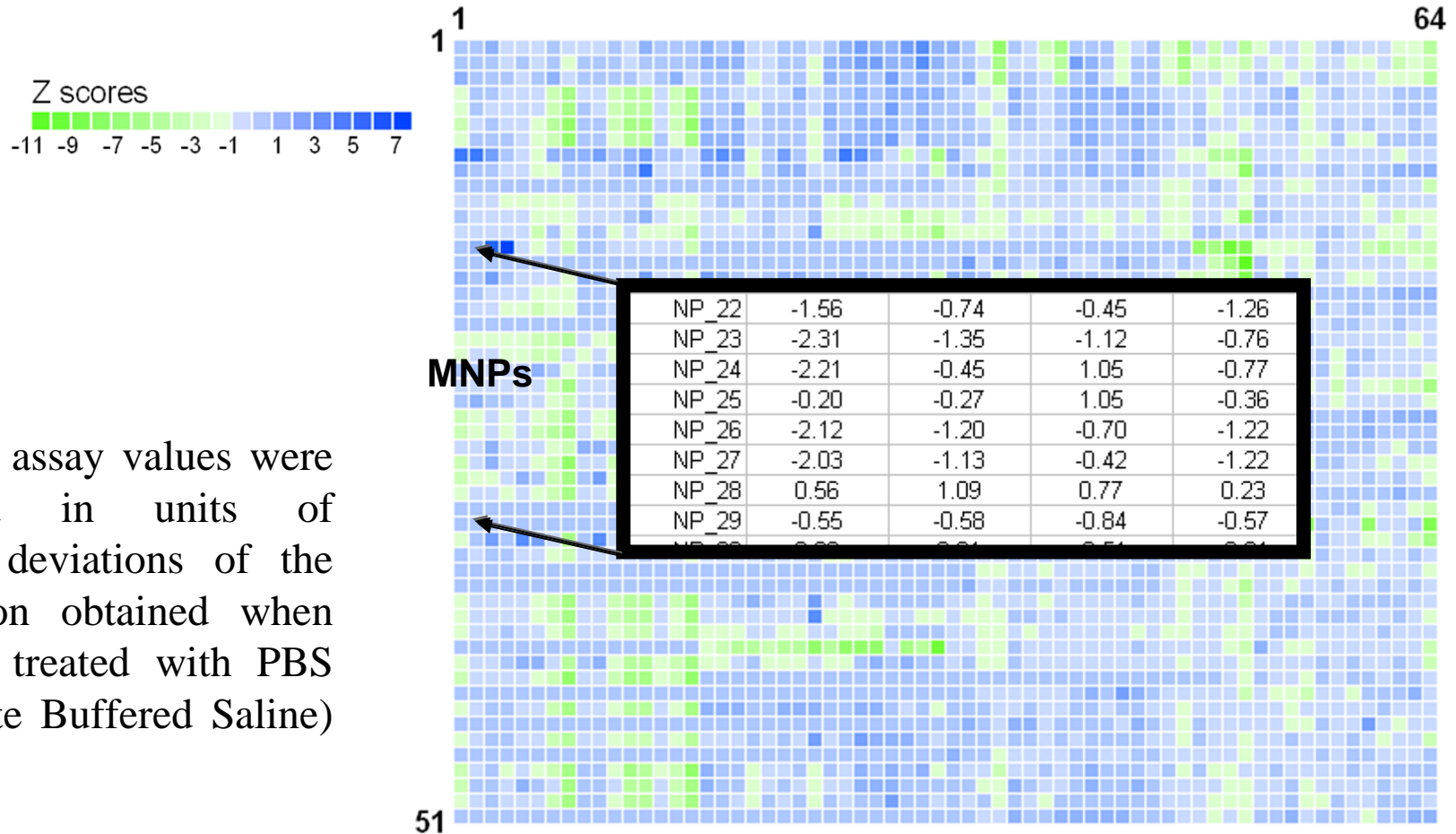
Recently¹, 51 diverse NPs were tested *in-vitro* against 4 cell lines in 4 different assays at 4 different concentrations (→ **51x64 data matrix**).

MNP	CLIO	PNP	MION	QD	Feridex IV	Ferrum Hausmann
#. particle	23	19	4	3	1	1



¹ Shaw et al. *Perturbational profiling of nanomaterial biologic activity. PNAS, 2008, 105, 7387-7392*

Case Study 1: Initial Activity Matrix



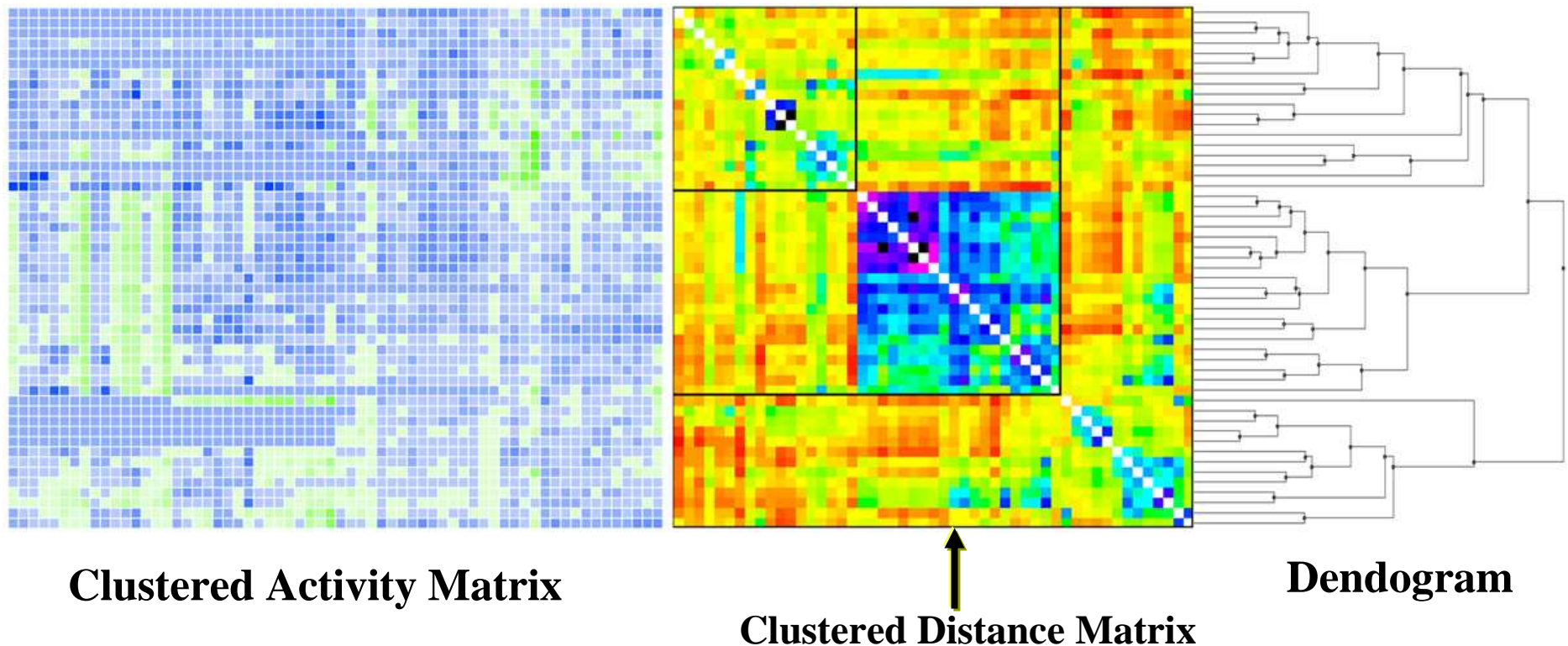
Z scores: assay values were expressed in units of standard deviations of the distribution obtained when cells are treated with PBS (Phosphate Buffered Saline) alone.

$$Z_{NP} = (\mu_{NP} - \mu_{PBS}) / \sigma_{PBS}$$

μ_{NP} : mean of control tests with PBS

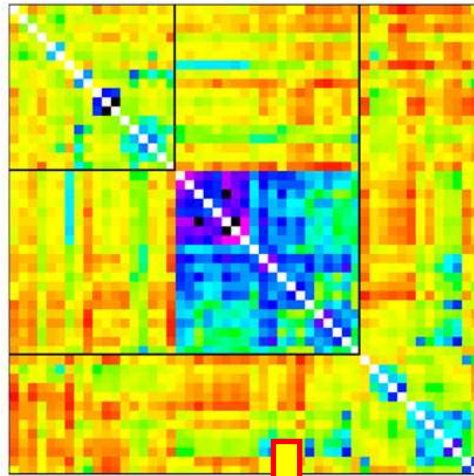
σ_{NP} : standard deviation of control tests with tests

Case Study 1: Hierarchical Clustering of The Activity Matrix



After the normalization of data, ISIDA/Cluster program* was used to cluster the activity matrix (51 * 64), using Johnson's hierarchical method, Euclidean metrics and complete linkage.

Case Study 1: Analysis of Clusters




NP type	CLUSTER 1	CLUSTER 2	CLUSTER 3	Total
CLIO	7	13	3	23
PNP	7	2	10	19
MION	0	4	0	4
Qt-dot	3	0	0	3
Feridex	0	1	0	1
Ferrum Hausmann	1	0	0	1
Total	18	20	13	51


NP Core	CLUST 1	CLUST 2	CLUST 3	Total
Fe ₂ O ₃	5	0	9	14
Fe ₃ O ₄	9	20	4	33
Cd-Se	3	0	0	3
Fe(III)	1	0	0	1
Total	18	20	13	51

A given metal core (i.e, Fe₃O₄) or NP category (i.e, Qt-dot), will induce similar biological effects in most cases, independent of the surface modifications.

Case Study 1: QNTR Matrix and Modeling Results

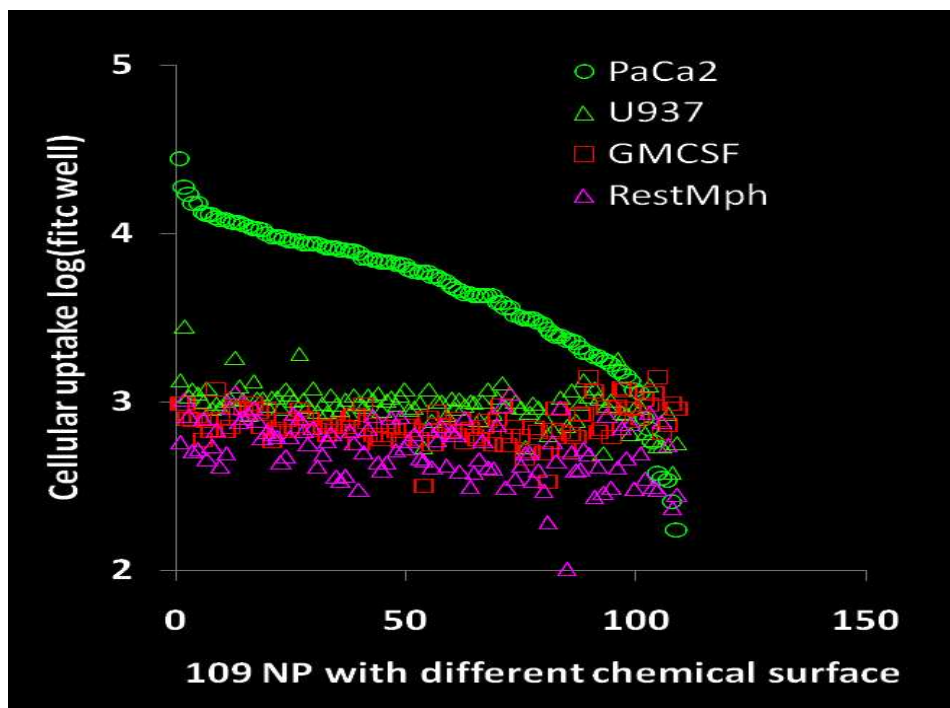
QNTR Matrix 

	Effect	Size	Zeta pot.	Relaxivities	
NP-01	High	0.4865	0.5278	0.2941	0.3986
NP-02	Low	0.4054	0.7222	0.4837	0.6476
NP-03	High	0.4324	0.5833	0.3529	1.0000
NP-04	Low	1.0000	0.5833	1.0000	0.7991
NP-05	High	0.3649	0.4722	0.2353	0.9403
NP-06	High	0.3919	0.6111	0.3333	0.9079
NP-07	High	0.5135	0.5833	0.4052	0.6270

Modeling Results 

Fold	MODELING SETS				EXTERNAL SETS				
	<i>n</i>	# models	% accuracy internal 5-fold CV	% accuracy	<i>n</i>	% accuracy	% CCR ^a	% Sensitivity (SE)	% Specificity (SP)
1	35	11	51.4 – 60.0	71.4 – 82.9	9	78	83	67	100
2	35	13	51.4 – 60.0	71.4 – 77.1	9	78	75	50	100
3	35	16	57.1 – 62.9	74.3 – 82.9	9	78	78	80	75
4	35	11	60.0 – 62.9	77.1 – 88.6	9	56	55	50	60
5	36	4	66.7	83.3 – 86.1	8	75	67	33	100
^a CCR – Correct Classification Rate; CCC = ½ (SE + SP)					44	73	73	60	86

Case Study 2: QNTR Study of NPs Uptake in PaCa2 Cells



PaCa2: Pancreatic cancer cells

U937: Macrophage cell line

GMCSF: Activated primary human macrophages

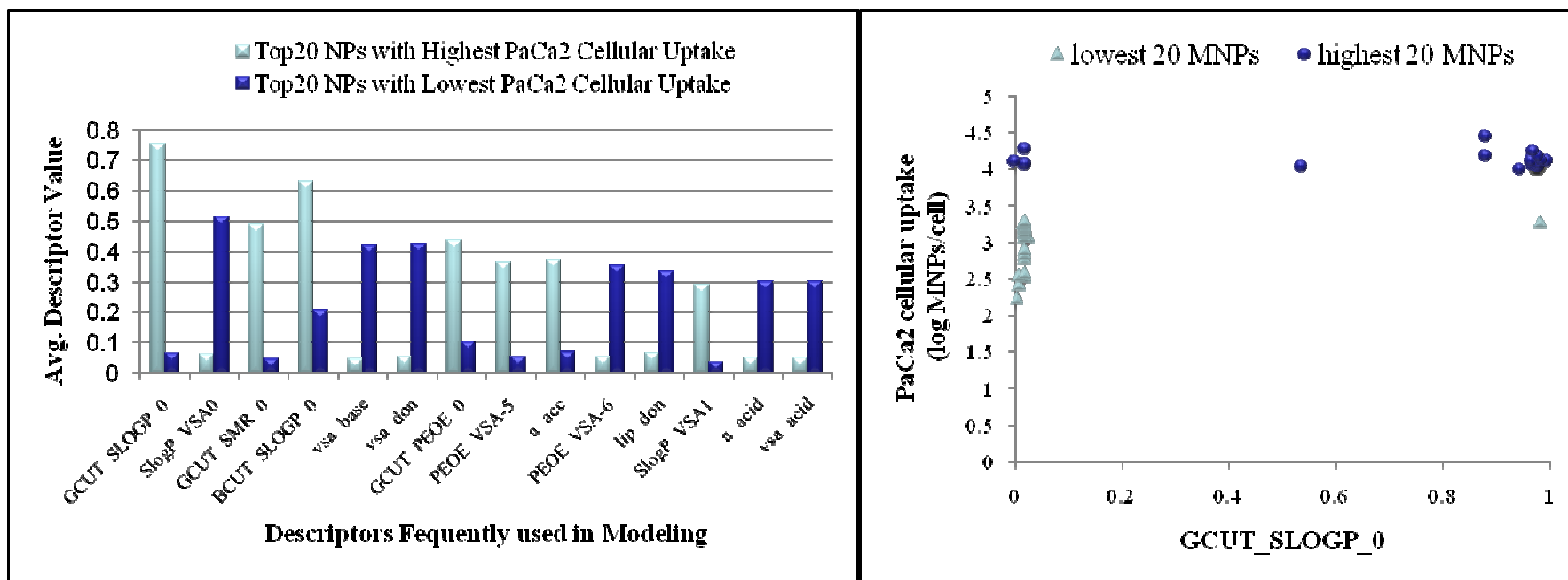
RestMph: Resting primary human macrophages

Recently, Weissleder et al.* investigated whether the multivalent attachment of small organic molecules on a same NP can modify its binding affinity to certain cells. 109 NPs possessing the same core (CLIO) were attached with different organic compounds on their surfaces

* Weissleder et al. *Nat. Biotechnol.*, 2005, 23 (11), 1418-1423

Case Study 2: Modeling Results And Descriptor Analysis

Fold	# comp. model	# comp. external	w/o AD		w/ AD		
			R _o ²	MAE	R _o ²	MAE	% cov
1	87	22	0.65	0.18	0.67	0.18	86
2	87	22	0.67	0.14	0.73	0.13	91
3	87	22	0.72	0.22	0.75	0.21	82
4	87	22	0.75	0.19	0.90	0.14	64
5	88	21	0.80	0.16	0.78	0.17	76
Average	87	22	0.72	0.18	0.77	0.17	80



Subtask 2: Conclusions

- Preliminary results demonstrate that QNTR models can successfully predict the biological effects of NPs from their descriptors either experimentally measured (e.g., case 1 study), or calculated (case 2 study).
- To increase the accuracy and impact of models on the experiments, we need additional systematic experimental data (structural and biological).
- QNTR approach may allow rational design or prioritization of novel NPs with desired target (physical and biological) properties.

Industrial Interactions and Technology Transfer

- **Potentially seamless interaction between the ESH Research Center and SRC member companies.**
- **Send nanomaterials to UNC for characterization and analysis.**
- **Analyze experimental data and build predictive QNTR models.**
- **Prioritize MNP design and toxicity testing.**
- **Provide continuous feedback of information for ESH and SRC member companies.**

Future Plans

Next Year Plans

- Subtask 1:
 - Complete the standard outlined assays for MNPs Set 1 and 2.
 - Carry out detailed physico-chemical characterization and additional biological assays to identify the cause of differential toxicity profile manifested by MNPs in Set 2.
- Subtask 2:
 - Establish a database of experimental nanotoxicity data
 - Develop extended QNTR models of all available nanotoxicity data

Long-Term Plans

- Obtain predictive knowledge of physical and chemical properties of MNPs that affect human cells and utilize this knowledge for improved MNP experimental design and prioritized toxicity testing.

Publications, Presentations, and Recognitions/Awards

- **Shalini Minocha and Russell J. Mumper, “In-vitro Assays to Assess the Toxic Potential of Manufactured Nanoparticles”, 2009 AAPS Annual Meeting and Exposition, Los Angeles CA, November 8-12, 2009.**
- **Shalini Minocha and Russell J. Mumper, “Characterization and in-vitro Evaluation of Potential Toxicity of Commercially available nanoparticles”, Chapel Hill Drug Conference, May 13-14, 2009, Chapel Hill, NC, USA.**
- **Denis Fourches, Lin Ye, Russell J. Mumper and Alexander Tropsha. Assessing the Biological Effects of Nanoparticles Using Quantitative Nanostructure – Activity Relationships. Spring 2009 ACS Meeting and Exposition, Salt Lake City, UT, March 22-26, 2009.**
- **Denis Fourches, Dongqiuye Pu, Russell J. Mumper and Alexander Tropsha. Quantitative Nanostructure-Toxicity Relationship (QNTR) Modeling. Nanotoxicology, manuscript in preparation.**
- **Shalini Minocha, Dongqiuye Pu, Alexander Tropsha and Russell J. Mumper, “Systematic Evaluation of Toxicity of Metal Based Nanoparticles”, Nanotoxicology, manuscript in preparation.**

Laboratory Scale Assessment of the Fate of CMP Nanoparticles Through Standard Waste Water Treatment Systems *(Customized Project)*

PIs:

- Reyes Sierra, Chemical and Environmental Engineering, UA
- Farhang Shadman, Chemical and Environmental Engineering, UA
- Ara Philipossian, Chemical and Environmental Engineering, UA

Graduate Students:

- Isabel Barbero, PhD candidate, Chemical and Environmental Engineering, UA
- Jeff Rottman, PhD candidate, Chemical and Environmental Engineering, UA
- Monica Rodriguez, MS candidate, Chemical and Environmental Engineering, UA
- Francisco Gomez, PhD candidate, Chemical and Environmental Engineering, UA

Undergraduate Students:

- Dustin Brown, Chemical and Environmental Engineering, UA

Other Researchers:

- Antonia Luna, Postdoctoral Fellow, Chemical and Environmental Engineering, AA
- Jim Field, Professor, Chemical and Environmental Engineering, AA

Cost Share (other than core ERC funding):

- Graduate Incentives for Growth Awards (GIGA) (\$25 K)
- Student Fellowship (Mexican Science Foundation, CONACyT) (\$20 K)

SRC/SEMATECH Engineering Research Center for Environmentally Benign Semiconductor Manufacturing

Objectives

- Investigate removal of CMP nanoparticles by interactions with the biosolids (*i.e.*, entrapment in sludge flocs, adsorption to cells, cell internalization).
- Assess the impact of municipal wastewater composition (eg. organic matter, salts, surfactants, pH, etc) on the aggregation behavior of CMP nanoparticles.
- Evaluate the removal of nanoparticles (NP) present in CMP effluents in a bench-scale wastewater treatment plant.

ESH Metrics and Impact

Reduction in emission of ESH-problematic material to environment

This study will lead to new insights on the interactions of NPs with typical components in semiconductor effluents, municipal wastewaters, and natural aquatic environments over a wide range of physicochemical conditions.

It will also provide information on the fate of NP present in CMP waste streams in municipal wastewater treatment systems. The knowledge gained can be utilized to determine if additional treatment steps are required to reduce environmental emissions of ESH-problematic chemicals, if any.

Materials and Methods

Commercial Slurries

Fumed Silica – Oxide CMP (30 nm)

Alumina – Cu CMP

Ceria – Oxide/STI CMP

Virgin Nanoparticles

Silica: 10-20 nm

Alumina: 50 nm

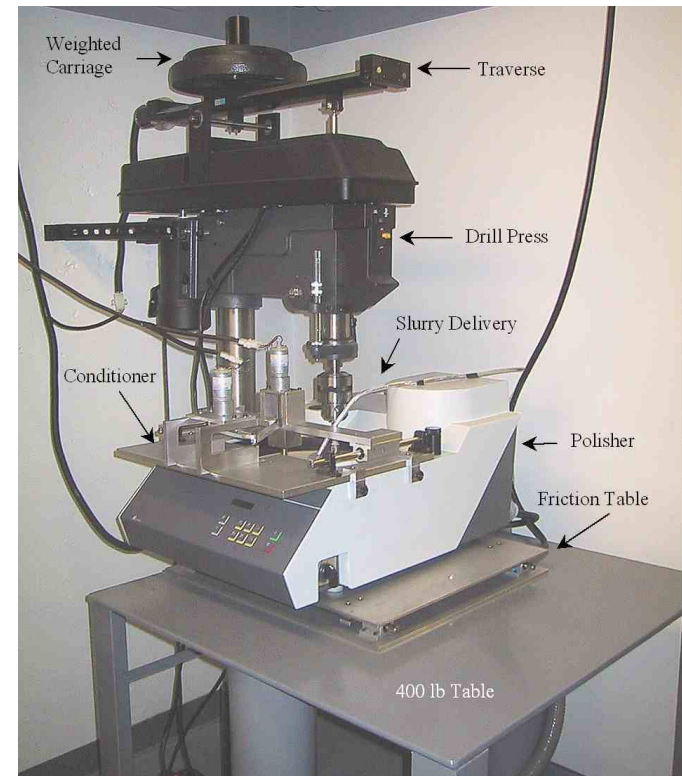
Ceria 20 or 50 nm

CMP waste:

Prepared at the pilot-scale CMP tool available at the UA

Particle size and Zeta potential:

Malvern Zeta Sizer Nano ZS



Polisher (100-mm) that will be used to prepare CMP waste effluents

Tasks

1. Impact of wastewater components on the aggregation behavior of CMP nanoparticles.
 - Organic compounds: eg proteins, aminoacids, humus, etc.
 - Polyelectrolytes
 - pH, Salts, divalent cations
2. Removal of CMP nanoparticles by biosolids
 - Adsorption isotherm experiments
 - Electron microscopy examination
3. Removal of nanoparticles in CMP effluent a lab-scale wastewater treatment plant
 - Lab-scale experiments with ceria slurry

Significant Aggregation of CeO₂, SiO₂ and Al₃O₂ Nanoparticles in Aqueous Solution

NP	Average Particle Size (nm)	
	Powder (Using TEM)	Aqueous medium (Using ZetaSizer)
CeO ₂	20	139
Al ₂ O ₃	50	175
SiO ₂	10-20	368

CeO₂, Al₂O₃ and SiO₂ NPs showed significant aggregation in aqueous solutions even at pH values considerably different from their respective isoelectric point.

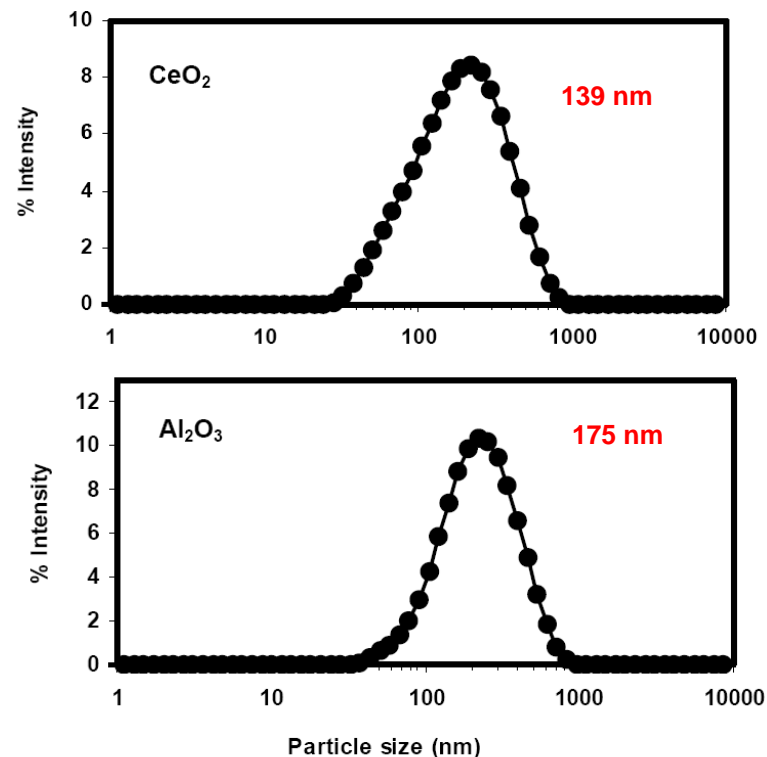


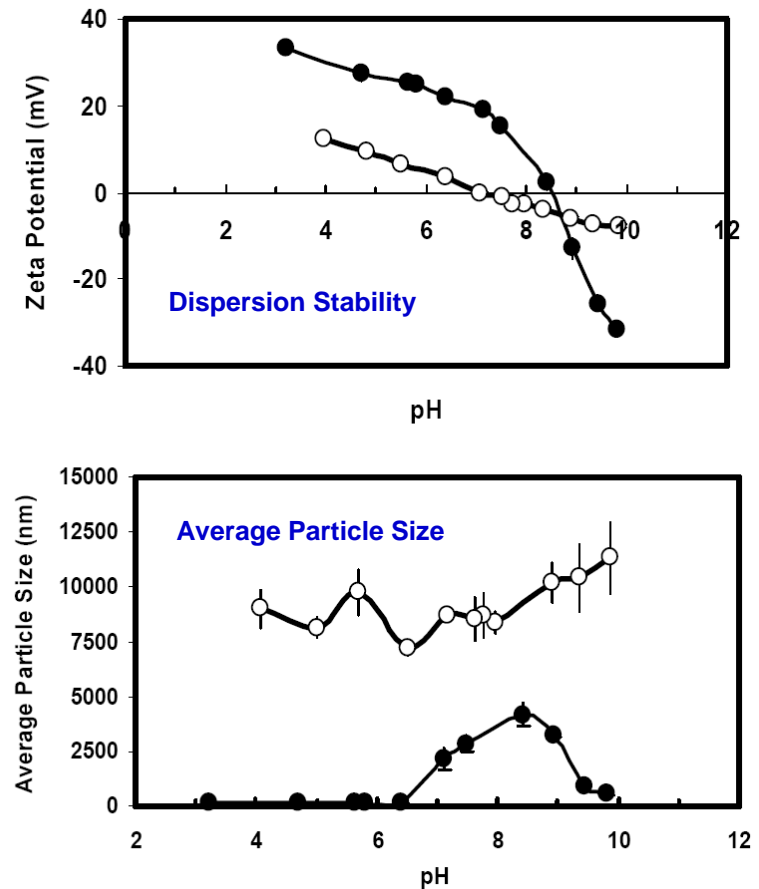
Fig. Particle size distribution of nano-CeO₂ and Al₂O₃ in pH-5.2 and pH-4.5 aqueous solutions, resp. Titration experiments showed that the dispersions exhibit high stability at these pH values.

Impact of pH and Dilution with Municipal Waste on the Stability of Al_2O_3 NP Dispersions

Z-pot: -20 to 20 mV
Dispersion is unstable

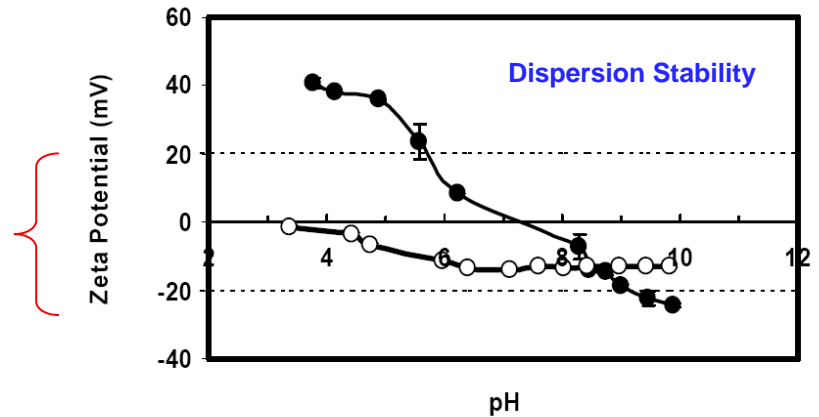
Dilution with municipal wastewater and circumneutral pH values promotes aggregation of alumina NPs.

Fig. Impact of pH on the zeta potential & average diameter of Al_2O_3 dispersions mixed with demineralized water (●) or filtered (20 nm) municipal wastewater (○).



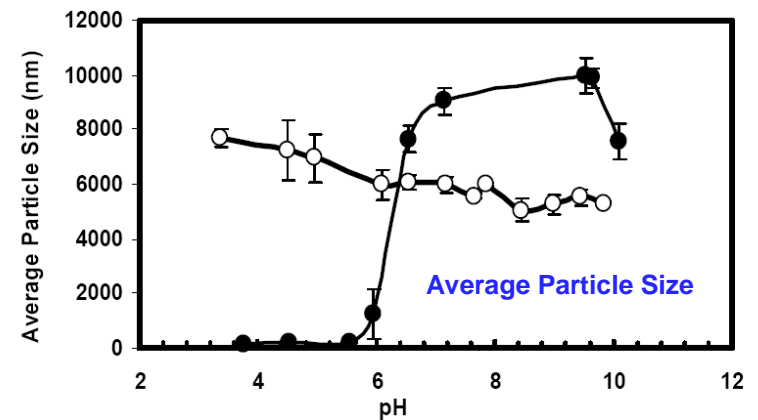
Impact of pH and Dilution with Municipal Waste on the Stability of CeO₂ NP Dispersions

Z-pot: -20 to 20 mV
Dispersion is unstable



Dilution with municipal wastewater and increasing pH promotes the aggregation of CeO₂ nanoparticles

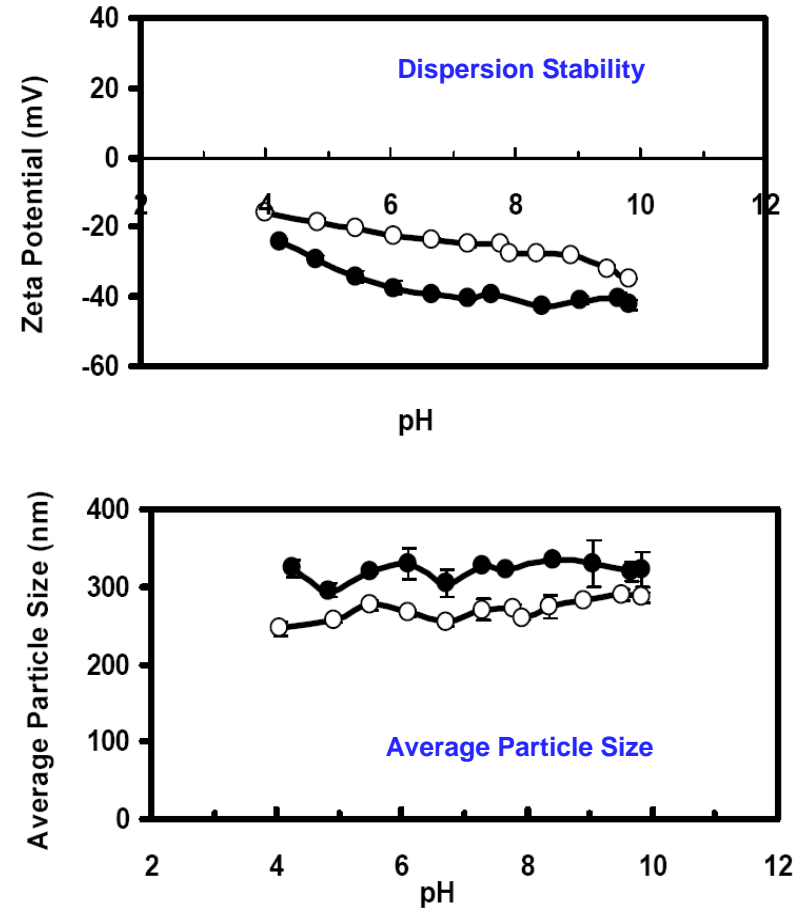
Fig. Impact of pH on the zeta potential & average diameter of CeO₂ dispersions mixed with demineralized water (●) or filtered (20 nm) municipal wastewater (○).



Impact of pH and Dilution with Municipal Waste on the Stability of SiO₂ NP Dispersions

The stability of SiO₂ NP dispersions was little affected by changes in pH or dilution with municipal wastewater

Fig. Impact of pH on the zeta potential & average diameter of SiO₂ dispersions mixed with demineralized water (●) or filtered (20 nm) municipal wastewater (○).

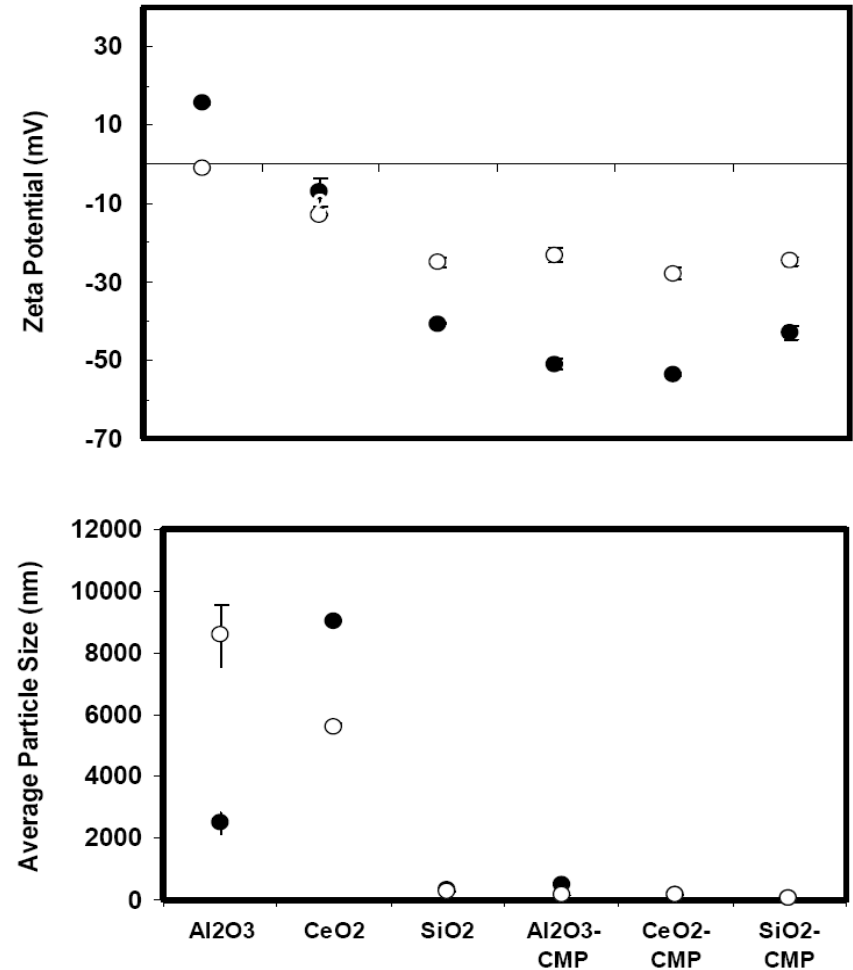


Impact of Dilution with Municipal Waste on the Stability of Al_2O_3 , CeO_2 , and SiO_2 NP Dispersions

Dilution of CMP waste with domestic wastewater (1:1) only caused a moderate decrease in the dispersion stability, probably due to high levels of surfactants in the slurry.

Considerably higher wastewater dilution resulting in increased destabilization of the NP dispersion is expected in the sewer.

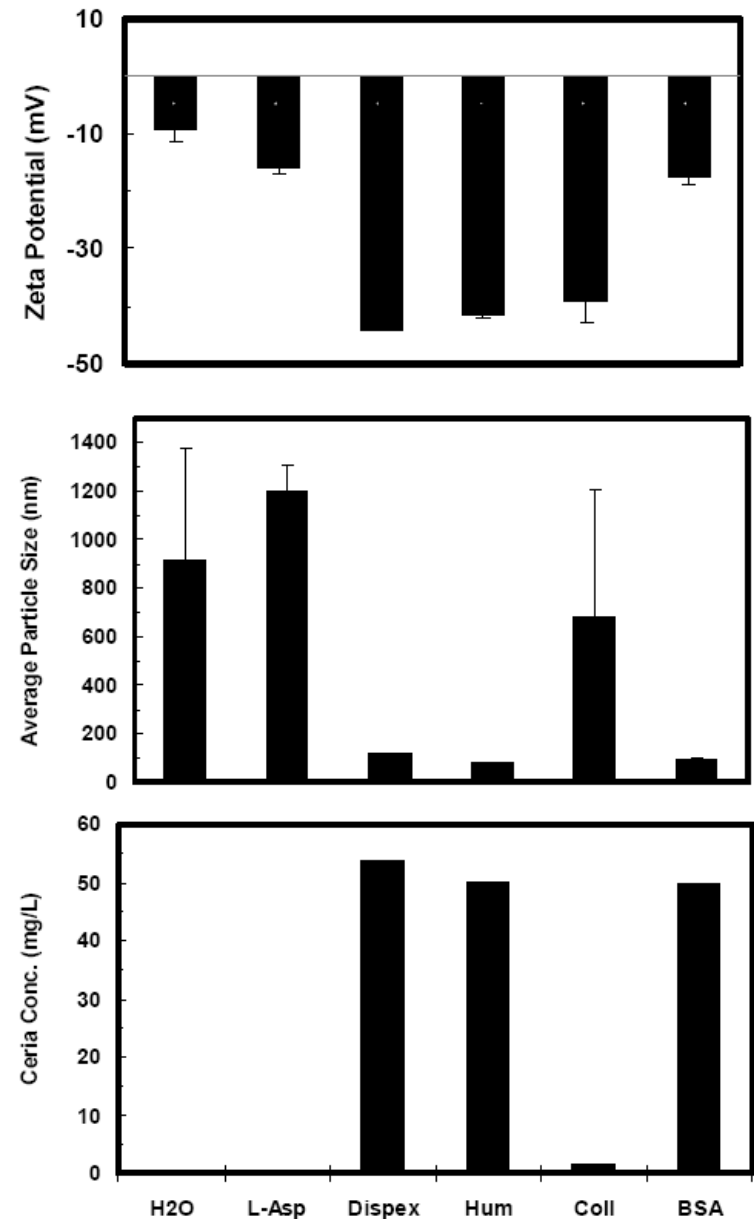
Fig. Stability of nano-sized CeO_2 , Al_2O_3 and SiO_2 dispersions, and CeO_2 , Al_2O_3 and SiO_2 -based CMP slurries diluted (1:1, v/v) with deionized water (●) and membrane-filtered (20 nm) municipal wastewater (○) at circum-neutral pH values.



Wastewater Components and NP Stability

Constituents in municipal wastewater alter the stability of the inorganic oxide dispersions. Some proteins, humic substances and synthetic dispersants stabilize NP dispersions (CeO_2 , Al_2O_3 , SiO_2) in the neutral to mildly alkaline range which is typical of municipal wastewaters.

Fig. Zeta potential (Top panel), average particle size (Middle panel), and residual ceria concentration in dispersions (Lower panel) after dilution (1/1, v/v) of a nano-sized ceria dispersion with solutions of different additives (200 mg/L). The final pH of the diluted dispersions was 6.8. Additives: L-Asp= L-aspartic acid; Dispex= Ammonium polyacrylate dispersant; Hum= Humic acid; Coll= Collagen; BSA= Bovine serum albumin.



Removal of CMP Nanoparticles by Activated Sludge

Aerobic activated sludge has a relatively high affinity for CeO_2 and Al_2O_3 NPs

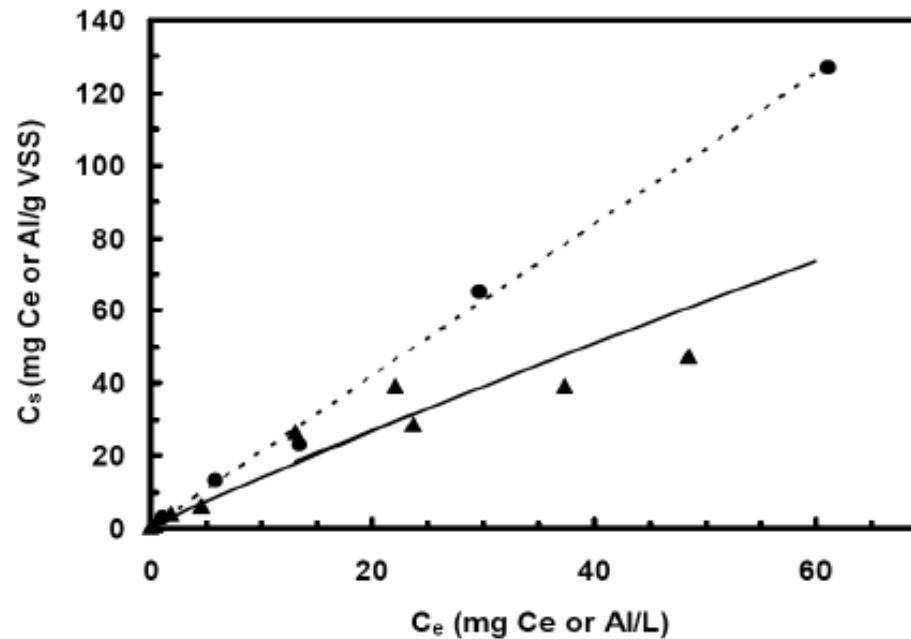
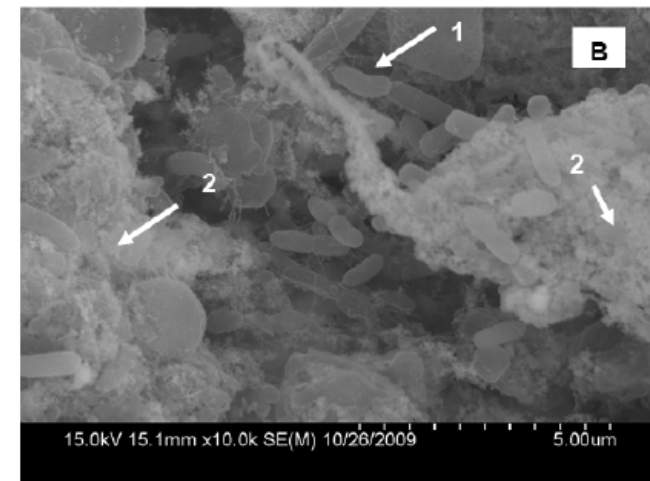
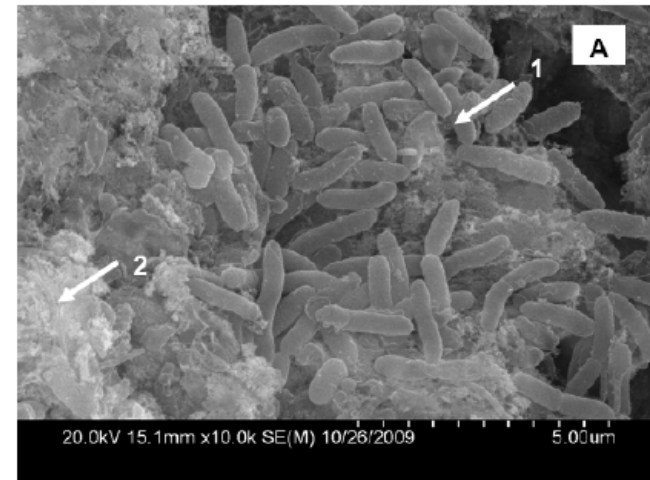


Fig. Partitioning of ceria (●) and alumina (▲) onto activated sludge collected from a municipal wastewater treatment plant. Experimental data fit to Freundlich model for ceria (dashed line) and alumina (solid line).

Removal of CMP Nanoparticles by Activated Sludge

SEM images of activated sludge collected from the bioreactor system fed with a wastewater containing CeO_2 NPs. The arrows indicate areas with bacterial cells (labeled 1), and areas where extracellular deposits (labeled 2) that are likely to contain large fractions of agglomerated ceria.

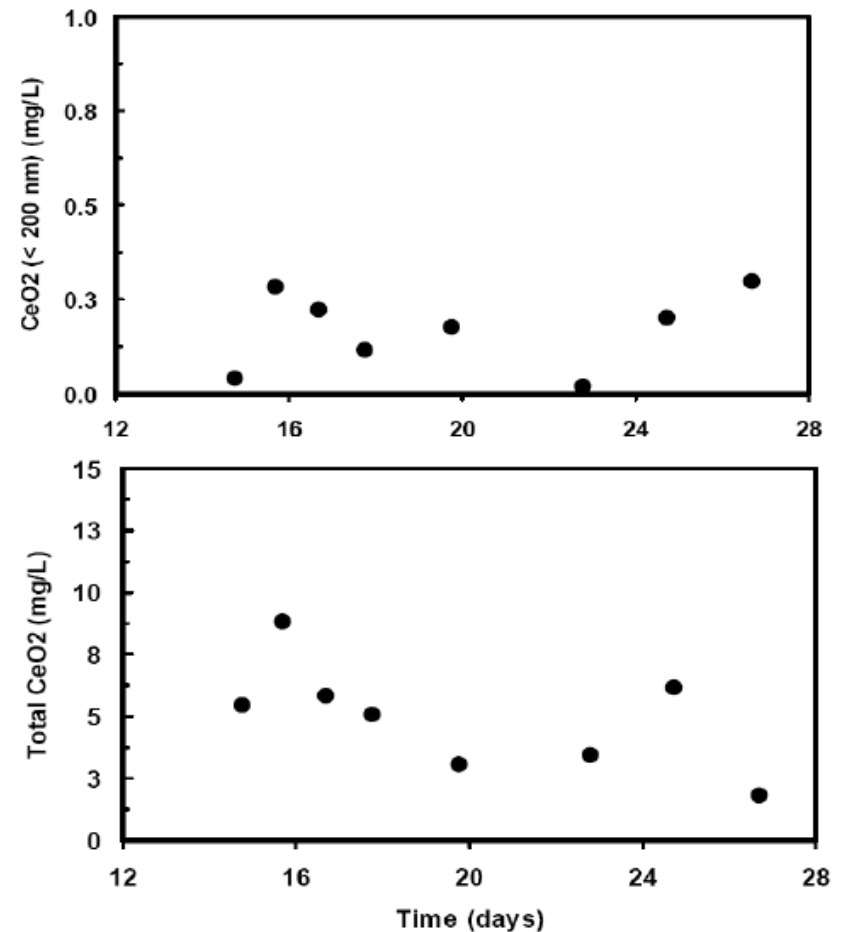


Removal of CMP Nanoparticles During Conventional Wastewater Treatment (Activated Sludge Process)

Conventional biological treatment provides high removal of CeO₂ NP.

NPs removed by adsorption onto the bacterial cell wall and entrapment into sludge flocs.

Fig. Concentrations of ceria (< 200 nm) (Top panel) and total ceria (Lower panel) in the treated effluent of a continuous lab-scale activated sludge system fed with nano-sized CeO₂ (75 mg/L)



Conclusions

- Treatment of effluents containing ceria or alumina NPs in conventional wastewater treatment plants is expected to result in a significant removal of the inorganic oxides from the treated effluent.
- Destabilization of the NP dispersions by constituents in the wastewater as well as association of the inorganic oxides with the activated sludge appears to be implicated in the removal mechanisms.
- SiO₂ NP dispersions were considerably more stable, even when diluted with municipal wastewaters or solutions containing proteins or amino acids that promoted aggregation of ceria and alumina NPs. These results suggest that a high fraction of SiO₂ NPs could escape wastewater treatment. Additional research is needed to test this hypothesis.

Industrial Interactions and Technology Transfer

- **Laurie Beu (ISMI / Sematech)**
- **Steve Brown (Intel)**
- **Reed Content (AMD)**
- **Art Fong (IBM)**
- **Peter Maroulis (Air Products)**
- **Brian Raley (Global Foundries)**
- **Tim Speed (IBM)**
- **Steve Trammel (ISMI / Sematech)**
- **Tim Yeakly (TI)**

Future Plans

Next Year Plans

- Writing scientific publications resulting from the project
- This 7-month project was completed on Nov. 2009
- Funding is being sought to continue research work on:
 - Fate and transport of SiO₂ and CeO₂ nanoparticles in aquatic environments, including wastewater and surface water
 - Innovative methods for the removal of abrasive nanoparticles from CMP wastewaters.

Publications, Presentations, and Recognitions/Awards

- Sierra-Alvarez, R., F. Shadman, A. Philipossian. 2009. Laboratory-Scale Assessment of the Fate of Chemical Mechanical Polishing (CMP) Nanoparticles Through Standard Wastewater Treatment Systems FATE Technology Transfer 09115058A-ENG. International SEMATECH Manufacturing Initiative, Inc. Austin, TX. Dec. 14, 2009.
- Three papers accepted for presentation by students at the 32nd Annual SESH International High Technology ESH Symposium and Exhibition. Scottsdale, AZ, April 26-29, 2010.
- Sierra-Alvarez, R et al. 2010. Removal of CeO₂ Nanoparticles in Semiconductor Manufacturing Effluents during Activated Sludge Treatment. 2010. 7th Leading Edge Conference on Water and Wastewater Technologies, Phoenix, AZ (June 2-4). (Accepted for presentation)
- Sierra-Alvarez, R., Barbero, I., M. Rodriguez, J. Rottman, F. Shadman, J.A. Field, R. Fate of Chemical Mechanical Polishing (CMP) Nanoparticles in Activated Sludge Processes (Paper in preparation)
- Field JA, Sierra-Alvarez. 2010. Nanoparticle Interaction with Biological Wastewater Treatment Processes. Brown Bag Water Sustainability Series, UofA Maricopa County Cooperative Extension. Phoenix, AZ. Jan 20.
- Barbero, I., M. Rodriguez, J. Rottman, F. Shadman, J.A. Field, R. Sierra-Alvarez. 2009. Evaluation of the Fate of Nanoparticles in CMP Wastewater during Standard Wastewater Treatment. 2009 Graduate Symposium, Dept Chemical and Environmental, UA, Oct. 10 (Poster, 1st prize)

Reducing Water and Energy Usage in Batch and Single-Wafer Rinsing Tools

**Jun Yan¹, Kedar Dhane¹, Davoud Zamani¹, Omid Mahdavi¹
Bert Vermeire² and Farhang Shadman¹**

¹ University of Arizona

² Arizona State University

Co-Sponsored by:

**ERC, Environmental Metrology Corp (EMC)
Freescale, and Samsung Electronics**

Objective and Approach

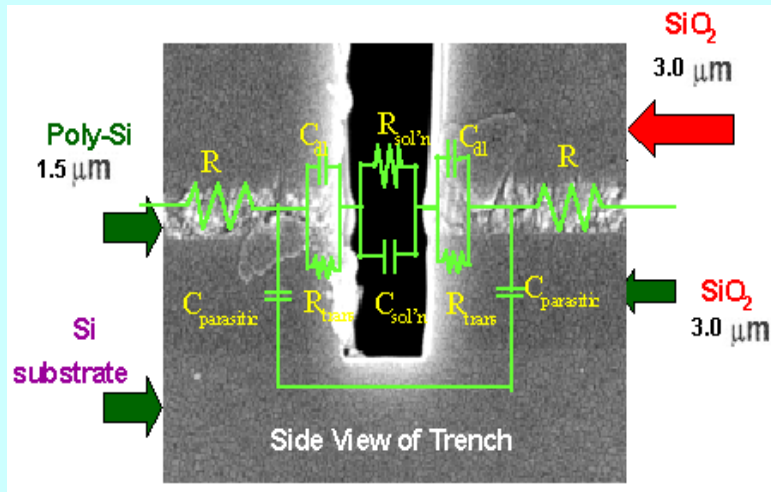
Objective:

- Investigate the fundamentals of cleaning, rinsing, and drying of micro- and nano-structures; develop new technologies (hardware, process models, and process recipes) to reduce water, chemicals, and energy usage during these processes.

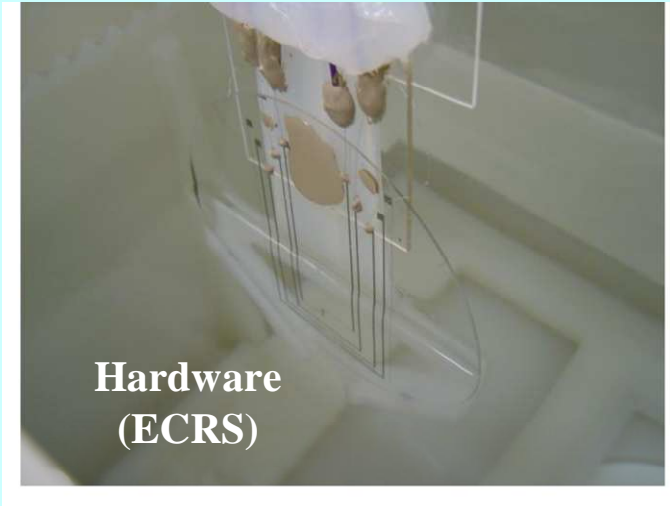
Method of Approach:

- Apply the novel ECRS metrology method for in-situ and real-time monitoring of the dynamics of batch and single-wafer surface preparation.
- Combine metrology with process modeling to identify the controlling steps (bottlenecks) in the cleaning, rinsing, and drying of small structures.

Background: In-situ Metrology (E CRS)



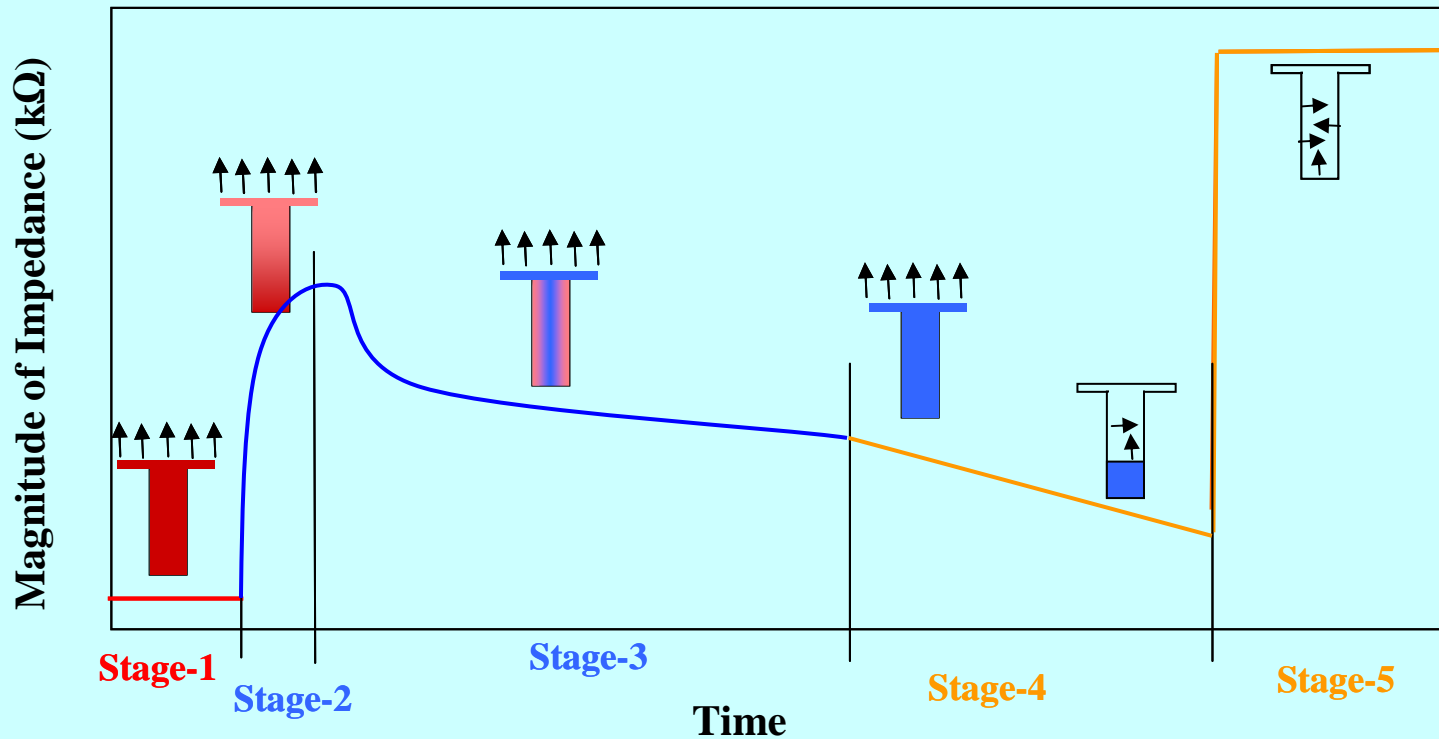
Solution (pH)	UPW (pH=7)	HCl(pH=6)	HCl(pH=5)
Resistivity (MΩ)	18	2.3	0.23
Resolution (ppt)	5	30	400



Key Features

- Real Time
- In-situ
- Online
- High Sensitivity
- Non-destructive
- Quick Response

Monitoring Capabilities of ECRS



Stage-1: Chemical Exposure

Stage-2: Rinsing -Purging of the Trench

Stage 3: Rinsing: Surface Reaction

Stage-4: Bulk Drying

Stage-5: Surface Drying

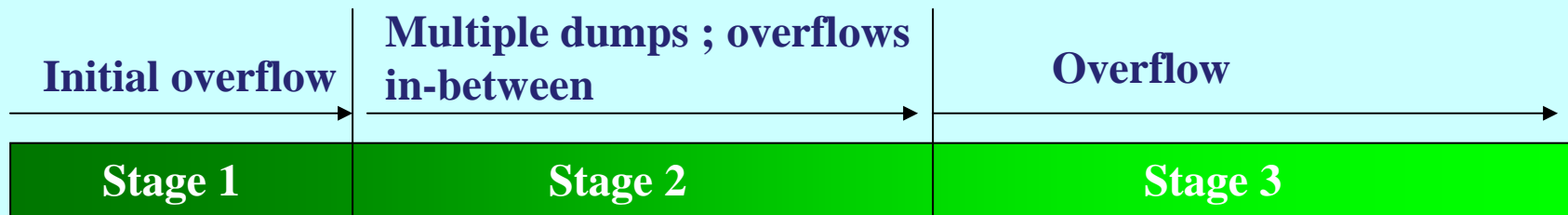
ECRS Application in Over-Flow and Quick-Dump Rinse Tools

Joint work with Freescale and EMC* on development of new low-water rinse processes using ECRS and process modeling.

Co-Investigators and Liaisons: Hsi-An Kwong, Marie Burnham, Tom Roche, Amy Belger, Stuart Searing, and Georges Robert

** EMC is a Engineering Research Center spin-off company that is formed for tech transfer and commercialization of ECRS technology*

Sample Results: Optimization of Rinse Recipe in OFR/QDR Combination



Process Parameters 520-621-9849

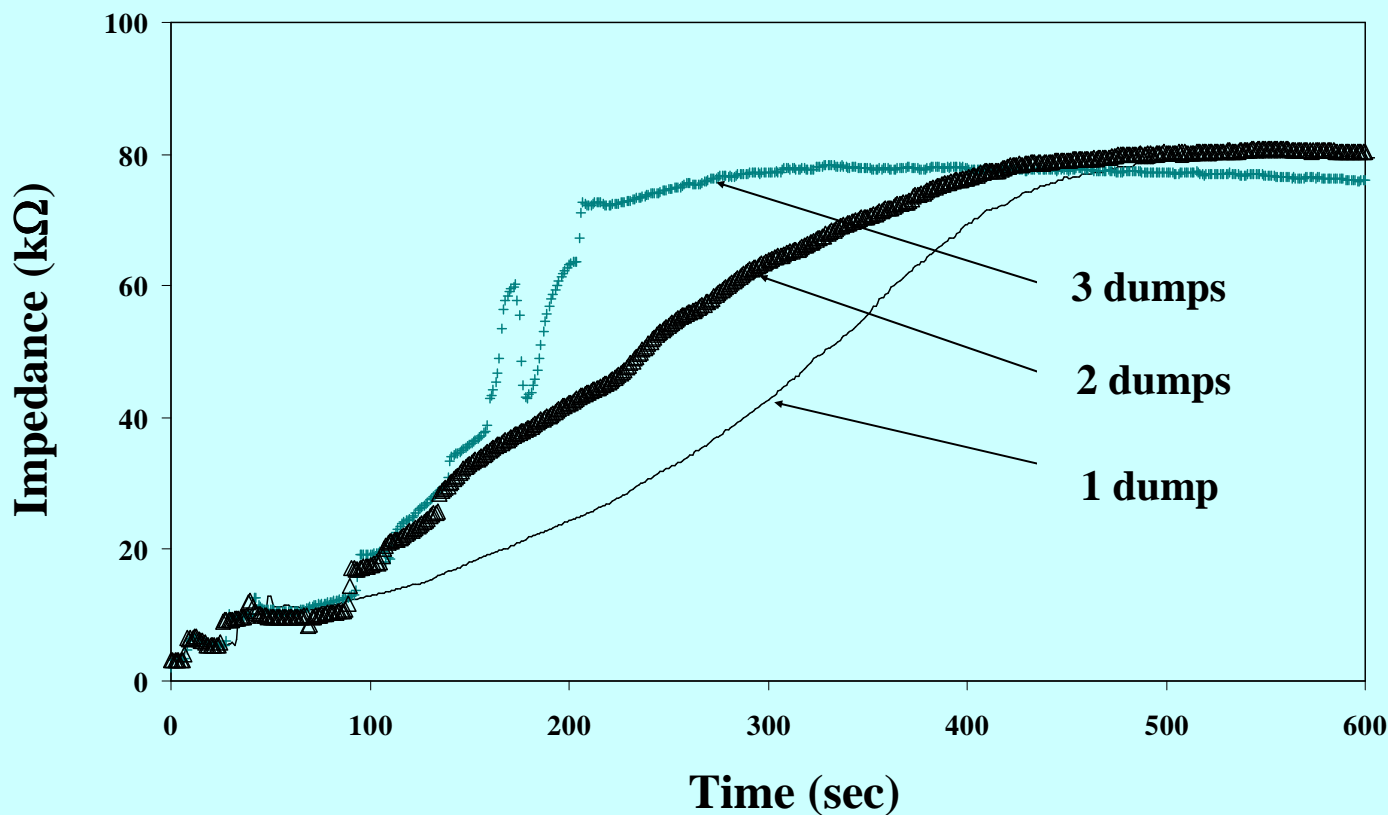
- Flow rates at different stages
- Time for every session of overflow rinse
- Number of quick dumps
- Water temperature at every session

Collaboration with Freescale to optimize existing rinse recipes is ongoing.

SRC/SEMATECH Engineering Research Center for Environmentally Benign Semiconductor Manufacturing

Effect of the Number of Dumps on the Post-APM Rinsing

Initial overflow for 5 sec; overflow in between for 5 sec;
flow rates are high flow at all stages; 30 ° C



ECRS Application in Single-Wafer **Spin Rinse**

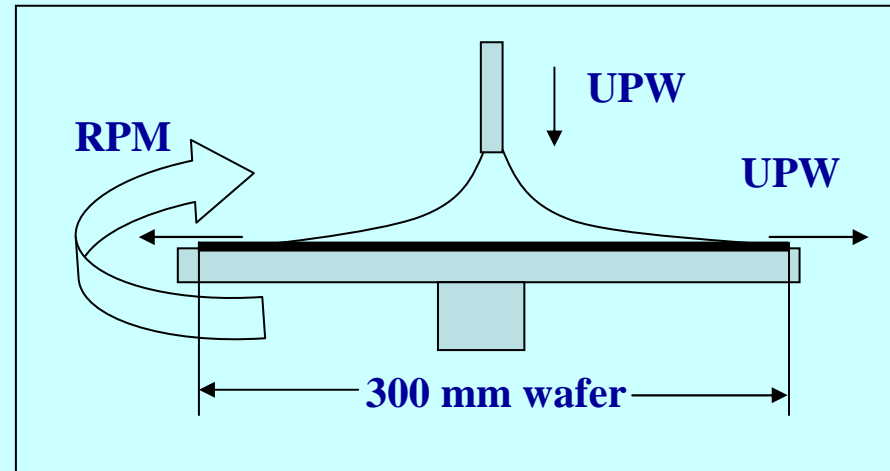
Joint work with Samsung and EMC on analysis of the dynamic of spins rinse and development of new low-water rinse processes.

Samsung Co-Investigator: Jeongnam Han

Application of ECRS to Single Wafer Rinsing and Drying



Experimental Setup



Process Model Schematic

- A single wafer tool equipped with ECRS is designed and set up.
- Combination of experiments and process model is used to study the effect of various process parameters.

Mathematical Analysis of Spin Rinsing

Multi-component species transport equations :

$$\frac{\partial C_i}{\partial t} = \nabla \cdot (D_i \nabla C_i + z_i F \mu_i C_i \nabla \phi) - u \nabla C_i$$

$$u_r = \frac{\rho \omega^2 r h^2 (1 - (1 - \frac{z}{h})^2)}{2\mu} \quad h = 0.782 \left(\frac{Q\mu}{\rho \omega^2 r^2} \right)^{1/3}$$

Surface adsorption and desorption:

$$\frac{\partial C_{S2}}{\partial t} = k_{a2} C_2 (S_{02} - C_{S2}) - k_{d2} C_{S2}$$

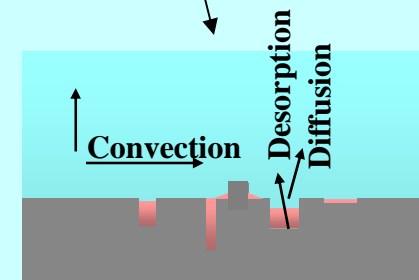
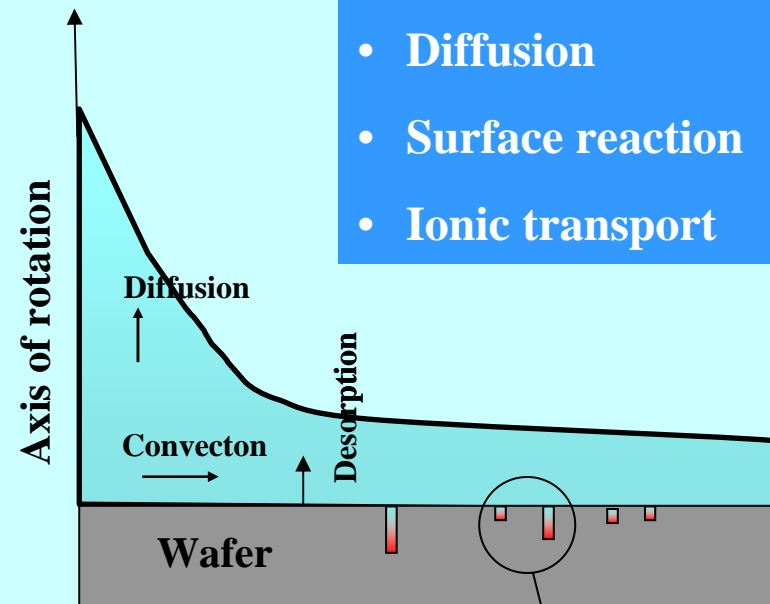
Poisson equation: $\nabla^2 \phi = -\frac{\rho}{\epsilon}$

where charge density: $\rho = F \sum_i z_i C_i$

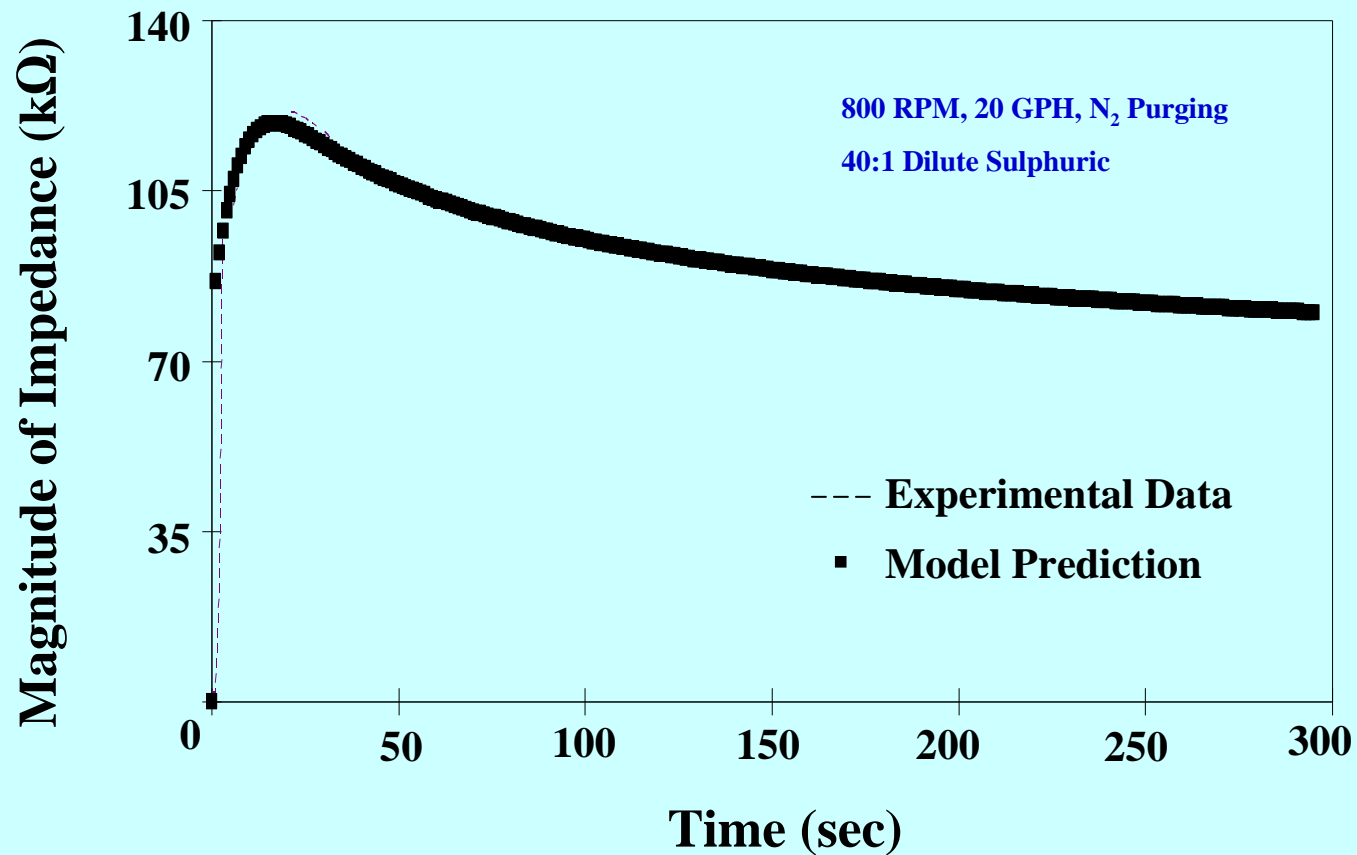
Ohm's law: $\vec{J} = \sigma \vec{E} \quad \nabla \times \vec{E} = 0$

where electrical conductivity: $\sigma = \sum_i \lambda_i C_i$

- Convection
- Surface Charge
- Diffusion
- Surface reaction
- Ionic transport



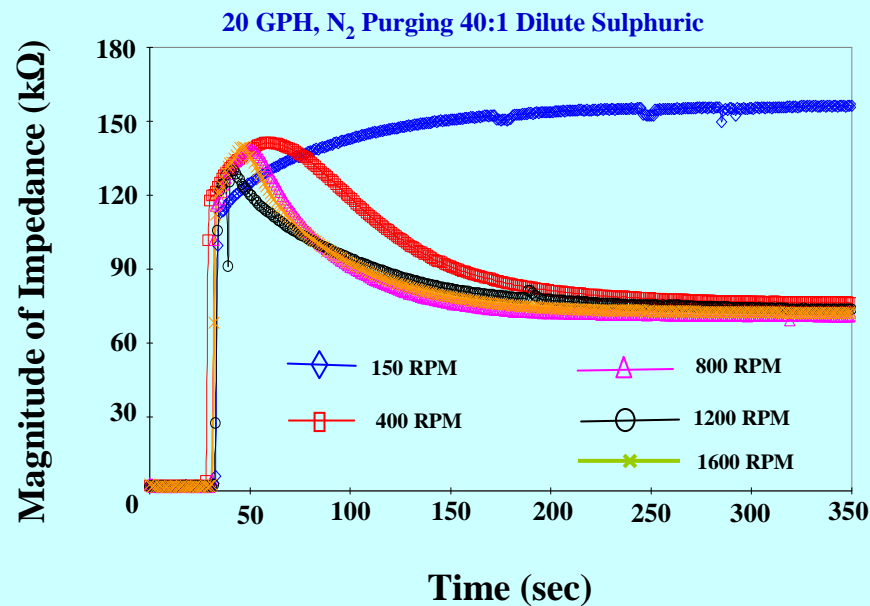
Validation of Process Simulation



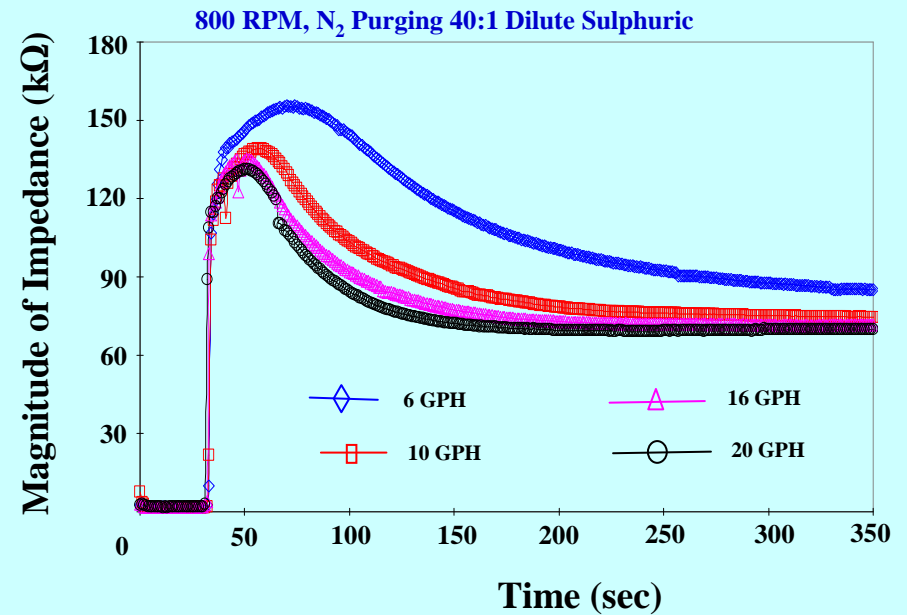
Simulation results are in good agreement with the experimental data

Effect of Process Parameters

Effect of Speed of Rotation

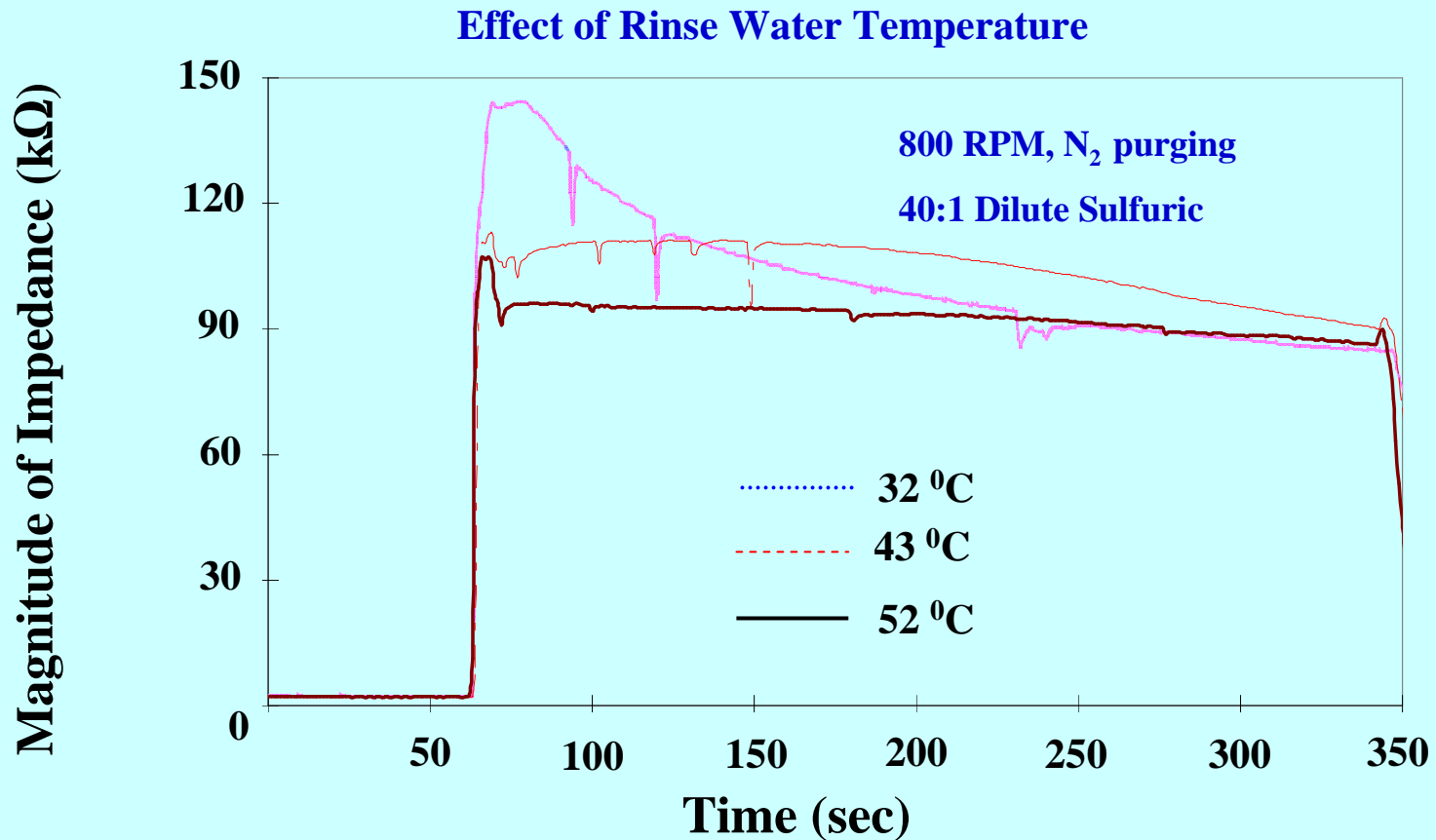


Effect of Flow Rate



- Gain in rinse efficiency diminishes as we reach an optimum speed of rotation and rinse-water flow rate.
- Speed of rotation and water flow rate can be optimized to reduce rinse time and increase throughput.

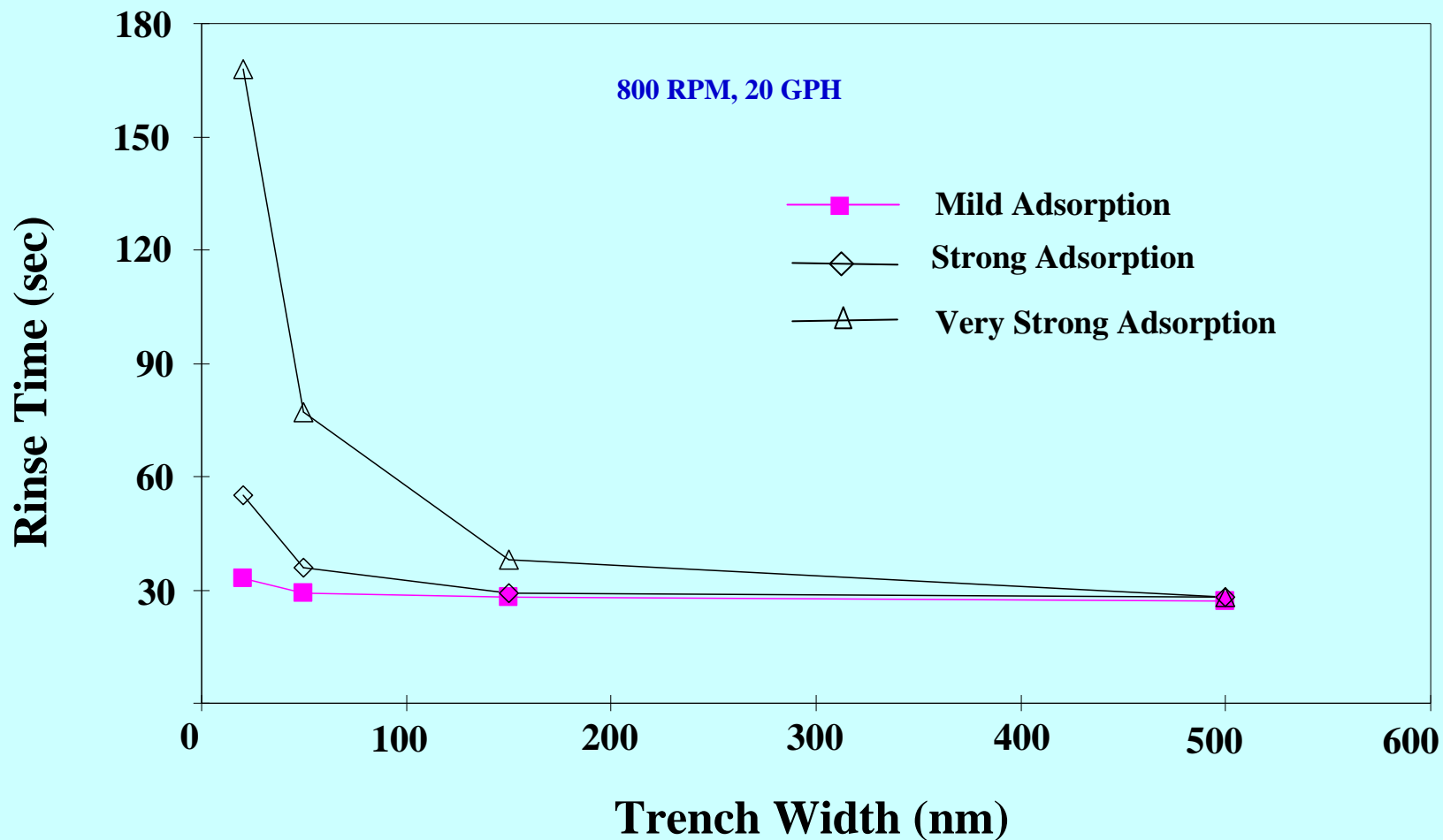
Effect of Process Parameters



Temperature has significant effect on enhancing both the early stage and the final stage of the rinse process.

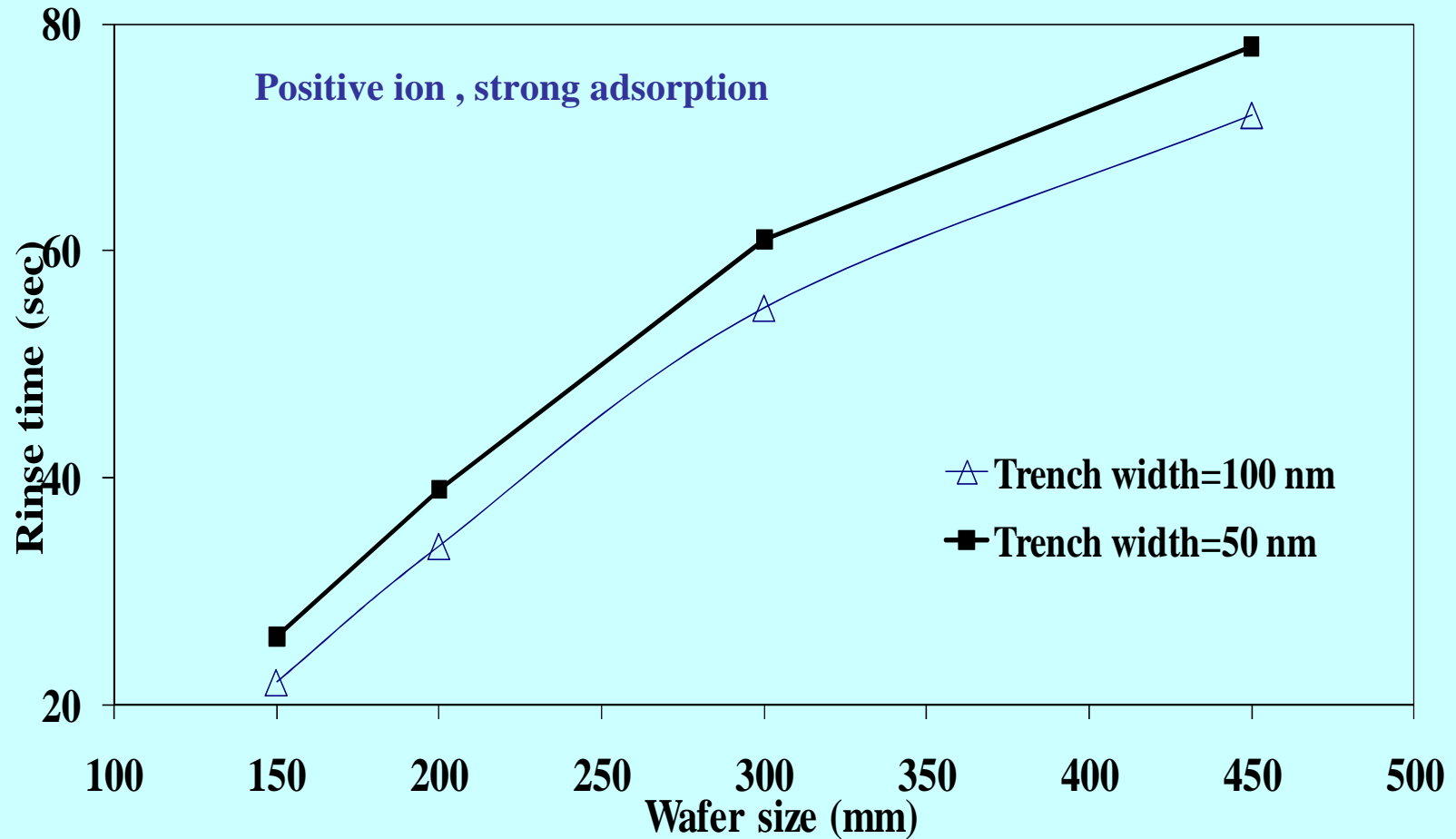
Effect of Feature Size

Rinse time to reach 10^{12} ions/cm² on the surface of the trench.



Effect of Wafer Size

Rinse time to reach 10^{12} ions/cm² on the surface of the trench.



Summary

- **Developed a method for integrating ECSR with single-wafer tools.**
- **Developed comprehensive process simulator and verified it for single-wafer rinsing; the simulator is applicable to rinsing and cleaning of fine structures on patterned wafers.**
- **Applied ECRS to determine the effect of key process parameters such as speed of rotation, flow rate, rinse water temperature, feature size, and wafer size.**
- **An integrated metrology method is under development for determining the extent of rinsing and drying and detecting the end points of each process step.**
- **Rinse and dry recipes and operating conditions can be optimized by applying the real-time and in-situ metrology using ECRS and the associated process simulator.**

Seed Project: Understanding, Characterizing and Controlling Pad Debris Generation during Copper CMP

PIs:

- **Takenao Nemoto, New Industry Creation Hatchery Center, Tohoku University**
- **Ara Philipossian, Chemical and Environmental Engineering, UA**

Graduate Students:

- **Yubo Jiao, PhD candidate, Chemical and Environmental Engineering, UA**
- **Zhenxing Han, PhD candidate, Chemical and Environmental Engineering, UA**

Other Researchers:

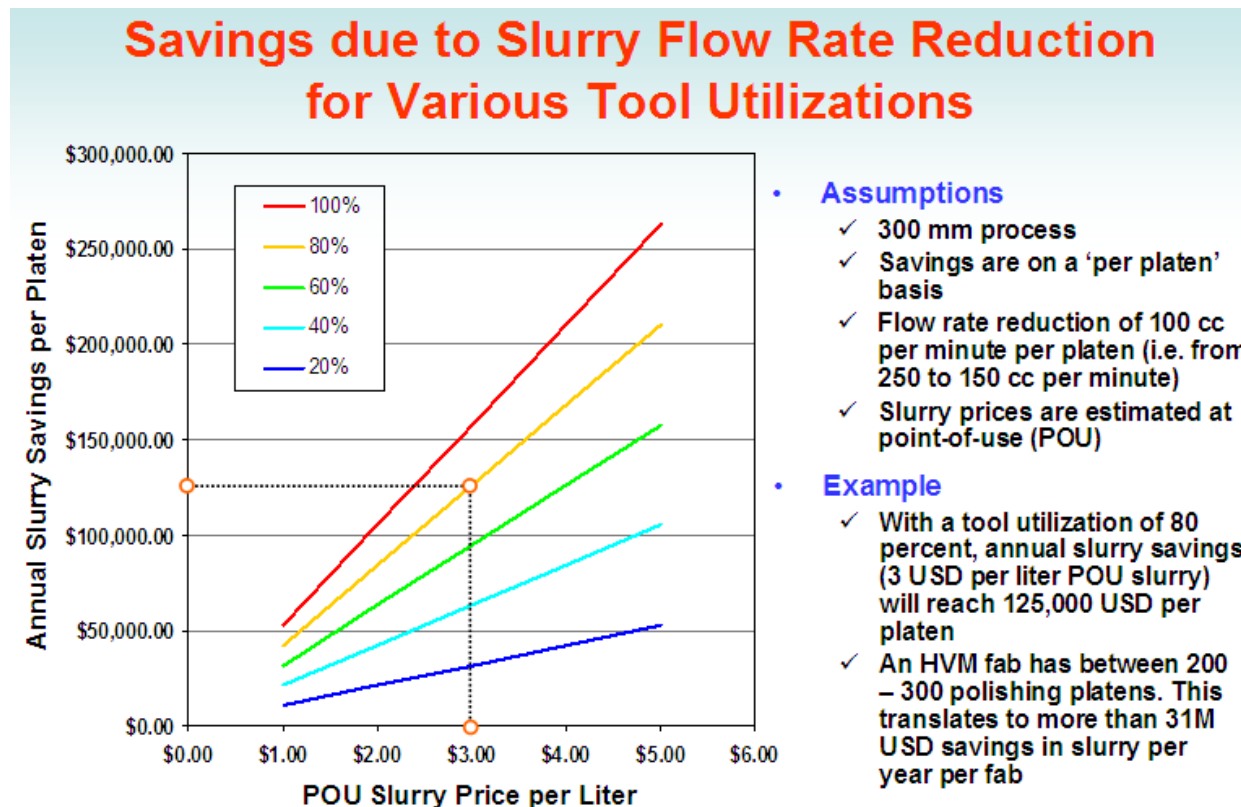
- **Yasa Sampurno, Research Associate, Chemical and Environmental Engineering, UA**
- **Yun Zhuang, Research Associate, Chemical and Environmental Engineering, UA**
- **Xun Gu, Ph. D. candidate, Graduate School of Engineering, Tohoku University**
- **Siannie Theng, Research Technician, Chemical and Mechanical Engineering, UA**

Objectives

- **Quantify the extent of pad debris generated during conditioning using different industry-standard pads and diamond disc conditioners**
- **Compare the polishing performance of standard vs. novel slurry injection methods on the extent of pad debris resident on the pad surface, polish performance and wafer defects during copper CMP**

ESH Metrics and Impact

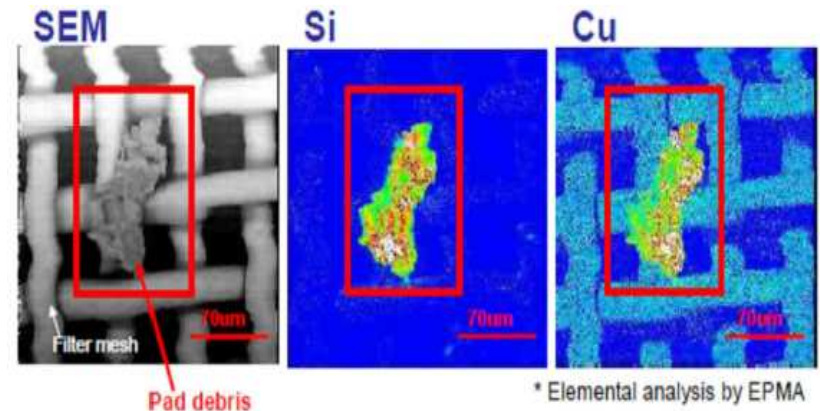
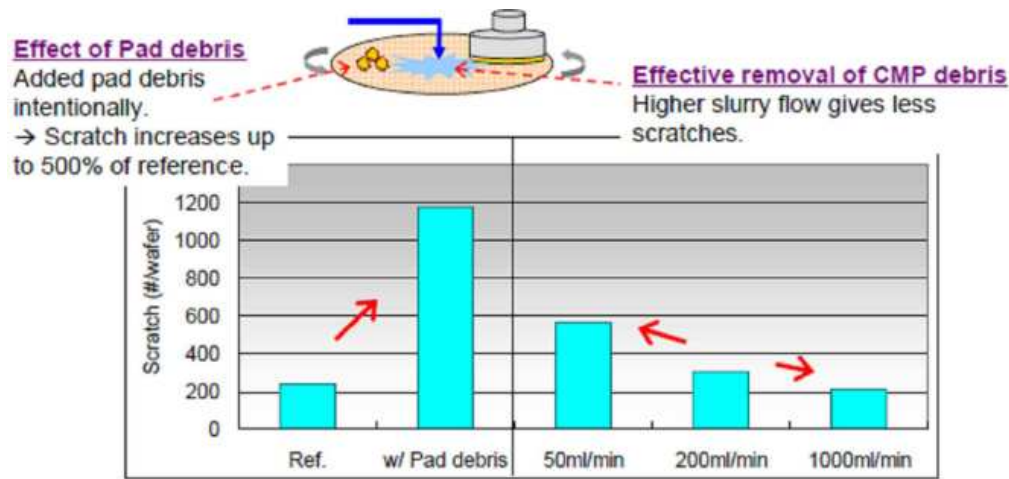
1. Increase yield by reducing wafer-level defects
2. Reduce slurry consumption (and associated waste) by 25 – 50 %
3. Increase pad life by more effectively removing conditioner-induced pad debris during polishing



Approach

- **Define and Implement a systematic characterization method for quantifying pad debris generated as a result of conditioning on the pad surface.**
- **Quantify the extent of pad debris generated during pad conditioning using different industry-standard pads and conditioning discs.**
- **Select a pad and a disc combination based on the above study. Perform polishing studies to determine whether extent of pad debris generation during polishing is correlated to wafer-level defects.**
- **Determine whether a novel slurry injection method (that also requires 2X less slurry) is effective in preventing pad debris from entering the pad-wafer interface.**
- **Determine whether the above novel injection method also reduces wafer-level defects.**

Effect of Pad Debris on Wafer-Level Defects



- ✓ Pad debris exhibits apparent effect on scratch generation.
- ✓ Scratch count decreases with higher slurry flow. Efficient debris removal would be one of the factors of scratch reduction.

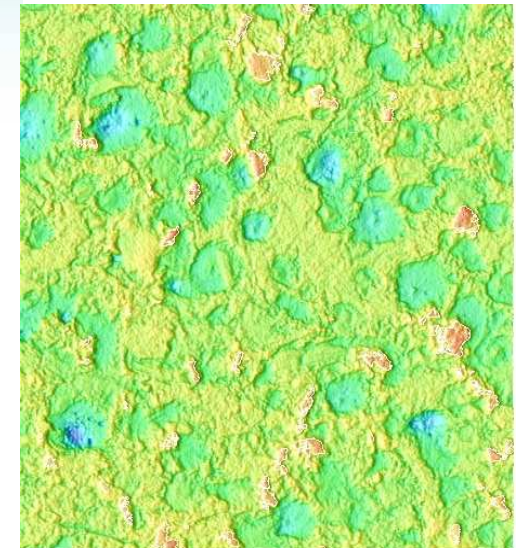
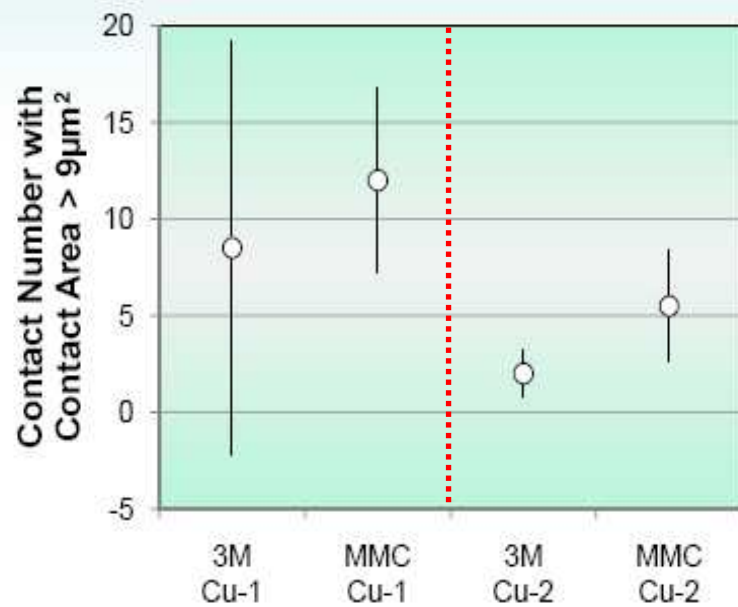
Elemental analysis suggests adhesion of silica particle and Cu-complex on the pad debris.

Source: JSR Corporation (2008)

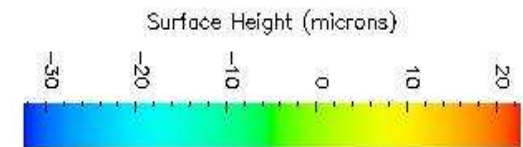
- Pad debris have been shown to be sources of scratch defects during CMP
- JSR's proposed solution is to reduce pad debris by increasing slurry flow rate by 5X
- This goes against EHS and COO objectives

Confocal Microscopy Images of Pad Debris

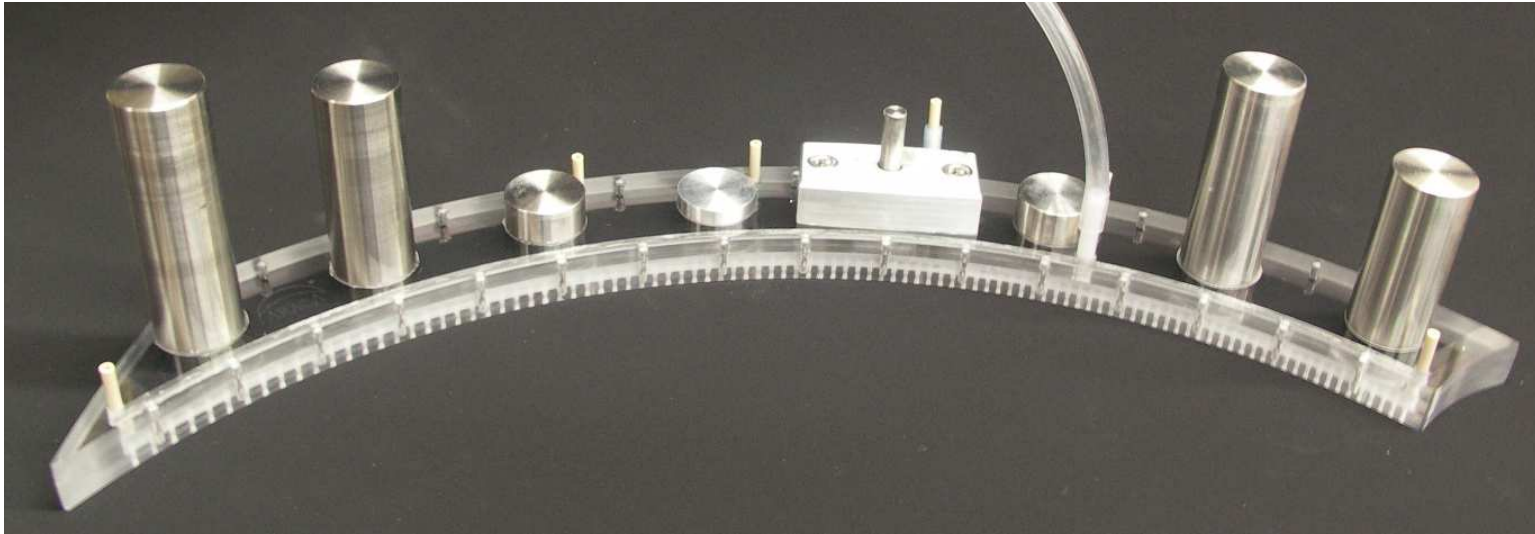
Based on an earlier joint study by UA and Tohoku University



- MMC disc generates more pad debris than 3M disc.
- We believe that pad debris is the source of defects during CMP.
- Cu - 2 process generates less pad debris than Cu - 1.

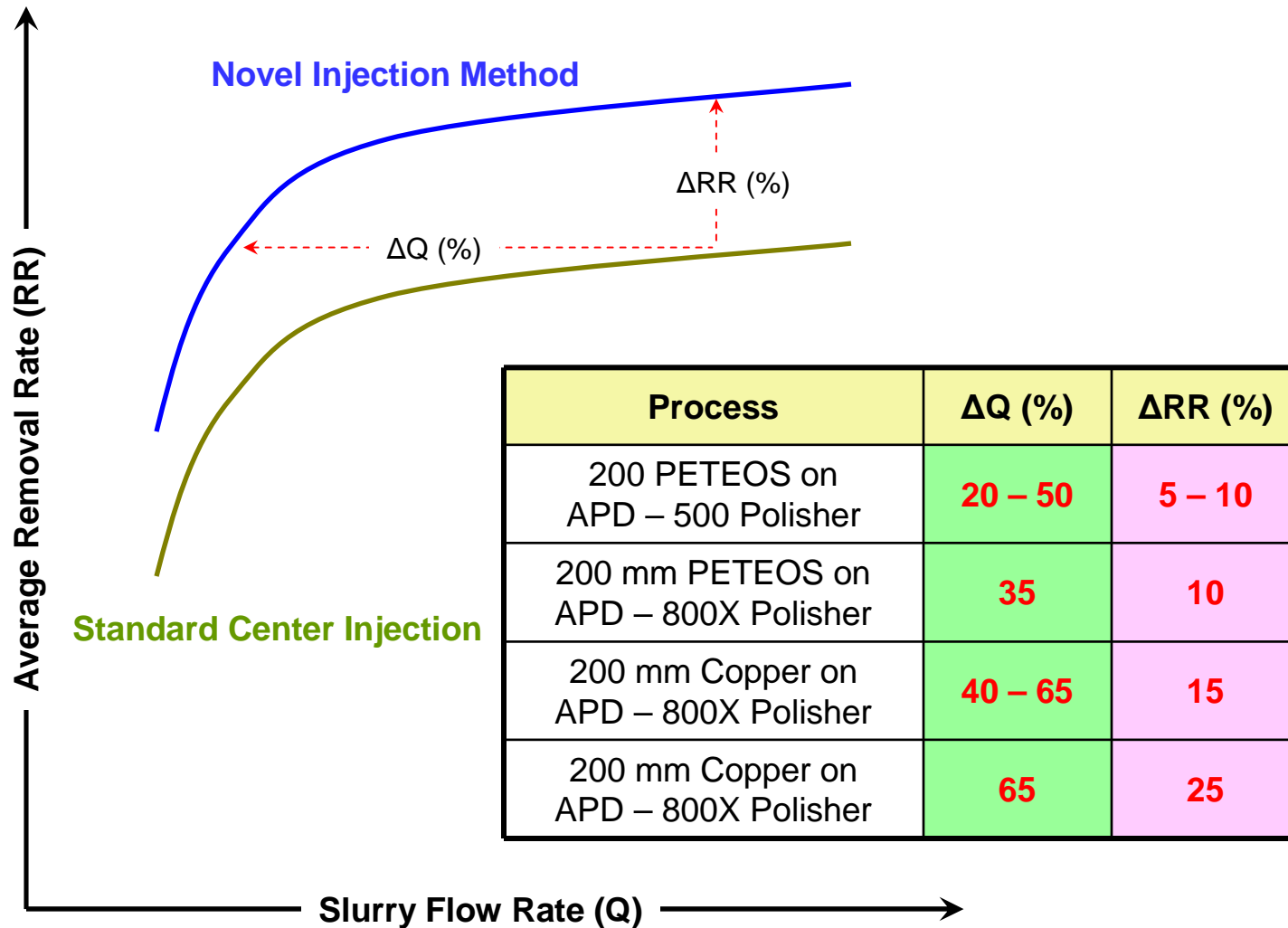


Novel Slurry Injection System



SRC/SEMATECH Engineering Research Center for Environmentally Benign Semiconductor Manufacturing

RR vs. Flow Rate Data Comparison



Benefits of Novel Slurry Injection System

- **Fresh slurry is applied exactly where it is needed**
- **The application method minimizes fresh slurry loss from the wafer or the retaining ring bow wave**
- **The device minimizes mixing of rinse water and used slurry with fresh slurry**
- **Preliminary results show that wafer-level defects are reduced**
- **The device can partially block foamed slurry from getting in the pad-wafer interface during polishing**
- **The design reduces slurry residue build-up on the pad**

It is not clear if the injection method will also be effective in preventing pad debris from getting into the pad-wafer interface during polishing – This study aims to address this matter

Novel Slurry Injection System

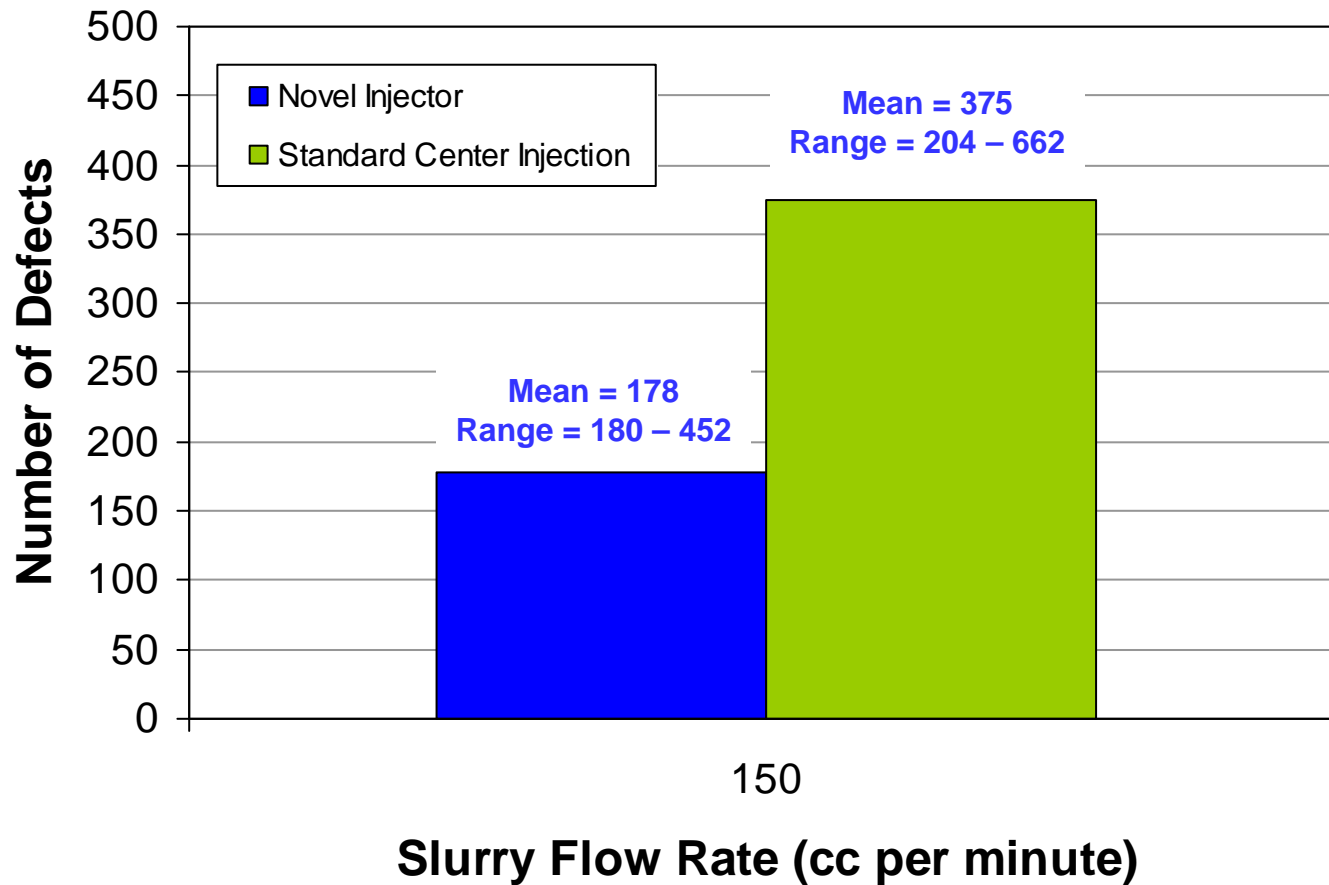
Removing Slurry Foam



- **Slurry foam is formed throughout polishing process**
- **Slurry foam is a major issue in IC manufacturing since most fabs are forced to change polishing parameters to suppress foam formation**
- **Novel slurry injection system can effectively screen out the foam from entering the polishing region without modifying polishing parameters**

Wafer-Level Defects Comparison

200 mm COPPER
on APD – 800X Polisher
(SP1 defects > 250 nm at 5 mm EE)



Industrial Interactions and Technology Transfer

Industrial mentors and contacts:

- **Leonard Borucki (Araca Incorporated)**
- **Tadahiro Ohmi (New Industry Creation Hatchery Center, Tohoku University)**

Plans (Only 1 Year Project)

- **Define and Implement a systematic characterization method for quantifying conditioner-induced pad debris.**
- **Quantify the extent of conditioner-induced pad debris using different industry-standard pads and conditioning discs.**
- **Select a pad and a disc combination based on the above study and perform polishing studies to determine whether pad debris generation correlates to wafer-level defects.**
- **Determine whether a novel slurry injection method (that also requires 2X less slurry) is effective in preventing pad debris from entering the pad-wafer interface.**
- **Determine whether the above novel injection method also reduces wafer-level defects.**

Retaining Ring Induced Frictional Pad Heating and its Effect on Pad Wear

PIs:

- Ara Philipossian, Chemical and Environmental Engineering, UA

Graduate Students:

- Zhenxing Han, Ph. D. student, Chemical and Environmental Engineering, UA
- Yubo Jiao, Ph. D. student, Chemical and Environmental Engineering, UA
- Xiaoyan Liao, Ph. D. student, Chemical and Environmental Engineering, UA

Other Researchers:

- Yasa Sampurno, Research Associate, Chemical and Environmental Engineering, UA
- Yun Zhuang, Research Associate, Chemical and Environmental Engineering, UA

Retaining Ring Induced Frictional Pad Heating and its Effect on Pad Wear

Cost Share (other than core ERC funding):

- **In-kind donation (retaining rings) from Entegris**
- **In-kind donation (slurry) from Fujimi**
- **In-kind donation (conditioner disc) from Shinhan**
- **In-kind donation (conditioner disc) from 3M**
- **In-kind donation (polishing pad) from Dow**
- **In-kind donation (polishing pad) from Cabot Microelectronics**
- **In-kind donation (wafer) from Intel**
- **In-kind support from Araca**

Objectives

- **Quantify the effect retaining ring materials, diamond disc conditioners, polishing pads and process conditions (i.e. pad temperature and polishing time) on pad cut rate and pad wear profile**
- **Determine whether or not temperature and/or time effects are the full explanation for pad wear profile differences in different processes**

ESH Metrics and Impact

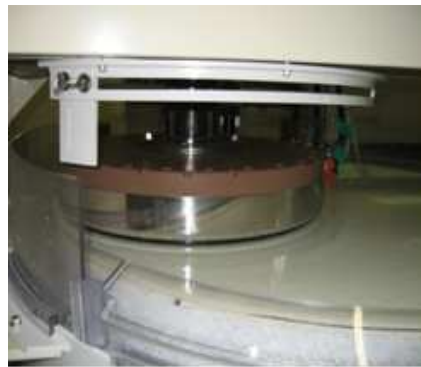
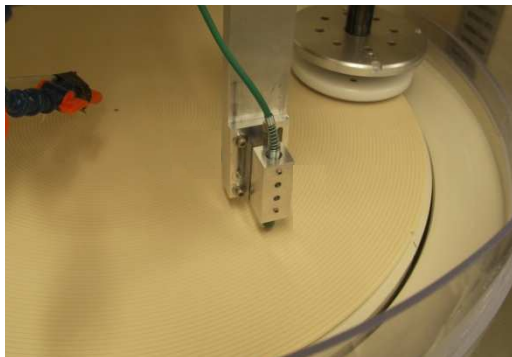
1. *Reduce slurry consumption by 15 %.*
2. *Reduce energy consumption by 15 %.*
3. *Increase pad life by 20 %.*

Approach

Our approach for this 2 – year program (6/2008 to 5/2010) is as follows:

- **Modify and integrate a previously built in-situ offline pad cut rate measurement device for UA's 300 mm polisher**
- **Measure pad wear at three platen temperatures for two different pads, two retaining ring materials and two retaining ring design using a 300 mm polisher equipped with platen heating/cooling**
 - **CMC D100 and Dow IC1000 pads**
 - **PEEK1, PEEK2 and PPS2 retaining rings**
 - **Platen temperature maintained at 15, 25 and 50 °C (Note: pad temperature is in between platen and room temperature)**
- **Use micrometry to verify pad cut rate (PCR) measurements obtained from the in-situ device**

Equipment for 300-mm Polisher



Pad cut rate measurement device (top) ... Neslab heater & chiller (center) ... Araca APD – 800 platen heating and cooling interface hardware (bottom)

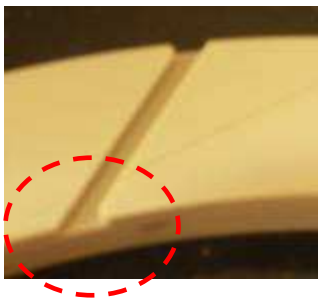
APD – 800 (300-mm polisher with automatic platen heating and cooling, 10-zone conditioner and in-situ frictional and pad temperature sensor)

Retaining Ring Materials and Slot Designs

PEEK



Design 1



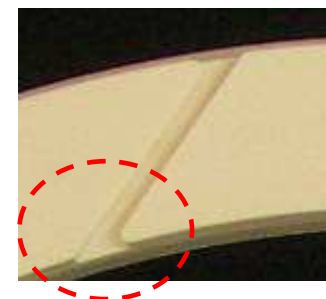
Design 2



PPS



Design 1



Retaining Ring Adaptor



Adaptor



Adaptor with the retaining ring installed



Overall setup on the APD – 800 carrier head

Retaining ring adaptor (courtesy of Araca and Entegris) has been successfully implemented. The adaptor enables the use of 300 mm industry standard retaining ring (i.e. for the AMAT Reflexion polisher) on APD – 800 300 mm polisher

Pad Cut Rate at Platen Temperature 25 °C

From Pad Cut Rate Measurement Device

Ring – Pad	Local Pad Cut Rate* (μ m/hr)				Average Local Pad Cut Rate (μ m/hr)
	0 – 2 hr	2 – 4 hr	4 – 6 hr	6 – 8 hr	
PPS1 – IC1000	14.7	12.1	10.0	-	12.2
PEEK1 – IC1000	36.6	19.4	20.5	-	25.5
PEEK2 – IC1000	N/A	N/A	19.9	25.6	22.8
PPS1 – D100	17.5	12.1	4.7	-	11.4
PEEK1 – D100	17.0	16.6	7.1	-	13.5
PEEK2 – D100	23.9	13.7	10.3	-	16.0

*** Measured by the pad cut rate measurement device at R = 12.25 every 2 hours.**

SRC/SEMATECH Engineering Research Center for Environmentally Benign Semiconductor Manufacturing

Pad Cut Rate at Platen Temperature 50 °C

From Pad Cut Rate Measurement Device

Ring – Pad	Local Pad Cut Rate* (μm/hr)			Average Local Pad Cut Rate (μm/hr)
	0 – 2 hr	2 – 4 hr	4 – 6 hr	
PEEK1 – IC1000	33.7	13.0	4.4	17.0
PPS1 – IC1000	32.9	27.9	21.3	27.4
PPS1 – IC1000 (Repeat Run)	22.3	27.9	10.8**	21.8
PEEK1 – D100	5.3	7.9	6.4	6.5
PPS1 – D100	< 4.0***	< 4.0***	< 4.0***	< 4.0

* Measured by the pad cut rate measurement device at R = 12.25” every 2 hours.

** Measured between 4 and 5.2 hours.

*** Within experimental error.

Pad Cut Rate Comparison

Platen Temperature at 25 and 50 °C

Ring – Pad	Local pad cut rate from pad cut rate measurement device (µm/hr)		Local pad cut rate from micrometry (µm/hr)		Global pad cut rate from micrometry (µm/hr)	
	25 °C	50 °C	25 °C	50 °C	25 °C	50 °C
PEEK1 – IC1000	25.5	17.0	29.6	23.8	27.5	20.3
PPS1 – IC1000	12.2	27.4	17.5	33.2	16.5	29.4
PPS1 – IC1000 (Repeat Run)	12.2	21.8	17.5	27.4	16.5	23.5
PEEK1 – D100	13.5	6.5	17.6	7.0	16.4	6.1
PPS1 – D100	11.4	< 4.0*	8.8	5.3	7.8	5.1

*** Within experimental error**

The pad surface contained moisture when the pad cut rate device was used to measure local pad thickness during the wear tests. The pad was dry when a micrometer was used to measure local pad thickness after the wear tests. This contributed to different local pad cut rate measurements obtained by the pad cut rate measurement device and micrometer.

[SRC/SEMATECH Engineering Research Center for Environmentally Benign Semiconductor Manufacturing](#)

Summary of Year – 1 Results

Platen Temperature 25 °C

- For both IC1000 and D100, global PCRs of PEEK1 and PEEK2 were **significantly higher** (by appx. 62 – 110 percent) than those of PPS1
- For both IC1000 and D100, global PCRs for the PEEK1 and PEEK2 were **similar**, indicating that the slot curvature design did not impact PCR
- For both PEEK1 and PPS1, global PCR for IC1000 was **significantly higher** (by appx. 68 – 112 percent) than D100
- PCR changed as a function of polishing time (possibly due to changes in pad properties in the ‘z’ direction)

Summary of Year – 1 Results

Platen Temperature 50 °C

- For IC1000, global PCR of PEEK1 was lower than that of PPS1 by 30 percent
- For D100, the trend was opposite: The global PCR of PEEK1 was **higher** than that of PPS1 by 16 percent
- For both PEEK1 and PPS1, global PCR for IC1000 was **significantly higher** than D100 (by appx. 233 to 476 percent)
- PCR changed as a function of polishing time (possibly due to changes in pad properties in the 'z' direction)

Summary of Year – 1 Results

Comparison of Platen Temperature at 25 and 50 °C

- For both IC1000 and D100, global PCR for PEEK1 at 50 °C was **significantly lower** than that at 25 °C (by appx. 35 – 169 percent)
- This was expected because both pads became softer at platen temperature of 50 °C
- For D100, global PCR for PPS1 at 50 °C was also **significantly lower** than that at 25 °C (by appx. 53 percent)
- However, for IC1000, the trend was reversed: Global PCR for PPS1 at 50 °C was **significantly higher** than that at 25 °C (by appx. 38 percent on average)

Industrial Interactions and Technology Transfer

Industrial mentors and contacts:

- **Don Hooper (Intel)**
- **Mansour Moinpour (Intel)**
- **Jason Zanotti (Intel)**
- **Cliff Spiro (Cabot Microelectronics)**

Future Plans

Next Year Plan

- Complete PCR tests on Dow IC1000 and CMC D100 pads using PPS1 and PEEK1 retaining rings at a platen temperature of 15 °C

Long-Term Plan

- Develop new (or augment existing) theories to explain the results

Investigation of the Relationship between Planarization and Pad Surface Micro- Topography

PIs:

- Ara Philipossian, Chemical and Environmental Engineering, UA

Graduate Students:

- Yubo Jiao, Ph. D. candidate, Chemical and Environmental Engineering, UA
- Zhenxing Han, Ph. D. student, Chemical and Environmental Engineering, UA
- Anand Meled, Ph. D. student, Chemical and Environmental Engineering, UA
- Xiaoyan Liao, Ph. D. student, Chemical and Environmental Engineering, UA

Other Researchers:

- Yasa Sampurno, Research Associate, Chemical and Environmental Engineering, UA
- Yun Zhuang, Research Associate, Chemical and Environmental Engineering, UA

Investigation of the Relationship between Planarization and Pad Surface Micro- Topography

Cost Share (other than core ERC funding):

- In-kind donation (conditioner disc) from Ehwa
- In-kind donation (conditioner disc) from Shinhan Diamond Industrial Co., Ltd.
- In-kind donation (conditioner disc) from 3M Company
- In-kind donation (polishing pad) from Rohm and Haas Company
- In-kind donation (polishing pad and slurry) from Cabot Microelectronic Corporation
- In-kind donation (wafer) from Intel Corporation
- In-kind support from Araca, Inc.

Objectives

- **Gain a deeper understanding and control of factors related to pad topography that affect planarization**
- **Prove that contact area can predict planarization behavior**

ESH Metrics and Impact

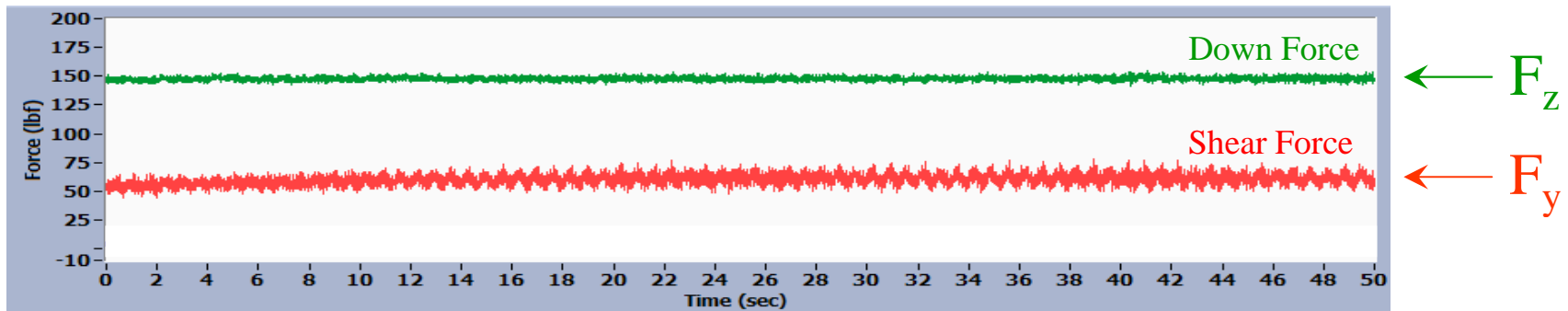
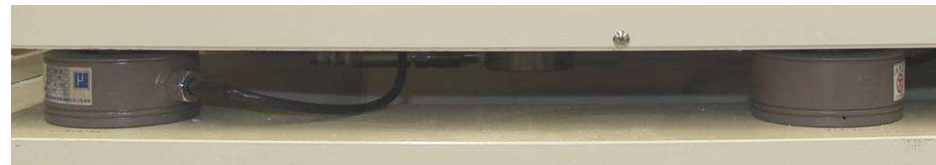
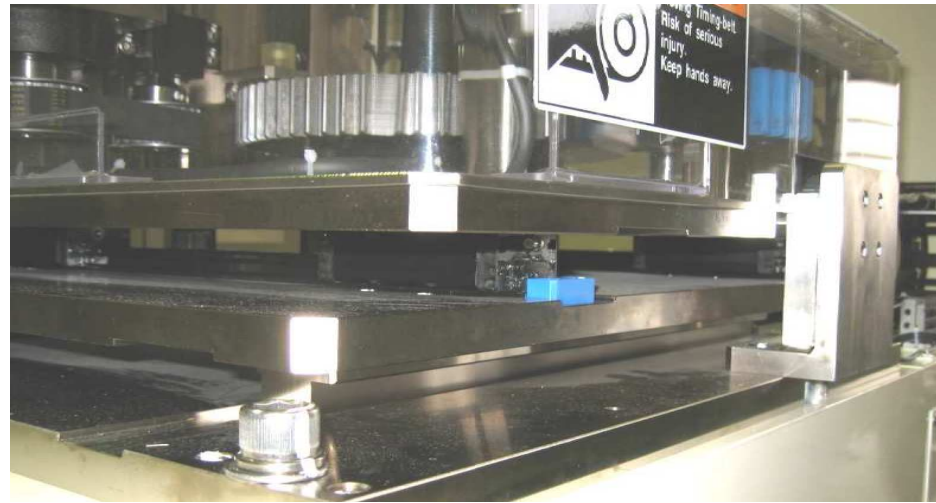
1. *Reduce slurry consumption by 30 %.*
2. *Reduce energy consumption by 20 %.*
3. *Increase pad life by 30 %.*

Approach

Our approach for this 3 – year program (6/2008 to 5/2011) is as follows:

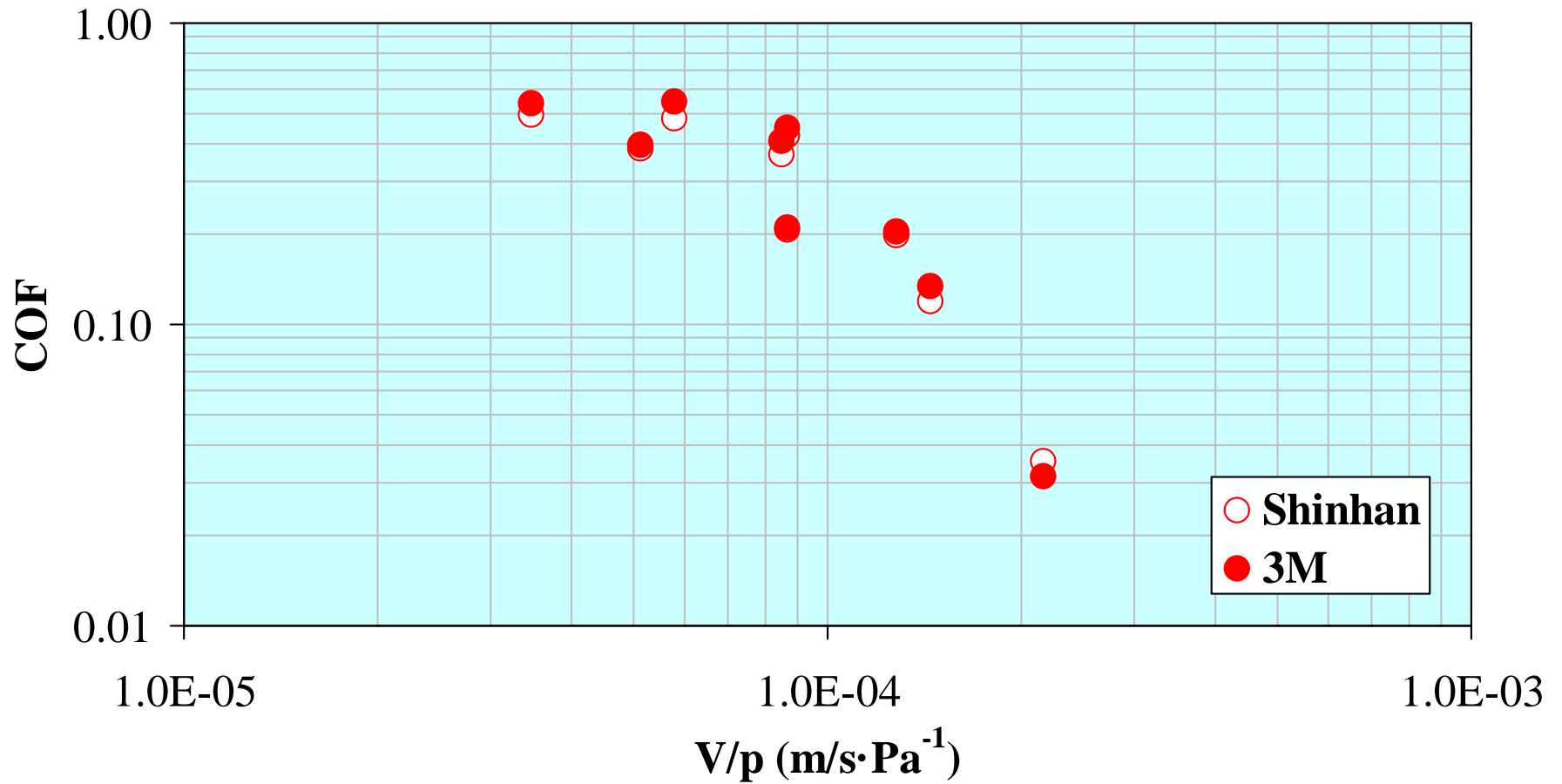
- Polish 300-mm wafers using a variety of conditions and consumables (i.e. pads with different hardness and porosity and diamonds with different levels of aggressiveness) known or expected to improve or degrade planarization efficiency
- Examine pad samples under static loading (at CMP-relevant pressures) using flat, and possibly patterned, sapphire windows (patterned windows would replicate the contact conditions on patterned wafers and would make it feasible to actually see which pad features affect planarization)
- Correlate planarization behavior with contact area characteristics
- Tie observational data together with rough surface contact and removal rate models

APD – 800 Polisher and Tribometer



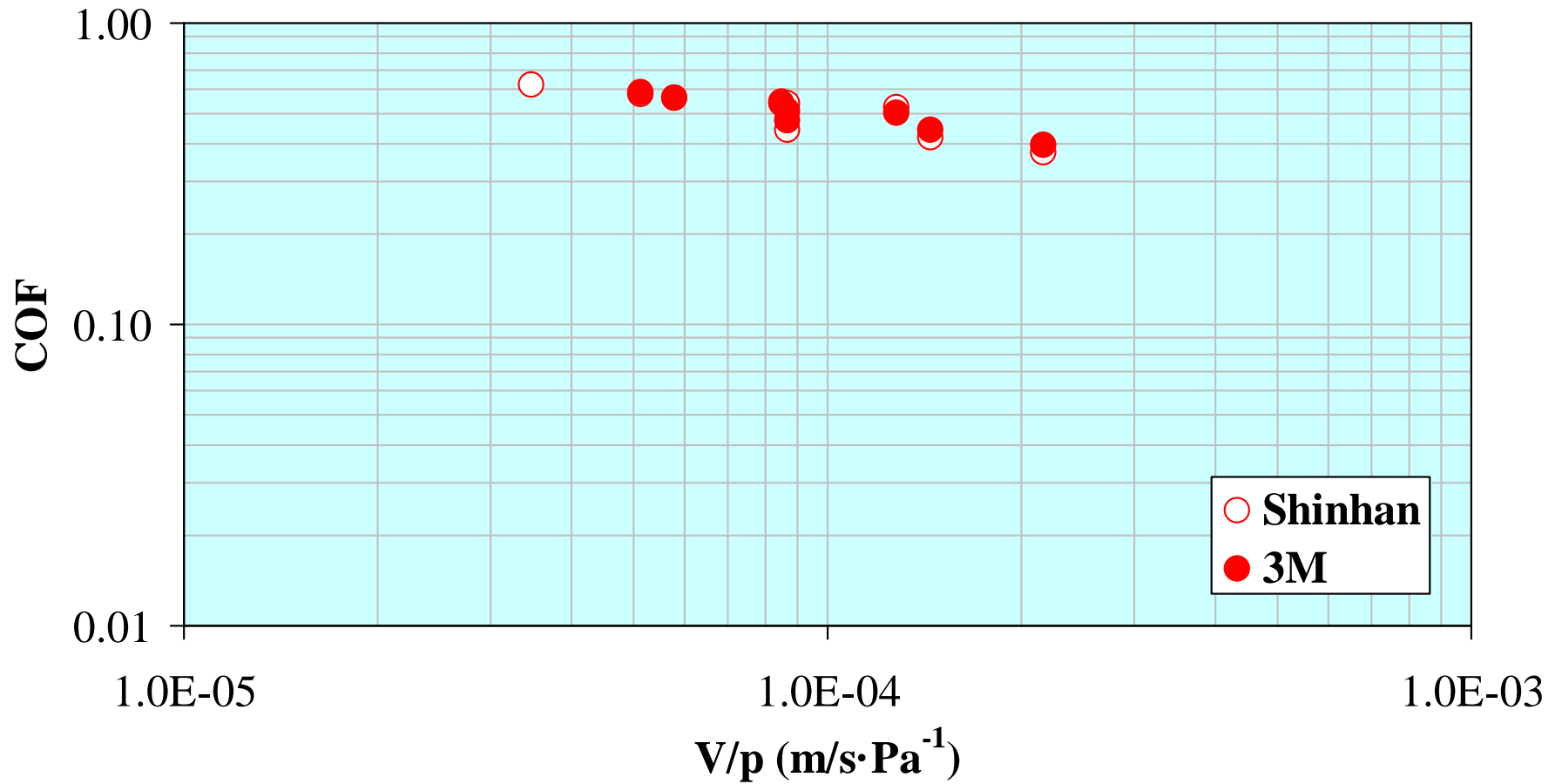
COF vs. V/p

IC1000



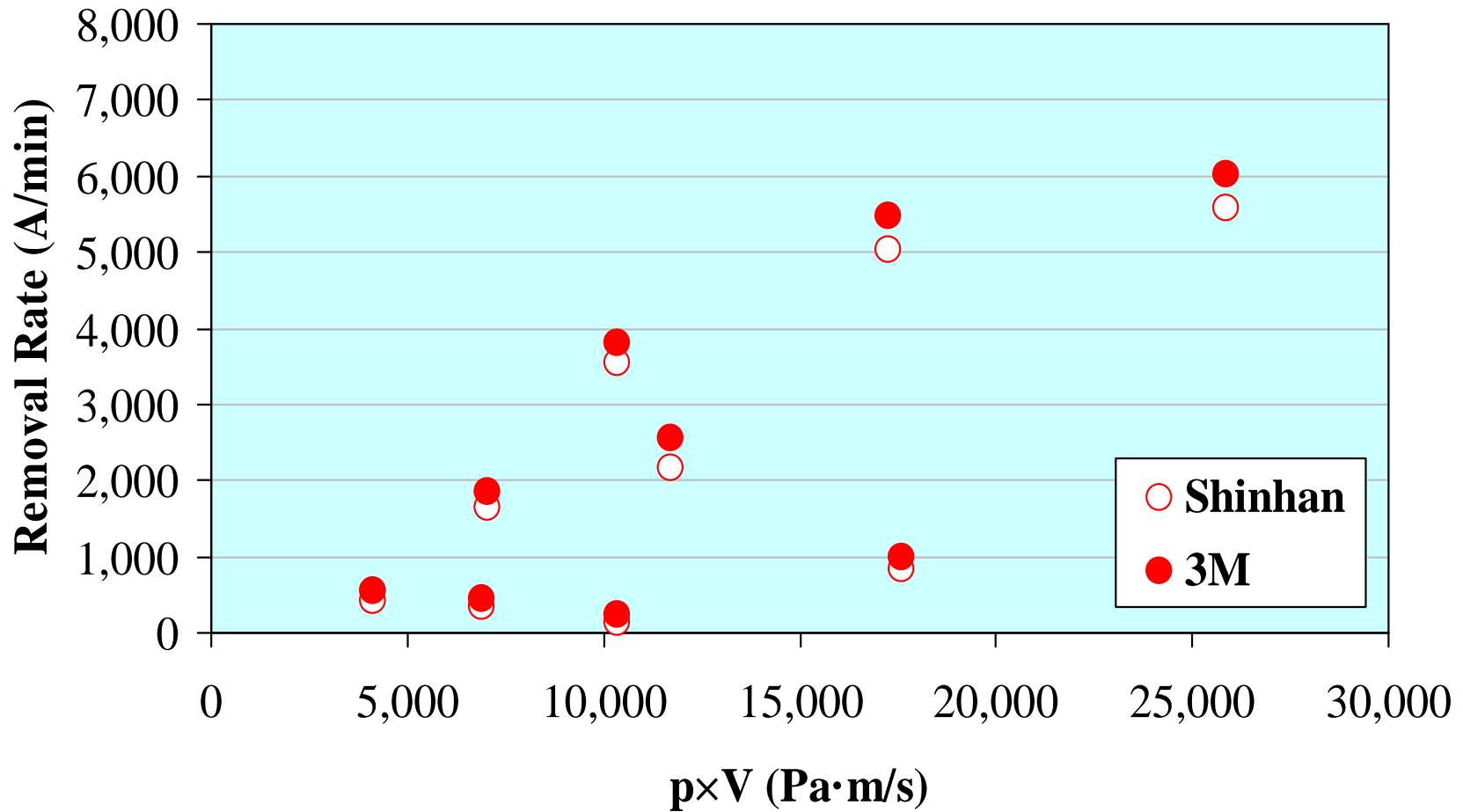
COF vs. V/p

D100



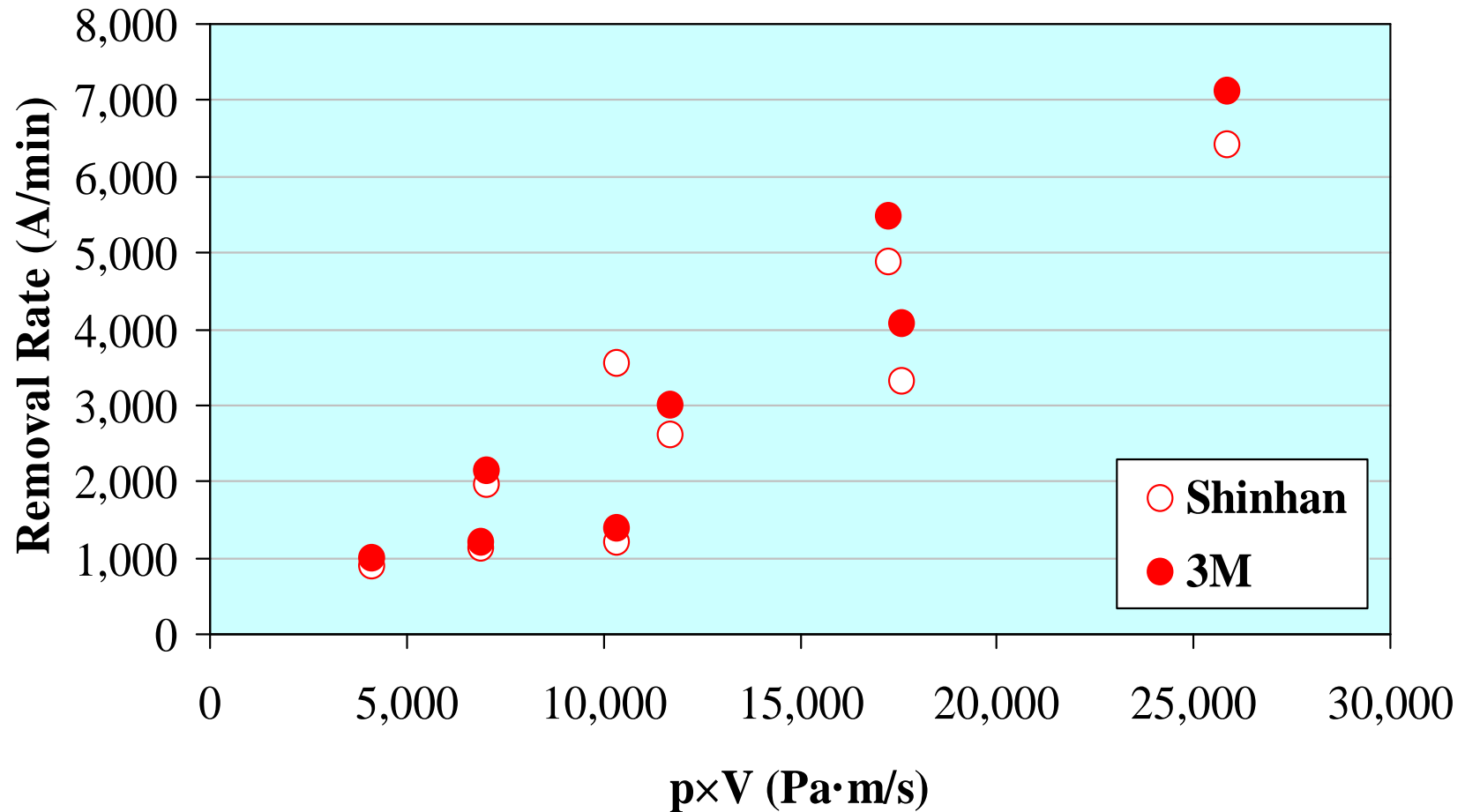
Removal Rate vs. $p \times V$

IC1000



Removal Rate vs. $p \times V$

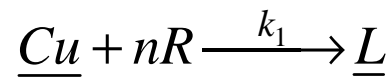
D100



2-Step Removal Rate Model

- Modified Langmuir-Hinshelwood model:

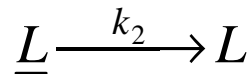
- n moles of reactant R in the slurry react at rate k_1 with copper film on the wafer to form a product layer L on the surface



$$k_1 = A \times \exp(-E_a / kT)$$

$$T = T_p + \frac{\beta}{V^{0.5+e}} \times COF \times p \times V$$

- Product layer \underline{L} is subsequently removed by mechanical abrasion with rate k_2



$$k_2 = C_p \times COF \times p \times V$$

- Abraded material L is carried away by the slurry

- The removal rate in this sequential mechanism therefore is a function of both thermal and mechanical attributes of the process

$$R R = \frac{M_w}{\rho} \frac{k_1 k_2}{k_1 + k_2}$$

Fitting Parameters

E_a	Activation Energy (eV)
A	Pre-exponential factor of chemical rate constant (mole \times m⁻² s⁻¹)
C_p	Proportionality constant of mechanical rate constant (mole/J)
e	Exponential factor of sliding velocity derived from pad heat partition fraction
β	A constant that depend on wafer size, tool geometry and properties of pad surface and bulk material (10⁻³ K/Pa(m/s)^{0.5-e})

Summary of Optimized Parameters

Based on Two Level Optimization Process

Fitting Parameters	IC1000 Shinhan	IC1000 3M	D100 Shinhan	D100 3M
E_a (eV)	1.267	1.267	1.267	1.267
A (10^{17} mole \times m ⁻² s ⁻¹)	7.734	7.734	7.734	7.734
C_p (10^{-7} mole/J)	1.640	1.536	1.550	1.667
e	1.562	1.901	1.006	0.740
β (10^{-3} K/Pa(m/s) ^{0.5-e})	1.967	2.133	1.143	1.176
RMS (A/min)	145	176	84	74

Summary of k_1/k_2

Pressure (PSI)	Velocity (m/s)	k_1/k_2			
		IC1000 Shinhan	IC1000 3M	D100 Shinhan	D100 3M
1.0	0.6	3.6	5.2	2.2	2.1
1.7	0.6	8.0	17.6	3.0	2.8
2.5	0.6	41.3	206.1	5.7	NA
1.0	1.0	2.3	2.5	1.3	1.5
1.7	1.0	2.4	3.4	1.7	2.1
2.5	1.0	7.0	14.5	2.9	3.7
1.0	1.5	3.6	4.7	1.0	1.1
1.7	1.5	1.1	1.2	1.3	1.8
2.5	1.5	2.7	3.6	2.3	3.3

Summary of Year – 1 Results

- **RR results for all combinations of 2 pads and 2 discs showed gross non-Prestonian behavior**
- **Compared to D100, the IC1000 pad exhibited a much faster transition from boundary lubrication to partial lubrication mode**
- **The 2-step Langmuir-Hinshelwood model successfully simulated the non-Prestonian RR results thus indicating that the observed scatter could be fully explained theoretically**
- **Wilcoxon Signed Rank test of simulation results showed that:**
 - **D100 exhibited a more chemically-controlled process (CCP) than IC1000**
 - **Shinhan exhibited a more CCP than 3M**

Industrial Interactions and Technology Transfer

Industrial mentors / contacts:

- **Don Hooper (Intel Corporation)**
- **Mansour Moinpour (Intel Corporation)**
- **Cliff Spiro (Cabot Microelectronic Corporation)**
- **Peter Ojerholm (Ehwa)**

Future Plans

Next Year Plans

- Repeat all of the tests (i.e. effect of pad and process conditions) and simulations performed in Year – 1 with the Ehwa disc
- Identify optimum polishing conditions and run 300 mm patterned wafers for pad analysis
- Examine pad samples under static loading using a flat sapphire window to determine wafer-level topography, pad-wafer contact and near-contact area, pad asperity shape and density and number of large pad debris

Future Plans

Long-Term Plans

- **Examine limited number of pad samples under static loading using a patterned sapphire window to better mimic the contact phenomena that the pad actually sees during patterned wafer polishing**
- **Determine contact area, pad asperity shape and density and number of large pad debris**
- **Correlate planarization behavior with contact area data**
- **Tie observational data together with rough surface contact and RR models**
- **Propose methodology for using confocal microscopy as part of a screening process or diagnostic technique for new consumables and processes**

Contamination Control in Gas Distribution Systems

Customized Project; Sponsored by Intel

PI:

- **Farhang Shadman, Ph.D., Professor of Chemical and Environmental Engineering, UA**

Co-PI:

- **Carl Geisert, Sr. Principal Engineer, Intel**

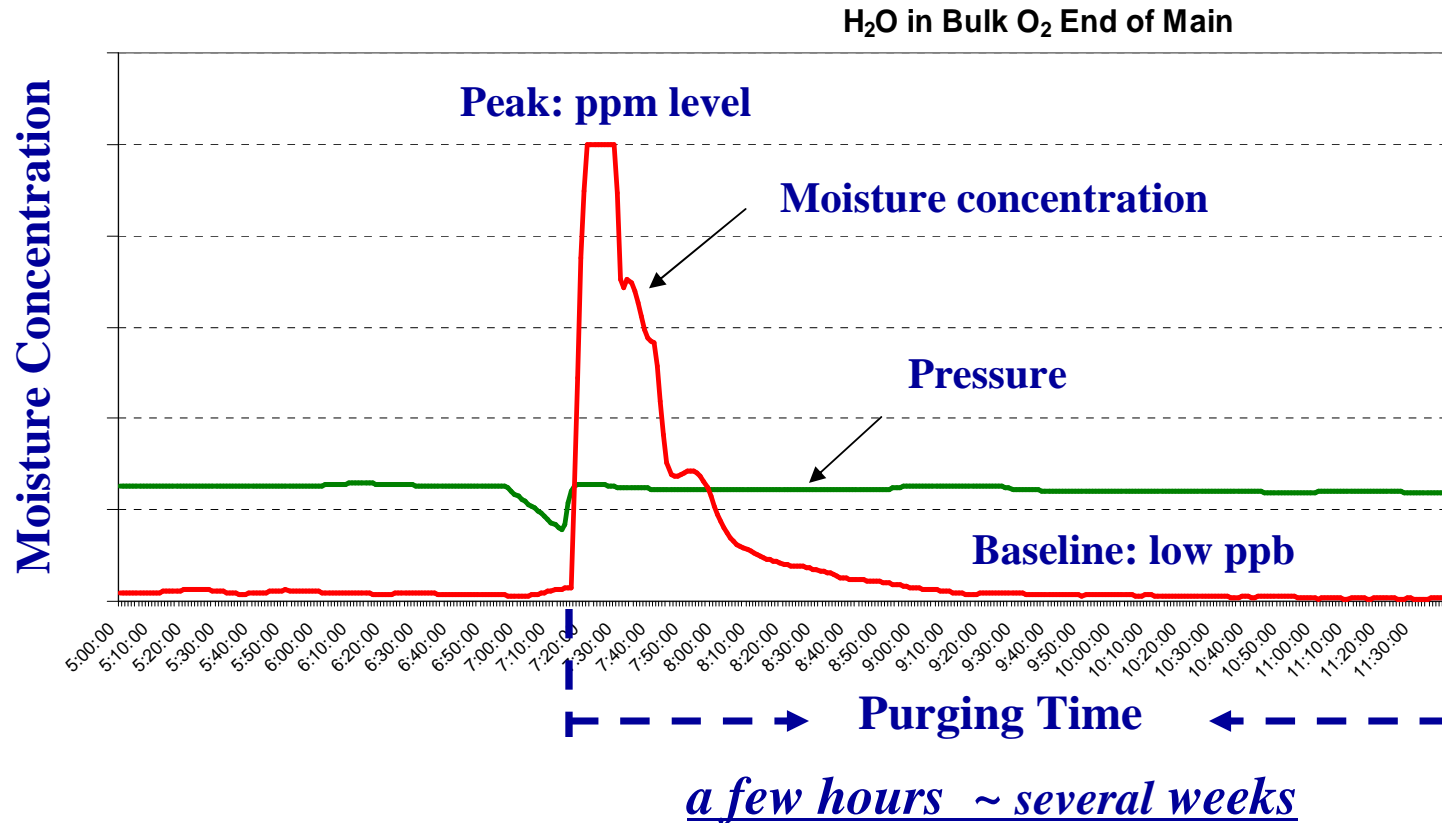
Research Engineer:

- **Junpin Yao: Ph.D., Postdoctoral, Chemical and Environ Eng, UA**

Graduate Students:

- **Hao Wang: Ph.D. student, Chemical and Environmental Engineering, UA**
- **Roy Dittler: Ph.D. student, Chemical and Environmental Engineering, UA**

Moisture Contamination & Dry-down



Fab closure due to contamination of the gas distribution system could result in revenue loss between \$5M and \$15 M/day

** Source: Intel*

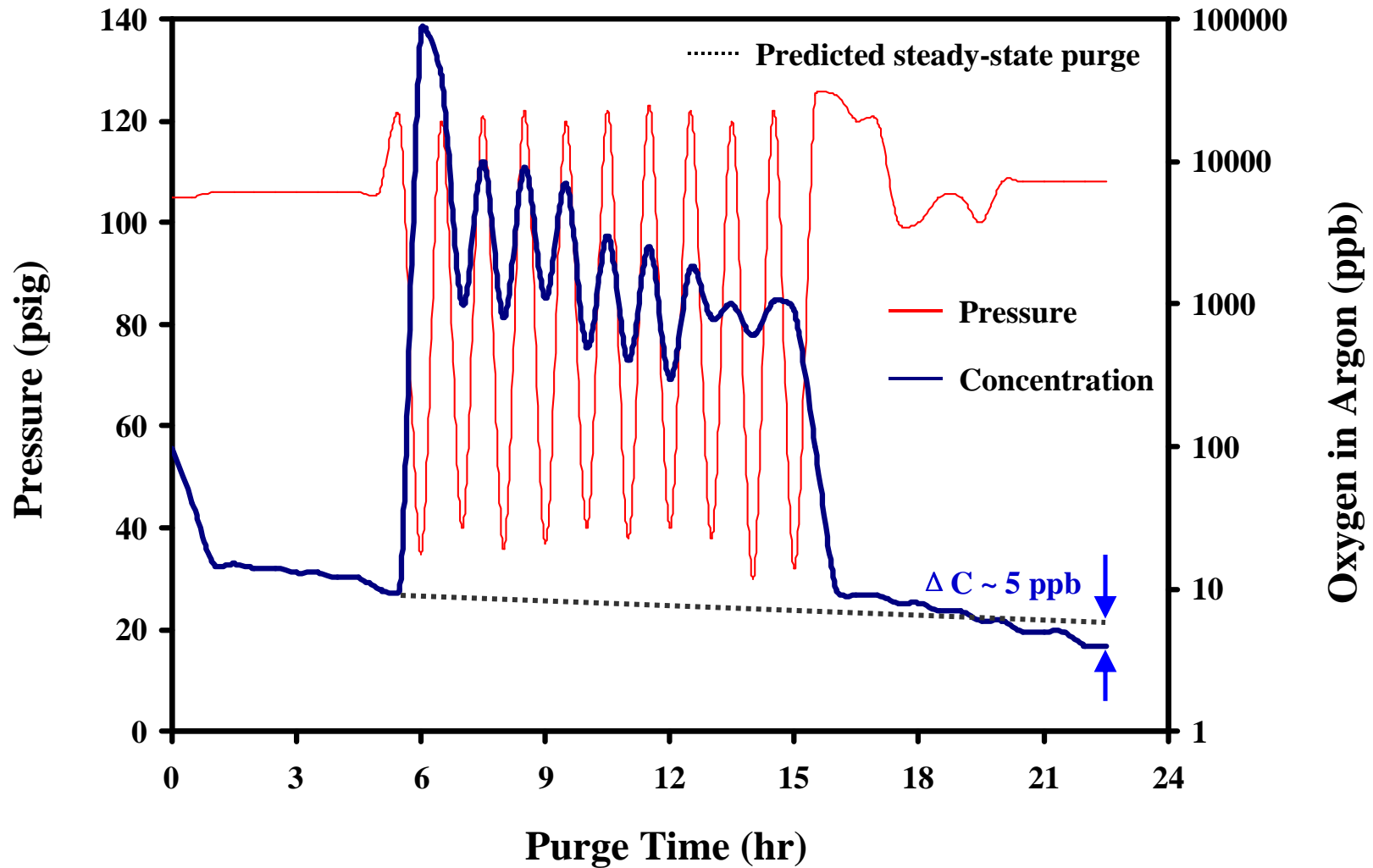
Objectives

- **Develop tools and techniques for analysis of contamination distribution and removal in ultra-pure gas distribution systems**
- **Develop and validate a user-friendly process simulator suitable for field application to minimize purge time and gas usage during system start up, system recovery, or during the operation of gas distribution systems.**
- **Develop a robust pressure-cyclic purge method as an alternate to conventional method**

ESH Impact

- **Significant reduction in the usage of resources (ultra-pure gas and energy) as well as reduction of down time during at start-up, recovery, or steady operation of the gas distribution systems**

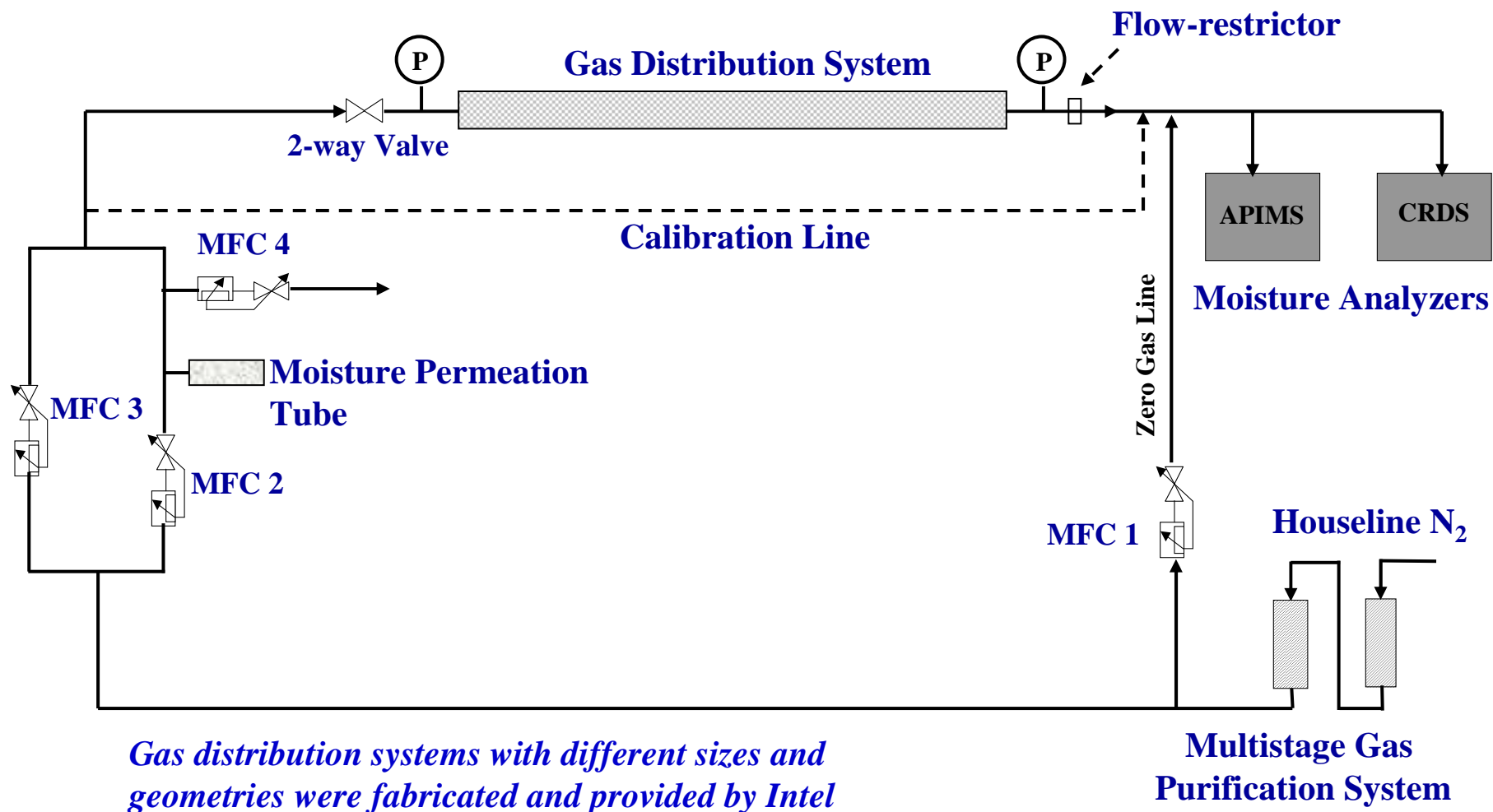
Impact of System Pressure



Cyclic purge may enhance the removal of contaminants

** Source: Intel*

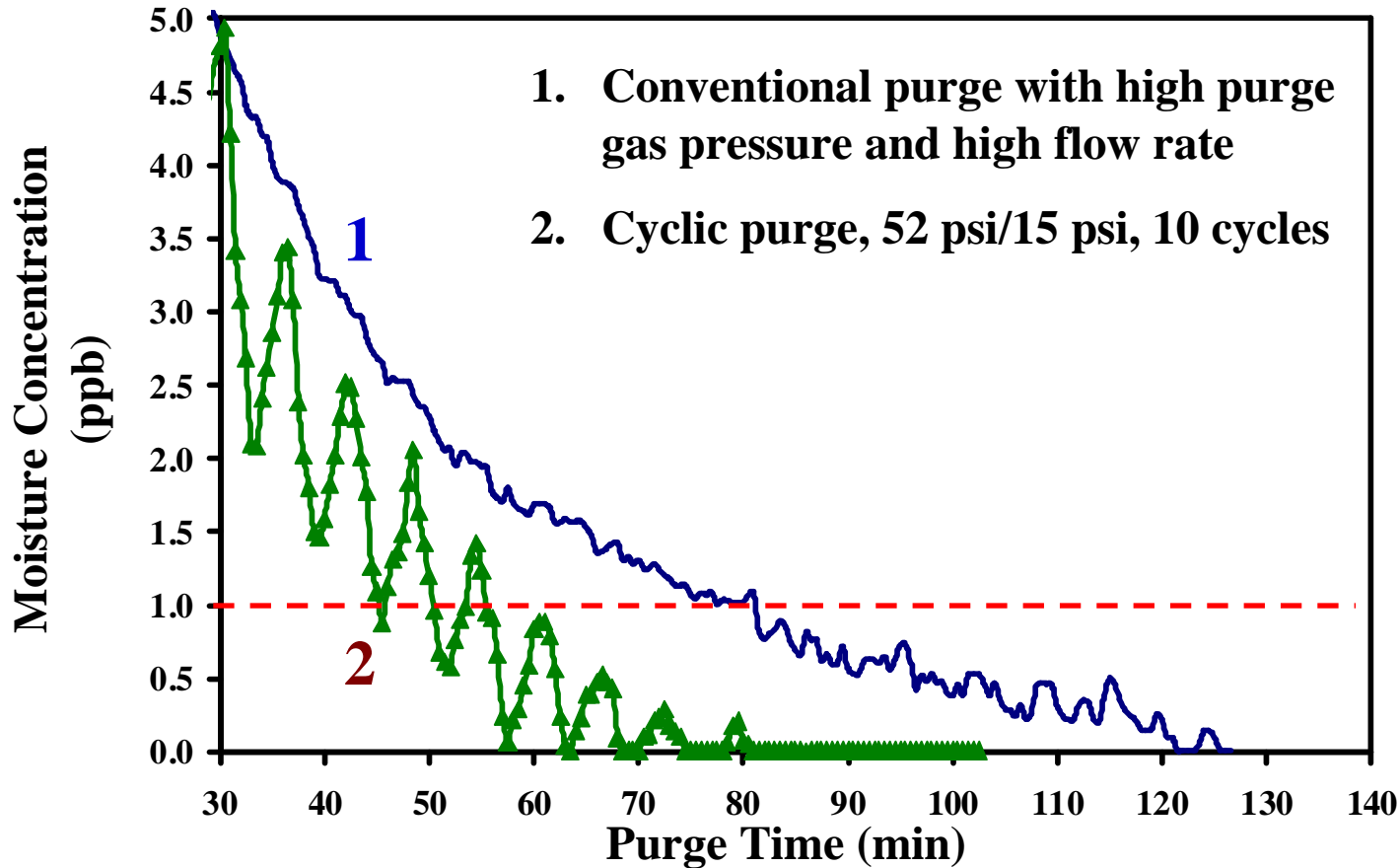
Experimental Set-up and Testbed



Cyclic Purge vs. Conventional Purge

Lab-scale system

EP SS pipe with 1.5 inch OD and 76 inch length. Initial conc. 90 ppb



To reach 1 ppb baseline: Cyclic purge save 32 minutes of purging time and 60 standard liter of purging gas

Process Model of Cyclic Purge

System Pressure:

$$\frac{\partial P}{\partial t} = -P \frac{\partial u}{\partial x} - u \frac{\partial P}{\partial x}$$

Velocity:

$$\frac{\partial u}{\partial t} = -\frac{RT}{PM} \frac{\partial P}{\partial x} - u \frac{\partial u}{\partial x}$$

Absorbed Moisture:

$$\frac{\partial C_s}{\partial t} = k_a C_g (S_0 - C_s) - k_d C_s$$

Gas Phase Moisture:

$$\frac{\partial C_g}{\partial t} = D_L \frac{\partial^2 C_g}{\partial x^2} + \frac{\partial D_L}{\partial x} \frac{\partial C_g}{\partial x} - u \frac{\partial C_g}{\partial x} - C_g \frac{\partial u}{\partial x} + \frac{4}{d} [(k_d C_s - k_a C_g (S_0 - C_s))]$$

C_s : moisture concentration on pipe wall, mol/cm²; C_g : moisture concentration in gas, mol/cm³;

k_{ads} : adsorption rate constant, cm³/mol/s; k_{des} : desorption rate constant, 1/s

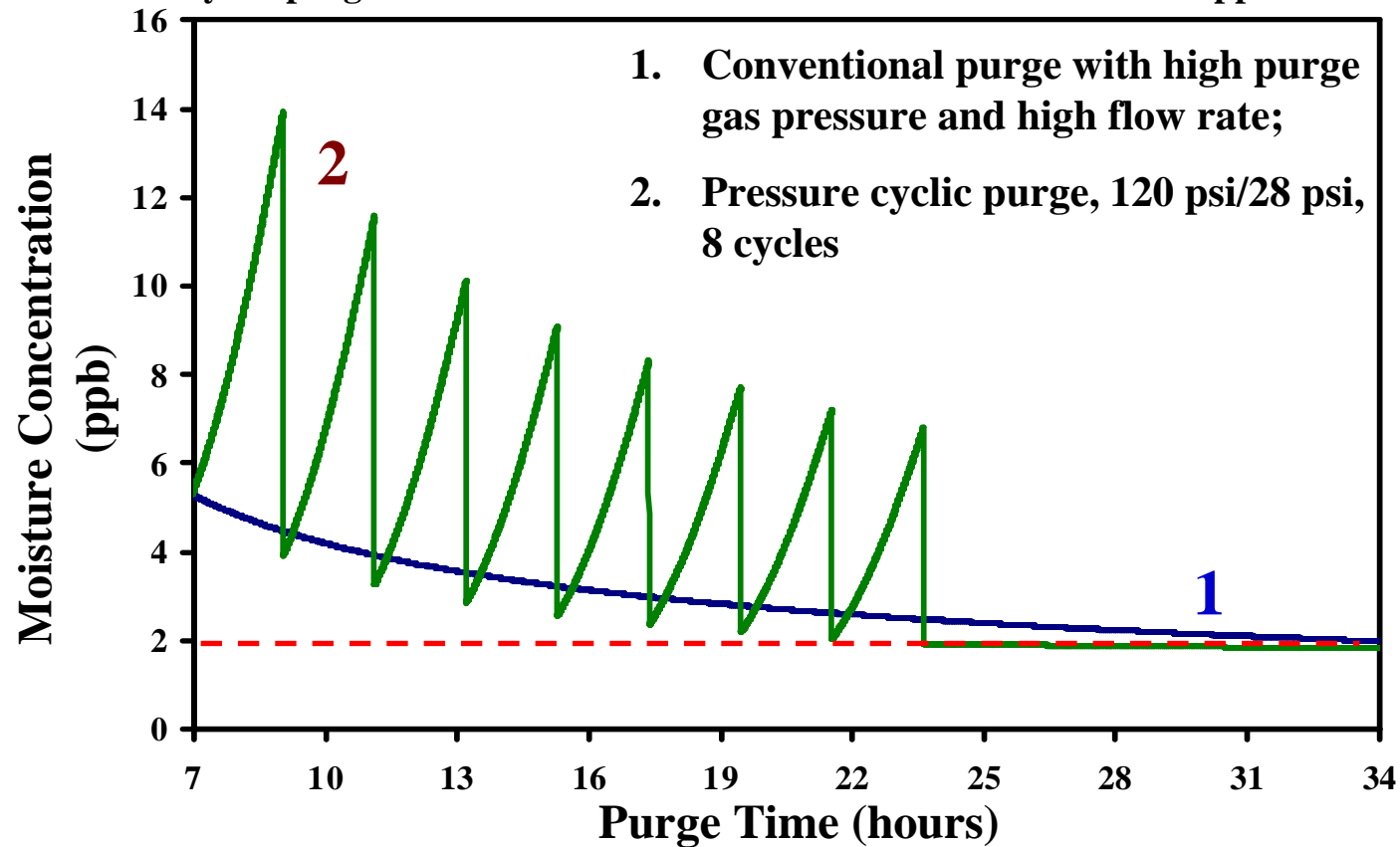
S_0 : site density of surface adsorption, mol/cm²; D_L : dispersion coefficient, cm²/s;

u : velocity, cm/s; d : diameter; P : pressure

Cyclic Purge vs. Conventional Purge

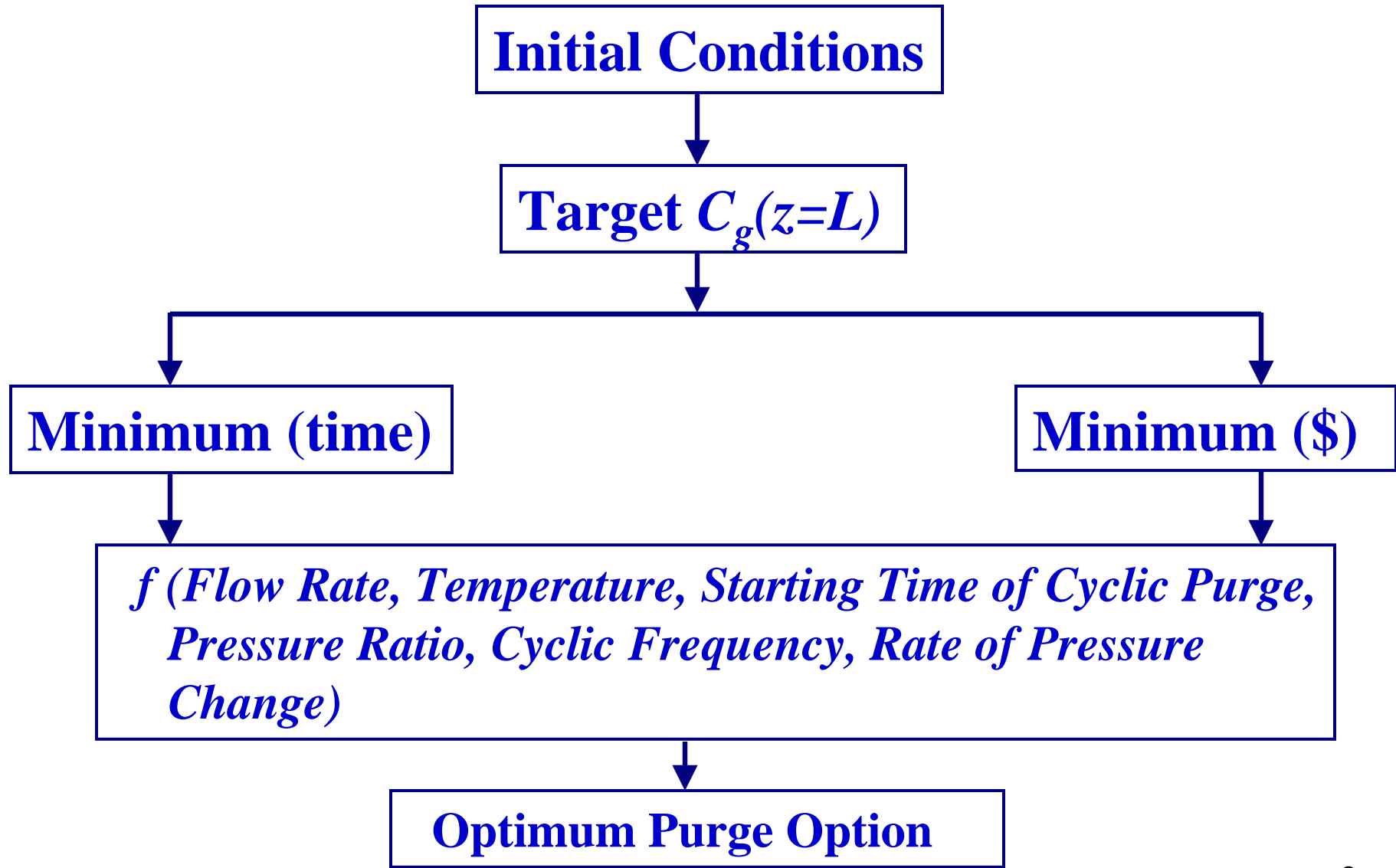
Industrial-scale system

EP SS pipe with 1.5 inch OD and 1640 feet length. Initial conc. 200 ppb;
cyclic purge starts when the moisture concentration reaches at 5 ppb

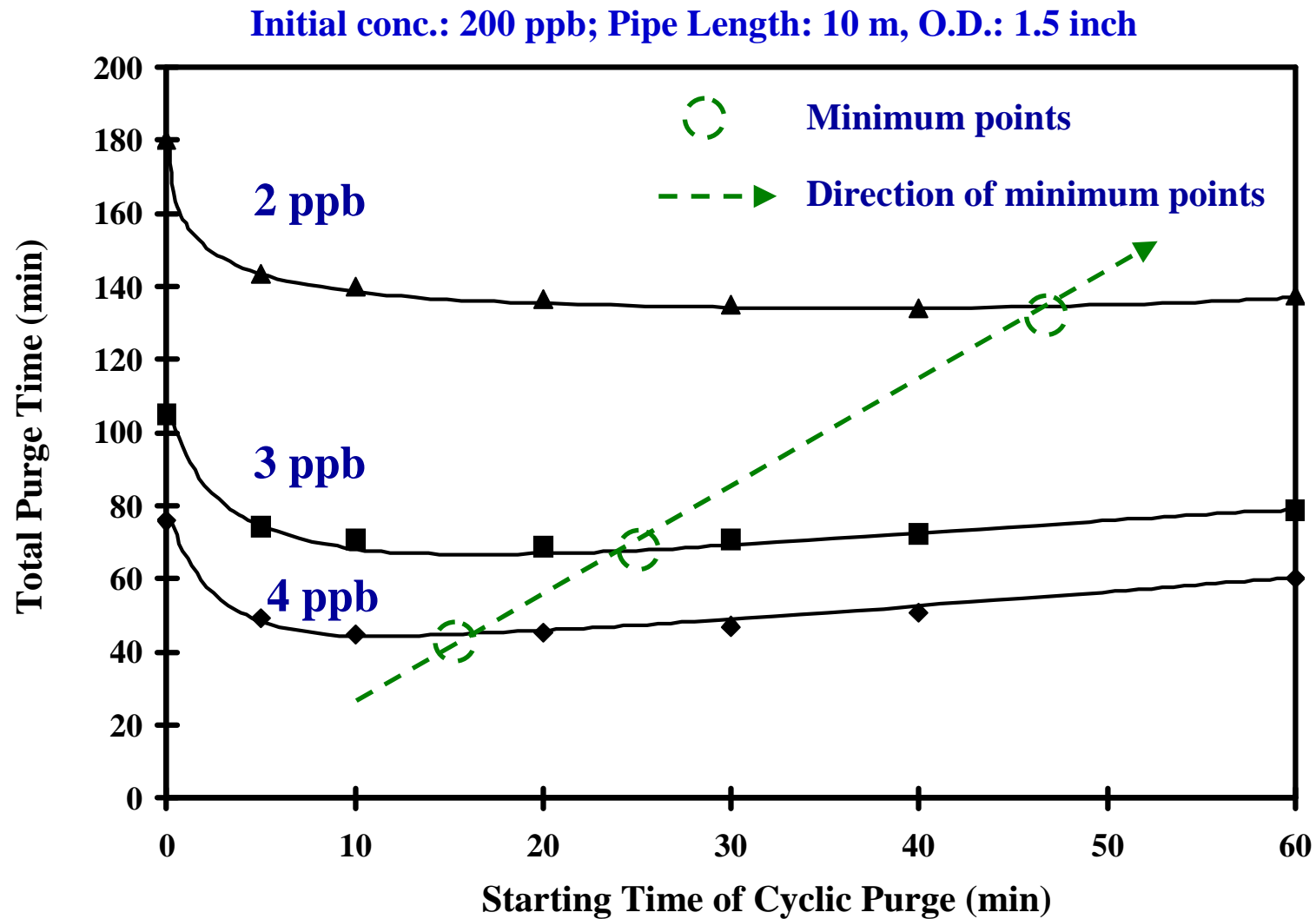


To reach 2 ppb baseline: Cyclic purge save 12 hours of purging time and 32,000 standard liter of purging gas

Optimization of Purging Process



Optimum Starting Time of Cyclic Purge



Highlights

- **Compared with traditional purge with high system pressure and high purging gas flow rate, pressure cyclic purge takes less purging time and less purging gas usage in order to reduce moisture concentration down to an acceptable level.**
- **Depending on the target baseline, the pressure cyclic purge must be started at an optimum time in order to minimize the time and gas usage to reach the target baseline**

Interactions and Future Plans

- Continue working with Intel on this customized joint project; initiate similar applications and studies for other members
- Prepare a process simulator for field applications

Presentations and Papers

- Lowering Material and Energy Usage during Purging Ultra-High-Purity Gas Distribution Systems (presenter), AIChE 2009 Annual Meeting, Nov. 2009, Nashville, Tennessee.
- Application of Pressure Cyclic Purge (PCP) in Dry-down of Ultra-High-Purity Gas Distribution Systems, under preparation and will be submitted to *Chemical Engineering Sciences*

Acknowledgements

- Intel: Val Strazds
- Tiger Optics LLC

Integrated Electrochemical Treatment of CMP Waste Streams for Water Reclaim and Conservation (Customized Project)

PIs:

- James Farrell, Chemical and Environmental Engineering, UA
- James C. Baygents, Chemical and Environmental Engineering, UA

Graduate Students:

- Francis Dakubo, PhD candidate, Chemical and Environmental Engineering, UA
- David Hubler, PhD candidate, Chemical and Environmental Engineering, UA
- Mark Brown, MS candidate, Chemical and Environmental Engineering, UA
- Pui Foon Lai, MS candidate, Chemical and Environmental Engineering, UA

Undergraduate Students:

- Jake Davis, Ritika Mohan, Kyle Kryger, Chemical Engineering, UA

Cost Share (other than core ERC funding):

- GEP Smith Fellowship (D. Hubler), Triffet Prize (D. Hubler), Mining Engineering Fellowship (F. Dakubo), NASA Space Grant Fellowship (K. Kryger), Water Sustainability Program Fellowship (R. Mohan)
- Water Resources Research Center (\$17K)

SRC/SEMATECH Engineering Research Center for Environmentally Benign Semiconductor Manufacturing

Objectives

- **Develop an electrochemical method for removing Cu^{2+} , H_2O_2 , colloidal abrasives, chelating agents and corrosion inhibitors from wastewater generated during CMP.**
- **Compare contaminant removal with industry benchmarks for use of reclaimed water.**
- **Build a prototype reactor and pilot test on real CMP wastewater.**
- **Compare the economic impact per gallon of water used in semiconductor industry to impact for other water uses.**

ESH Metrics and Impact

1. *Reduction in emission of ESH-problematic material to the environment*

- Eliminate the disposal problems associated with membrane concentrates.
- Eliminate the disposal of Cu-laden nanoparticles into hazardous waste landfills.

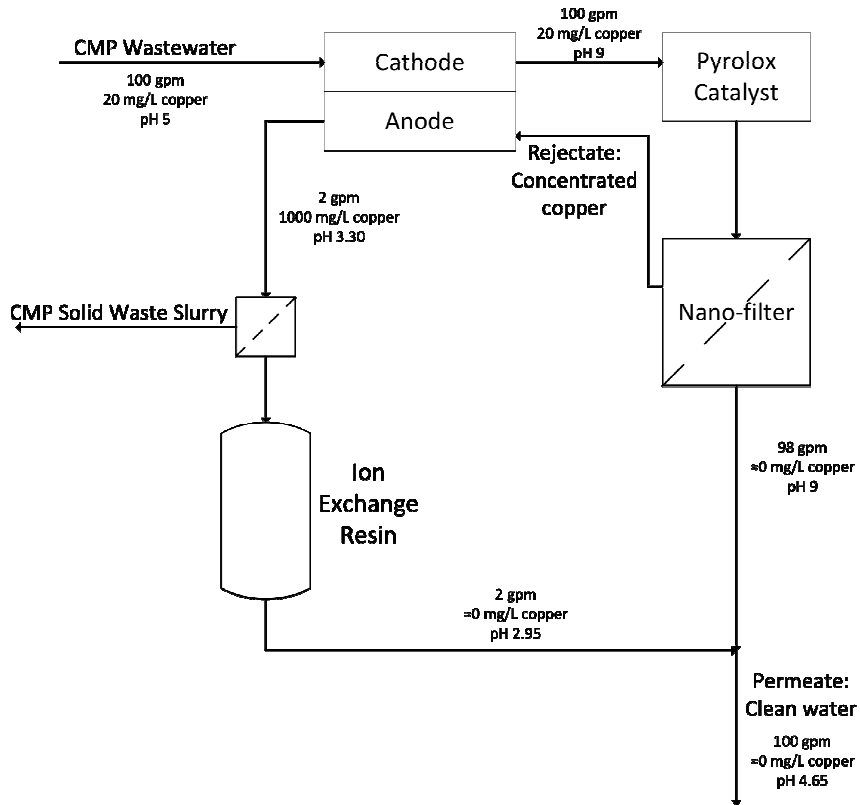
2. *Reduction in the use of natural resources (water and energy)*

- Reclaim CMP wastewater for use in mechanical systems.
- CMP wastewater accounts for up to 30% of fab water use.

3. *Reduction in the use of chemicals*

- Eliminate the need for pH adjusting chemicals and reducing agents that add to TDS load.
- Eliminate the need for activated carbon regeneration.

Electrochemical Treatment System



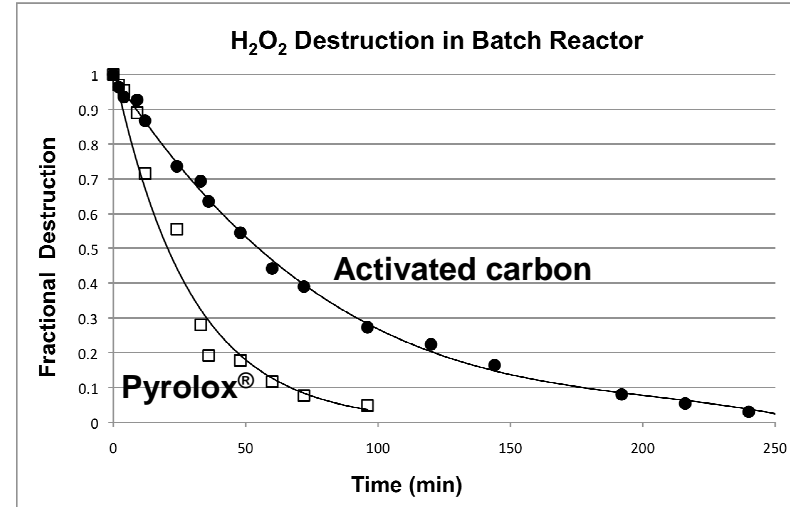
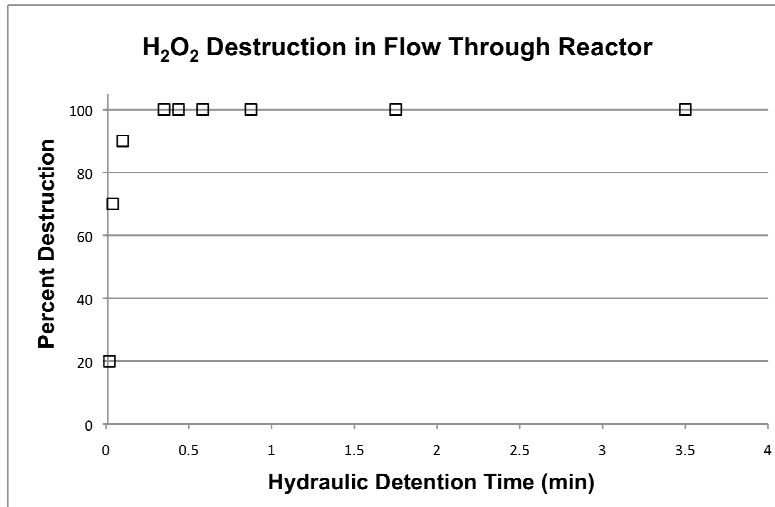
System combines standard filtration unit operations with:

- 1) novel H_2O_2 destruction catalyst
- 2) electrochemical pH manipulation
- 3) electrochemical ion exchange regeneration

Advantages of electrochemical treatment:

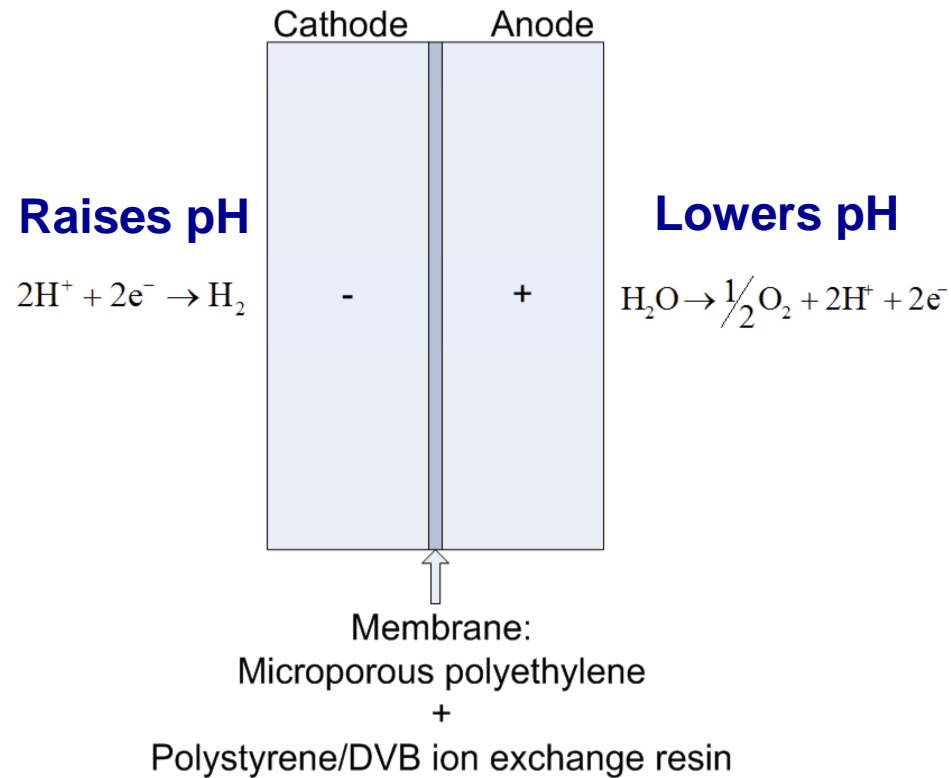
- 1) elimination of chemical additives (e.g., pH adjusting chemicals)
- 2) elimination of secondary waste stream production requiring further treatment or disposal (e.g., ion exchange brines)
- 3) small footprint, low capital and operating costs

Peroxide Destruction Catalyst



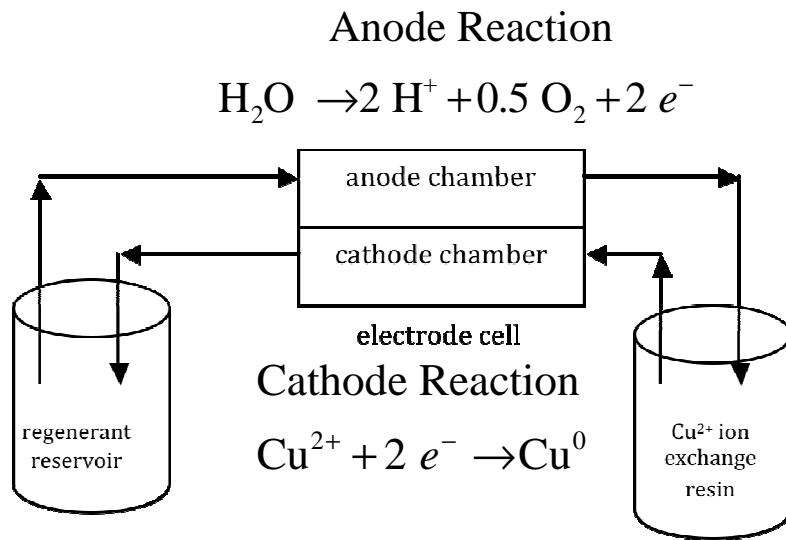
- Conducted tests on six possible peroxide destruction catalysts
- Conducted tests on ultrasonic, O₃ and UV-light peroxide destruction
- Pyrolox[®] (pyrolusite= β -MnO₂) catalyst determined to be the most effective
- Pyrolox[®] is commercially available and used for removing Fe²⁺ from drinking water

Membrane for Electrochemical pH Manipulation



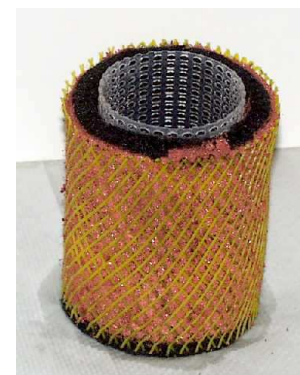
- Developed a novel membrane that is resistant to pinhole leaks common with conventional membranes
- Novel membrane will be useful in other electrochemical applications

Electrochemical Ion Exchange Regeneration



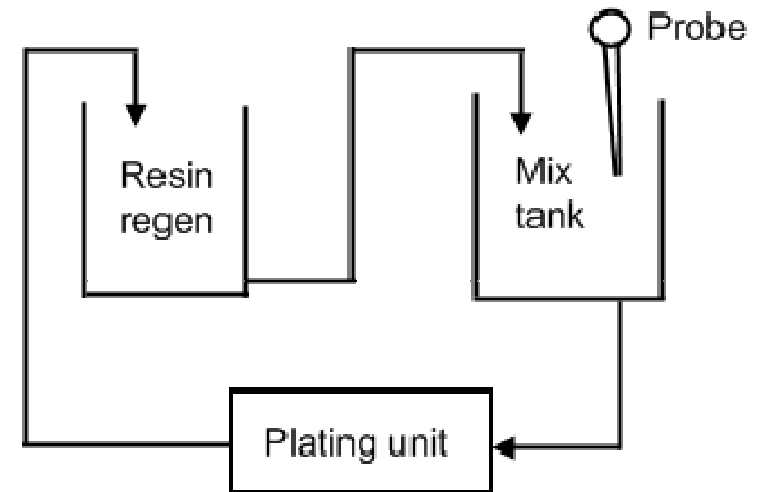
Power cost = \$8.40/m³-resin

Cu value = \$240/m³-resin



Mathematical Model for Ion Exchange Regeneration

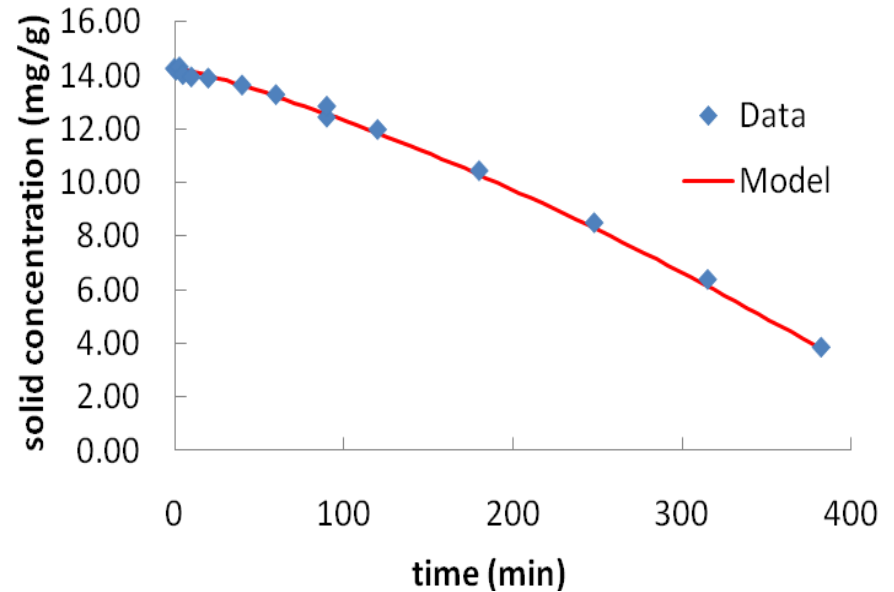
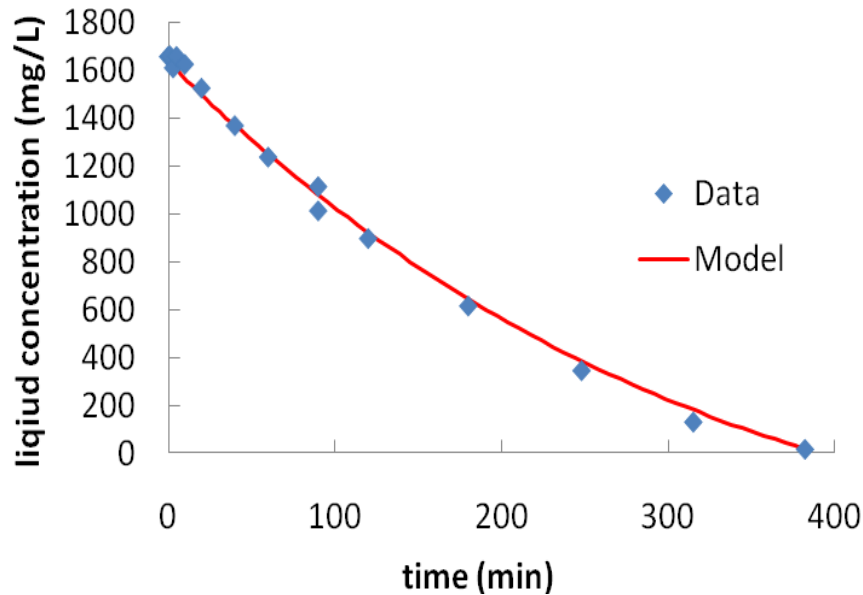
- Cu plating rate can be limited by mass transfer or applied current
- Trade-off between Cu plating rate and Faradaic efficiency
- Mathematical modeling used to optimize the plating rate for cost or time considerations



Liquid mass balance:
$$\left(V_{MIX} + V_P + \varepsilon V_{RR} \right) \frac{dc}{dt} = -k_0 A + V_{RR} K_m \left[c_{eq}^l (c_s) - c \right]$$

Solid mass balance:
$$V_{RR} \frac{dc_s}{dt} = -V_{RR} K_m \left[c_{eq}^l (c_s) - c \right]$$

Resin Regeneration Modeling



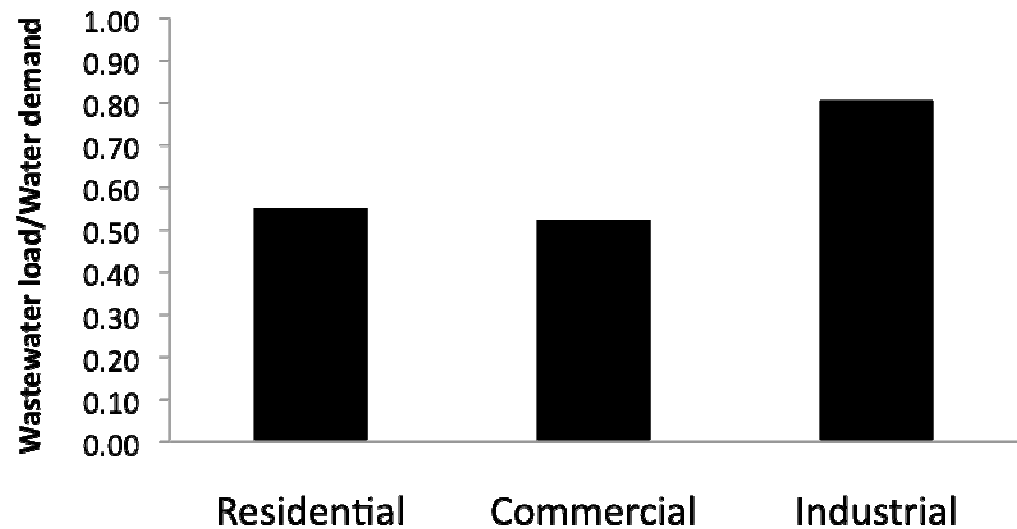
- Modeling can predict both liquid and solid phase Cu²⁺ concentrations
- Modeling will be used to scale-up from prototype to full scale system

Parameters: $V_{MIX} = 6.0$ L; $V_{RR} = 3.4$ L; $V_P = 3.0$ L; $\varepsilon = 0.3$; $K_m = 0.162$ min⁻¹; $k_0A = 110.7$ mg/min
Isotherm: $c_{liq} = (1/(1.97 \times 10^{-3})) \times (c_{sol}/(18.6 - c_{sol}))$, c_{liq} in mg/L, c_{sol} in mg/g

Economic Impact of Semiconductor Water Use

- Evaluate the economic benefits of selected uses of water
- Question: Is high volume semiconductor manufacturing a rational use of water, especially in a semi-arid community?

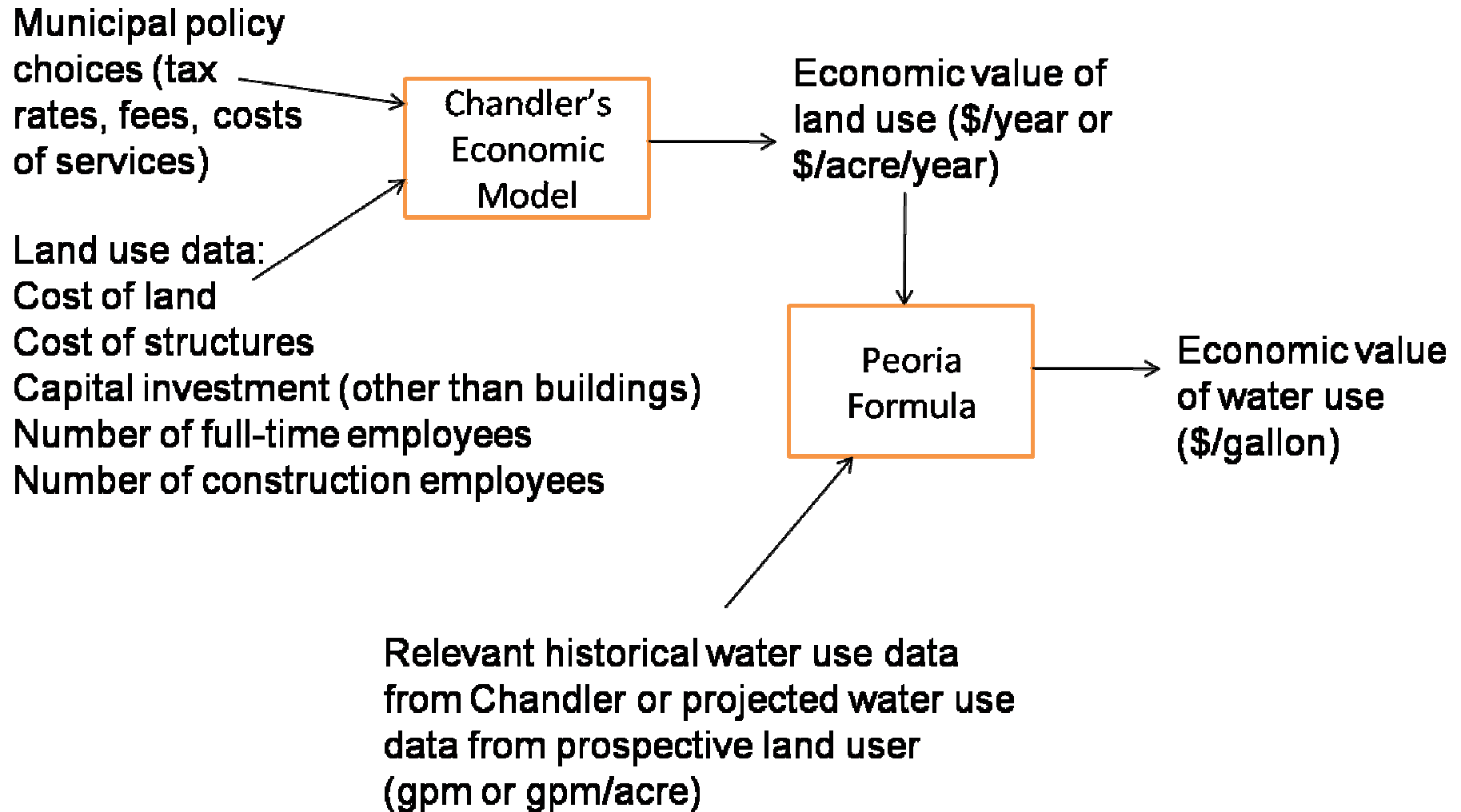
Fraction of water returned by different land users:



- Not just a matter of total water use, as industrial users can return more water to the city, and semiconductor HVM can go beyond other industrial users

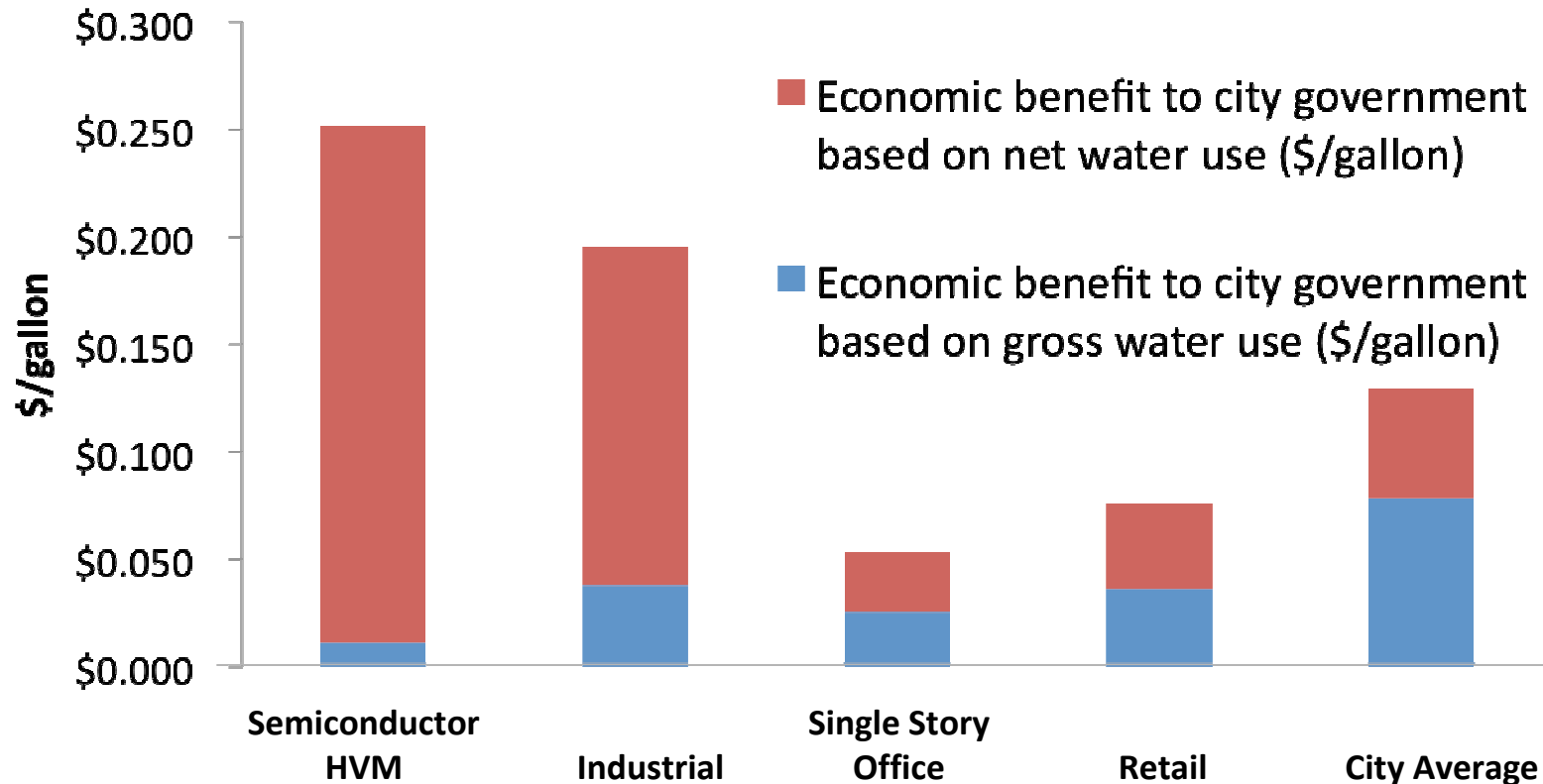
Economic Impact of Semiconductor Water Use

Method for evaluating economic impact per gallon:



Economic Impact of Semiconductor Water Use

Economic benefit to city government:



- Semiconductor HVM is a reasonable use of water in semi-arid or arid communities, as long as infrastructure exists to recapture value from wastewater streams.

Industrial Interactions and Technology Transfer

- **Don Hooper, Intel Corporation**
- **Dan Hodges, Intel Corporation**
- **Allen Boyce, Intel Corporation**
- **Avi Fuerst, Intel Corporation**

- **Sharon Megdal, Water Resources Research Center, UA**
- **Christine Mackay, Economic Development Director, Chandler, AZ**

Future Plans

Next Year Plans

- Pilot test of complete system

Long-Term Plans

- Apply electrochemical treatment methods to other wastewater streams

Publications, Presentations, and Recognitions/Awards

- **David Hubler: Triffet Prize and GEP Smith Fellowship**
- **Francis Dakubo: Department of Mining Engineering Fellowship**
- **Kyle Kryger: Ella Philipossian Memorial Scholarship & Pillars of Excellence Award**
- **David Hubler: First Place Award, University of Arizona 2009 Student Showcase, B.P.A. Division, November 6-7, 2009, Tucson, AZ**
- **“Economic Benefit of Commercial and Industrial Water Uses in a Semi-arid Municipality,” presented at the Arizona Hydrological Society/American Institute of Hydrology 2009 Hydrological Symposium, August 30-September 2, 2009, Scottsdale, AZ**
- **“Electrochemical Methods for Water Reclaim in Semiconductor Manufacturing,” presented at the International Conference on Microelectronics Pure Water, November 11-12, 2008, Mesa, AZ**
- **“Electrochemical Water Treatment using Diamond Film Electrodes,” presented at the University of Illinois at Urbana-Champaign, November 7, 2008**

Optimization of Dilute Ammonia-Peroxide Mixture (APM) for High Volume Manufacturing Through Surface Chemical Investigations (Intel Customized Project)

PIs:

- Srimi Raghavan, Material Science and Engineering, UA
- Jinhong Zhang, Mining and Geological Engineering, UA

Graduate Students:

- Shariq Siddiqui, PhD candidate, Material Science and Engineering, UA

Cost Share (other than core ERC funding):

- Horiba SC-1 monitor on loan

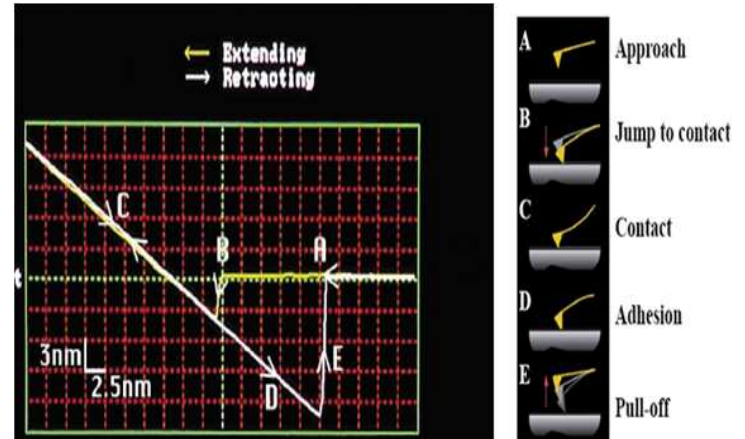
Objectives

- 1) Optimization of ammonia-peroxide mixtures (APM) for particle removal through interaction force measurements using atomic force microscope (AFM).
- 2) Investigate the stability of ammonium hydroxide and hydrogen peroxide in APM solutions as a function of temperature and dilution ratio.

Experimental Approach

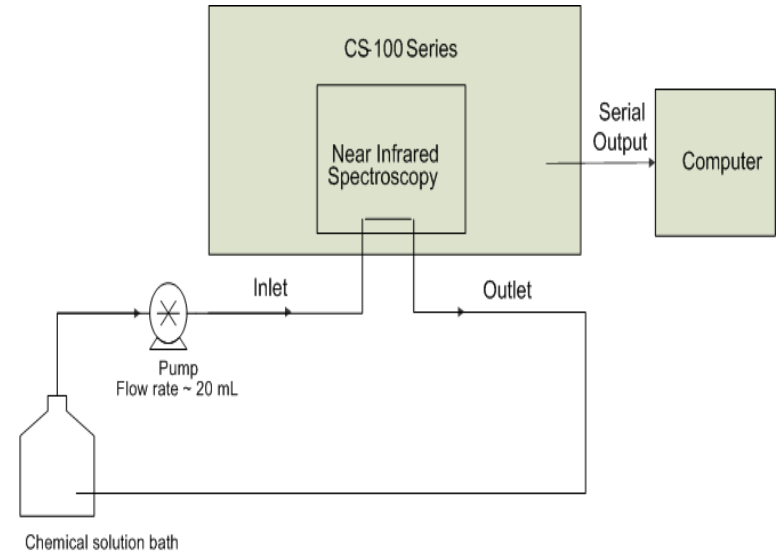
1) Adhesion or repulsive forces measured using atomic force microscope (AFM).

- p-type Si (100) substrate etched in dilute HF(1:100)
- Silicon tip
 - spring constant = 0.12 N/m, radius = 3 nm.
 - etched in dilute HF (1:100)



2) NH_4OH and H_2O_2 concentrations measured using Horiba CS-100C composition monitor.

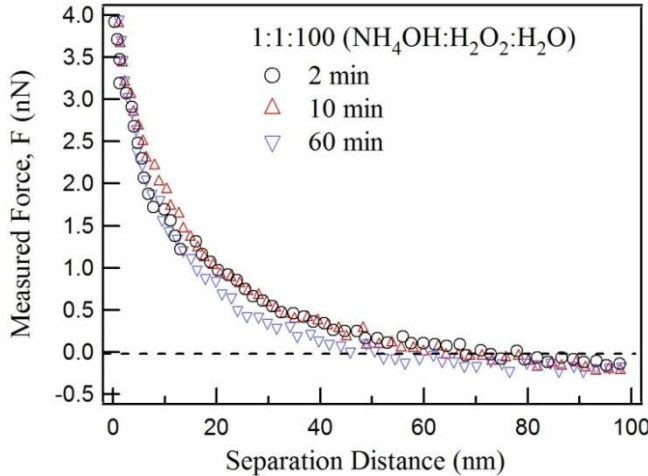
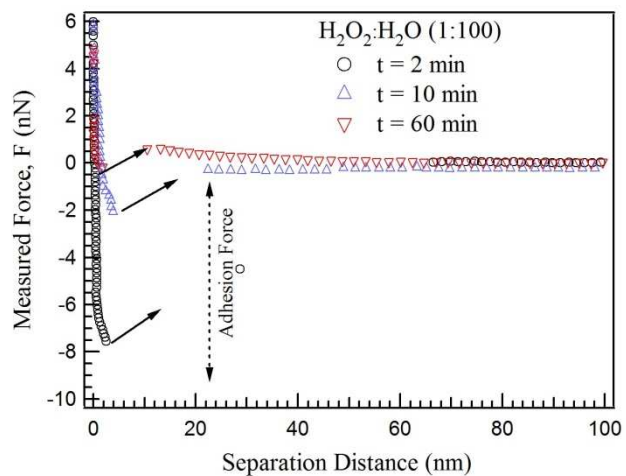
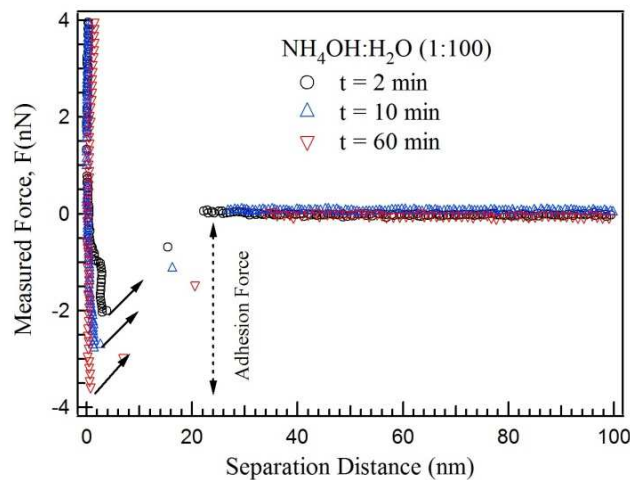
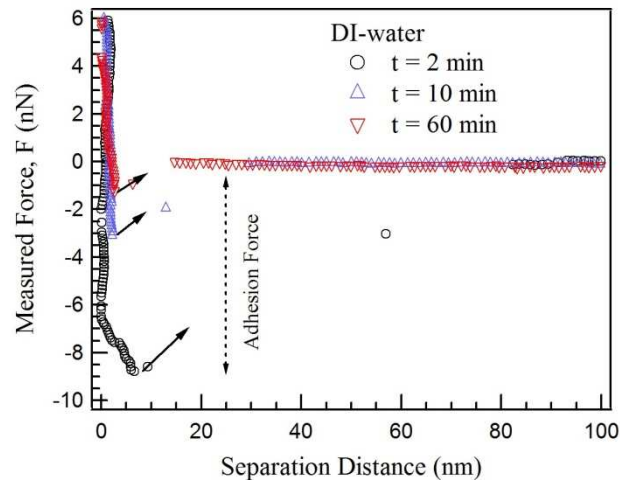
- Solutions: 1:1:5 and 1:1:50 ($\text{NH}_4\text{OH}:\text{H}_2\text{O}_2:\text{H}_2\text{O}$)
- $T = 24, 40, 50$ and 65°C



RESULTS –Part I

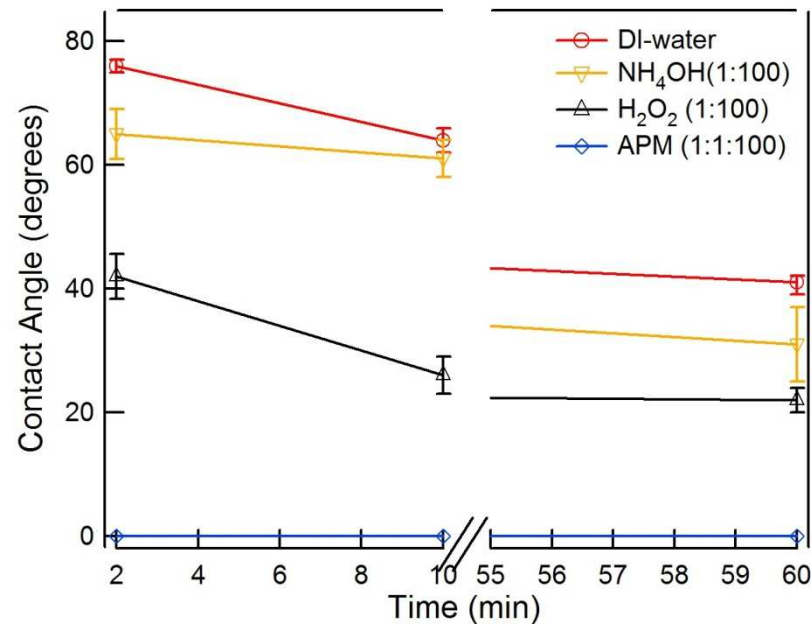
Force measurements between *H-terminated Si surface* and a *H-terminated Si tip* in dilute APM (1:1:100) solution and its components.

Force Measurements between a H-terminated Si surface and a H-terminated Si tip in APM Solution & Components



- Adhesion force exists between Si surface and Si tip in DI-water, $\text{NH}_4\text{OH}:\text{H}_2\text{O}$ (1:100) and $\text{H}_2\text{O}_2:\text{H}_2\text{O}$ (1:100) solutions.
- Only repulsive force was measured between Si surface and Si tip in a dilute APM 1:1:100 solution.
- Infact, in APM solutions covering the range 1:1:100 to 1:1:500, only repulsive forces were measured within 2 min of immersion time.

Wettability of Si Surfaces in Ammonia-Peroxide Mixture (APM)

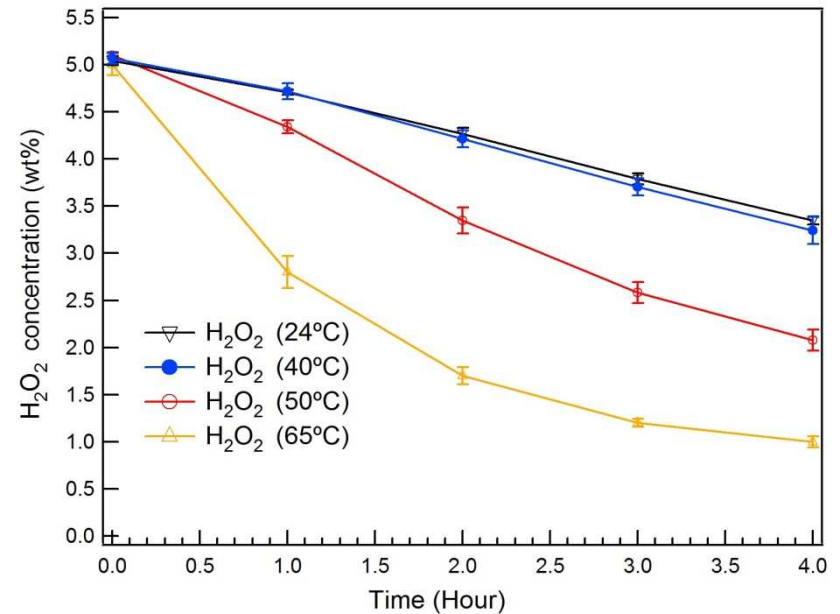
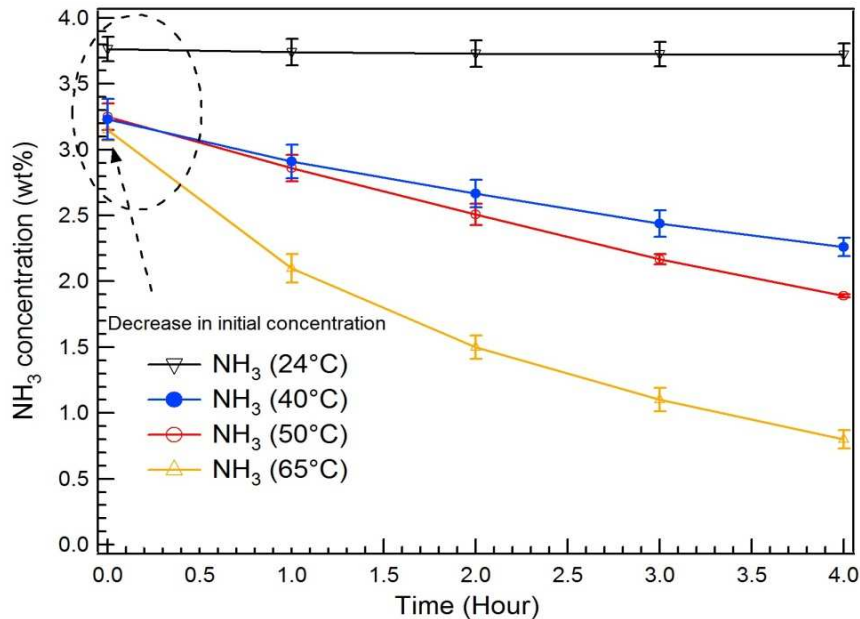


- Contact angle of DI water and NH₄OH solution on HF etched silicon decreases with time; in dilute peroxide solution contact angle decrease is more rapid- in all cases, it does not go below 20° even at 60 min---reason for adhesion force measured in these solutions.
- In 1:1:100 APM solution HF etched silicon becomes hydrophilic within two minutes---Reason for absence of any attractive force.

RESULTS –Part II

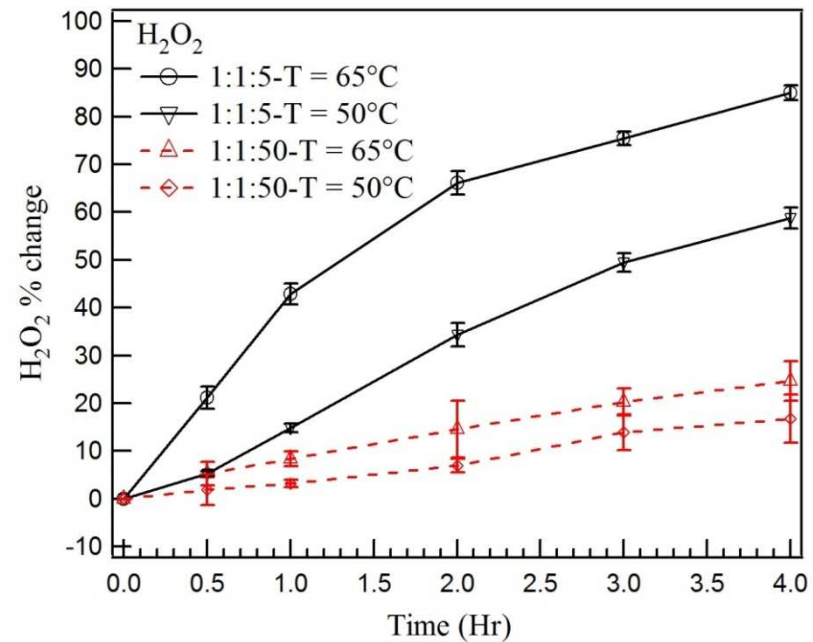
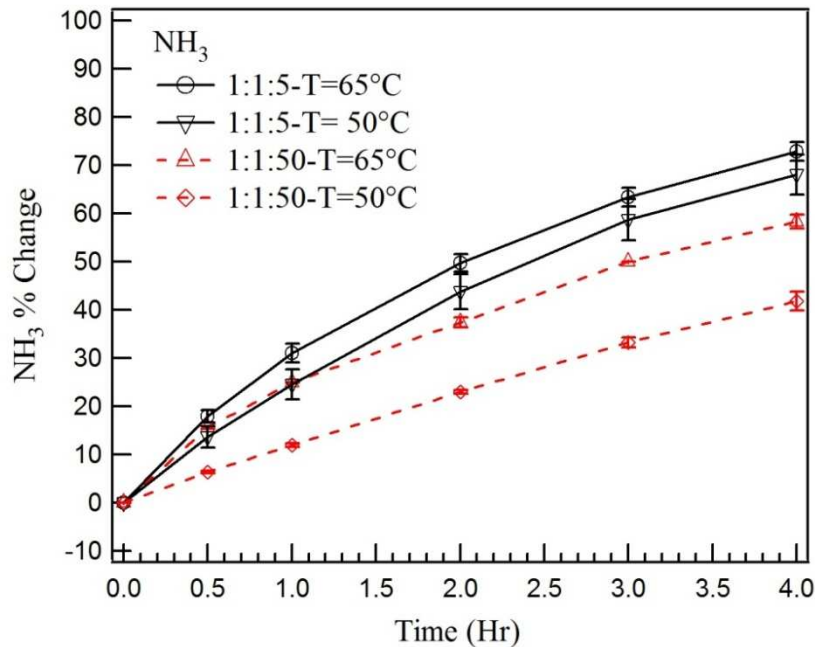
Measurement of the stability of *ammonium hydroxide* and *hydrogen peroxide* in APM solutions using Horiba SC-1 composition monitor.

Decomposition of NH_4OH and H_2O_2 in 1:1:5 APM Solution



- Ammonia decomposition increases with temperature.
 - In one hour, ammonia concentration decreased by 30% at 65°C .
- Increase in temperature results in higher hydrogen peroxide decomposition.
 - Time for 50% decomposition is roughly 2.8 and 1.0 hr at 50°C and 65°C, respectively.

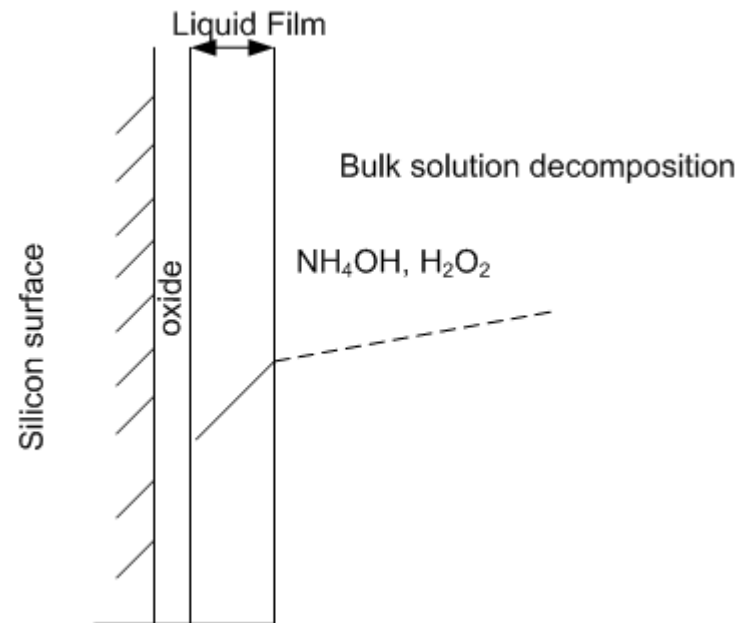
Effect of Dilution on NH_4OH and H_2O_2 Decomposition



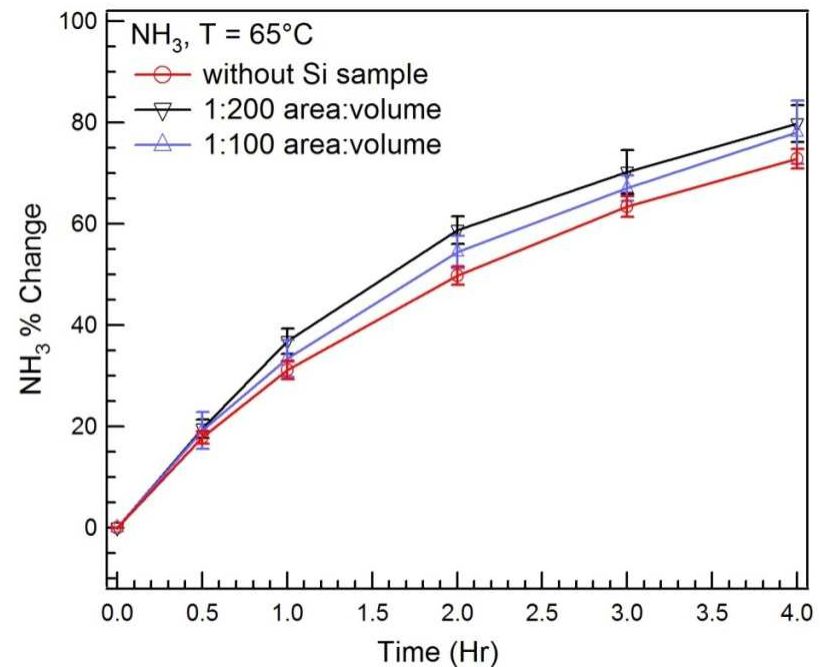
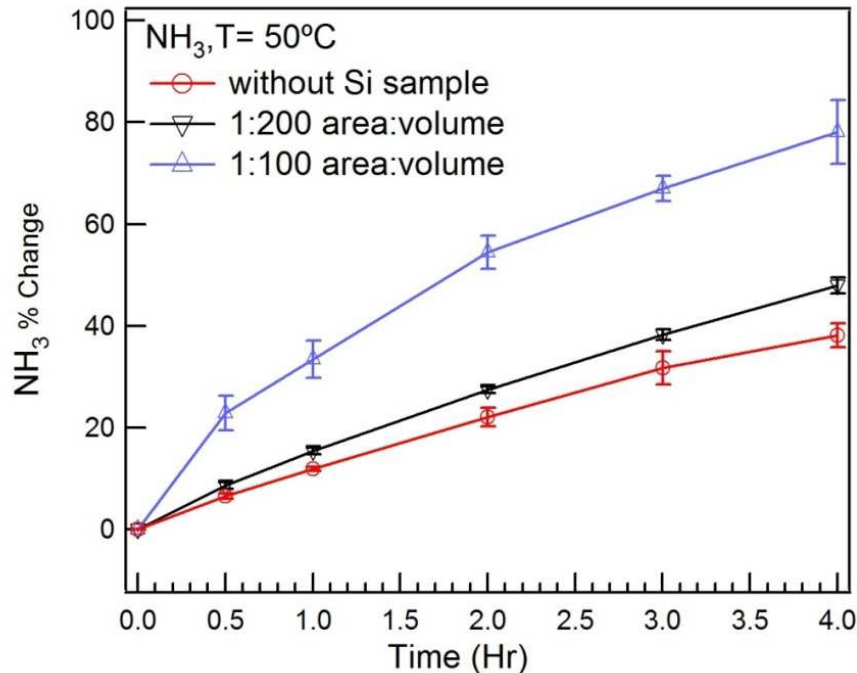
- Extent of decomposition of both ammonium hydroxide and hydrogen peroxide decreases with dilution of APM solution.
- In four hours, ammonia concentration decreased by 30% in a dilute (1:1:50) APM solution vs. 65% decrease in a conventional (1:1:5) APM solution at 50°C.
- Hydrogen peroxide decomposition measured to be less than 15% in four hours at 50°C and 65°C for a dilute APM (1:1:50) solution.

Does silicon surface play a role in the decomposition of ammonium hydroxide and hydrogen peroxide?

- Silicon surface may act as a catalyst
- Consumption of H_2O_2 and NH_4OH by formation and etching of oxide film.

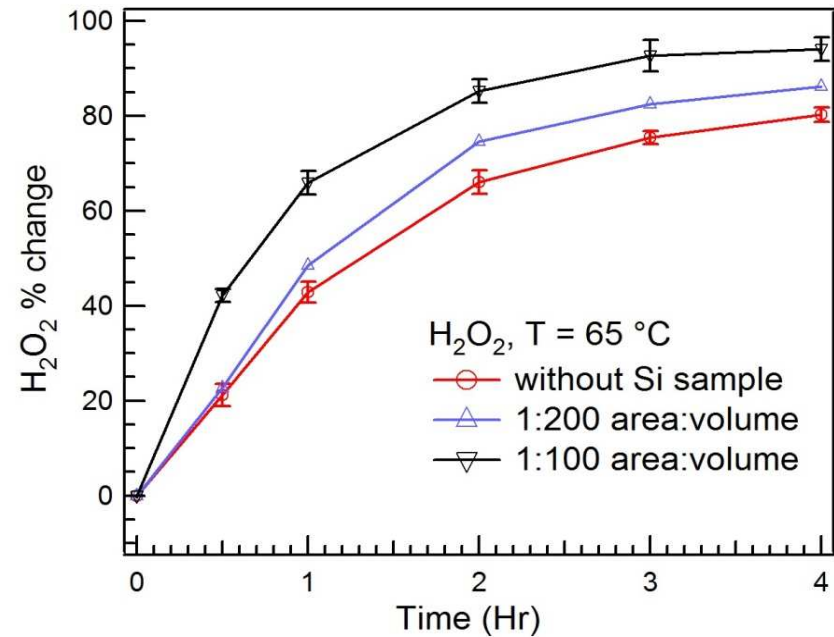
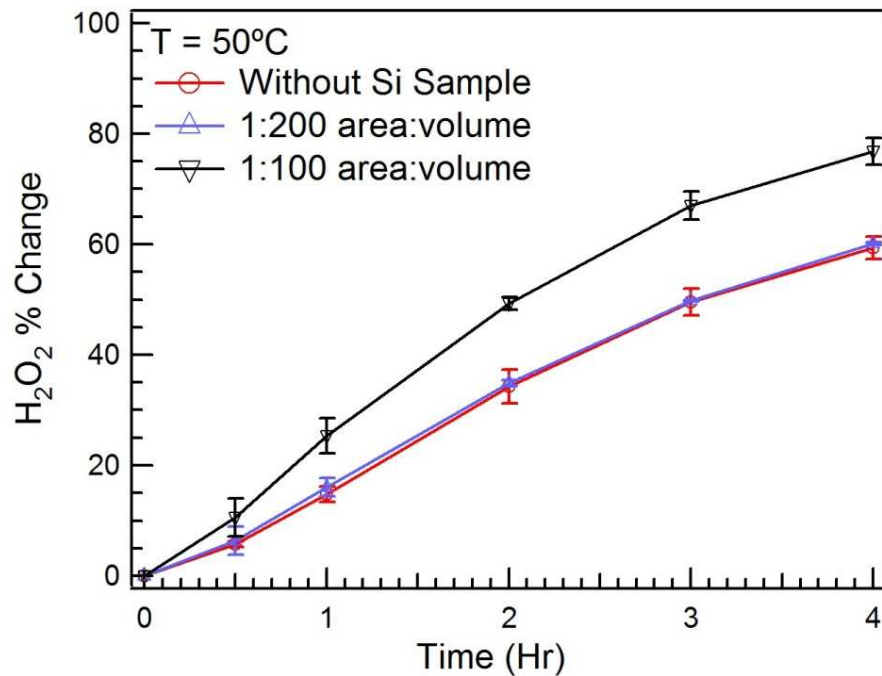


NH₄OH Decomposition Induced by Si Surface in 1:1:5 APM Solution



- At 50°C, when the Si surface area to solution volume increases, ammonia decomposition increases with temperature.
 - This perhaps indicates surface mediated decomposition.
- At 65°C, area to volume ratio is not significant---bulk decomposition

H₂O₂ Decomposition Induced by Si Surface in 1:1:5 APM Solution



- Higher surface area results in higher hydrogen peroxide loss due to oxidation and catalytic decomposition

Highlights

- Adhesion forces prevailed between H-terminated Si surface and a H-terminated Si tip in DI water, ammonium hydroxide and hydrogen peroxide solutions up to 60 min.
- Interaction force measurements in dilute APM (1:1:100) solution showed repulsive forces between Si surface and Si tip within 2 min.
- Ammonium hydroxide and hydrogen peroxide decomposition increases with temperature for a conventional APM (1:1:5) solution
- At 50°C, surface area of silicon exposed to solution affects ammonia and peroxide loss
- Dilute APM solution (1:1:50) showed less decomposition at elevated temperatures when compared to 1:1:5 solution

Future Plans

- Interaction force measurements at elevated temperatures (40, 50 and 65°C)
- Measurements of stability of ammonium hydroxide and hydrogen peroxide in APM in the presence of trace metal ions.
 - Proposed metal ions are: Fe²⁺ and Fe³⁺

Industrial Interactions

Industrial Mentor

- **Avi Fuerst, Intel Corporation**
- **Barry Brooks, Intel Corporation**
- **Eric Hebert, Horiba Inc.**

Destruction of Perfluoroalkyl Surfactants **using Boron Doped Diamond Film** **Electrodes** *(Task Number: 425.018)*

PI:

- **James Farrell, Chemical and Environmental Engineering, UA**

Graduate Students:

- **Kimberly C. Carter, PhD candidate, Chemical and Environmental Engineering, UA**

Undergraduate Students:

- **none**

Other Researchers:

- **Zhahui Liao, Postdoctoral Fellow, Chemical and Environmental Engineering, UA**

Cost Share (other than core ERC funding):

- **\$100 k from National Science Foundation, Small Grants for Exploratory Research**

Destruction of Perfluoroalkyl Surfactants in Semiconductor Process Waters Using Boron Doped Diamond Film Electrodes

(Task Number: 425.018)

Subtask Subtitles:

Susceptibility of PFAS oxidation and reduction products to biodegradation under conditions relevant to municipal wastewater treatment plants.

Development of an adsorptive method using hydrophobic zeolites and/or anion exchange resins for concentrating PFAS compounds from dilute aqueous solutions.

PI:

- **Reyes Sierra, Chemical and Environmental Engineering, UA**

Graduate Students:

- **Valeria Ochoa, PhD candidate, Chemical and Environmental Engineering, UA**

Undergraduate Students:

- **Chandra Kathri, Chemical and Environmental Engineering, UA**

Other researchers

- **Sandra Hernandez, PhD candidate, University Autonomous of Coahuila, Mexico**

Cost Share (other than core ERC funding):

UA/NASA grant (to C. Kathri) / CONACyT grant (to S. Hernandez)

SRC/SEMATECH Engineering Research Center for Environmentally Benign Semiconductor Manufacturing

Objectives

- **Determine the feasibility of electrochemical destruction of perfluoroalkyl surfactants (PFAS) in aqueous waste streams.**
- **Determine the susceptibility of PFAS compounds and their oxidation products to microbial degradation.**
- **Determine the degree of electrolysis required to generate products that are readily biodegraded in municipal wastewater treatment plants.**
- **Develop an adsorptive method for concentrating PFAS compounds from dilute aqueous solutions.**
- **Test the proposed multistep treatment scheme on real semiconductor wastewaters containing PFAS compounds.**

ESH Metrics and Impact

1. Reduction in emission of ESH-problematic material to environment.

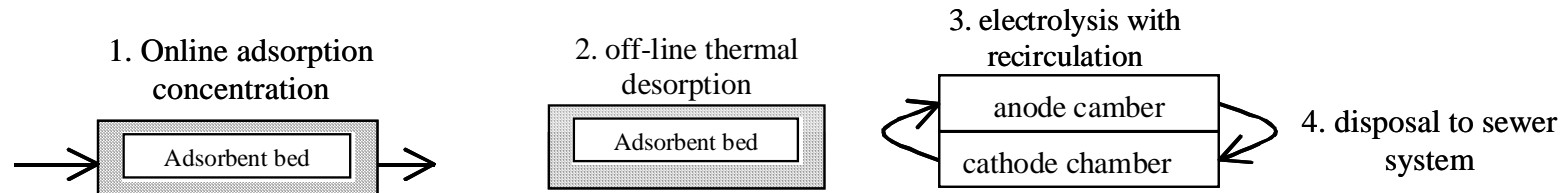
- 100% destruction of perfluoroalkyl surfactants in wastewaters
- technology can also be used for destruction of other ESH-problematic organic compounds

2. Reduction in the use of natural resources (water and energy).

- energy savings by avoiding costly reverse osmosis (RO) separation
- water savings by recovering all the treated wastewater (no RO retentate disposal)
- energy savings by avoiding combustion of PFAS compounds in RO retentate

3. Securing the critical use exemption status for PFAS and related compounds in the semiconductor industry.

Proposed Treatment Scheme



Multi-step treatment scheme:

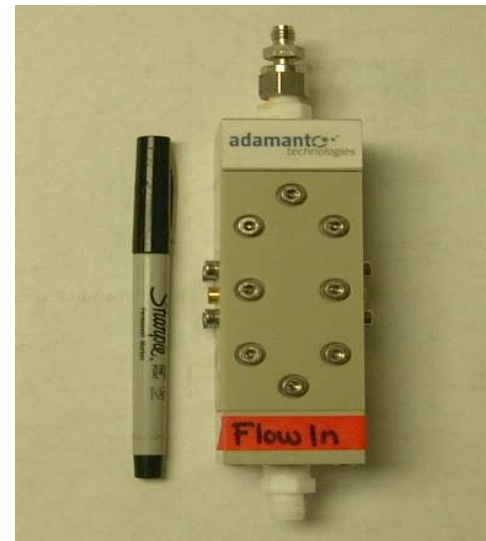
- 1. Concentrate PFAS from dilute aqueous solutions on an adsorbent or ion exchange resin.**
- 2. Desorb PFAS into a concentrated solution.**
- 3. Recirculate concentrated PFAS solution through a BDD electrode reactor for electrolytic destruction.**
- 4. Dispose of biodegradable electrolysis products to the sanitary sewer system.**

Experimental Systems



Rotating Disk Electrode (RDE) Reactor

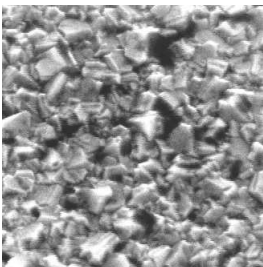
- no mass transfer limitations
- electrode surface area = 1 cm^2
- solution volume = 350 mL
- $a_s = 0.00286 \text{ cm}^2/\text{mL}$



Parallel plate flow-cell

- rates similar to real treatment process
- electrode surface area = 25 cm^2
- solution volume = 15 mL
- $a_s = 1.67 \text{ cm}^2/\text{mL}$

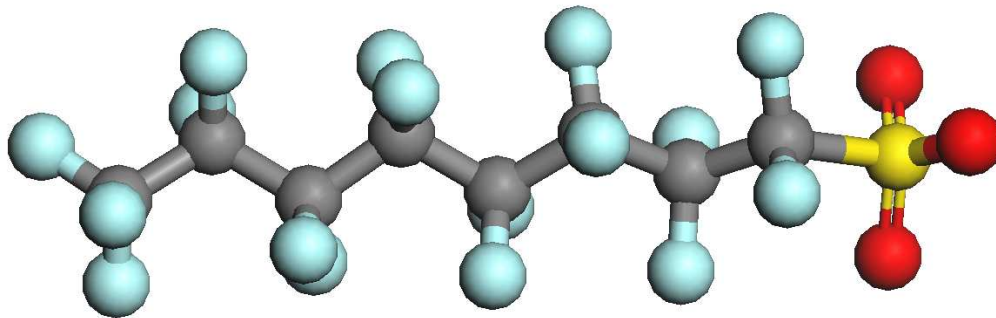
Boron Doped Diamond Film Electrodes



- Diamond film grown on p-silicon substrate using CVD
- Boron doping provides electrical conductivity
- Highly stable under anodic polarization
- No catalyst to foul or leach from electrode
- Emerging technology being adopted for water disinfection

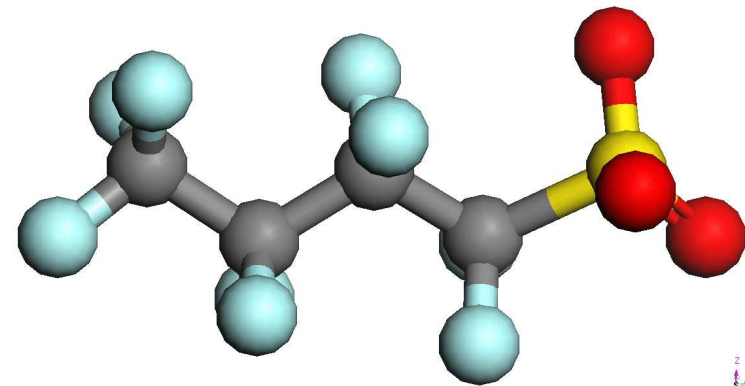
Target Compounds:

perfluorooctyl sulfonate (PFOS)



Most widely used PFAS.

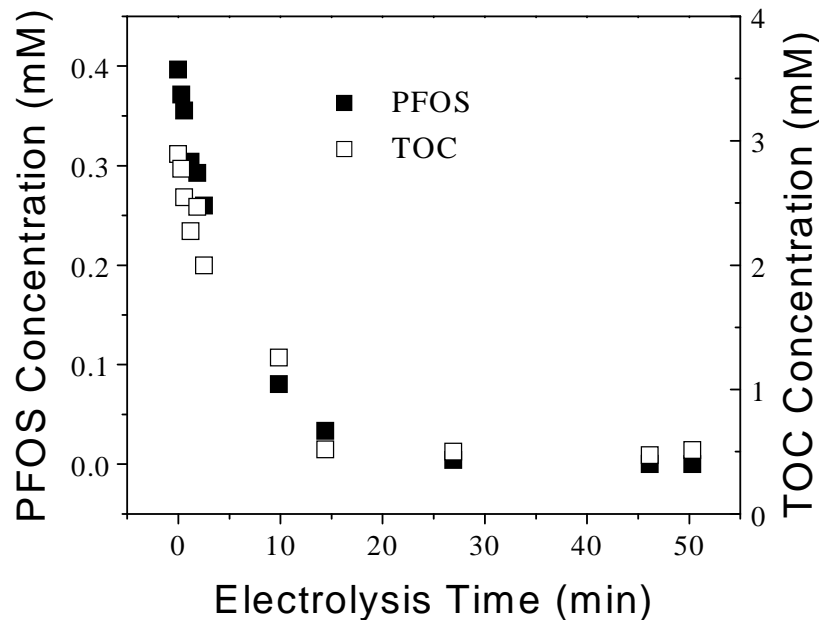
perfluorobutyl sulfonate (PFBS)



Potential replacement for PFOS.

Experimental Results:

Flow Through Reactor



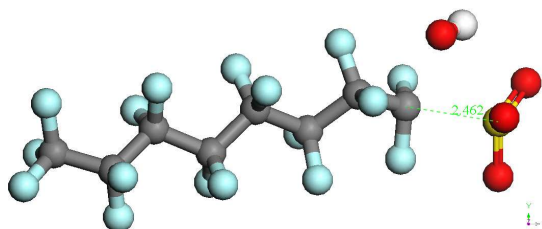
PFOS & total organic carbon (TOC) concentrations as a function of electrolysis time for the flow-cell operated at a current density of 20 mA/cm².

- PFOS can be rapidly removed from water with a half-life ~7 min.
- Reaction rates are first order in PFOS concentration.
- No build-up of fluorinated organic reaction products.
- Similar results observed for PFBS.
- Measured activation energy for PFOS oxidation is low (4.2 kJ/mol).

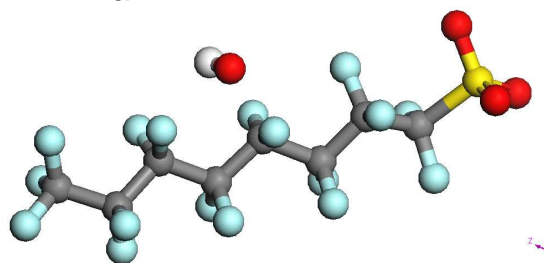
Quantum Chemistry Modeling: Activation Energies for HO• Attack

Transition State Structures

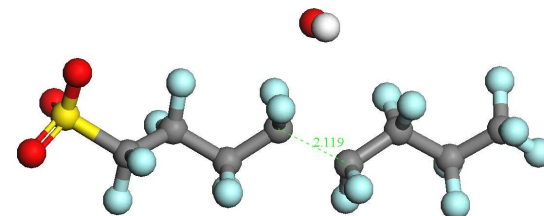
$E_a = 123$ kJ/mol



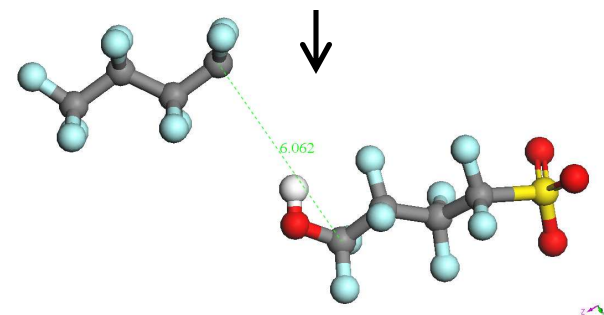
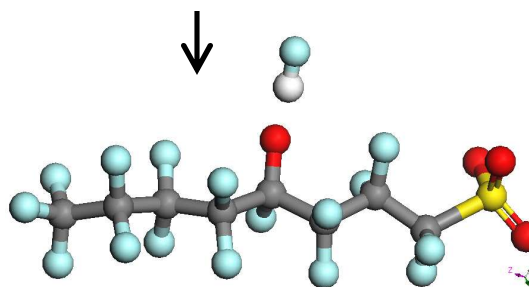
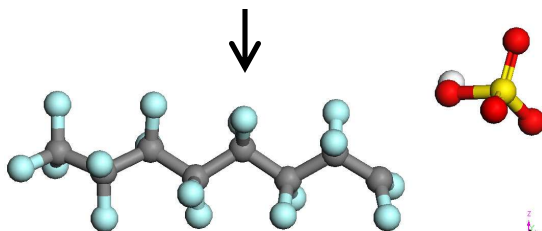
$E_a = 241$ kJ/mol



$E_a = 169$ kJ/mol



Final Products



- Activation energies are much higher than those observed for compounds that readily react with hydroxyl radicals at room temperature. This suggests that the oxidation rate limiting mechanism at BDD electrodes does not involve hydroxyl radicals.

SRC/SEMATECH Engineering Research Center for Environmentally Benign Semiconductor Manufacturing

Reaction Mechanisms

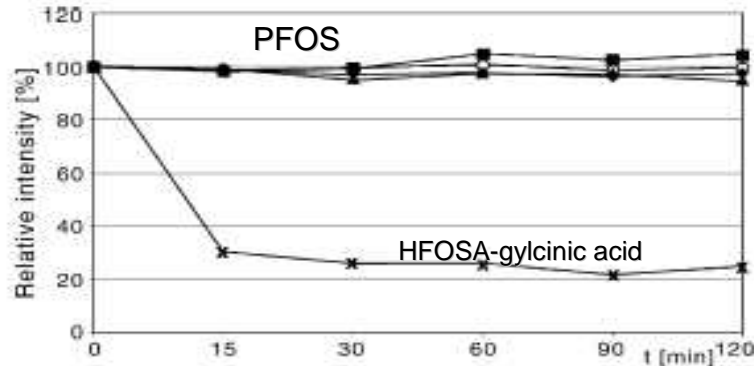


Fig. 1. Graphs of elimination for PFOS and HFOSA-glycinic acid under AOP treatment over a period of 120 min applying different AOP reagents (PFOS treated with: O_3 ▲; O_3/UV ■; O_3/H_2O_2 ◆; Fenton ○; HFOSA-glycinic acid treated with: O_3/UV ×).

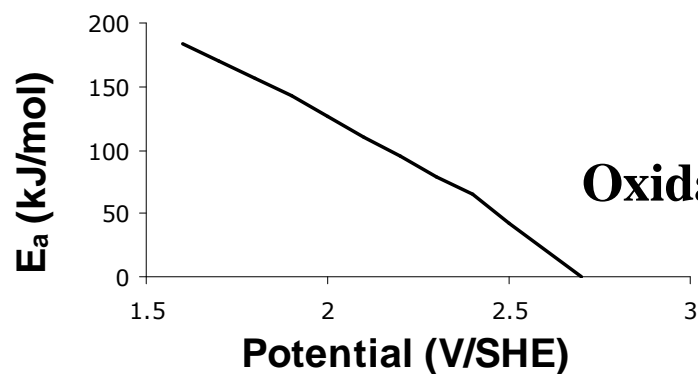
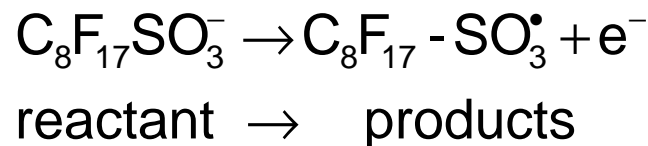
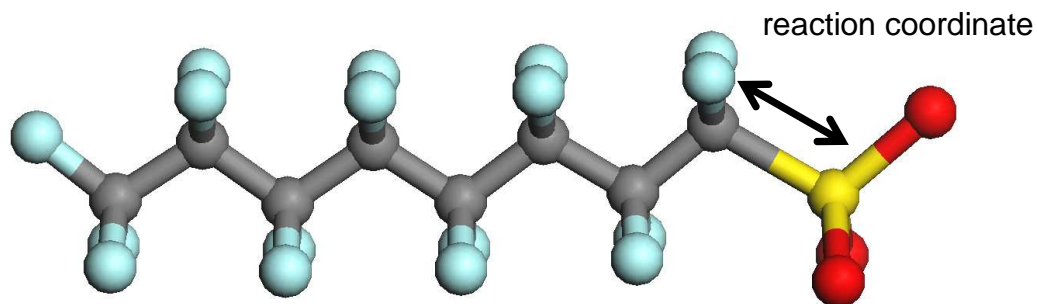
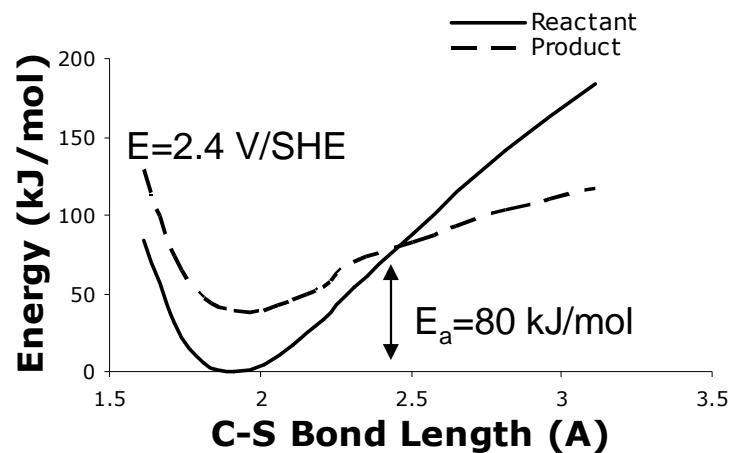
PFOS unreactive with:

1. O_3
2. O_3/UV
3. H_2O_2/O_3
4. $H_2O_2/Fenton (Fe^{2+}/Fe^{3+})$

Schroder and Meesters, *J. Chromatog. A.*, 2005.

- High activation energies for oxidation by HO^\bullet is consistent with absence of PFOS reactivity with H_2O_2 based oxidation methods.
- **Oxidation by BDD electrodes is much more powerful than peroxide based oxidation methods.**

Quantum Chemistry Modeling: E_a for Direct Electron Transfer

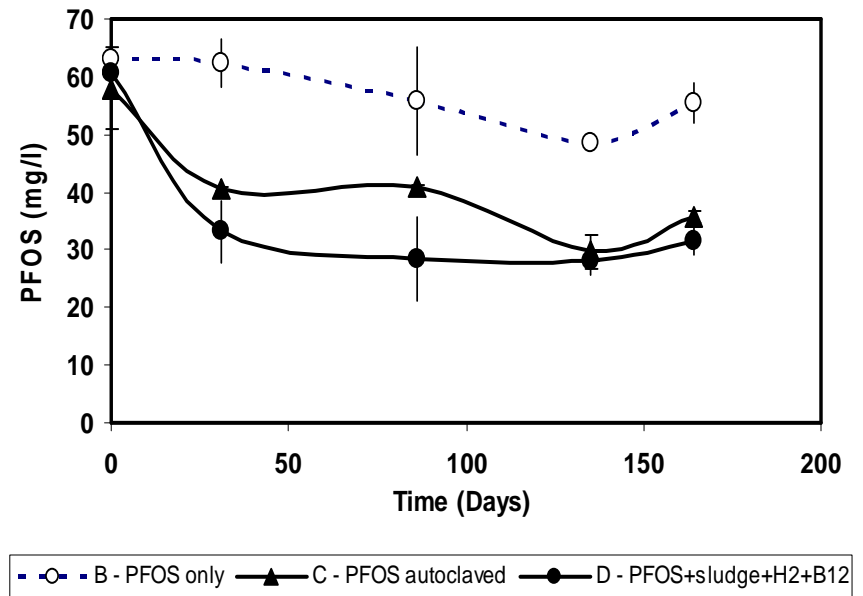


Oxidation becomes activationless at $E > 2.7$ V/SHE.

Results:

Microbial Degradation of PFOS and PFBS Electrolysis Products

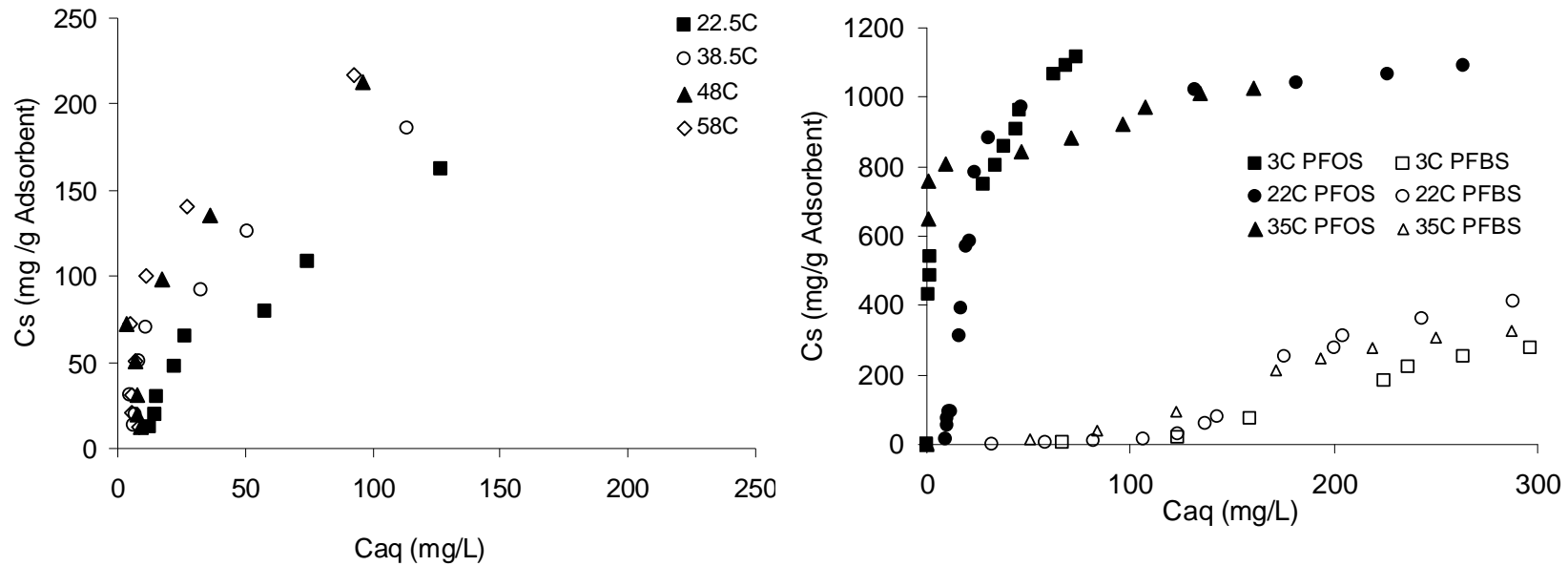
Time course of the anaerobic degradation of PFOS electrolyzed for 24 h. Abiotic control (■), killed sludge control (▲) and full treatment (●).



Products of PFOS and PFBS electrolysis are very persistent.

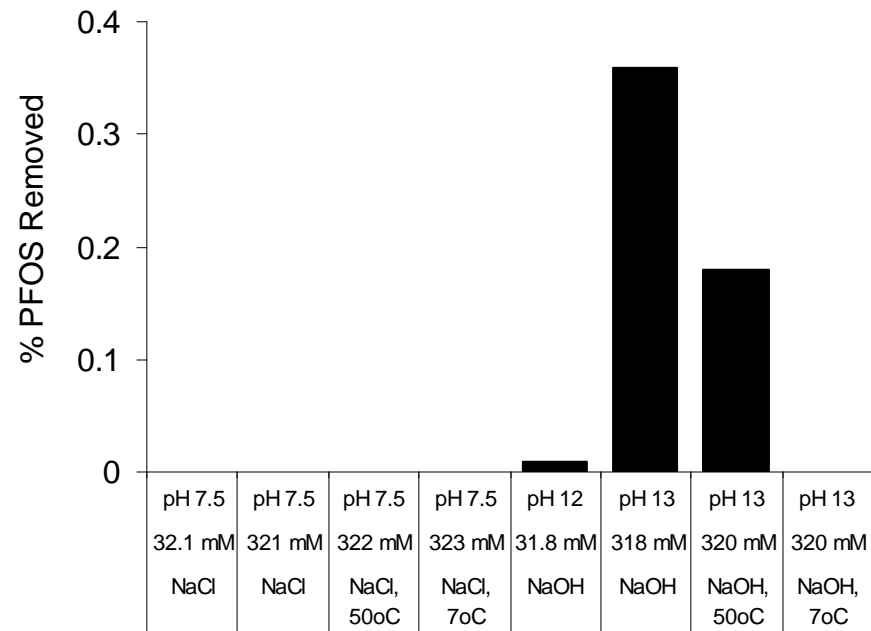
- ❖ Electrochemical treatment of FPOS and PFBS for up to 24 and 96 h, resp., did not enhance the compound's anaerobic biodegradation even after extended incubation (> 1.1 years).
- ❖ PFOS partly adsorbed by microbial sludge.

Adsorbent Testing



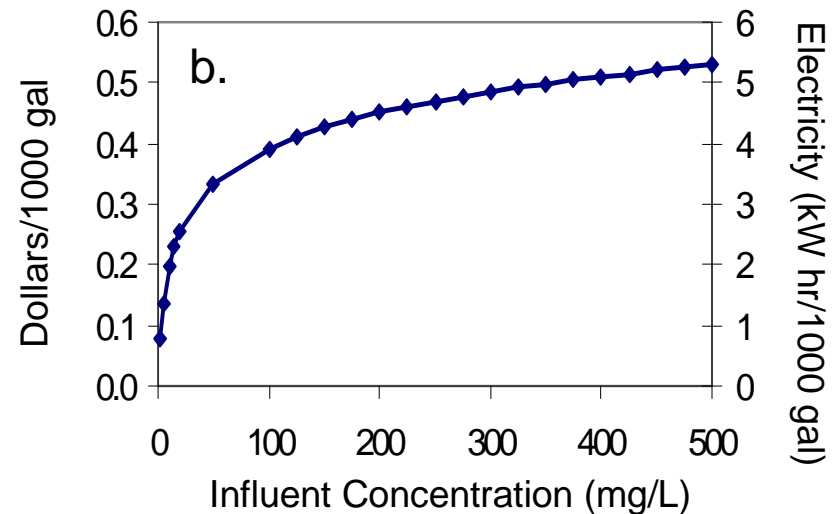
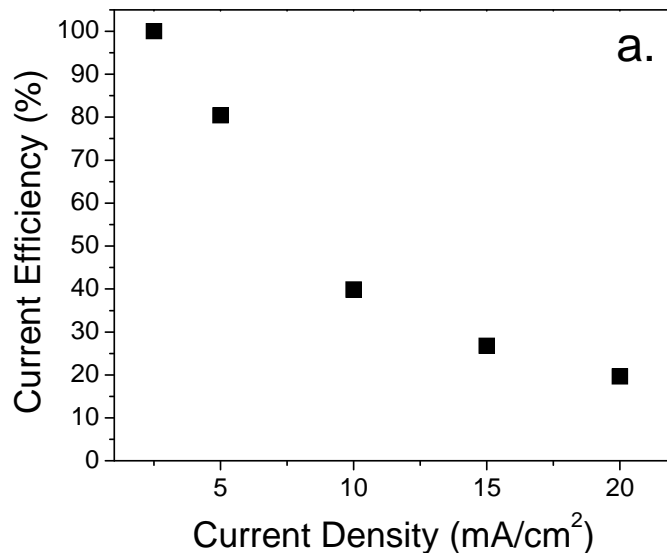
- Measured adsorption isotherms on GAC, ion exchange resins and zeolites
- Greater adsorption at higher temperatures (endothermic)

Adsorbent Regeneration Testing



- PFOS is irreversibly adsorbed to ion exchange resin.
- Reverse osmosis (RO) is only viable concentration method.

Current Efficiencies and Treatment Costs



- a) Faradic current efficiencies for PFOS oxidation based on 34 mol e⁻ per mol of PFOS.
b) Electrical power requirements and costs required to reach a final PFOS concentration of 1 mg/L (2.5 μM) as a function of the influent PFOS concentration. Costs based on flow-cell operated at a current density of 20 mA/cm² and an energy cost of \$0.10/kW hr.

- Electrical power costs are small compared to other treatment methods.
- To reduce the size of the electrochemical cell, concentration of dilute solutions via reverse osmosis is recommended prior to electrochemical oxidation.
- Capital costs for a 10 liter per minute flow-cell are ~\$2500.

Conclusions

- ❖ PFOS and PFBS are rapidly mineralized to CO₂ and fluoride ions at BDD electrodes without detectable intermediate products.
- ❖ No evidence for the microbial degradation of PFOS and PFBS was observed after extended incubation (> 1.0 yr).
- ❖ PFOS and PFBS are adsorbed by hydrophobic zeolites, activated carbon, and ion exchange resins.
- ❖ Adsorption to ion exchange resins is irreversible.

Industrial Interactions and Technology Transfer

- **Walter Worth, Sematech, Walter.Worth@ismi.sematech.org**
- **Tim Yeakley, Texas Instruments, t-yeakley@ti.com**
- **Thomas P. Diamond, IBM, tdiamond@us.ibm.com**
- **Jim Jewett, Intel, jim.jewett@intel.com**
- **Laura Mendicino, Freescale Semiconductor,
Laura.Mendicino@freescale.com**

Future Plans

Next Year Plans

- **Finish adsorbent regeneration tests by April 1, 2010.**

Long-Term Plans

- **Identify partners for pilot testing on RO concentrates containing organic compounds.**

Publications, Presentations, and Recognitions/Awards

- Carter, K. E.; Farrell, J. “Oxidative Destruction of Perfluorooctane Sulfonate using Boron Doped Diamond Film Electrodes,” *Environ. Sci. Technol.* 2008, 42, 6111-6115.
- Liao, Z.; Farrell, J. “Electrochemical Oxidation of Perfluorobutane Sulfonate using Boron Doped Diamond Film Electrodes,” *J. Applied Electrochem.*, 2009, 39, 1993-1999.
- Carter, K. E.; Farrell, J. “Removal of Perfluorooctane and Perfluorobutane Sulfonate from Water via Carbon Adsorption and Ion Exchange,” *Separation Science and Technology* 2010, in press.
- Ochoa-Herrera, V.; Sierra-Alvarez, R. “Removal of Perfluorinated Surfactants by Sorption onto Granular Activated Carbon, Zeolite and Sludge,” *Chemosphere* 2008, 72, 1588-1593.
- Torres, F. J.; Ochoa-Herrera V.; Blowers, P.; Sierra-Alvarez, R. ”*Ab initio* Study of the Structural, Electronic, Vibrational, and Thermodynamic Properties of Linear Perfluorooctane Sulfonate (PFOS) and its Branched Isomers,” *Chemosphere* 2009, 76,1143-1149.
- Torres, F. J.; Ochoa-Herrera V.; Blowers, P.; Sierra-Alvarez, R. Response to “Comment on: *Ab initio* Study of the Structural, Electronic, Vibrational, and Thermodynamic Properties of Linear Perfluorooctane Sulfonate (PFOS) and its Branched Isomers,” *Chemosphere* 2009, 77, 1457–1458.
- J. Farrell, “Electrochemical Water Purification using Boron Doped Diamond Film Electrodes” presented at the University of California at Los Angeles, 10/30/07.
- J. Farrell, “Electrochemical Water Treatment using Diamond Film Electrodes,” presented at the University of Illinois at Urbana-Champaign, 11/7/08.
- James C. Baygents and James Farrell. “Electrochemical Methods for Water Reclaim in Semiconductor Manufacturing,” presented at the International Conference on Microelectronics Pure Water, November 11-12, 2008, Mesa, AZ.